NASA SP-392

The Space Telescope

NATIONAL AERONAUTICS AND SPACE ADMINISTRATION

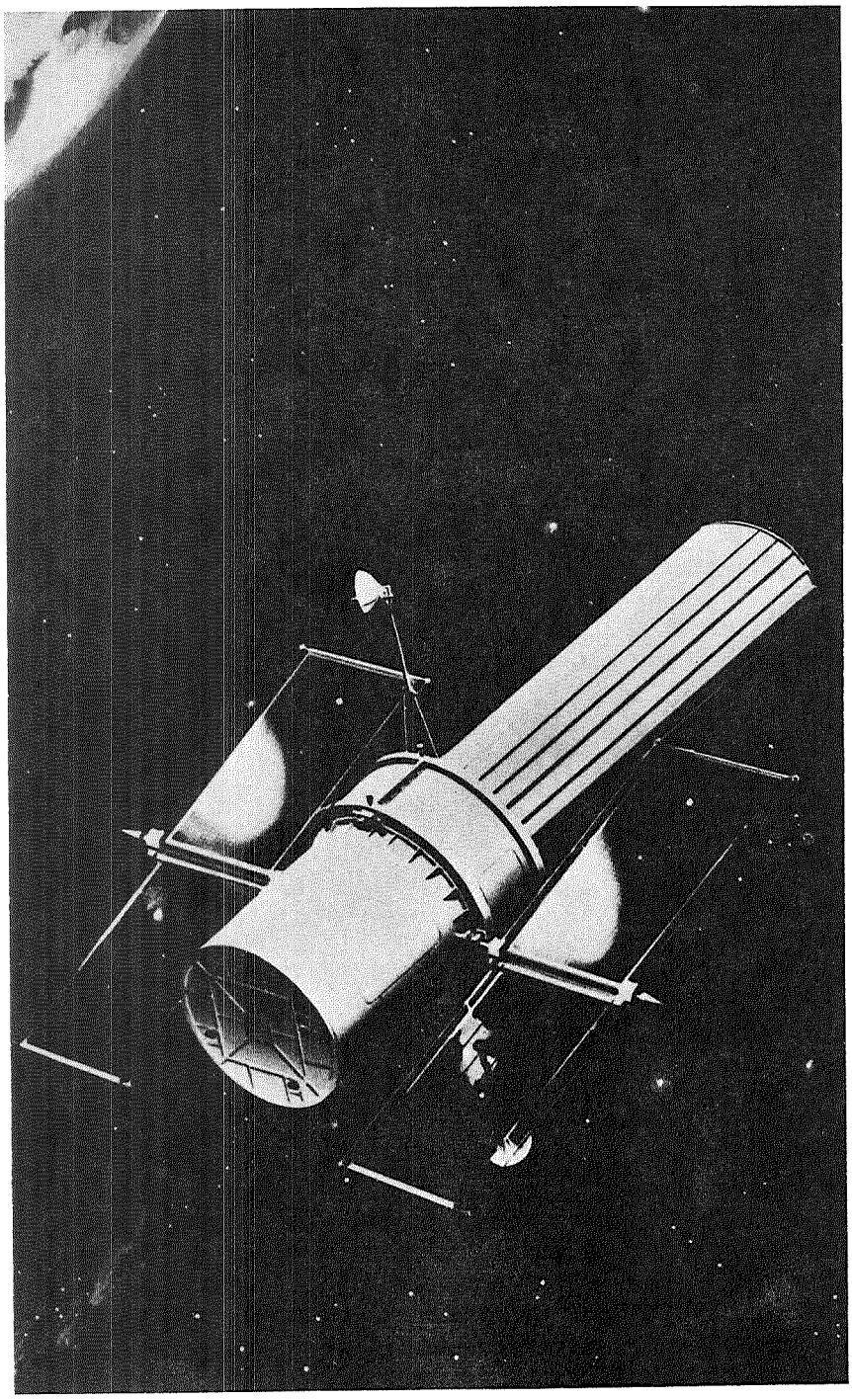

THE SPACE TELESCOPE

NASA SP–392

THE SPACE TELESCOPE

This volume contains the authors' summaries of their papers on the Space Telescope presented at the 21st annual meeting of the American Astronautical Society at Denver, Colorado, August 26–28, 1975

Scientific and Technical Information Office 1976
NATIONAL AERONAUTICS AND SPACE ADMINISTRATION
Washington, D.C.

Library of Congress Cataloging in Publication Data

Main entry under title:

The Space telescope.

(NASA SP ; 392)
"This volume contains the authors' summaries of their papers on the space telescope presented at the 21st annual meeting of the American Astronautical Society at Denver, Colorado, August 26-28, 1975."
Includes author index.
1. Orbiting astronomical observatories–Congresses. 2. Telescope, Reflecting–Congresses.
I. American Astronautical Society. II. Series: United States. National Aeronautics and Space Administration NASA SP ; 392).
QB88.S72 522'.29'19 76-7920

For sale by the Superintendent of Documents
U.S. Government Printing Office, Washington, D.C. 20402
Price $2.30 Stock Number 033-000-00644-6

FOREWORD

For over a decade, astronomers have been developing a new approach to observational astronomy and astrophysics because of the exciting new windows opened to space astronomy with the advent of the first Earth satellite. Since then, the ultraviolet portion of the spectrum has revealed new data about the stars and the universe. The proposed Space Telescope will unveil an exciting portion of the electromagnetic spectrum from the far ultraviolet to the near infrared and will make high-resolution observations in the visible portion that cannot be made from ground-based telescopes.

With the Space Telescope we will be on the threshold of new discoveries in space astronomy. It will allow astronomers to detect stars that are 50 times fainter than those observable with the most powerful ground-based instrument—the 5-meter (200-inch) Hale Telescope at Palomar. It will expand our understanding of the content, scale, structure, and evolution of the universe with a capability not possible with ground-based observatories.

The Space Shuttle, which NASA is developing for the early 1980's, will have the capability to launch the Space Telescope into its proper orbit. With the Space Shuttle to provide in-orbit maintenance, instrument update, and refurbishment for a period of 10 to 15 years, the Space Telescope will become a permanent observatory in space.

Launch of the Space Telescope will inaugurate a new era for astronomy and astrophysics. It is anticipated that it will provide an insight into new energy mechanisms and answers to many questions about the universe. Historically, astronomy has opened up new vistas that ultimately have very practical applications to our everyday terrestrial activities and problems. To predict what the contributions from the Space Telescope will be and when they will happen is folly; that they will occur is certainty.

Noel W. Hinners
Associate Administrator
for Space Science

PREFACE

The papers and summary papers that follow were presented at the Twenty-first Annual Meeting of the American Astronautical Society held in Denver, Colorado, on August 26 to 28, 1975. They should provide an insight into the activities of the scientific and industrial teams that have been engaged in solving the challenging problems of the Space Telescope.

Since its inception as a feasibility study effort in the early part of this decade, many of the concepts including the systems and subsystems for the proposed Space Telescope were outgrowths of the Orbiting Astronomical Observatory, the Apollo Telescope Mount, and other spacecraft developed during the past 16 years. Both the scientific and engineering teams have worked diligently to overcome the difficult tasks encountered in defining the Space Telescope.

I wish to thank the authors of the papers and summaries for their efforts in making this publication possible. It is my hope that the readers will gain an appreciation for the contributions of those associated with one of the most exciting projects in space astronomy, the Space Telescope.

M. J. Aucremanne
Program Manager–Space Telescope
Office of Space Science

CONTENTS

IV. MIRROR DEVELOPMENT

V. PRECISION POINTING AND CONTROL SYSTEMS

VI. DATA MANAGEMENT

VII. MAINTAINABILITY AND OPERATIONS

POTENTIAL FOR ADVANCEMENT OF SPACE ASTRONOMY

Arthur D. Code
University of Wisconsin

The opportunity to carry out astronomical studies in space has been the realization of a dream nurtured by astronomers for centuries. Such studies have already provided many exciting discoveries and surprises and significantly advanced our understanding of the universe in which we live. The Space Telescope represents a quantum jump in this intellectual adventure.

Space astronomy provides distinct advantages over the traditional techniques of ground-based astronomy by greatly expanding the utility of the experimental approach. It is now possible to perform in situ measurements with space probes and to obtain and return samples of planetary and interplanetary material. Previously we had to be content with analysis of those few meteorites or cosmic particles that came to us from outer space. Today we can go look. For the most part, however, experimental astronomy is restricted to the solar system and astronomy remains basically an observational science. However, observations from outside the terrestrial atmosphere provide several distinct advantages. First, the absence of atmospheric absorption greatly expands the available electromagnetic spectrum. Only in the extreme ultraviolet does the interplanetary and interstellar hydrogen interfere with our clear view of stars and galaxies. Second, the sky brightness is significantly reduced due to the absence of night sky emission and scattered light (the reduction of sky brightness depends upon the wavelength but is on the order of a factor of 3 or 4). Finally, in orbit, astronomical instruments are no longer plagued by the erratic fluctuations of the sea of air above a ground-based observatory. Absent are the debilitating effects of atmospheric tremor, scintillation, and differential refraction that astronomers refer to as "seeing" disturbances. The spatial resolution is no longer limited by Earth's atmosphere but rather by the optical system itself. Above Earth's atmosphere the stars are sharp, steady pinpoints of light; the sky is dark; and the spectrum is free of atmospheric absorption. To date, space observations have primarily capitalized on this freedom from atmospheric absorption. Rocket and satellite measurements in the X-ray region have opened a new and exciting chapter in astrophysics by providing a view of the high-energy processes occurring in space. Many X-ray sources are compact objects, some of which may be the ultimate collapsed objects—black

holes. Satellite observations in the ultraviolet have been of significance in all areas of stellar astronomy. The great hydrogen halos discovered surrounding comets have changed concepts of the structure of these objects, indicating that H_2O is the primary icy constituent. The extended constant luminosity behavior of the nova, FH Serpentis, which was discovered by ultraviolet observations, has significantly modified the interpretation of these cataclysmic events. The observations of a sharp peak in the interstellar extinction curve at 220 nanometers have provided new insight into the nature of interstellar dust grains, while measurements of many interstellar resonance lines in the ultraviolet reveal the essential features of the dynamic interplay between stars and the interstellar medium. The extension of measurements over most of the electromagnetic spectrum has made it possible for the first time to determine empirically fundamental parameters of main sequence stellar structure, such as effective temperatures and luminosities; many other fascinating problems are under investigation using satellite observations of variable stars, clusters, and galaxies. These and other observations will be continued by a variety of techniques such as the International Ultraviolet Explorer, sounding rockets, and Space Shuttle sortie missions. The Space Telescope promises to extend these absorption-free measurements to much fainter limiting magnitudes and yield higher precision than currently is possible. It is, however, in the area of high spatial resolution that the Space Telescope will make its most profound impact.

Let me illustrate the dramatic improvement in spatial resolution obtainable by the following comparison. It is possible by sophisticated techniques such as speckle interferometry to achieve angular resolutions of the order of two Airy disks with a ground-based telescope, despite atmospheric degradation; that is, it is possible to approach diffraction-limited performance. The signal-to-noise ratio S/N for interferometric observations is shown to be proportional to the observing time τ and inversely proportional to the square of the diameter of a point image in the focal plane θ and to the square root of the number Q of individual exposures of length τ:

$$\frac{S}{N} \approx Q^{1/2}\, \tau\, \theta^{-2}\, f[\lambda, D, \epsilon, F]$$

where λ = wavelength, D = diameter of telescope, ϵ = fraction of light blocked from the secondary mirror by the secondary mirror and its support, and F = focal length of telescope. In ground-based observations the maximum exposure time τ is limited by the length of time for which the stellar image or speckle pattern is stationary, and this does not exceed 0.1 second. The angular size θ of a typical stellar image observed from the ground is on the order of 1 second of arc. Therefore, for ground-based telescopes,

$$\tau\, \theta^{-2} = 0.1$$

On the other hand, a space telescope can carry out observations for most of an orbit (approximately 30 minutes) without significant temporal changes in the

image distribution. We assume that the optics are capable of putting most of the light from a point source within a 0.2-second-of-arc diameter (in fact, this is a rather conservative estimate for the Space Telescope). Therefore, because

$$\tau \sim 30 \text{ minutes}$$
$$\sim 2 \times 10^3 \text{ seconds}$$

and

$$\theta \sim 0.2 \text{ second of arc}$$

then

$$\tau \theta^{-2} = 5 \times 10^4$$

Comparing $\tau\theta^{-2}$ for the Space Telescope to that for a ground-based telescope, we see that the signal-to-noise ratio with the Space Telescope is approximately 5×10^5 greater than the signal-to-noise ratio achievable from the ground. Therefore if Q exposures are obtained on the ground to achieve S/N equal to that of the Space Telescope, then

$$Q^{1/2}\tau\theta^{-2} = 5 \times 10^4$$
$$Q = 2.5 \times 10^{11}$$

and

$$Q\tau = 2.5 \times 10^{10} \text{ seconds}$$
$$\approx 800 \text{ years}$$

Thus it would therefore require some 2.5×10^{11} individual exposures (or 800 years of exposure time) with the ground-based telescope to achieve the same signal-to-noise ratio obtainable in space during a single orbit of the Space Telescope.

Before reviewing some of those areas in which it is expected that the Space Telescope will make its most significant contributions, let me briefly describe an astronomer's view of the universe. In the beginning, some 10 billion years ago, there was an expanding hot dense condensation of matter and radiation. As this primordial mass expanded, the simplest of all atoms, hydrogen, became the primary constituent along with a lesser amount of helium. Later density fluctuations within the primordial medium caused condensations of massive clouds of hydrogen and helium, which on further collapse and fragmentation under the forces of self-gravitation resulted in condensations of galactic masses. As individual galaxies formed, perhaps with the violent events we see now as quasars, further condensations occurred, driven by shock waves produced in the collapsing mass. Thus stars were born, stars not too unlike our Sun but with at least one very essential difference. These stars were composed of only hydrogen and helium, with no traces of carbon, nitrogen, oxygen, iron, and other heavy elements present in the Sun and here on Earth. As these first stars contracted, the temperature increased until thermonuclear reactions set in.

Hydrogen in the deep interior was first converted to helium, providing the light we see radiating from stars. As the central hydrogen fuel was consumed, the temperature rose and helium nuclei began to fuse to form carbon; in the final stages of the star's life heavier elements appeared and their amounts increased. For those stars more massive than the Sun, a significant fraction of their mass was then returned to the interstellar medium, in some cases by violent explosions producing what astronomers call supernova and in other cases by less energetic losses of mass such as those resulting in planetary nebula. By these processes the interstellar medium became enriched in heavy elements and new stars were formed and the cycle repeated. The very atoms of which each and every one of us are made were formed in the center of some star in the distant past, and that these atoms should collect into the complex amino acids and proteins that form living organisms is not nearly so unlikely as was once thought. In the interstellar medium from which stars form, atoms condense into solid particles to form dark clouds of dust, and in these dust clouds modern radio astronomy reveals organic molecules not too different from these essential amino acids. The formation of complex organic compounds appears to be a natural and likely event that has been duplicated in simple laboratory experiments. It is believed that in the formation of stars like the Sun, matter condenses and forms planets that orbit about the central star, and that on those favorable planets, through the womb of time, self-organizing systems have evolved by the process of mutation and adaptation and thus we are assembled here today. This scenario describes the framework of our general view of the origin and evolution of the universe. In detail much remains to be learned, and each step is subject to uncertainty and some to controversy; it is however a fair description to say that this is what astronomy is about and it is in this arena that the Space Telescope displays its potential.

The scientific potential of the Space Telescope (formerly called the Large Space Telescope or LST) was first explored in depth in 1969 in the National Academy of Sciences publication *Scientific Uses of the Large Space Telescope* (ref. 1). Each of the current Space Telescope Instrument Definition Teams has prepared a compilation of the scientific objectives, and many of the exciting research programs were presented at the Washington meeting of the American Institute of Aeronautics and Astronautics in 1974 (ref. 2). Let me survey these areas by simply listing the titles of the papers presented at that Aerospace Sciences Meeting: "Cosmology With the LST" by Allan Sandage, "Contents and Structure of Galaxies as Observed With LST" by Ivan King, "Observing Quasars With LST" by Margaret Burbidge, "A Breakthrough for Astrometry" by Laurence Frederick, "Infrared Capability With LST" by Gerry Neugebauer, "LST–A Window on Stellar Nurseries" by George Herbig, "LST Looks at Stellar Death" by John Bahcall, and "Solar System Astronomy From the LST" by Harlan Smith.

I commend these papers to your attention. Had I the time, I could hardly do better than each of these imaginative authors has already done. Rather let

me single out one specific problem to illustrate the point that the Space Telescope does indeed represent a quantum jump in astronomical instrumentation.

The area I have chosen is the cosmological problem, a field that captures the imagination of all inquiring minds. If the Space Telescope is capable of making significant contributions to the cosmological problem, it then is a tool that necessarily has the capability required for most of the other investigations.

The cosmological problem in its most restricted sense is the problem of determining the appropriate geometry for describing the universe. The more ambitious program of describing the present structure and origin and evolution of the universe might more properly be called the cosmogonic problem. For the present let us consider the restricted problem of choosing the most appropriate world model. Is the universe finite or infinite, bounded or unbounded, closed or open?

The geometry may be completely specified by the metric. The metric is usually described in terms of the coefficients for each coordinate in space as they appear in the line element or differential distance between two points. For example, if we write

$$ds^2 = g_{xx}\, dx^2 + g_{yy}\, dy^2 + g_{zz}\, dz^2$$

in a simple three-dimensional space, then ordinary flat cartesian coordinates are given by

$$g_{xx} = g_{yy} = g_{zz} = 1$$

In general these coefficients, called the components of the metric tensor or the metric, are not constant. For example, in spherical coordinates

$$ds^2 = dr^2 + r^2\, d\theta^2 + r^2 \sin^2 \theta\, d\phi^2$$

In discussing the geometry of the universe, we are interested not only in where an event occurs but at what time it happened; hence a four-dimensional space is used where time is the fourth coordinate. The line element is written in a shorthand form as

$$ds^2 = g_{\mu\nu}\, dx_\mu dx_\nu$$

where μ and ν take on the values 1, 2, 3, and 4; hence, in general, we may have terms like $g_{23}\, dx_2 dx_3$ as well as terms like $g_{11}\, dx_1{}^2$. In principle, the metric may be found from examining those simple consequences of the prevailing geometry. For example, in flat space the sum of the angles of a triangle equals 180°, while in a positively curved space, like the surface of a sphere, the sum of the angles is greater than 180°. In a negatively curved space, like the open space of a saddle surface, the sum of the angles is less than 180°. Astronomical observations do not directly yield simple accurate distances and angles, and one must examine the more complex relations between observed quantities such as brightness, doppler shift and number counts, and the geometry of space. The approach taken is to predict the observational relations that would exist for a

given world model and choose the appropriate world model on the basis of the success of such predictions.

World models may be constructed within the framework of the general theory of relativity. General relativity is based upon two fundamental principles. The first is the principle of covariance, which simply states that the laws of physics should be independent of the observer and hence expressible in a form that is invariant to the particular choice of coordinate systems. The second principle, that of equivalence, also recognizes that there is no particular unique coordinate system or absolute frame of reference when it states the equivalence of inertial and gravitational mass. It is not possible to distinguish between a force and a coordinate acceleration. This means that by a suitable coordinate transformation, a force field can be transformed away. In a free-falling elevator we could say that we are falling under the attraction of the gravitational force of Earth or equivalently that we are moving uniformly in a coordinate system in which the grid spacing becomes progressively closer as we approach Earth. That is, we can choose complex laws of physics and a simple geometry or a simple law of motion, namely that all particles follow a simple path, a geodesic, and employ a complex geometry. The presence of matter has curved space and determined the appropriate metric. Planets move in near-elliptical orbits simply because the solar mass has curved space and the shortest path in this geometry is an ellipse. The equivalence or relation between the underlying geometry or metric and the distribution of mass and energy in the universe is the field equation:

$$f(\text{metric}) = F(\text{mass energy})$$

One of the beauties of this field equation as formulated by Einstein is that it contains implicitly all the conservation laws of physics and yet is the very simplest equation connecting the metric, described by the values of $g_{\mu\nu}$, and the mass of the universe. Other cosmological formulations such as the Brans-Dicke cosmology or the steady-state universe modify the field equations, but the recipe remains the same. Given the distribution of mass and energy in the universe, we can determine the appropriate geometry or metric; or, conversely, the determination of the metric specifies the large-scale physical structure of the universe. From the metric or values of $g_{\mu\nu}$ we can determine the invariant line element or interval between two events:

$$ds^2 = g_{\mu\nu}\, dx_\mu dx_\nu = \text{invariant}$$

The equation of motion of a particle in the universe is then described by the simple path of a geodesic in this space:

$$\delta \int ds = 0$$

The equation of motion is the equation of the geodesic, which says that the path is a minimum. Now when applying these concepts to the gross structure

of the universe, it is both necessary and reasonable to make a basic simplification. Over a sufficient volume of the universe, it is reasonable, although not necessarily true, to assume that irregularities average out and on a large scale the universe is homogeneous and isotropic:

$$g_{\mu\nu} = 0 \qquad \text{if } \mu \neq \nu$$

and

$$ds^2 = c^2\, dt^2 - R(t)^2\, du^2$$

That is, the universe looks the same at any place and in any direction. This is the cosmological principle. It means that the line element cannot contain any cross-product terms such as $dxdy$ or the universe would look different depending upon whether we looked in the $+x$ or $-x$ direction. The line element can therefore be written in a form in which the three spacelike coordinates du^2 simply vary in scale as a function of time by the factor $R(t)$. In other words, the universe is radially symmetric. The history of the universe is then described by the scale factor $R(t)$. In a closed universe this can be viewed as simply the temporal behavior of the radius of the universe.

Without prejudicing the discussion by a choice of a particular world model, let us consider the local behavior of $R(t)$. By expanding $R(t)$ around the point in four-space here and now that ($R = R_0$ and time $= t_0$), we obtain

$$R(t) = R_0 + (t - t_0)\dot{R}_0 + \frac{1}{2}(t - t_0)^2 \ddot{R}_0 + \ldots$$

The Hubble constant H_0 is determined from the slope of the velocity-distance relation in the near vicinity of our own galaxy, where the difference between different models is insignificant:

$$H_0 = \frac{\dot{R}_0}{R_0}$$

If the time scale τ is defined as

$$\tau = (t_0 - t) H_0$$

then

$$\frac{R(t)}{R_0} = 1 - \tau + \frac{1}{2}\tau^2 \frac{1}{H_0{}^2} \frac{\ddot{R}_0}{R_0} + \ldots \tag{1}$$

and if an acceleration parameter q_0 is defined as

$$q_0 = -\frac{\ddot{R}_0}{H_0{}^2 R_0}$$

then

$$\frac{R(t)}{R_0} = 1 - \tau - \frac{1}{2} q_0 \tau^2 + \ldots$$

The chief uncertainty in the determination of H_0 is the accuracy of the extragalactic distance scale and whether the measurements have been extended far enough to be in the region of "pure Hubble flow"; that is, to large enough velocities that local velocity fields are unimportant. The Hubble constant establishes the time scale τ while the acceleration parameter q_0 is a measure of the curvature of space. The linear term given by the Hubble constant is found observationally to be positive. The universe is currently expanding at a rate somewhere between 50 and 100 kilometers per second per megaparsec. If we know $R(t)$ we can determine the behavior of all pertinent observational parameters. For example, the matter density of the universe is simply

$$\rho = \rho_0 \left(\frac{R_0}{R(t)} \right)^3$$

which is related to the number of galaxies that may be observed at different magnitude limits. It is rather easy to demonstrate that the very important red shift parameter $z = \Delta\lambda/\lambda$ is given by

$$1 + z = \frac{R_0}{R(t)}$$

in any cosmological model. To the first order we can see from the expansion given in equation (1) that $z \approx \tau_0$, and because τ_0 is the length of time in units of the Hubble time for light to travel a distance d, which is to this order the distance of the galaxy,

$$\tau_0 = \frac{d}{c} H$$

The expansion velocity cz is

$$cz = dH$$

the linear velocity-distance relation appropriate for small values of z.

The field equations of general relativity yield a set of simple solutions if the pressure p and the cosmological constant Λ are set equal to zero. In the present epoch the pressure term is exceedingly small compared to the gravitational interaction of masses, because collisions between galaxies or clusters of galaxies are very rare; thus $p = 0$ is an excellent approximation. The cosmological constant is a term occurring in the most general formulation of the field equation representing some large-scale interaction not known in terrestrial physics. We do know that if there is a cosmological constant, it is exceedingly small because it does not manifest itself on the scale of the solar system. Models based on the assumption $p = \Lambda = 0$ are referred to as the Friedmann universe. For closed Friedmann universe models ($q_0 > 1/2$),

$$R(t) = A(1 - \cos \psi)$$

and

$$ct = A(\psi - \sin \psi)$$

For flat Friedmann universe models ($q_0 = 1/2$),

$$R(t) = Kt^{2/3}$$

For open Friedmann universe models ($q_0 < 1/2$),

$$R(t) = A(\cosh \psi - 1)$$

and

$$ct = A(\sinh \psi - \psi)$$

The following equation is true for all Friedmann universe equations:

$$A = \frac{c}{H_0} \frac{q_0}{|2q_0 - 1|^{3/2}}$$

The constant A appearing in these solutions is a function of H_0 and q_0 only. Thus we see that the model is completely specified by H_0 and q_0, hence the importance of these two parameters. For a closed universe, $q_0 > 1/2$, the solution is a periodic function. In figure 1 the behavior $R(t)$ is shown for Friedmann models. A flat universe continues to expand proportional to $t^{2/3}$, q_0 re-

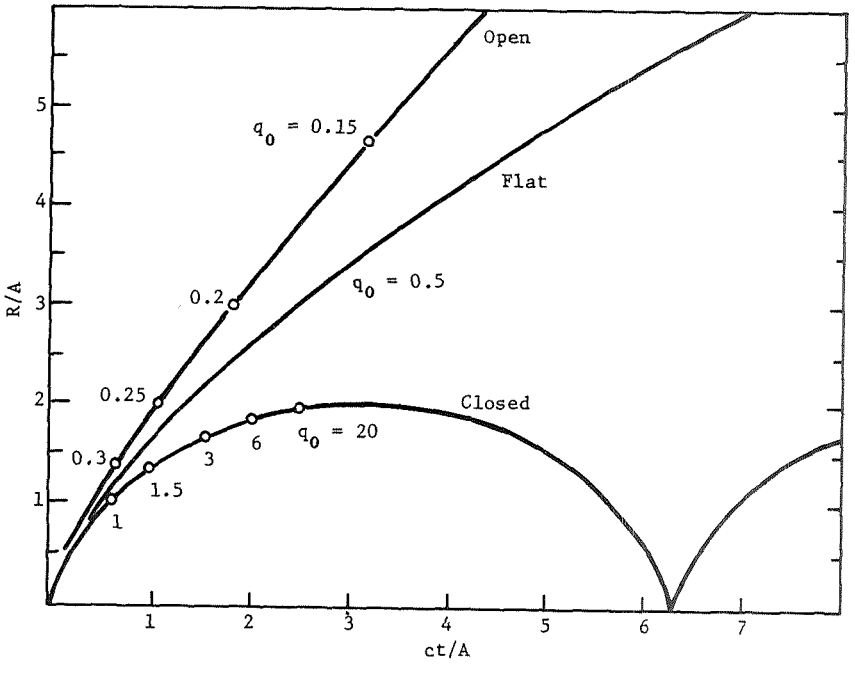

Figure 1.–Behavior of $R(t)$ for Friedmann models.

maining equal to 1/2 at all times. If the density of the universe is sufficiently high, gravitational interactions will decelerate the expansion and the universe will ultimately contract again as shown by the cyclical curve for a closed universe. The total energy of the universe, in this case, is negative and the system is bound; it did not have escape velocity. The critical density above which the universe is closed is given by inserting 1/2 for q_0 into the equation for the density of a Friedmann universe:

$$\rho_0 = \frac{3}{4\pi} q_0 H_0{}^2$$

For current values of H_0, this density is more than an order of magnitude larger than the observed density of the universe; and unless there is appreciable "missing" or unobservable mass, the universe is open. It is possible, however, that locally the density exceeds the appropriate critical density for which space is closed; we then say we are dealing with a "black hole."

Now while this closed model gives a periodic or pulsating universe, the Friedmann conditions are certainly violated as $R(t)$ approaches zero and the density approaches infinity. In a high-density state, it is no longer valid to neglect the pressure or the energy density of radiation, and thus unless very special conditions prevail, the universe will not bounce and repeat its history as suggested by the curve.

The open universe indicated by the curve with the systematically decreasing value of q_0 continues to expand indefinitely. If we knew observationally the value of q_0, we would then know our present location on one of these sets of curves. If, in addition, we knew the value of the Hubble constant, we would then know the scale of these curves and hence the age of the universe and its dimensions. Now let us return to the observational evidence available for relating these model universes to the "real" physical universe. We know that currently all distant galaxies give red doppler shifts and hence indicate that we are presently in an expanding universe. Of the variety of observational relationships that can be used to test the space metric, the most powerful using ground-based data is, in fact, the relation of this doppler shift to the observed magnitude of galaxies. As mentioned previously, the doppler shift $1 + z$ is given by $R_0/R(t)$. The total energy received from a galaxy decreases as the fourth power of $R(t)/R_0$ or as $(1 + z)^{-4}$. The energy is reduced by one factor of $1 + z$ due to the reduction in energy of a photon and by another factor of $1 + z$ resulting from the decreased rate of arrival of the photons. A factor of $(1 + z)^2$ accounts for the change in solid angle in which the photons are observed as a result of the geometry.

In figure 2, the relation between the total power received, expressed as the bolometric magnitude m_b, and the logarithm of the doppler shift cz is shown for different values of q_0 for Friedmann models. The curve labeled $q_0 = -1$ represents the results for the steady-state cosmology. Significant differences between models set in at magnitudes fainter than the 18th or having a log cz

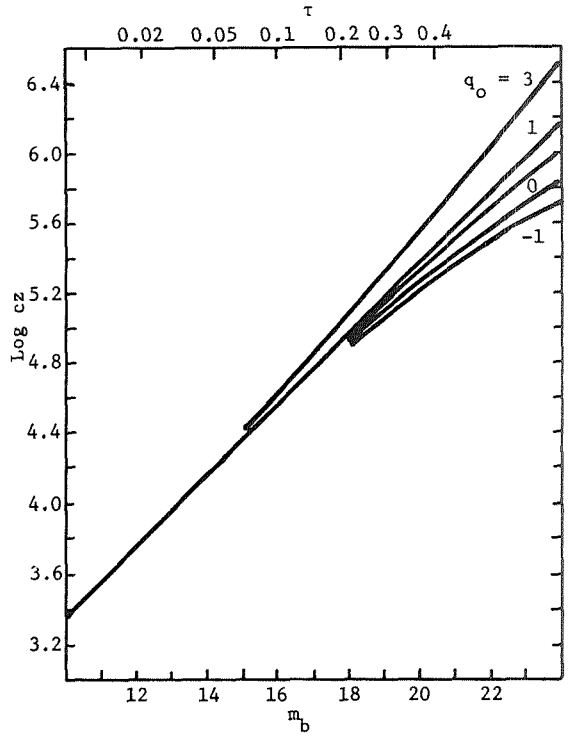

Figure 2.–Relationship between power received and doppler shift.

greater than 5 (corresponding to $z > 1/3$). The time τ scale indicated on the upper margin corresponds to the times for $q_0 = 1$. At about the 19th magnitude, one is looking back through nearly half the history of the universe. The curves plotted in figure 2 refer to the variation in observed bolometric magnitude of an object of fixed luminosity, namely to a "standard candle." This standard candle is usually taken as the brightest galaxy in a cluster. The determination of the luminosity of this standard candle is intimately connected to the determination of the extragalactic distance scale and the Hubble constant; the extension of the curve to larger red shifts involves determining the extent to which the brightest galaxies in clusters are really the same and making a variety of other corrections.

Figure 3 shows the results of a discussion by Sandage and Hardy (ref. 3) that summarizes the data as of that time. The data presented are for 97 clusters or groups of galaxies and the straight line corresponds to $q_0 = 1$. The magnitude given is the total corrected V magnitude. We do not observe the bolometric magnitude but only the magnitude of the object over some selected bandpass, in this case the V magnitude centered near 550 nanometers. The V

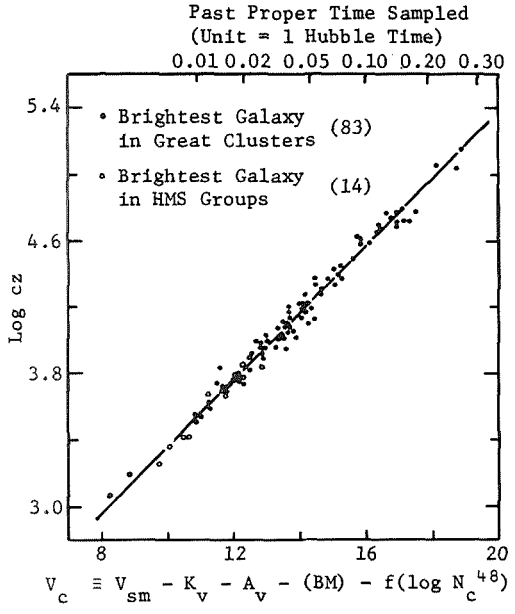

Figure 3.–Relation of the brightest galaxy in each of 97 clusters with the doppler shift of the cluster.

magnitude of a nearby star of known spectral type differs from the bolometric magnitude by a simple determinable constant. The V magnitude of a distant galaxy V_c is not so simply related to its bolometric magnitude, and the corrections applied are indicated along the abscissa of this figure. The magnitude has first been corrected for the fact that observations with a given focal plane aperture may not include all the light from a galaxy V_{sm}. The second correction K_ν, called the K term, takes into account the fact that for a red-shifted galaxy, one is not observing the same spectral region with the fixed bandpass as for an object in the rest frame. The third term A_ν corrects for the decrease in brightness caused by extinction produced by interstellar dust grains in our own galaxy. The last two corrections attempt to correct for differences in the brightness of the brightest galaxies in clusters depending upon the kind of cluster and the richness, or population, of the cluster. It is clear that the step from observation to our theoretical models is not a simple one and each correction is subject to uncertainty. Moreover, one very essential consideration has been neglected. It may very well be that, due to evolution, those distant galaxies sampled back in time are significantly brighter or fainter than the nearby galaxies of the present epoch. We shall return to the question of evolution presently, but for the moment let us see what can be said about the choice of metric if evolutionary corrections are small.

As noted before, the difference between different world models does not

become significant until at least the 18th magnitude, and thus figure 3 gives little information on the value of q_0. In figure 4 I have plotted the results for the most distant clusters for which we had observational data in 1973. These data are taken from reference 3. The deviation in magnitudes from the curve $q_0 = 1$ is plotted against the red shift parameter z on a linear scale. The range of magnitude differences for the closer clusters is indicated by the arrows in the lower portion of the plot. While a formal least-squares solution could be made for the best value of q_0, it appears clear from the diagram that q_0 is really undetermined. It is probably inconsistent with the steady-state cosmology or a value of q_0 much in excess of two, but otherwise is uncertain.

Obviously, what is required to derive information on q_0 from the Hubble diagram is to improve the precision of the magnitude determination and to extend the results to large values of z and therefore to fainter objects and to increase the total number of clusters observed.

The Space Telescope should be capable of obtaining spectra for red shifts to $z \sim 1$, while the photometric precision at this limit would be appreciably better than current ground-based photometry. At larger red shifts the ability of the

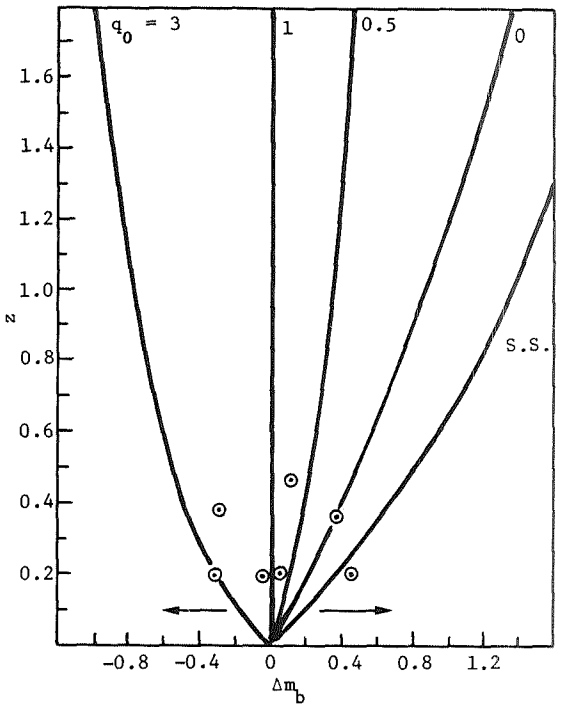

Figure 4.—Red shift as a function of change in bolometric magnitude for various values of the acceleration parameter.

Space Telescope to carry out observations in the ultraviolet may prove advantageous. The most important aspect of ultraviolet observations, however, will probably be the leverage provided to allow for galaxy evolution. This is very difficult to determine in the spectral region available to ground-based telescopes. The extension of spectral energy distributions to the far ultraviolet, however, would give a very strong hold on the hot star component in the galaxy, which exhibits the most rapid evolution. Observations would be needed of both small red shifts and the largest values of z possible to provide the sensitivity required to calculate the evolution of galaxies with time. The Space Telescope could also provide information on evolution by extending galaxy counts to much fainter limits, because the effect of evolution on the apparent value of q_0 has the opposite sign for number counts than for the red shift-magnitude relation.

The most fundamental contribution of the Space Telescope to the cosmological problem, however, will be in the refinement of our knowledge of the distance scale and the brightness of the brightest cluster galaxies. The extragalactic distance scale is based upon the observation of individual objects of various kinds in nearby galaxies. The cepheid variable stars, for example, are luminous pulsating stars whose absolute magnitudes can be determined from their period of pulsation. The very brightest stars in our own and nearby galaxies also provide a valuable distance indicator that can be used to somewhat greater distances than the cepheid variables. A different type of distance indicator is provided by the angular diameter of the largest H (II) regions or ionized hydrogen regions. At the top of figure 5, the distances to which these types of distance indicators are applicable are indicated schematically for typical ground-based observation. Here the limiting B magnitude for suitably accurate photometry is taken to be 22d magnitude, and the angular resolution to be of the order of 1 second of arc. Immediately below the figure some of the galaxy groups and clusters are given. It is only from these few nearby groups and the Leo and Virgo cluster that we can apply these basic distance indicators and thus connect the brightest cluster galaxies to these distance determinations. To increase the available statistics on the brightest cluster members, one must resort to a number of indirect arguments having considerably weaker foundation. The bottom of figure 5 shows the domain of the cepheids, brightest stars, and H (II) regions accessible to the Space Telescope if the performance is conservatively taken to be $B \approx 26$ magnitude and $\theta \approx 0.1$ seconds of arc. Distance indicators in thousands of galaxies become possible, and the number of clusters that can be studied is substantially increased.

In this discussion I have restricted myself to only a few classical approaches to the cosmological problem. The Space Telescope offers alternatives. In addition, I have confined the discussion to the problem of selecting the appropriate geometry. The Space Telescope can make very substantial contributions to the broader questions of the origin and evolution of the universe. I hope, however, I have convinced you that the solution of the cosmological problem is within our grasp.

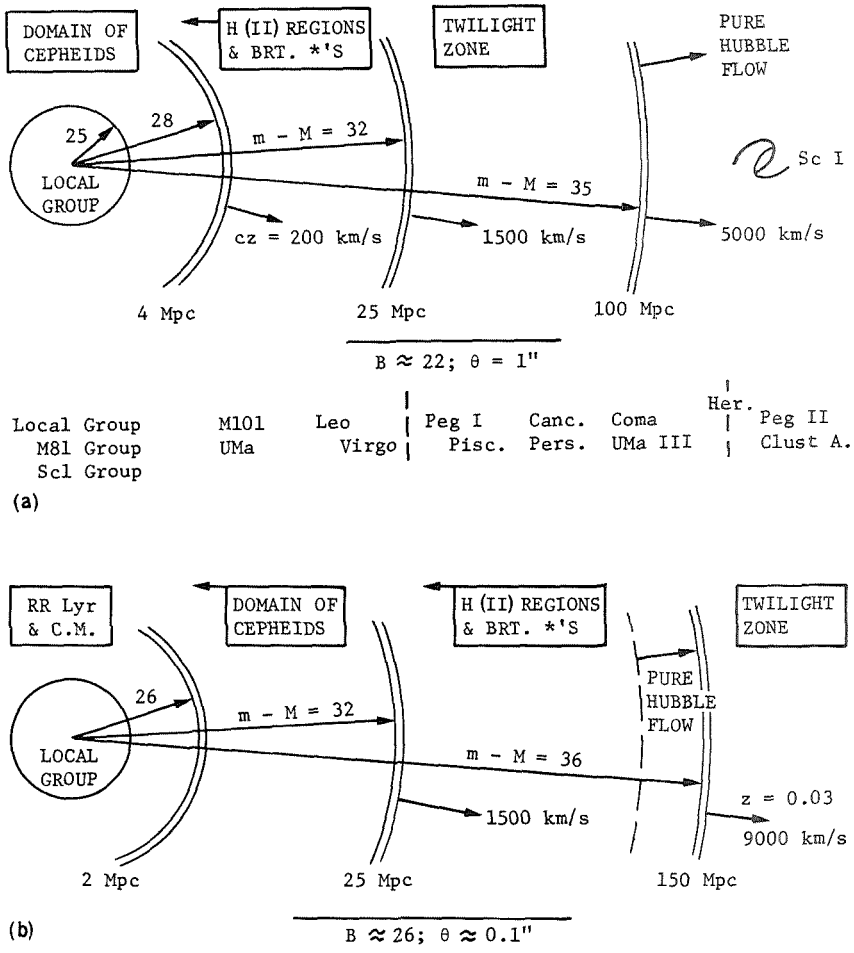

Figure 5.–Yardsticks available for galaxies at various distances. (*a*) Current. (*b*) Future with the Space Telescope.

The Space Telescope is an exciting adventure, and whether it comes to pass here and now, it will come to pass. For thus it is that the primordial hydrogen atoms, of which I spoke, have, over 10 billion years of dynamic history, arranged themselves in such as we, so that they can ask from whence they came.

REFERENCES

1. Space Science Board Ad Hoc Committee on the Large Space Telescope: *Scientific Uses of the Large Space Telescope.* National Academy of Sciences, 1969.
2. *Large Space Telescope–A New Tool for Science.* Papers presented at the 10th Annual Meeting, American Institute of Aeronautics and Astronautics (New York), Jan. 1974.
3. Sandage, A.; and Hardy, E.: *The Astrophysical Journal,* vol. 183, 1973, p. 743.

CONCEPTS OF OPERATION

C. R. O'Dell
NASA Marshall Space Flight Center

As the first true astronomical space observatory, the Space Telescope will be faced with the operational requirements of both the traditional ground-based observatories and its predecessor satellite programs. Moreover, it will have its own set of new constraints and requirements. These all combine to make the Space Telescope a challenging system to operate efficiently, and efficient operation will be a necessity because the scientific demand for the use of the Space Telescope will be very high, and the cost per year of observing time will significantly exceed that of traditional telescopes.

What I shall address in this paper is the subject of operations in the broadest sense, and mention what I believe are the relevant points in moving from idea, through observation, to interpreted result. The actual control of spacecraft operations will be through a Mission Operations Center. Although it will be working with the Tracking and Data Relay Satellite System, this aspect of operations will not be particularly different from earlier astronomical satellites and will not be discussed in detail here. There are, however, two requirements that are special for the Space Telescope.

Object acquisition and guidance are new problems for the Space Telescope because of the precision required. Acquisition presents a new challenge because of the faintness of the objects being observed. Although methods using precise gyros are sufficient for most imaging experiments, these are insufficient for locating the correct star into a scientific instrument entrance aperture that is comparable in size to the Space Telescope's minute images. The problem is further compounded by the need to work often on faint objects in crowded fields of view. When the object is isolated and bright, we can use a signal from the source itself to do the fine centering. However, in the faint-object/ crowded-field case we must obtain an image of the field, then use that information to make the final setting. Almost all Space Telescope observations will demand an essentially continuous guidance with a stability only a small fraction the size of the stellar image. Because we will be observing faint stars, the reference signal for guidance will have to come from guide stars, some 10 minutes of arc away from the object field. The guidance system must know where to look for these stars, acquire them automatically, and then initiate the guidance signal. This required preplanning and automation are among the real challenges of Space Telescope operations.

SCIENTIFIC REQUIREMENTS

After the scientist establishes his desired observing goals, in terms of a limited or multifaceted approach, he must formulate the observing needs to reach these goals. Using information of Space Telescope systems capabilities and procedures, he can turn these observing needs into a proposed observing program. These observing proposals will be solicited continuously and normally collected periodically at times 6 to 12 months before the observations would begin. Technical evaluation follows. This evaluation is combined with the scientific justification to allow a peer group review by other scientists prior to selection. This peer group will select, according to scientific merit and feasibility, a set of observing programs to fill the time period in question.

The nature of these programs will vary enormously. Some will be one-shot measurements while others will require multiple observations. Some will require intensive observations during one part of the year when a particular part of the sky is optimally located, while others will require occasional observations throughout the year. Many different brightness levels will be addressed, and some programs may even wish to use more than one scientific instrument.

The observer must then work with a specialist staff of scientists working for the Space Telescope program to prepare a list and sequence of specific scientific instrument operations to be executed in the performance of his program. The requests for the use of scientific instruments must be compiled into an optimum observatory observing schedule. This optimization will consider the requirements for turning individual scientific instruments on and off; calibration needs; demands for observations at specific times; solar, lunar, and terrestrial glare; communications requirements; and setting slewing rates for the telescope as a whole.

The final, optimized observing program will in large part be performed without immediate scientist user participation. However, in two areas the scientist will have to work closely with the Mission Operations Center staff. The first of these will be in the quick look at some of the data, where changes in the observing program may be demanded by the nature of the source at that specific time. The second will be in the acquisition of faint objects and/or of objects in crowded fields. In the latter case, the observer scientist will work with an acquisition scientist who does the actual field recognition and spacecraft commanding, with the observer scientist beside him, if necessary.

SCIENTIFIC DATA OUTPUT

Once the observation is made, the process of turning data into information begins. After temporary onboard storage and transmittal to the ground and the Mission Operations Center, the scientifically relevant data (which can include spacecraft status data) are extracted and put into a form to allow straightforward data reduction. Data reduction is expected to be a detailed process.

Because the data processing requirements will be essentially identical for various observations with one scientific instrument, this process will be centralized, with the user scientist working with a data scientist. During this process, field distortion corrections will be applied, photometric calibrations determined, and spectral response calibrated. All these processes will be applied and then the scientist user can select from several formats in which to collect his reduced data. Basically the intent is to centralize those functions that are common to many observing programs and carry the data reduction up to the step of data analysis. The data then belong to the scientist to do with as he pleases.

These data will also be stored in a readily accessible form. Experience amply shows that proprietary use of his own data is an essential ingredient in obtaining the best science. Observance of this tradition of proprietary rights is balanced by the fact that this is a nationally funded facility. We expect to balance these two opposing pressures by keeping the data in storage until 1 year after data reduction, after which time the data can be distributed upon request.

There are several plans describing the function of a scientist in performing Space Telescope operations; however, the preferred ones must recognize that scientific excellence flourishes only under a free enterprise system while the Space Telescope itself is a complex system demanding continued involvement of the agency developing it.

PROGRAM STATUS

James A. Downey III
NASA Marshall Space Flight Center

The concept of placing an astronomical observatory in Earth orbit is not a recent one. Scientific advisory groups, individual scientists, and various persons of vision have recognized the exciting possibility of putting a major astronomical facility in space above the obscuring effects of Earth's atmosphere. The idea of a large optical observatory in orbit predates the space era. Today a number of telescopes already have been flown in space and have observed celestial objects in various regions of the electromagnetic spectrum. These present systems, along with the advance of aerospace technology in general and the coming availability of the Space Shuttle, have paved the way for accomplishment of the Space Telescope project. The Space Telescope will be an astronomical observatory that will operate in space for more than a decade.

DESCRIPTION AND STATUS OF DEFINITION

The Space Telescope is an automated satellite that will be delivered to orbit by the Space Shuttle. Scientific data from its scientific instruments (SI) will be transmitted to Earth via telemetry through the Tracking and Data Relay Satellite in geosynchronous orbit. The Space Telescope differs from existing automated satellites in that it can be retrieved from orbit and returned to Earth by the Space Shuttle for refurbishment. Also, it will be equipped to permit in-orbit maintenance and repair by a spacesuited astronaut. As the Space Telescope operational era evolves, a high degree of in-orbit maintenance and servicing will be possible. The Space Telescope is a relatively safe and inert payload from the standpoint of presenting a hazard to the Space Shuttle and its crew; it has no onboard propellants and will carry no pyrotechnic devices.

The current overall status of the Space Telescope program is that more than one-half the definition effort (phase B) has been completed. Early definition was based on a configuration with a primary mirror of 3.0-meter (118-inch) diameter. However, since May 1975 all effort has been concentrated on a 2.4-meter (94-inch) Space Telescope. The events and rationale leading to this change will be discussed later in this paper. The remaining part of the definition contracts will be completed by March 1976, and the program is aimed at a new development start in the 1977 fiscal year.

The fiscal year 1977 new start plan reflects release of the RFP's for the development contracts in June 1976, leading to the award of contracts early in 1977. Development of the Space Telescope system will require a period of approximately 6 years, with launch in late 1982 or early 1983.

There is an intrinsically long development time associated with certain elements of the Space Telescope; e.g., the primary mirror. The project plan has approached the development schedule on a basis of minimizing costs. Obviously, there are no launch window considerations in the case of the Space Telescope. Planning of various events in the development schedule can be optimized from a standpoint of cost effectiveness.

As a result of recent reviews of the Space Telescope definition contracts, development cost estimates have been refined. These cost estimates have been submitted to NASA Headquarters for review and evaluation. Development costs are not discussed in this paper because of the current review activity in NASA. The next key milestone from an overall program standpoint is inclusion of Space Telescope development as a fiscal year 1977 new start in NASA's budget plans. This decision will be made next month by NASA top management. Submission of the Space Telescope as a new start in NASA's fiscal year 1977 budget will be the starting point in review and approval of initiation of the Space Telescope execution phase by the Office of Management and Budget and the Congress.

The balance of this paper discusses some of the early history of the Space Telescope program and concentrates on the recent decisions and work that remains to be done in the definition phase. By spring of 1976, Space Telescope definition will have been completed. More time and resources will have been expended on definition of the Space Telescope than in the planning of any previous NASA scientific mission. Consequently, definition will be exceptionally thorough, providing high confidence that the Space Telescope can be developed to achieve the required scientific performance within predicted costs.

Feasibility studies were completed in 1972, and project responsibility was assigned to Marshall Space Flight Center. Goddard Space Flight Center (GSFC) also plays a significant role in the project, having responsibility for the scientific instrument definition and development. George Levin, the GSFC Space Telescope Study Manager (the Space Telescope was formerly called the Large Space Telescope or LST), is providing a paper on the Space Telescope SI; therefore, the status of the SI is not discussed in detail in this paper.

In late 1972, NASA decided to proceed with definition and development of the Space Telescope by letting separate contracts for the definition and development of the telescope portion, which is referred to as the optical telescope assembly (OTA), and the spacecraft, called the support systems module (SSM). The SI will be developed by principal investigators (or investigator teams) from the astronomical community. (In the present definition phase, the OTA contractors have responsibility for the combined definition of the OTA and SI,

based on requirements established by the scientific community.) We refer to the contracting approach being used in this program as the "associate contractor" approach. NASA will have overall systems engineering management responsibility but will receive support in systems engineering and integration by the SSM contractor.

The Space Telescope definition effort was initiated in 1973. Scientists were selected in the summer of 1973 to participate in the definition. Their guidance and assistance have been invaluable. Contracts for the definition of the OTA and SI were awarded in August 1973 to Itek and Perkin-Elmer Corp. Originally these contracts were for a duration of 17 months, but extensions have been implemented to carry the work through February 1976. The initial work on the SSM was started in-house by Marshall Space Flight Center in August 1973. The in-house definition of the SSM was completed in the fall of 1974. In December 1974, contracts for further definition of the SSM were awarded to Boeing, Lockheed, and Martin Marietta. These contracts are for 15 months' duration and will be completed early next year.

The 1975 fiscal year was the first year that the Space Telescope was identified as a specific and separate line item in the NASA budget submission to Congress. After passage of the fiscal year 1975 Authorization Bills, the House Appropriations Subcommittee recommended the funding requested for the Space Telescope be denied. The Senate subsequently favored reinstatement of funding for the Space Telescope. Ultimately, as a result of the actions and resolution of the Joint House/Senate Conference Committee, NASA received $3 million fiscal year 1975 for Space Telescope definition. This was approximately one-half the amount of funding requested by NASA for the Space Telescope. Furthermore, this funding was appropriated with the stipulation that NASA pursue definition of a lower cost program involving substantial international participation. Definition of the 3.0-meter (118-inch) Space Telescope system had not matured to the state that accurate cost predictions were available. However, the intent of Congress was clear and action was taken by NASA to readjust the program objectives to reduce overall project cost and complexity.

In the fall of 1974, the OTA contractors, who had been defining a 3.0-meter (118-inch) telescope system, were asked to recommend a lower cost system. What was being sought was a smaller size system that would cost less but still provide acceptable scientific performance. Both contractors performed studies which indicated that significant cost savings and increased confidence in cost and schedule estimates could be achieved by reducing the aperture of the telescope to 2.4 meters (94 inches). When the SSM contracts were awarded in December 1974, Boeing, Lockheed, and Martin Marietta were requested to do 4-month studies to evaluate the cost and performance characteristics of three systems having primary mirror sizes of 1.8, 2.4, and 3.0 meters (71, 94, and 118 inches). The result of these studies showed that significant cost savings could be achieved by reducing the size from 3.0 to 2.4 meters (118 to 94

inches). However, further reduction to 1.8 meters (71 inches) did not result in significant savings. Also, the 1.8-meter (71-inch) system degraded science performance to the extent that the class of scientific investigations envisioned for the Space Telescope would not be achievable. Above the 2.4-meter (94-inch) size there is somewhat of a "step function" in higher cost and complexity. Therefore, in May 1974, the NASA Headquarters decided that all further Space Telescope effort should be based on the 2.4-meter (94-inch) size system. This decision was a sound one, primarily because of the engineering margins available with the 2.4-meter (94-inch) system and the higher overall confidence that cost targets can be met and program objectives attained.

During the earliest NASA studies of the Space Telescope, the principal efforts were directed at basic technology and subsystem performance. A high-quality optical system is necessary to take maximum advantage of the viewing potential in space. Questions were raised about the ability to figure the primary mirror of a Space Telescope to the accuracies required to achieve near-diffraction-limited performance. Furthermore, the structure of the Space Telescope would have to be very stable dimensionally in the orbital environment to keep the mirrors alined in proper focus during scientific observations. Additionally, the higher the potential optical performance of the Space Telescope and the finer the detail of the optical image, the greater the demands on the spacecraft stabilization system to hold the image steady during long-term observations. A number of advanced development activities have been accomplished that studied and resolved these and other technical areas of concern to the Space Telescope program.

NASA sponsored an advanced technical development effort with Itek to figure a 1.8-meter (71-inch) mirror to the accuracies required by the Space Telescope program. This contract with Itek was successfully completed in June 1974. The mirror was figured to better than 1/60 of a wave (measured at 632.8 nanometers), exceeding the design goal for optically figuring the primary mirror. This 1.8-meter (71-inch) mirror was made of the same low coefficient-of-thermal-expansion material that will be used for the Space Telescope primary mirror. The 1.8-meter (71-inch) mirror admittedly is somewhat smaller than the 2.4-meter (94-inch) primary mirror; however, we now have utmost confidence that the 2.4-meter (94-inch) mirror can be figured to Space Telescope program requirements.

To build a telescope mirror support structure using traditional structural materials would put severe demands on the thermal control system to achieve telescope performance and focus during scientific observations. Fortunately, the technology of graphite epoxy materials has progressed rapidly. Graphite epoxy has attractive properties for a variety of aerospace applications. A property that is of particular significance to the Space Telescope is that graphite epoxy structural members can be fabricated in a manner to provide an extremely low thermal coefficient of expansion. (Also, graphite epoxy is a stiff material and has exceptional strength/weight properties.) Making structural

components of the telescope portion of the Space Telescope, or optical bench, out of graphite epoxy with its low coefficient of expansion relaxes significantly the performance requirements of the spacecraft thermal control system. NASA has accomplished in-house work and sponsored advanced development efforts to investigate the basic materials properties of graphite epoxy for Space Telescope applications. Also, there were concerns about the fabricability of graphite epoxy structures for use on the Space Telescope, particularly techniques to make appropriate joints at the intersection of structural members. However, a full-scale graphite epoxy truss for a 3.0-meter (118-inch) Space Telescope has been completed by Boeing. This truss is being tested. Also, General Dynamics/Convair has fabricated a Space Telescope half-scale structural shell out of graphite epoxy. The cylindrical shell design is an alternate approach to the truss for forming the principal structure of the telescope.

The requirements on the Space Telescope spacecraft stabilization and control system are demanding. We have specified a design goal of maintaining stabilization of 0.007 second of arc during a scientific observation. This might appear intuitively to be an unachievable goal. However, the Orbiting Astronomical Observatory spacecraft has demonstrated stabilization performance of 0.01 second of arc (and even better for short periods). The Orbiting Astronomical Observatory achieved this stabilization using a reaction-wheel-actuated control system, and this type is planned for use on the Space Telescope. The Martin Marietta Corp. has developed a fine-pointing simulation facility that is used to investigate pointing control and motion disturbance effects on a simulated Space Telescope system. This simulator, which is in a seismically quiet location, can resolve motions of a few ten-thousandths of a second of arc. Lockheed has built a structural simulator of the Space Telescope system and is investigating induced vibrations in the simulated structure using components similar to those that will be used on the Space Telescope. Of particular interest are vibrations from reaction-wheel imbalance and the propagation of these vibrations to the focal plane region of the telescope.

These areas of investigation and other advanced development effort, sponsored both by Government and industry, have provided the assurance that Space Telescope development is achievable and practical. Certainly the technology exists today for its development. In addition, a significant part of the Space Telescope effort to date has been devoted to the testing and breadboarding of certain critical subsystems and components. Demonstration of performance of various OTA and SSM subsystems in my opinion has been a most important contribution of the NASA- and industry-sponsored work accomplished to date. The principal challenge that lies ahead is not further technological effort and advanced development work, but application of engineering design principles and systems engineering practices to implement the Space Telescope as a complete flight hardware system.

The Space Telescope system is designed in a modular fashion with respect to the SI. The instruments are not interdependent in any way, and each on-axis

instrument is designed separately to a common interface specification. Individual instruments may be added or removed without affecting the other elements of the system. This modularity in instrument design represents a principal difference between the early Space Telescope designs and the current approach being pursued during the present definition effort. The easy interchange of instruments during the operational life of the Space Telescope provides the ability to update instruments to address the problems of greatest scientific interest during the long projected lifetime of the Space Telescope observatory. Also, as the instrument and detector technology evolve, the Space Telescope can be updated to benefit from future state-of-the-art instrumentation. There is a strong analogy in this respect to the operation of the great Earth-based astronomical observatories. The basic telescope optics and structure remain essentially unchanged; however, the scientific problems being addressed and instrumentation used at the large ground observatories have evolved with time.

The scientific participants in the Space Telescope phase B definition activity have established minimum scientific performance requirements. It will be necessary for the system to provide performance equal to (or exceeding) these requirements to effectively address the class of scientific problems envisioned for the Space Telescope. The overall challenge of the Space Telescope program is to meet these requirements in a most cost-effective manner. A current listing of some of the overall parameters of the Space Telescope system is as follows:

Primary mirror	2.4-meter (94-inch) diameter
Primary *f* number	2.3
System *f* number	24
Angular resolution	0.1 second of arc
Spectral range	115 nanometers to 1 millimeter
Encircled energy	60 percent at 0.15-second-of-arc diameter
System wavefront error	$\lambda/20$ at 632.8 nanometers (λ = wavelength)
Spacecraft stability	0.007 second of arc
Weight (typical)	6800 kilograms (15 000 pounds)
Length (typical)	13 meters (44 feet)
Diameter (typical)	4.3 meters (14 feet)

With the current designs, we are able to maintain a healthy engineering margin without incurrence of significant additional cost. For example, we have a design target of $\lambda/20$ for the overall wavefront error at the focal plane of the OTA. The image quality available to the SI is affected both by the intrinsic optical quality of the system and the ability of the spacecraft control subsystem to stabilize the optical axis of the system during an observation. We have set a design target of 0.007 second-of-arc stabilization for the spacecraft. With an OTA wavefront error of $\lambda/20$ and stabilization of 0.007 second of arc, the minimum scientific performance of encircled energy of 60 percent at 0.15-second-of-arc diameter (which relates to the profile of the point-spread

function of a stellar image) is met with reasonable margin. The encircled energy criterion still can be achieved if the telescope performance is reduced to $\lambda/14$ and the stabilization is reduced to 0.010 second of arc. Furthermore, if the optical performance is maintained at $\lambda/20$, the spacecraft could drop to 0.02 second of arc and the encircled energy performance criterion would still be met. Margins such as this are necessary in definition of the system to provide assurance of cost and schedule predictions. During the execution phase of a program, when hardware is being manufactured and tested, margins can prove to be the salvation in preventing delays and associated cost overruns when the manpower being applied to the program is near its peak.

We have been working actively with the European Space Agency (ESA) concerning their potential commitment to the Space Telescope. They have expressed potential interest in providing an SI and associated detector, furnishing the solar array and possibly other elements of the SSM power subsystem, and in supporting Space Telescope operations. Other areas of involvement are also under consideration by ESA. The Europeans will make a preliminary decision next month concerning their participation. ESA will be compensated for its contributions to the program by a share of total observing time no less than the fraction of the cost of the total project which ESA contributes in areas of mutual interest. A detailed working agreement concerning NASA/ESA Space Telescope cooperation has been drafted.

During the balance of the phase B effort, particularly in the second half of the SSM contracts, interfaces between the various elements of the Space Telescope system will be better defined. There is a number of interfaces to be resolved, including the Space Telescope to Space Shuttle interfaces, the Space Telescope to the Tracking and Data Relay Satellite System communications interface, the OTA to SSM interface, physical/optical interfaces between the SI and the OTA, and power and data interfaces to the SSM. The Space Telescope project will be making a number of interface decisions by October 1, based primarily on the technical material provided in the recent design reviews by the two OTA/SI phase B contractors and the three SSM phase B contractors. These interfaces are defined in general terms, but they will be "hardened up" in preparing final specifications for the development phase.

We do not anticipate that the basic designs of the OTA or SSM will change significantly during the balance of the definition phase. The Space Telescope systems engineering and integration will be emphasized. Particular attention will be devoted to test and integration planning. Of course, costs will continue to receive prominent attention. Costs will be of key importance in all decisions that are made. The balance of phase B will be mainly a "fine tuning" of presently available information and updating of cost and schedule estimates. We do not believe that the Space Telescope design, program plans, or cost estimates will change significantly.

It is our plan to initiate the Space Telescope development phase with performance-type specifications indicating requirements, not design solutions.

However, the RFP's for the development phase will include detailed interface specifications that will form the boundary conditions for the various elements of the Space Telescope system. It is our intention to procure the lowest cost system that will provide acceptable performance. Furthermore, we will be willing to trade performance for cost, particularly in areas where significant cost savings can be realized. We are wary of proposed sophisticated solutions and complex designs. If one is considering a trade between sophistication and performance versus simplicity and somewhat reduced performance, it is usually prudent to adopt the simpler approach. Also, flight-proven components and subsystems and standard components will be used whenever practical. Use of space-proven equipment is doubly beneficial by reducing both development cost and performance risk.

CONCLUSION

The technology and advanced development work to assure the success of the Space Telescope program has been accomplished and demonstrated. The Space Telescope system, as presently defined with the 2.4-meter (94-inch) primary mirror, meets scientific requirements. Appropriate engineering margins with this design are available. The exceptionally long and thorough definition phase, which will be completed in March 1976, will provide high confidence in the reasonableness and appropriateness of design approaches, specification requirements, and cost estimates. We are certain that all program objectives can and will be achieved.

SCIENTIFIC INSTRUMENTS

George M. Levin
NASA Goddard Space Flight Center

The Space Telescope scientific instruments (SI) represent a unique design challenge. The Space Telescope is to be a permanent national astronomical space observatory. SI for the spacecraft are being designed as facility instrumentation that will be replaceable during the life of the observatory. To reduce the down time of the Space Telescope, the instruments are being designed for manned onboard serviceability. The SI must be capable of serving the broader needs of the astronomical community.

These basic mission requirements have been translated into specific design approaches. The Space Telescope focal plane assembly is configured around standard SI modules. Each module contains one SI. The thermal, electrical, mechanical, and data interfaces between all modules and the focal plane assembly are identical. Figures 1 and 2 show the two concepts of the focal plane assembly under study. Each concept has four standard axial SI modules that share the light in the focal plane.

At present, there are seven SI under design for the first Space Telescope mission. These are the *f*/24 field camera, the *f*/48 and *f*/96 planetary camera, the high-resolution spectrograph, the faint object spectrograph, the infrared photometer, the high-speed point/area photometer, and the astrometer.

f/24 FIELD CAMERA

The design of the *f*/24 field camera is geared toward the study of faint extended and point sources, and for search and survey work. The instrument system is designed so that the *f*/24 field camera can be operated simultaneously with the other scientific instruments.

The *f*/24 field camera (fig. 3) consists of the 70-millimeter Secondary Electron Conduction Orthicon (SECO) camera submodule, a 1:1 relay, filter assembly, standard star calibration system, internal source calibration system, and capping shutter assembly. These subsystems are mounted on an optical bench in the SI module. The optics are housed in a forward bay that is enclosed with a thermal shroud whose temperature is thermostatically controlled. The SECO is mounted to the optical bench in an aft bay. The aft bay has a thermal reflector to increase the view factor of the SECO submodule to the outer wall of the instrument module.

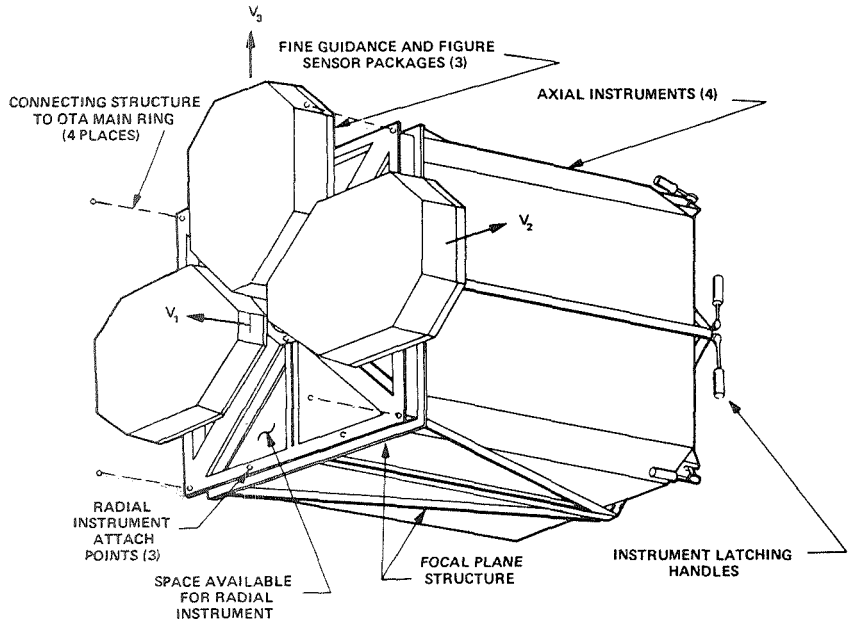

Figure 1.–Focal plane assembly, concept 1. (OTA = optical telescope assembly.)

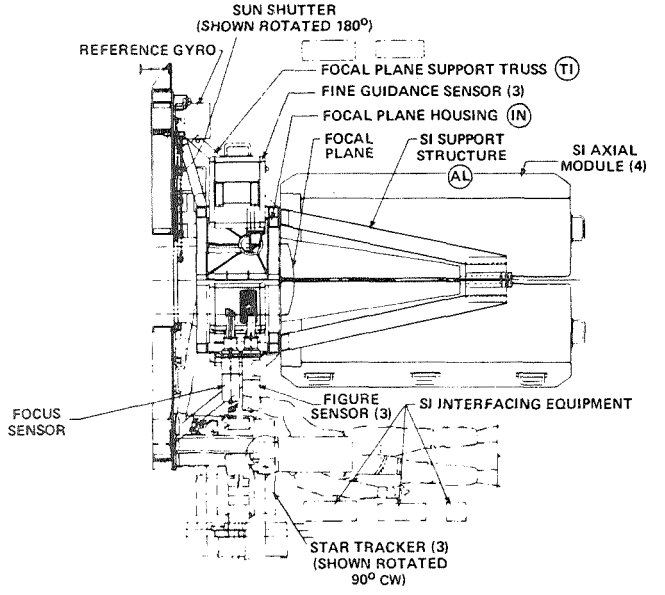

Figure 2.–Focal plane assembly, concept 2.

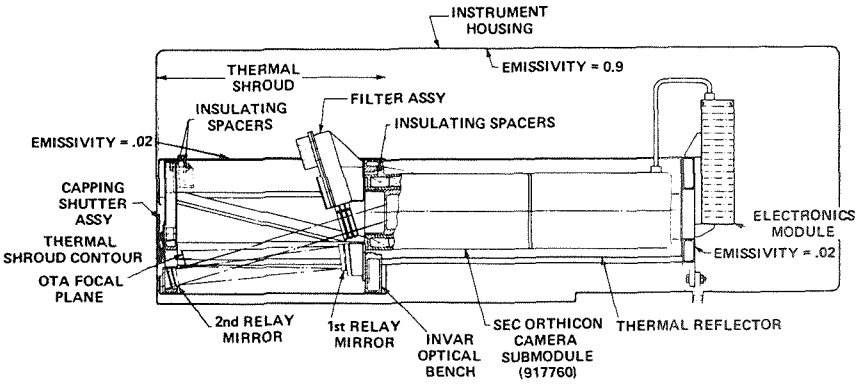

Figure 3.–*f*/24 field camera.

f/48 AND *f*/96 PLANETARY CAMERA

The design of the *f*/48 and *f*/96 planetary camera is primarily for the study of imaging photometry at high angular resolution for high surface brightness or multiple bright sources. The planetary camera (fig. 4) has an optical system with two selectable focal lengths imaging on a charge-coupled device detector cooled to -40° C. The optical system consists of two independent, two-mirror relays nested together in such a way as to have two separate entrance apertures in the focal plane and a common output focal plane. Switching between the relays is accomplished by means of a multiposition capping shutter.

The wavelength range of the planetary camera is from 180 to 1200 nanometers. The field of view at *f*/48 and *f*/96 is 17 by 17 and 8 by 8 seconds of arc, respectively. The camera is to have 0.1-second-of-arc resolution at *f*/48 and to be diffraction limited at *f*/96.

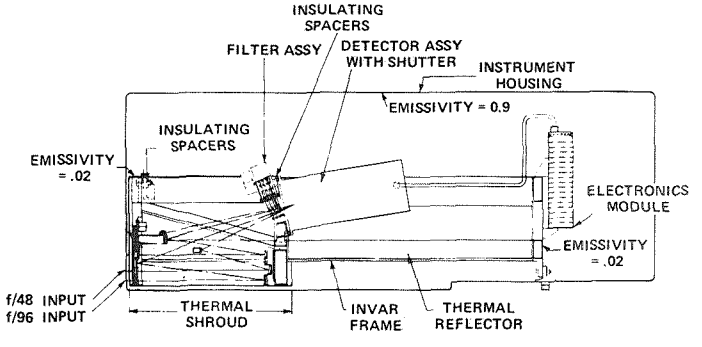

Figure 4.–*f*/48 and *f*/96 planetary camera.

HIGH-RESOLUTION SPECTROGRAPH

The high-resolution spectrograph is designed for use in imaging spectroscopy of point or extended sources. The instrument (fig. 5) consists of interchangeable slits, a collimator, interchangeable echelles and first-order gratings, interchangeable cross-dispersers, detector selector and compensator for orbital-velocity doppler shifts, and two SEC Orthicon camera submodules. The principal operating mode of the high-resolution spectrograph is as an echelle spectrograph with spectral resolution of 3×10^4 and 1.2×10^5. A secondary spectral resolution of 10^3 was also specified. The wavelength range of the design is from 115 to 410 nanometers. This wavelength range is divided such that the first SECO camera (with a CsI photocathode and a MgF_2 window) covers 115 to 170 nanometers and the second SECO camera (with a bialkali photocathode and an SiO_2 window) covers 170 to 410 nanometers.

FAINT OBJECT SPECTROGRAPH

The faint object spectrograph is a composite instrument covering a broad spectral range and intended for imaging spectroscopy at moderate resolving power. Both point, or stellar, and extended sources are to be observed. Time variations, spectral profiles of broad emission and absorption features, and continuum flux distributions are to be measured for primarily faint targets.

The main components of the faint object spectrograph (fig. 6) are gratings used in a Wadsworth mount, three intensified-charge-coupled device camera submodules, a collimator, an image slicer, a slit jaw camera, and a spectral reference source. The wavelength range is from 90 to 800 nanometers. It is

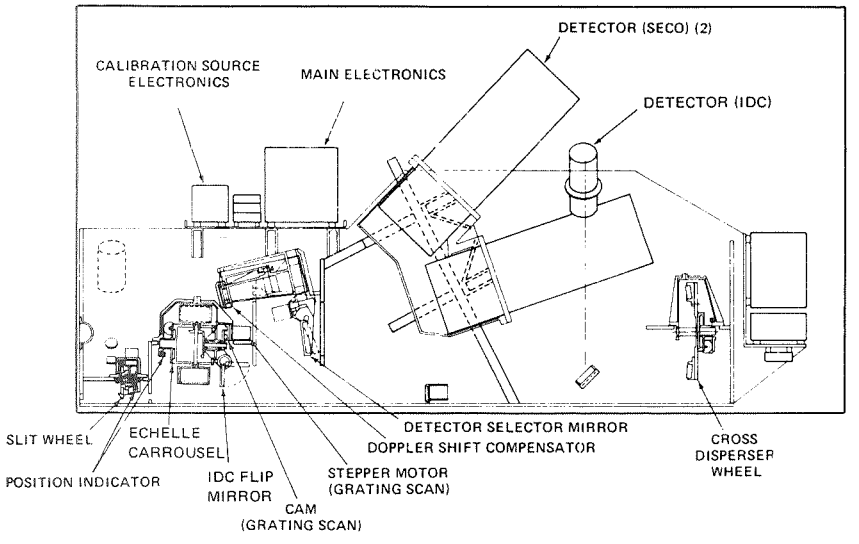

Figure 5.–High-resolution spectrograph. (IDC = image dissecting camera.)

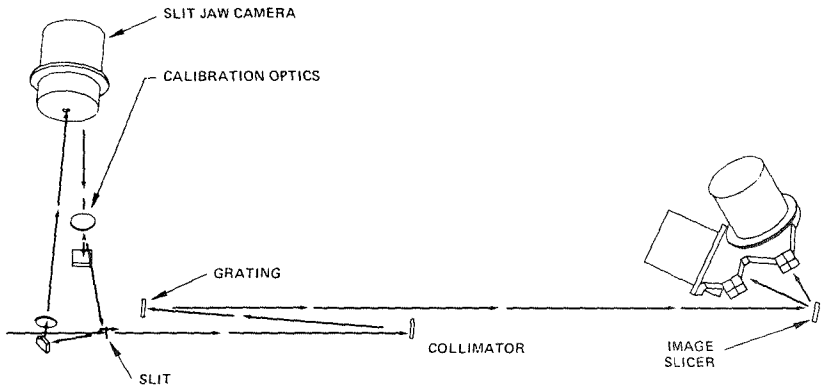

Figure 6.–Faint object spectrograph.

divided into three regions. The first is from 90 to 190 nanometers, and its intensified-charge-coupled device camera has a CsI photocathode and a MgF_2 window. The second region covers the range from 180 to 400 nanometers and has a bialkali photocathode and SiO_2 window. The third covers the range from 380 to 800 nanometers and has an S-25 photocathode and an SiO_2 window.

INFRARED PHOTOMETER

The infrared photometer is primarily intended for use in the photometry of point or extended sources in mid- and far-infrared wavelengths. By commanding the telescope to move in a prescribed systematic manner, the photometer can scan a particular area of scientific interest. When scanning, the photometer can determine the surface brightness of infrared sources. In addition, the photometer can accurately determine the position of new infrared sources by scanning the area surrounding a nominal spacecraft pointing and determine the location of the peak signal.

Background-limited performance requires detector cooling to less than the lambda point of He; i.e., 2.2 K. In addition, offset signals caused by background must be suppressed. Cryogen life and dewar design are significant design drivers of the infrared photometer.

The infrared photometer concept (fig. 7) is based on the use of superfluid helium to achieve the necessary detector cooling. A focal plane chopper provides the required background suppression. Cooled apertures matched to the diffraction size of the beam and cooled field mirrors provide the remaining background suppression. Multiple apertures and filters along with a beamsplitter provide instrument flexibility. In certain target cases, acquisition is handled in a special peak-up mode to determine the largest signal magnitudes encountered during the scan. Using the results of this determination, the telescope is automatically commanded to the new pointing.

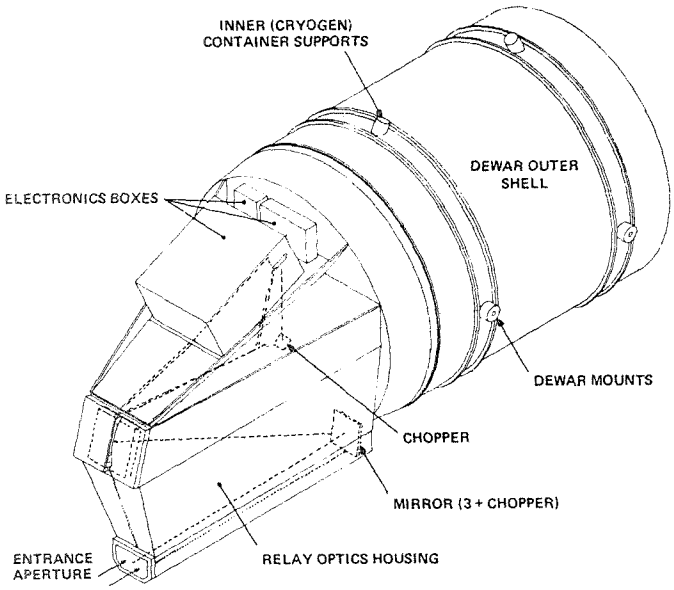

Figure 7.–Infrared photometer.

The general arrangement and construction of the dewar and relay optics are shown isometrically. The system consists of three separable modules: the dewar, the instrument mounted within the dewar, and the external optics assembly. The electronics are mounted on the optics housing but are thermally isolated.

The dewar outer shell and relay optics will be at, or near, ambient container temperatures. The chopper and electronics will be above ambient temperature. The optical relay system will be sensitive to temperature gradients that may cause bending misalinement; however, it will not be very sensitive to the uniform temperature level. To preclude temperature gradients, it will be necessary to thermally insulate the heat-producing elements such as the electronics from the structure and provide means to transfer this energy to the SI container. Low-power heaters and insulation may be necessary on the optical housing to control gradients under various operating conditions.

The entrance aperture will require a cover to preclude contamination. As a minimum, a removable aperture cover for use during ground handling will be necessary.

HIGH-SPEED POINT/AREA PHOTOMETER

The basic utility of an ultraviolet-visible photometer operating in a photon-counting mode with an optional analog mode capability is its capability to obtain precise measure of the constant or time variable intensities over a wide

dynamic range of astronomical signal strengths. The data collected can be from either point sources or celestial fields of small angular size. Such a photometer makes feasible a variety of observing programs extracting the maximum information content possible. In addition, high time resolution and flexible sequencing allow observations of a variety of unusual time-related phenomena.

The first element of the high-speed point/area photometer is the contamination door, which is used to exclude contaminants during prelaunch, launch, return, and maintenance operations and is used as backup to the shutter, which is next in reaction time and can quickly shut out unwanted incoming light in the case of inadvertent acquisition of a source whose intensity is bright enough to damage the sensors (fig. 8).

An aperture wheel assembly is mounted at the telescope *f*/24 focus and provides selectable field stops. The two filter wheels follow the aperture wheel assembly. These filter wheels provide spectral bandpass discrimination. The next element is the primary mirror carrousel. The carrousel contains space for mirrors on each of the six sides of the turret. Four of these are used, one each for the two point detectors, and one each for the *f*/24 and *f*/96 images. Each of the mirrors is figured for the optical system in which it functions and is so placed on the carrousel to direct the beam to the desired detector or secondary mirror. The two point detectors receive their input from primary mirrors on the carrousel and are mounted to the bench rods, receiving their input from the primary mirrors on the carrousel. They, in turn, direct the beam to the area detector forming images at *f*/24 and *f*/96.

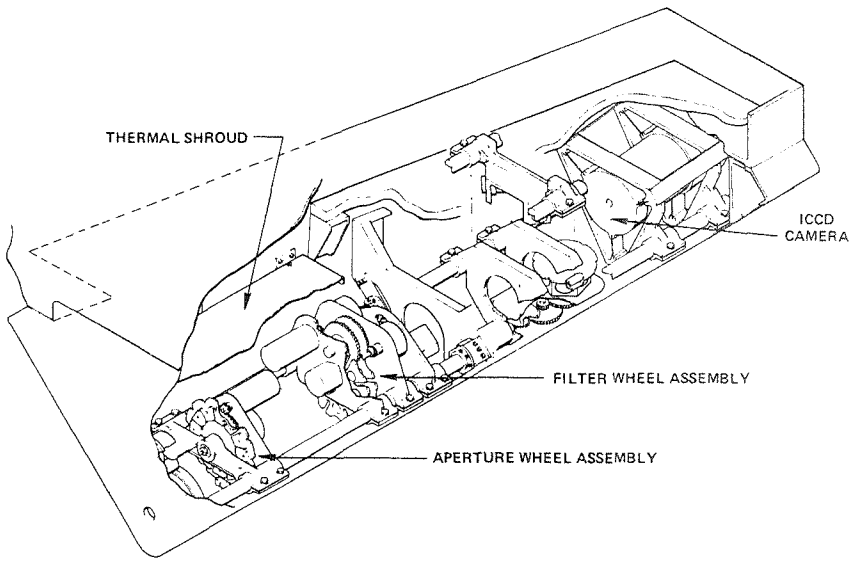

Figure 8.–High-speed point/area photometer. (ICCD = intensified-charge-coupled device.)

The final element is the intensified-charge-coupled device area detector. Mounted to the optical bench rods, it connects through a flexible thermally conductive copper web strap to a radiator.

Graphite epoxy is used for the optical bench rods to minimize thermal deformation. The rods are supported at midpoint and aft end on flexures to allow only minimal stress to be induced in the rods from deformation of the shell.

ASTROMETER

The astrometer is designed to measure parallaxes and proper motions 10 times more accurately than is presently possible, to measure angular diameters for stars and the nuclei of galaxies, and to determine individual masses through observations for about 100 spectroscopic binaries.

Wide-field astrometry for studies of parallax and proper motions requires a wide field of view (effective area equivalent), uniform image quality (over that effective area), stable positional accuracy within the field of view (±0.002 second relative to other objects in the field of view), and occasional serendipitous operation regardless of which instrument is prime. Narrow-field astrometry for single stars and close double stars requires high angular resolution (diffraction limited) and high time resolution (100 microseconds ±2 percent).

Two different concepts of astrometry instrumentation are under study. In the first concept, a modified multiplex area scanner (fig. 9) is employed for the wide-field studies. The high-resolution camera and the area photometer may also be used to supplement and expand the capabilities of the astrometric multiplexing area scanner for astrometric measurements.

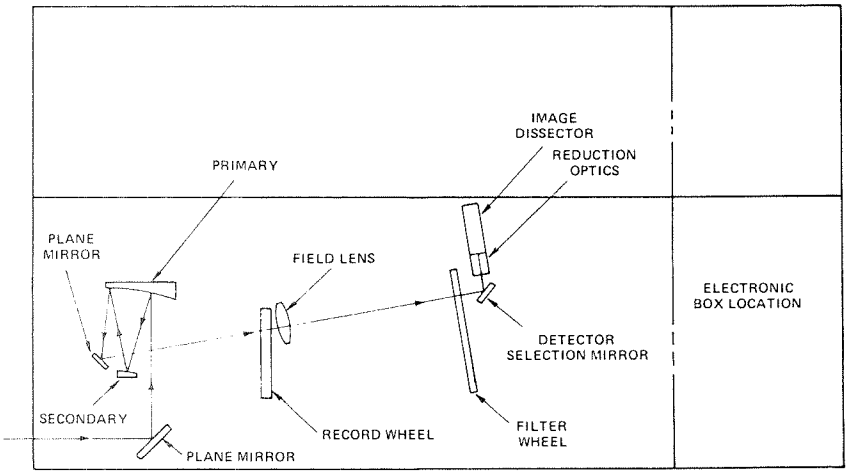

Figure 9.–Astrometer (astrometric multiplexing area scanner) optical schematic.

In the second concept, the fine guidance system for the optical telescope assembly is used for wide-field measurements. This fine guidance system is modified to include a high-performance reticle. For narrow-field astrometry, the fine guidance system software is modified to include the necessary multi-target search and measure routines as well as handling the encoded signals as data. The high-resolution camera and the area photometer are used for astrometric measurements.

1

Mission Analysis and Operations

SCIENTIFIC OPERATION PLAN

Donald K. West
NASA Goddard Space Flight Center

A Space Telescope Science Institute has been proposed for the Space Telescope. If this Science Institute is adopted by NASA, it will be responsible for proposal selection, telescope time schedules, science planning, and the implementation of investigator's programs. Guest investigators as well as principal investigators' will normally come to the Institute to perform their astronomical observations. During an observing run, the investigator will participate in the verification of the observing plan, real-time target acquisition, the analysis of quick-look data, changes to the observing plan, and the specification of data reduction procedures. Data processing is performed to the user's specification to the point where scientific judgment is required. At this point, the data are given to the user in the form and format of his choice for scientific analysis.

The purpose of this paper is to describe a Space Telescope ground system that is compatible with the operational requirements of the Space Telescope. The goal of this approach to the ground system is to minimize the cost of postlaunch operations without seriously compromising the quality and total throughput of Space Telescope science. The resulting system is able to accomplish this goal through optimum use of existing and planned resources and institutional facilities.

REQUIREMENTS

Mission and data operations conceptual studies for the Space Telescope have been completed at Goddard Space Flight Center. The results of these studies showed that all of the mission operations requirements could be met through the slightly modified use of hardware and software resources developed for the Orbiting Astronomical Observatory. Scientific operational requirements, however, call for the development of new resources in three areas.

The first of these new requirements involves the development and operation of a scheduling and science planning system for the guest investigators. The support requires sophisticated hardware and software systems to accomplish long-range observatory scheduling and science planning.

The second new requirement concerns the real-time operation of the scientific instruments and spacecraft pointing control system to accomplish

closed-loop-to-ground target acquisition and positioning in the scientific instruments apertures. Extended real-time contact periods and ground target acquisition systems are needed to meet this new requirement.

The third and most demanding new requirement is in science data management. The Space Telescope will transmit several images per orbit that will require preprocessing and image processing of millions of data points per day. Preprocessing of raw telemetry data is needed to sort out the science data and output it in a format suitable for data reduction tasks, such as image processing. Processing of 10^9 bits per day is a Space Telescope requirement that identified the need for a significant new resource.

COST CONSTRAINTS AND GUIDELINES

Ultimately, a Space Telescope Science Institute will desire autonomous dedicated computer facilities to maximize the scientific flexibility and data throughput in the planning of observations and the final science data processing and analysis.

The Goddard Space Flight Center (GSFC) has identified a scientific operations solution that will meet the Space Telescope requirements within the limits of current cost ceilings. The plan is centered on sharing existing and planned data facilities at Goddard with the Space Telescope program. The hardware and software facilities identified for the Space Telescope have broad data handling and processing capability extending well beyond the requirements.

To develop a completely viable Space Telescope ground system that will effectively interface the Science Institute with the Mission Operations Center (MOC) and the GSFC shared facilities, it is necessary to define the following set of system guidelines:

(1) The Mission Operations Center will be located at Goddard Space Flight Center.
(2) The Space Telescope Science Institute will be located at Goddard or a part of its operational staff will be colocated at Goddard.
(3) Raw data will be acquired, stored, and preprocessed by the Telemetry Operations Processing System (TELOPS).
(4) Routine image processing hardware and system software is to be provided by the GSFC Image Processing Facility.
(5) The Science Institute will be responsible for providing scientific applications programs and calibration data for image processing to the Image Processing Facility.
(6) Custom data processing is to be done by the Science Institute.

IDENTIFICATION OF NEW RESOURCES

Following the above cost constraints and ground system design guidelines, a study of existing and planned resources was performed. The results of this

study revealed that most of the Space Telescope's requirements could be met by observational and data processing software and hardware resources currently in development at GSFC. These facilities will be fully operational several years prior to launch of the Space Telescope and can be made available to the Space Telescope program if their effective use can be assured. The effective use of these shared facilities is strongly dependent on the proximity of the user. Three distinct resources have been identified.

(1) The International Ultraviolet Explorer is an international space observatory that will host at least 50 guest observers per year. Software and hardware for long-range guest observer scheduling and real-time target acquisition systems are currently being developed for a 1977 launch. These International Ultraviolet Explorer systems are ideally matched with Space Telescope requirements for guest observer support and real-time closed-loop-to-ground target acquisition.

(2) The Space Telescope requirements for the preprocessing of 10^9 bits per day of science data can be satisfied by using the Telemetry Operations Processing System. This system, currently being built at Goddard, is sized to handle data volume and preprocessing requirements several orders of magnitude greater than those of the Space Telescope.

(3) The Image Processing Facility under development at Goddard is a large-scale computer system that will process up to 2×10^{11} image bits per day. In addition, the Image Processing Facility is able to accommodate the scientists' need for making changes in calibration data sets, scientific algorithms, and applications programs.

TELEMETRY OPERATIONS PROCESSING SYSTEM

The Telemetry Operations Processing System serves as an online digital interface between the Spacecraft Tracking Data Network (STDN) and the Space Telescope ground system. It provides spacecraft and user support in near real-time with a storage and processing capacity to handle large volumes of data. The features of the system include data capture, data staging, data editing, rapid access online storage, off-line data archival, 24 hour and 7 day per week operation, and a fail-safe protect system. System capacity characteristics are online data input from the Spacecraft Tracking Data Network on 22 lines simultaneously, 20 lines with a bit rate up to 108 000 bits per second each, combined peak rate of up to 2.6 million bits per second, processing capacity of 450 million data points per day, and online storage of 169 billion bytes.

IMAGE PROCESSING FACILITY

The general function of the Image Processing Facility is to provide standard image processing support to users. Image processing functions include

preprocessing, annotation and guiding, radiometric calibration, geometric corrections, editing, data merging, reformatting, product generation, near real-time transmission, enhancement, and differencing. Geometric corrections are performed on the basis of image correction data and reference control points (relative or absolute). The primary purpose of geometric corrections is temporal registration of data. Algorithms are resampled using nearest neighbor and sin x/x approximation (at least cubic). The processing volume is 10^{11} bits per 16 hours, and input-output is in the form of high-density tapes or general computer-compatible tapes.

GROUND SYSTEM PLANNING AND DATA FLOW

The major functional elements that will make up the Space Telescope ground system are shown in figure 1. Those elements that will provide institutional support services to the Space Telescope are shaded. The Mission Operations Center and the proposed Science Institute will contain all the elements dedicated to the Space Telescope.

An observation request will originate with the principal or guest investigators in the form of target coordinates, time and duration of observations, measurement accuracy, and instrument configuration. The planning computer receives observing plans from the Science Institute via terminals, punched card, or tape input. Mission control inputs current spacecraft constraints to the planning computer, which translates the observing plan into 24 hours of Space Telescope commands. This command message will be approved by the Mission Operations Center for transmission to the Space Telescope via the Spacecraft

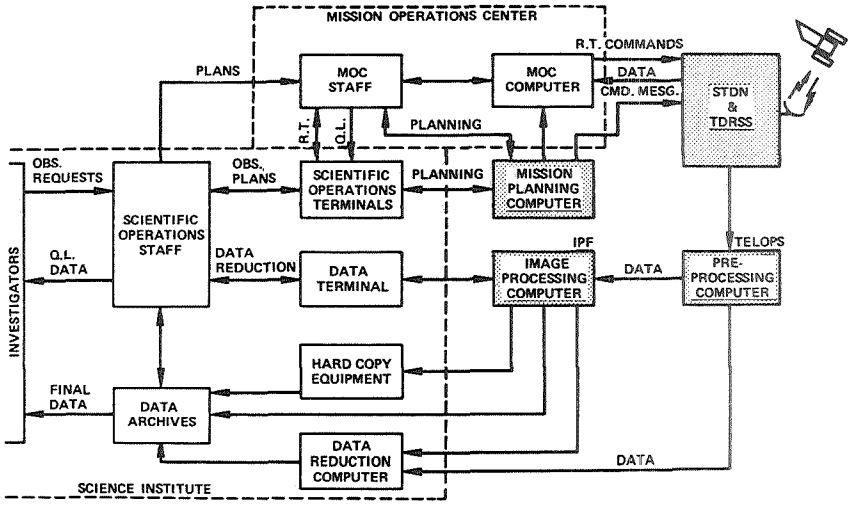

Figure 1.–Ground system interfaces. (Q.L. = quick look; R.T. = real time.)

Tracking Data Network (Tracking and Data Relay Satellite System (TDRSS)). Real-time operation, such as target acquisition, will be accomplished by direct command of the Space Telescope by the Mission Operations Center computer in response to requests from terminals in the Mission Operations Center and the Science Institute.

The Space Telescope transmits science and engineering data that will be relayed by the Spacecraft Tracking Data Network to the Mission Operations Center and the Telemetry Operations Processing System at GSFC. Engineering data are available in the Mission Operations Center for spacecraft monitoring and analysis. Science data in quick-look form will be available to the users in the Science Institute by the Mission Operations Control computer or the Telemetry Operations Processing System. The Telemetry Operations Processing System receives, stores, and preprocesses large quantitites of science data for image processing by the Image Processing Facility, which will then output the reduced data to the Science Institute. Final data reduction and products will be processed to the point where scientific analysis is required. Reduced data are given to the user for his analysis and to the National Space Science Data Center for timely distribution to the general scientific community.

SCIENTIFIC INTERFACES

The question of how guest astronomers interface with the Space Telescope is a central one. Staff astronomers, night assistants, and technicians will assist guest astronomers in the daily functions: specification of target sequences, target acquisition, identification, and slit monitoring; scientific instrument command requirements and operation in real-time and stored command memory mode; the specification and evaluation of all science and instrument engineering data processing and its storage and distribution; the specification and requirement development for all science operation ground support hardware and software systems and changes; and the maintenance of instrument calibration and image processing data sets, programs, and algorithms.

The interface between astronomers and the Space Telescope in orbit is the planning computer. Standard computer terminals will be used to initiate programs on the planning computer. Similar interactive display/control computer terminals will interface with the operations (command-control) computer in the Mission Operations Center for real-time operation.

The interface between astronomers and the data processing facility will be standardized and predefined in terms of the number and type of data reduction processes available and in the types of output and formats available to the user for his analysis. The user will have the capability of reviewing scientific data in condensed (quick-look) form prior to image processing. This interface will also allow the timely update of scientific algorithms, applications programs, and calibration data.

FUTURE DEVELOPMENT

This scientific operations plan was developed to meet the immediate requirements of the Space Telescope within the prelaunch budgetary constraints. The plan described here not only accomplishes this goal but, in addition, contains modular design concepts that offer considerable flexibility for future development of facilities dedicated to the Space Telescope.

SPACE TELESCOPE OPERATIONS, A TYPICAL DAY

William J. Pragluski and Robert H. Brown
Martin Marietta Corp.

The development of operational time lines provides visibility between the degree to which science objectives of the Space Telescope mission can be achieved and realistic design requirements on the flight and operations systems. The mission time line presented here encompasses approximately 3 weeks of mission time corresponding to a point in the mission after the initial in-orbit checkout of the Space Telescope. The over 300 orbits of time line using several target types makes possible a statistical approach to evaluating the Space Telescope design requirements and their impact on science mission design flexibility.

The results of this analysis demonstrate the significant contribution the Space Telescope can make in the science of astronomy. It can not only provide new, fundamental data on the nature of the universe, but it will also provide more accurate data on the yardsticks used in virtually all astronomical analyses.

SCIENCE OBJECTIVES

Cosmology is high on the list of priorities. The Space Telescope's light-gathering potential allows the observation of targets over five magnitudes dimmer than possible from the surface of Earth. This allows taking direct measurements at a distance where the many theories on the nature of the universe (i.e., flat and infinite, curved space, closed) and its origin result in theoretically different results.

Precise measurements of interstellar medium, binary stars, and stellar parallaxes will provide far more accurate data on the abundance of mass in the universe and the relationship between the target's stellar characteristics and the relative distances in space. These yardsticks are fundamental in properly interpreting the data gathered by all telescopes, both orbiting and on Earth's surface.

The Space Telescope can also make significant contributions to solar system astronomy. It cannot compete with highly sophisticated spacecraft of the Viking type that can take in situ measurements, but it will provide considerable data on the outer planets and comets that equal the quality and quantity of the data from precursors of the Pioneer type.

MISSION OPERATIONS PROFILE

A time line for mission operations and typical instrument usage sequences is simulated to determine the data quantity performance of the Space Telescope. The event times and standardized presentation plots for the mission operations profile are generated by a time line computer program. The time line program includes an ephemeris generator and a set of routines to calculate the event times shown for orbital day/night cycles, sidereal revolution numbers, viewing of representative science targets (constrained by Sun, Moon, Earth, and stray light), South Atlantic Anomaly encounters, target slewing maneuvers, and ground station to Tracking and Data Relay Satellite contacts.

COMMAND AND DATA OPERATIONS SUMMARY

Several operations profile segments have been developed and are representative of integrated science sequences that could be used during the Space Telescope operational mission phase. Analysis of the information presented by these profiles furnishes summary statistics related to uplink command storage volumes and science data quantity.

Command Storage

The Space Telescope is being designed as an autonomous, on-orbit operations system for periods of up to 24 hours. The onboard Data Management Subsystem has the responsibility for receipt, storage, and dissemination of commands for the subsequent automatic execution. These time-tagged commands are generated in the Mission Control Center and uplinked periodically to the Space Telescope via the Tracking and Data Relay Satellite System. Requirements are, therefore, established for ground generation and onboard storage systems to accommodate the command volume required for the scientific operations of the Space Telescope.

The scientific instrument and supporting subsystem command requirements for a 24-hour period depend upon the particular observation sequence performed. The previously mentioned operation profile segments have been evaluated for determination of command requirements. The data of figure 1 present the results of these evaluations.

The command storage volumes were determined on an orbit-by-orbit basis for the various profile segments. The number of orbits requiring particular volumes of commands are plotted versus the volume of commands (fig. 1). The distribution indicates three distinct groupings. The first grouping is the result of long exposures where the commands required per orbit are low. The second grouping represents orbits in which the exposure times are short, several frames of science data are taken, and many commands are required. The third grouping is representative of the initial operational checkout phase where an extremely large number of data frames are taken per orbit, and even larger volumes of commands are required. The volume of commands required on a

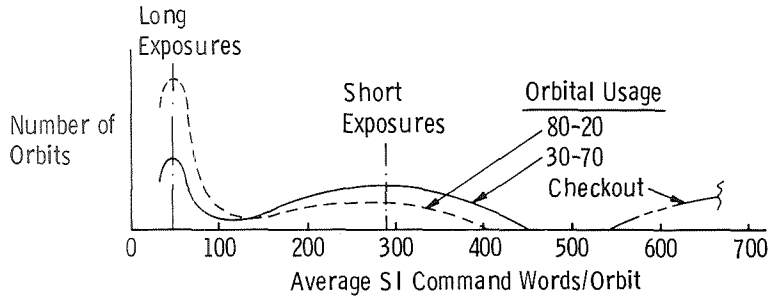

Figure 1.–Typical command storage distribution. (SI = scientific instrument.)

daily basis is a result of the number of orbits requiring long exposures versus those requiring short exposures for data acquisition. This relationship is referred to as the orbital usage percentage. The standard planning cycle for the Space Telescope would suggest equal probabilities of the orbital usage being anywhere between a 10 to 90 relationship (extensive calibration segments) and a 90 to 10 relationship (extensive observations of faint objects). The scientific instrument checkout usage is a special case that approaches a 0 to 100 relationship.

The data of this figure indicate mean values for long-, short-, and checkout-exposure distributions. The long-exposure commands have minimum impact on daily command storage requirements. The short-exposure mean is the predominate factor in the derivation of a 24-hour requirement for the operational mission. This factor, when combined with orbital usage considerations, has resulted in a recommended daily storage capability of 1500 words. The checkout usage mean places a two-orbit requirement on command storage. The data of this figure show that the recommended 1500-word storage capability is satisfactory for accomplishment of two orbits of science instrument checkout exposures.

Science Data Quantity

Scientific data quantities, in terms of data bits and data frames, are also dependent upon the particular observation sequence being performed. The various profile segments were again evaluated on an orbit-by-orbit basis to derive these quantities for the orbital usage relationships. The data of figure 2 show bit volume ranges per orbit for long-exposure and short-exposure data frames. The trends of these data curves in the short-exposure range show only minor variations with orbital usage. The apparently large deviation in the long-exposure range is caused by a difference in downlinking philosophies. Onboard instrument detector integration over multiorbits was assumed on the 80 to 20 orbital usage profile segment, whereas ground integration on an orbit-by-orbit basis was assumed on the 30 to 70 orbital usage segment. Both

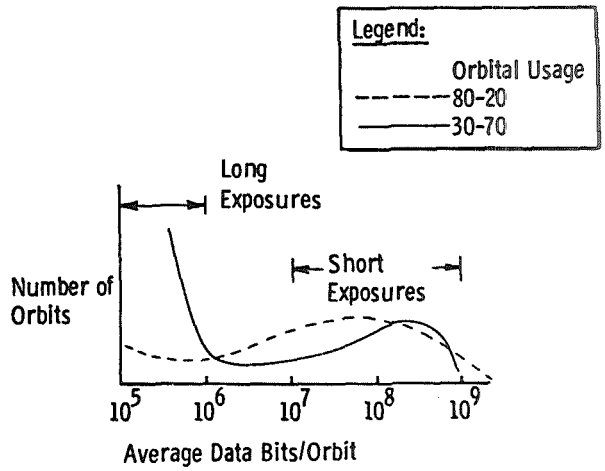

Figure 2.–Typical science data bit distribution.

procedures are viable candidates for Space Telescope operations. An accumulation of scientific data bits from the various profile segments shows an overall average for recorded and downlinked data of 2.8×10^9 bits per day and a maximum of 3.7×10^9 bits per day.

The distribution of individual science instrument frames, based on the accumulation of data from the various profiles, is presented by the data of table 1. This distribution shows that the instrument usage being planned for

TABLE 1.–*Space Telescope Science Objectives Summary*

Scientific instrument	Percent of frames	Field of contribution to science objectives
f/24 field camera	36	Cosmology, extragalactic studies, young and binary stars, stellar parallaxes, and the solar system
Faint object spectrograph	24	Cosmology, extragalactic studies, quasars, the interstellar medium, and binary and old stars
High-speed point/area photometer	22	Cosmology, quasars, stellar parallaxes, and old stars
Infrared photometer	16	Extragalactic studies, young stars, and the solar system
High-resolution spectrograph	2	Quasars, the interstellar medium, young stars, and the solar system
Astrometer	–	Binary stars and stellar parallaxes
f/48 and *f*/96 planetary camera	–	Quasars and the solar system

the Space Telescope will furnish data for significant contributions to the field of astronomy.

CONCLUSIONS

The time line developed in this paper demonstrates that the Space Telescope, with a cost-effective payload of scientific instruments, can perform a wide variety of astronomy experiments. With careful mission planning, its use (i.e., useful science time per orbit) will be high, allowing it to support a large segment of the astronomical community in a timely fashion. In addition, it can perform this mission without demanding excessively expensive requirements on either the flight hardware design or the operations system.

MISSION ANALYSIS

Frank M. Friedlaender
Lockheed Missiles & Space Co., Inc.

The Space Telescope will be one of the first large scientific payloads to be launched and supported by the Space Shuttle. This payload will have a 2.4-meter (94-inch) diameter, near-diffraction-limited mirror in conjunction with four interchangeable instruments. The current family of instruments from which these four instruments will be selected for the initial launch in 1982 consists of an *f*/24 field camera, faint object spectrograph, high-speed point/area photometer, infrared photometer, *f*/48 and *f*/96 planetary camera, astrometer, and high-resolution spectrograph. The Space Telescope is designed for long-duration operation with periodic maintenance and refurbishment cycles after extended observational periods.

The instrument complement can be changed for any specific observation period, and allows measurements from 120 nanometers in the ultraviolet to 1 millimeter in the infrared. The interchangeability of instruments as well as of other spacecraft components provides this observatory with long-term capability. Maintenance can be performed in orbit with support of the Space Shuttle, or, using the Space Shuttle as the transporter, major refurbishment can be accomplished on the ground.

This Earth-orbiting observatory will open a new era of astronomy because it can see 7 times farther and 350 times as much volume as the best ground-based telescope. It also has 10 times better resolution and 10 times the frequency spectrum of ground-based systems. It is this greatly expanded astronomical capability in conjunction with the environmental constraints imposed by an orbital observatory that provides the mission planner with a unique challenge.

SCIENTIFIC OPERATIONS

The planning for scientific observation is shown in figure 1 and contains both a long-term and short-term sequence. The long-term sequence is performed several months prior to the observations, and the short-term sequence is performed just days prior to the observation. The interaction of the targets, instruments, observation time frame, and environment provide the ingredients that make up the fabric of each experiment. Each experiment, in turn, consists of a target and one or more instruments operating in a number of

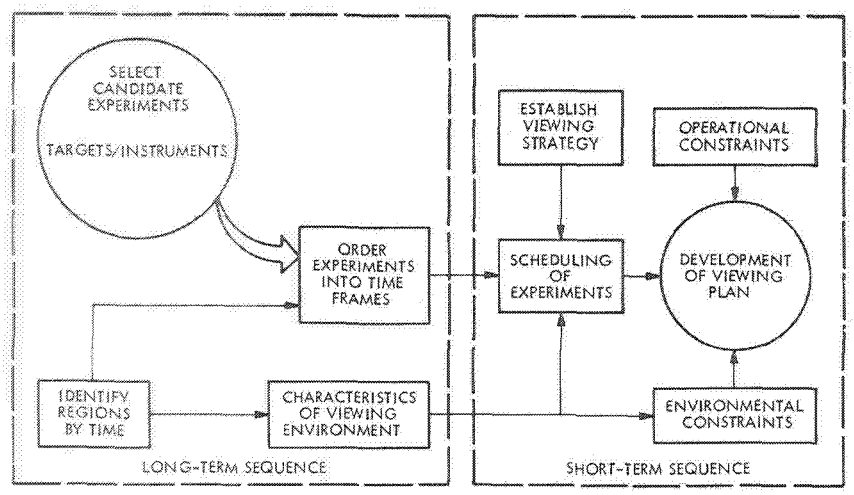

Figure 1.–Science observation planning sequence.

modes. As part of the long-term planning sequence, the optimum time must be chosen to conduct the experiment, with consideration given to both the time of year and the environment. The environment includes background phenomena such as zodiacal light and integrated starlight radiance, proximity to bright objects, passage through the South Atlantic Anomaly, and whether the observation is in sunlight or in Earth's shadow.

SUPPORT OPERATIONS

Although the scientific mission operation phase is the key mission phase in satisfying the scientific objectives of the Space Telescope, it is only one of several flight phases. To gain some perspective on the overall operation, figure 2 shows the flight phases in the context of the total mission scenario. This figure shows all the events from the integration of the spacecraft until its final return to Earth. The optical system and the instruments are integrated into a payload element, which is then mated to the spacecraft bus. This is now the Space Telescope, which goes to systems test, launch site, and into orbit. Several in-orbit maintenance actions are repeated until the mission is completed. In-orbit maintenance actions are expected to have a frequency of 1 to 2 years, with Earth return in 4 to 7 years. Planning for all mission phases is considerably broader in scope than planning for the science portion only.

The Space Telescope deployment, shown in figure 3, is one of the first significant events in the flight operation sequences. The Space Shuttle remote manipulator system is used to erect the telescope on the sill of the Space Shuttle bay, the solar arrays are deployed, the antennas are deployed, a direct communication link is established, and the telescope is raised from the sill and

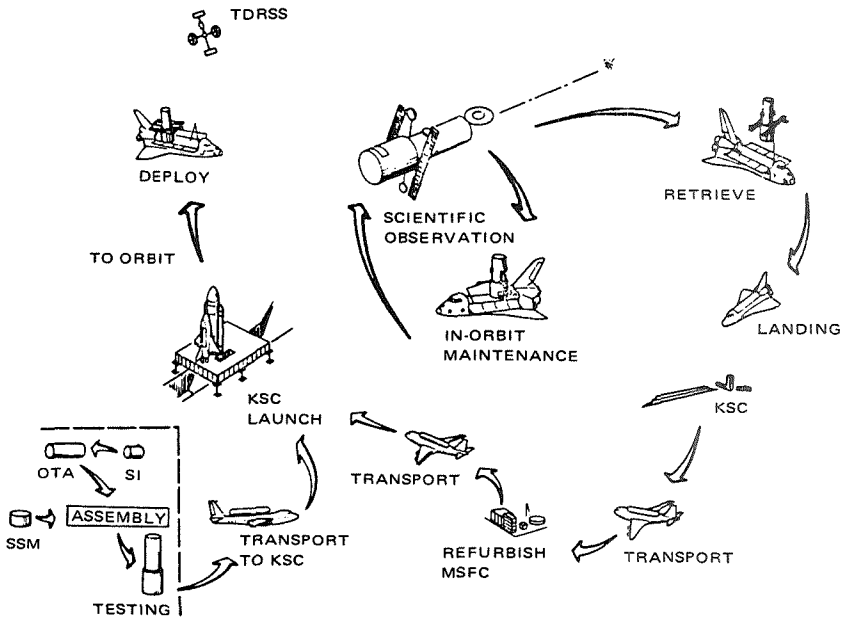

Figure 2.—Space Telescope operational phases. (KSC = Kennedy Space Center; MSFC = Marshall Space Flight Center; OTA = optical telescope assembly; SI = scientific instruments; SSM = support systems module; and TDRSS = Tracking and Data Relay Satellite System.)

released as the Space Shuttle backs away. The Space Telescope is then completely checked out while the Space Shuttle flies in escort mode for several days.

Another area of particular interest to the mission planner is the maintenance and refurbishment of the telescope throughout its life cycle. Both in-orbit maintenance and Earth refurbishment have been included. In-orbit maintenance consists of the replacement of those elements called "orbit replaceable units" that can be readily replaced in orbit. The replacement consists of routine replacement of limited-life components such as batteries, components that have failed during the operational period and thereby caused reduced system performance, and components that are not expected to last until the next maintenance action. Ground refurbishment consists of major actions such as recoating the mirror, changes that affect vehicle interfaces, and updating of instruments and equipment. The periodic maintenance action also permits the planned replacement of selected electronic components that are potentially subject to radiation damage. Radiation damage is caused primarily by repeated passages through the South Atlantic Anomaly. Electronic components have different levels of susceptibility to radiation damage, depending upon their composition. Although the minimum lifetime is approximately 15 years, it is

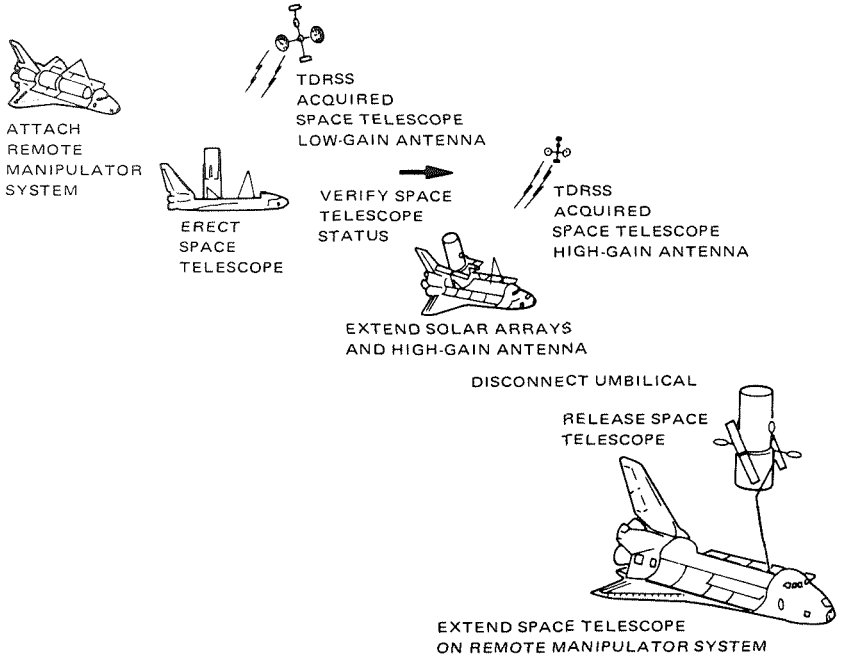

Figure 3.–Deployment of the Space Telescope.

advisable to plan for the replacement of these components on a regular schedule. The periodic replacement of components can provide both the lifetime and flexibility for an extended mission.

CONCLUSIONS

The inherent characteristics of the periodic Space Shuttle revisits and Earth-return capability provide this astronomical observatory with a capability for growth that should be incorporated into every phase of its development. Not only must the design allow for a change in technology, such as allowing higher data rates, more computer storage, and greater instrument capability, but the integration and testing of these systems with new capabilities must be accomplished without having to rebuild the spacecraft whenever an improvement occurs. It is, however, this basic growth process in the development that will permit the Space Telescope to become an outstanding astronomical facility initially and to grow with the constantly improving technology that will allow the observatory to continue probing the frontiers of science.

ACKNOWLEDGMENT

The work described in this paper was supported by NASA contract NAS8-31313.

AUTOMATION OF THE SPACE TELESCOPE

William W. Warnock and C. William Case
Martin Marietta Corp.

Phase B studies are being conducted by several contractors for the three sections of the Space Telescope: the optical telescope assembly, the scientific instruments, and the support systems module. In addition, a wide variety of supporting disciplines are being researched under advanced technological development contracts. Candidate scientific instruments for the Space Telescope are listed in table 1, along with one important characteristic for each.

TABLE 1.—*Candidate Scientific Instruments*

Instrument	Characteristic
Astrometer	Positional accuracy: ±0.002 second of arc
Faint object spectrograph	Spectral resolution: 10^4
High-resolution cameras	Imagery with high spatial resolution
High-resolution spectrograph	Spectral resolution: 10^5
Infrared photometer	Wavelength range: 2 to 1000 micrometers
High-speed point/area photometer	Time resolution: 100 microseconds

AUTOMATION CONSIDERATIONS

Maximum science return from the Space Telescope requires maximum use of the observatory, which will produce large data volumes (3×10^9 bits per 24 hours). The automation of the Space Telescope can be separated into two categories: onboard and ground. Trade studies are being conducted by Martin Marietta and the other two support system module contractors for determining the best designs for accomplishing the automation functions.

Onboard Automation

The onboard subsystems must have the capability for a variety of processing functions related to the operation of the scientific instruments and spacecraft control functions. General instrument-related processing functions include observation sequencing, target acquisition and slit centering, data encoding, merging of science and engineering data, fault detection and safing, and bulk data storage management. Some specialized onboard functions are doppler

shift correction for the high-resolution spectrograph, data buffering for the high-speed point/area photometer, and data storage for photon-counting detectors. Onboard spacecraft control functions include pointing control, support systems module subsystem fault detection and safing, and engineering data formatting and command handling.

The Data Management Subsystem will provide most of these functional capabilities. Six basic Data Management Subsystem concepts have been considered, with emphasis being placed upon cost effectiveness and scientific instrument accommodation flexibility. The difference among these concepts lies in the number of computers employed and the separation/integration of command and telemetry functions with the computers. The need for a support systems module computer to perform pointing-control functions has been firmly established. The currently preferred concept has separate command and telemetry systems, a support system module processor, and a subsequencer/microprocessor within each scientific instrument. This approach enables standardization and yet gives great flexibility and growth potential for later instrument designs.

Ground Automation

Automation of the ground systems required for flight operations is necessary for efficient use of the Space Telescope. A brief description of the functional requirements for these systems is best provided by the following NASA guidelines (from ref. 1; note that the Space Telescope was formerly called the Large Space Telescope or LST), subject to change as a result of trade study conclusions:

(1) All Space Telescope scientific operations shall be managed by a Science Institute, and the responsibilities of the Institute shall include control of science viewing requirements; science mission planning; pointing verification; quick-look science evaluation and attendant mission changes; final calibration determination; guest observer selection and interface; and science data management, including preprocessing, processing, and analysis.

(2) The Science Institute will establish observation requirements and perform the science viewing mission planning and a Mission Operations Center will perform the integrated mission planning including the science requirements, spacecraft constraints, support requirements, and Space Shuttle support as required. Execution of the mission plan shall be the responsibility of the Mission Operations Center. Responsibilities shall include such items as spacecraft command and control, status monitoring, and contingency control.

(3) The Mission Operations Center will perform the data processing and evaluation of the engineering and selected science data in support of overall evaluation of the spacecraft.

CONCLUSIONS AND SUMMARY

The Space Telescope observatory will function in a manner similar to a ground-based, automated, general-purpose optical observatory, with some

exceptions including the following: (1) a radiofrequency communications link will be required by the Space Telescope for commands and telemetry; (2) onboard computer(s) will be required by the Space Telescope for several types of processing and control; (3) operating constraints will be different; (4) observatory status monitoring will include different sets of variables; and (5) fault detection, isolation, and recovery will require different techniques.

Automation of astronomical observatories can be used to maximize science return within cost constraints. While automation of ground-based optical observatories is not required for many types of observations, it must be used for the Space Telescope. Trade studies are being conducted to determine the best methods for satisfying the large variety of Space Telescope automation requirements.

REFERENCE

1. *LST Project Requirements and Guidelines Document,* revision 2, NASA/Marshall Space Flight Center, June 25, 1975.

II

Telescope Performance

SCIENCE PERFORMANCE CONSIDERATIONS FOR THE DESIGN OF THE SPACE TELESCOPE

Damon D. Ostrander and James C. Tuttle
Martin Marietta Corp.

Any attempt to quantify science performance necessarily hinges on using appropriate and valid performance criteria. For the purposes of this paper, a combination of several performance criteria is used to describe the quality and quantity of the data that the Space Telescope will provide. Computerized mathematical models of the optical system (including detectors) are used to evaluate these performance measures. These models are analytical in nature as opposed to the ray-tracing approaches used for optical design and assume that distortion and aberrations of the image are negligible. These assumptions are valid for the purposes of preliminary design and greatly reduce computational costs. All the performance measures are based on a determination of the optical point spread function and the modulation transfer function. These performance criteria are used to evaluate the effect of pointing instability, wavefront error, and aperture size on total performance. Three aperture sizes are evaluated at different levels of performance. Combinations of wavefront error and pointing instability that give performance at each level are determined.

METHOD

A summary of the performance measures chosen and their salient characteristics is provided in table 1. The measures are of two basic types: measures related to the light sensitivity or "speed" of the telescope (and therefore related to the quantity of data obtainable in a given time) and measures of the spatial resolution of the telescope (which relates to the quality of data obtainable). Some parameters of the models used for performance measure evaluation are shown in the table, and their influence on the performance measures is rated as high or low in sensitivity. The large variation in sensitivity among the performance measures emphasizes the need to understand and choose suitable measures.

RESULTS

The Space Telescope science performance measures were used to evaluate the effect of aperture size on mission performance. The data in table 2 show a

TABLE 1.–*Performance Measure Characteristics*

Performance		Definition	Sensitivity of selected parameters				
Type	Measure		Aperture diameter	Secondary mirror obscuration	Detector characteristics	Optical wavefront error	Line of sight pointing stability
Light sensitive exposure time	Faint object sensitivity	Limiting visual magnitude attainable to $S/N = 10$ in 4 hours in diffraction disk in central maxima	High	Low	Low	High	Low
	Spectral sensitivity	Spectrograph limiting visual magnitude attainable to $S/N = 2$ in 4 hours in central maxima of monochromatic line image; slit = 0.1 × 1 second of arc	High	Low	Low	High	Low
Spatial resolution	50 percent modulation transfer function response	Spatial period in seconds of arc, which gives 50 percent modulation transfer function response	High	Low	High	High	Low
	Contrast (Rayleigh criterion)	Separation in seconds of arc of 2 identical stars that gives an image center intensity 26.5 percent less than the peak intensity	High	High	–	Low	High
	Encircled energy	Angular radius in seconds of arc containing 60 percent of total energy entering aperture	High	High	–	High	Low
	Full-width half intensity	Point spread function diameter at the half-intensity point in seconds of arc	High	Low	–	High	Low

TABLE 2.–*Performance Comparison*

Performance measure	Aperture diameter		
	1.8 meters (71 inches)	2.4 meters (94 inches)	3 meters (118 inches)
Faint object sensitivity (visual magnitude limit)	26.8	27.4	27.8
Spectral sensitivity	21.2	22.2	23.0
Contrast ratio (separation = 0.1 second of arc), percent	53	88	96
Encircled energy (within 0.075 second-of-arc radius), percent	63	66	76
Full-width half intensity, seconds of arc	0.072	0.054	0.044

performance comparison of three aperture sizes, each with a root-mean-square pointing error of 0.005 second of arc and a root-mean-square wavefront error of $\lambda/20$. (λ is the standard symbol for wavelength.) For this comparison, the performance measure of faint object sensitivity was evaluated using a mathematical model of an *f*/24 camera with a Secondary Electron Conduction Orthicon (SECO) detector. The 50-percent response is determined for an *f*/96 camera with a SECO detector. Spectral sensitivity is determined for a faint object spectrograph using a slit width of 0.1 second of arc, a SECO detector, and a spectral resolution ($\lambda/\Delta\lambda$) of 1600. An equal weighted sum of these measures shows that from a science data aspect, a 2.4-meter (94-inch) telescope achieves about 77 percent of the total performance achieved by a 3.0-meter (118-inch) system and a 1.8-meter (71-inch) telescope about 53 percent.

For each aperture, a selection of pointing stability and optical quality requirements can be made based on science-related performance data. For example, in figure 1 curves are presented that indicate values of wavefront

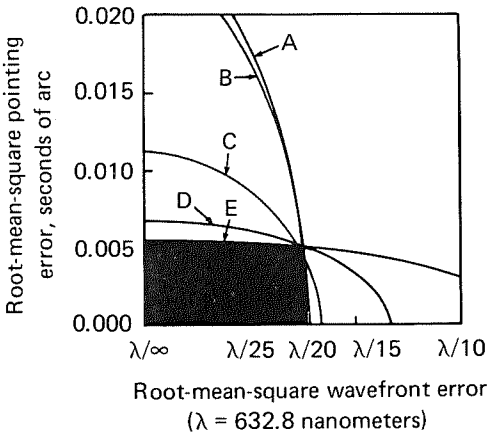

Figure 1.–Systems that will have performance equivalent to a 3-meter (118-inch) diffraction-limited system. *A:* encircled energy; *B:* 50 percent modulation transfer function response; *C:* faint object sensitivity; *D:* contrast; *E:* full-width half intensity.

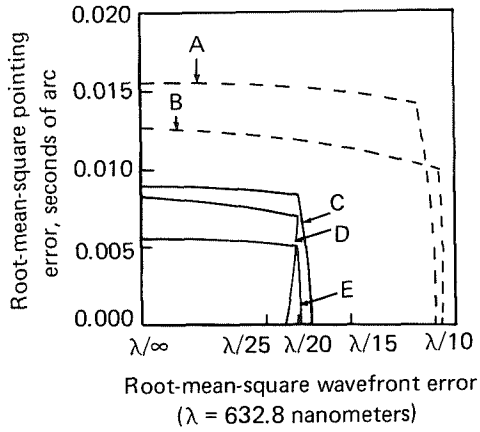

Figure 2.–Equivalent performance with different aperture diameter systems. *A:* 2.4-meter (94-inch) system–equivalent to 2-meter (79-inch) near-diffraction-limited (NDL) system; *B:* 3-meter (118-inch) system–equivalent to 2.4-meter (94-inch) NDL system; *C:* 2-meter (79-inch) NDL system; *D:* 2.4-meter (94-inch) NDL system; *E:* 3-meter (118-inch) NDL system.

error and pointing error which give performance equivalent to a 3-meter (118-inch) near-diffraction-limited system. The shaded region represents the combinations of design values that would result in a system capable of meeting 3-meter (118-inch) near-diffraction-limited performance requirements for all the indicated performance measures. The measures that establish the design requirements are observed as the boundaries of the shaded region. A cost-effective system can be found by selecting the minimum cost point on the boundary.

The same concept can be used to compare different aperture size systems. Figure 2 shows the boundaries of the acceptable design regions for 3-meter (118-inch), 2.4-meter (94-inch), and 2-meter (79-inch) near-diffraction-limited systems. The dashed curves indicate the extent that a larger diameter system can be degraded and still reach the near-diffraction-limited performance of a smaller system.

CONCLUSIONS

Improvement of line-of-sight pointing stability and optical quality (wavefront error) provides limited improvement in telescope performance as compared to improvement obtained by increasing aperture size. A large aperture system of modest quality can easily outperform a diffraction-limited system of smaller aperture size. A large aperture allows design margins and relaxed tolerances that may result in lower total cost to get performance comparable to smaller systems. If faint object sensitivity and spectral sensitivity are taken as performance measures of more than average importance, then the sensitivity of performance to aperture diameter is even more pronounced. A cost-effective combination of optical quality and pointing stability should be chosen based on data relating the effects of each on total performance.

OPTICAL PERFORMANCE CONTROL

Terence A. Facey
Perkin-Elmer Corp.

To achieve maximum scientific use of the Space Telescope, the optical performance of the system must be essentially equal to the theoretical optimum. To insure this, the Space Telescope will be equipped with an optical performance control subsystem that will monitor the optical performance of the telescope periodically and provide corrective data to ground controllers.

The sensing elements of the performance control subsystem are the focal plane wavefront sensors, three of which are required. A plane wave from a stellar source entering the telescope is aberrated by imperfect optical surfaces and misalinement of optical elements. The function of the wavefront sensor is to quantify the aberrations in this wavefront and telemeter to the ground station a set of pupil optical path difference maps for the telescope. On the ground, these maps will be used to generate the error signals that can be used to realine the secondary mirror and, if necessary, correct the figure of the primary mirror.

A set of general control equations has been developed that allows separation of the secondary mirror position errors in the presence of small primary mirror figure errors. The residual errors caused by the primary mirror only are then available for figure correction use by actuators, or for postexposure image processing.

A perturbation analysis was undertaken for the Space Telescope optical design. Motions of the secondary mirror in each of its five significant degrees of freedom (roll about the optical z-axis is of no consequence) are manifest as changes in five aberration coefficients. Thus, secondary mirror position is potentially describable by a set of five simultaneous linear equations. Such a set of equations may be expressed in matrix form as

$$[M_{ij}]\,[\epsilon_j] = [A_i] \tag{1}$$

where M_{ij} are the influence coefficients, ϵ_j are the alinement perturbations, and A_i are changes in the aberration polynomial coefficients. Numerically, then,

equation (1) becomes, for the Space Telescope,

$$\begin{bmatrix} -0.24 & -0.24 & -23.34 & 1.67 & 1.67 \\ 0 & 0 & 0 & -0.08 & 0 \\ 0 & 0 & 0 & 0 & -0.08 \\ 0 & -2.57 & 0 & 1.56 & 0 \\ -2.57 & 0 & 0 & 0 & 1.56 \end{bmatrix} \begin{bmatrix} x \\ y \\ z \\ \theta \\ \phi \end{bmatrix} = \begin{bmatrix} A_4 \\ A_5 \\ A_6 \\ A_7 \\ A_8 \end{bmatrix}$$

The determinant of the matrix is 0.9865 and its elements are in units of micrometers aberration per millimeter perturbation (or micrometers per milliradian). This equation may be inverted (eq. (2)) to solve for the secondary mirror errors, given the aberration polynomial coefficients deduced from the optical path difference map of the telescope pupil, as measured at a single point in the field:

$$\begin{bmatrix} 0 & 0 & -7.59 & 0 & -0.39 \\ 0 & -7.59 & 0 & -0.39 & 0 \\ -0.043 & -0.816 & -0.816 & -0.004 & -0.004 \\ 0 & -12.5 & 0 & 0 & 0 \\ 0 & 0 & -12.5 & 0 & 0 \end{bmatrix} \begin{bmatrix} A_4 \\ A_5 \\ A_6 \\ A_7 \\ A_8 \end{bmatrix} = \begin{bmatrix} x \\ y \\ z \\ \theta \\ \phi \end{bmatrix} \quad (2)$$

Thus, if we assume a perfect (or at least statically perfect) primary mirror, the secondary mirror may be correctly alined in all five degrees of freedom from the information contained in a pupil optical path difference map measured by a single wavefront sensor located off-axis at a known field position in the telescope focal plane.

The ability to separate tilt and decenter components of the secondary mirror misalinement is dependent on the ability to measure small amounts of astigmatism. However, for misalinements that cause astigmatism of amounts below the measurement limit of the wavefront sensor, it is practical to correct the coma by either tilt or decenter adjustment—whichever is most easily accomplished. This obviously assumes that the sensor is more sensitive to astigmatism than any other instrument in use. The wavefront sensors are located toward the edge of the scientific data field and therefore "see" more astigmatism than do scientific instrument entrance apertures. More generally, equation (1) is written

$$[A_i(h)] = [M_{ij}(h)]\,[\epsilon_j] + [P_i] \quad (3)$$

where $M_{ij}(h)$ expresses the field dependence of M_{ij} in equation (1) and P_i is the

aberration polynomial coefficient change caused by primary mirror distortions.

Equation (3) suggests that the field-independent nature of the primary induced coefficient changes will allow them to be separated from values of A_i' to yield secondary mirror position errors uncorrupted by primary mirror effects if measurements are made at more than one field position.

The odd field dependence of misalinement-induced aberrations suggests the use of two orthogonal locations in the field. The focus error in the wavefront introduced by axial z misalinement of the secondary is also field independent and therefore yields a singularity in the 5 by 5 matrix of $[M_{ij}(h_1)] - [M_{ij}(h_2)]$.

Elimination of focus information A_4 and the axial degree of freedom z from equation (3) allows elimination of $[P_i]$ to yield secondary position errors in x, y, θ, and ϕ uncorrupted by primary mirror effects:

$$[A_i(h_1)] - [A_i(h_2)] = \{[M_{ij}(h_1)] - [M_{ij}(h_2)]\} \{\epsilon_j\} \tag{4}$$

The secondary mirror position control equation becomes:

$$\begin{bmatrix} 3.79 & -3.79 & 1.94 & -1.94 \\ -3.79 & -3.79 & -1.94 & -1.94 \\ -6.25 & -6.25 & 0 & 0 \\ 6.25 & -6.25 & 0 & 0 \end{bmatrix} \begin{bmatrix} A_5' \\ A_6' \\ A_7' \\ A_8' \end{bmatrix} = \begin{bmatrix} x \\ y \\ \theta \\ \phi \end{bmatrix} \tag{5}$$

in which

$$A_i' = A_i(h_1) - A_i(h_2)$$

Thus the secondary mirror may be controlled in four degrees of freedom (everything except focus) without confusion from primary mirror effects by two figure sensors located at equal field heights but situated at right angles to one another in the focal plane.

The focus error signal remains a combined error resulting from secondary despace Δz, primary mirror radius of curvature change Δr, and small contributions resulting from decenter and tilt errors.

These effects may be separated by observing changes in the focus coefficient A_4 and in the third-order spherical aberration coefficient A_{11} and by addition of the measured coefficient changes from two diametrically opposite field positions.

In this way, small corrupting effects of focus errors caused by secondary tilt or decenter are removed due to their odd field dependence, allowing the focus errors caused by secondary axial position error Δz and primary radius of curvature error Δr to be separated by a pair of simultaneous equations:

$$\begin{bmatrix} A_4(h) \\ A_{11}(h) \end{bmatrix} + \begin{bmatrix} A_4(-h) \\ A_{11}(-h) \end{bmatrix} = 2 \begin{bmatrix} P_{11} & P_{12} \\ P_{21} & P_{22} \end{bmatrix} \begin{bmatrix} \Delta z \\ \Delta r \end{bmatrix} \tag{6}$$

In the event, and this is the case for the Space Telescope, that the system thermal and structural designs are such that no significant pure radius of curvature change of the primary is likely, then this last procedure is unnecessary, and all focus error may be attributed to secondary despace and corrected accordingly.

IMPACT OF FOCAL PLANE DYNAMICS ON IMAGE QUALITY

William J. Pragluski, Peter W. Abbott, and Jack F. Eastman
Martin Marietta Corp.

The Space Telescope has a large aperture telescope that has the potential for near-diffraction-limited performance. This performance potential provides the possibility of very-high-resolution photography, photometry, and spectroscopy as well as viewing of very faint objects, well beyond the performance of the largest ground-based telescopes.

To achieve this potential, the Space Telescope's pointing and stability requirements are quite precise. A pointing accuracy of 0.01 second of arc and stability of 0.007 second of arc are design goals, compared to a diffraction-limited image size of 0.13 second of arc (i.e., 37 micrometers at the focal surface). Even the smallest microvibrations of the telescope structure can induce apparent image motions at the focal surface that are of the same order of magnitude as the image size. If true, this would seriously affect the image quality and, hence, the performance of the Space Telescope scientific mission.

The parameter used herein to compare the effects of focal plane dynamics on image quality is the size of the "blur circle." This parameter defines the area over which over 400 rays, passing through the telescope assembly, are splayed at the focal surface over and above the normal diffraction image size. Although other criteria, such as the root-mean-square wavefront error, Strehl ratio, or modulation transfer function were evaluated, the use of the blur circle parameter and its impact on the image quality is the easiest to visualize.

STRUCTURAL DYNAMICS ANALYSIS

The precise pointing requirements of the Space Telescope require an accurate mathematical model of the structure if the impact of microvibrations at the focal surface are to be reliably predicted. The system disturbances are both known (i.e., reaction wheel static and dynamic imbalance, internal moving parts, etc.) and undefined (i.e., bearing noise, thermal creaking, etc.).

Structural mass, stiffness, and damping are critical characteristics in the analysis. The model developed is broken into three basic structural elements: the support systems module, the optical telescope assembly, and appendages.

Each of these elements is further broken down into several substructures and these are combined using the technique of modal coupling with appropriate boundary conditions. The coupled system includes 177 degrees of freedom and 130 modes below 100 hertz.

OPTICAL PERFORMANCE ANALYSIS

Optics Model

The telescope modeled in this analysis is a standard 2.4-meter (94-inch) two-mirror Ritchey-Chretien design. Both mirrors are figured as hyperboloids. The system is designed to be free of spherical aberration and coma. The image quality in the field is limited by astigmatism.

Sensitivities

The on-axis sensitivity data for defocus are approximately linear with displacement. The slope is nearly equivalent to the first order approximation of the square of the result of subtracting 1 from the secondary mirror magnification. Using the arbitrary criterion that the blur circle diameter should be less than one tenth the Airy disk diameter (37 micrometers) results in a maximum allowable deflection of 1.0 micrometer.

The on-axis sensitivity to decenter is somewhat lower than that for defocus (an order of magnitude). The sensitivity, over the range of decenter investigated, is very nearly proportional to the product of the secondary mirror magnification and the displacement.

The basic data at field positions of 80 and 135 millimeters (3.15 and 5.31 inches) show that the effect of astigmatism masks the effect of structural deflections until the deflections are greater than 2 to 5 micrometers. The blur circles, in either case, are of the same order in size as the Airy disk diameter. If the effect of this aberration could be completely compensated for, the conclusion on the sensitivities would be the same as described for the on-axis results. However, physical limitations will play a part in the amount of compensation that can be accommodated. Structural deflections begin impacting the image quality at approximately 0.25 micrometer.

The sensitivities to tilt of both the primary and secondary mirrors were evaluated over a range of tilts between 10^{-8} and 10^{-9} radians. The range was selected as representative after survey of the structural dynamics analysis results. The data show that deflections of this order of magnitude do not affect the data quality. The effect of primary mirror tilts on the centerline image quality is just beginning to be felt at tilts of 10^{-8} radians.

RESULTS

The structural analysis presented results in the apparent star motions at the focal surface shown in figure 1. These data show relatively small responses at

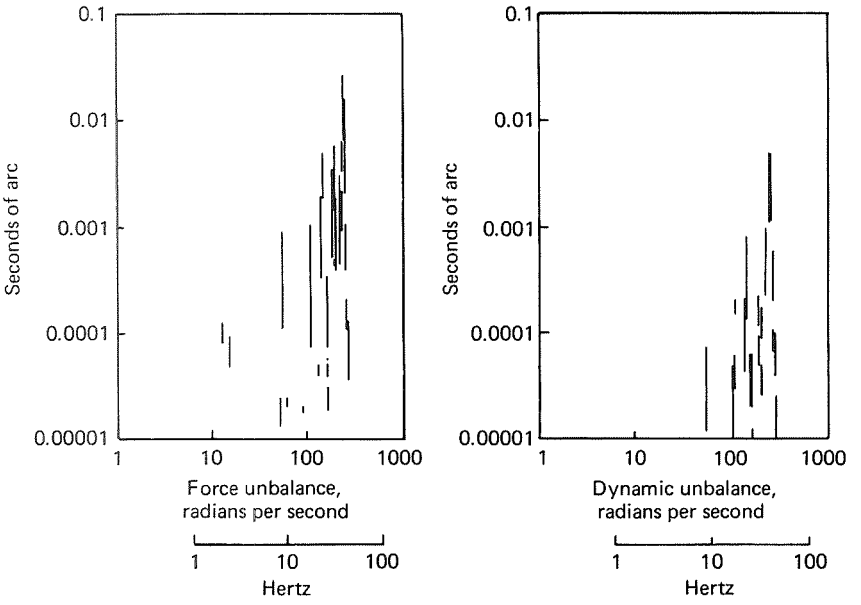

Figure 1.–Image motion induced by reaction wheels. (*a*) 1.5×10^{-6} kilogram-meter. (*b*) 0.35×10^{-6} kilogram-square meter.

low frequencies and excessive responses at around 30 hertz. The low-frequency data (1 to 10 hertz) reflect characteristics after the lower frequency elements (notably antenna booms and solar array structure) had been beefed up, using the weight margin available on the Space Shuttle, as a result of earlier analyses. This frequency regime is critical from a vehicle control system interaction (stability) point of view and the weight margin used there is well spent to minimize potential problems.

The excessive responses (compared to the 0.007-second-of-arc stability limit) near 30 hertz result primarily from the bending of the secondary mirror support structure from its attachment near the primary mirror. A more detailed analysis is required to evaluate the possibility of alleviating these adverse responses by stiffening the structure. However, the probability of exciting these modes has been minimized by modifying the Space Telescope control law (momentum management) such that the reaction wheel speeds will be well below 30 hertz during science observations. The higher wheel speeds will only be used during large slew maneuvers, between targets, when no science data are being taken.

The composite effect of structural deflections on blur circle diameter is shown in figure 2. These data show both the static (no dynamics) diameter as a function of field position as well as the envelope of the five dynamics cases (below 25 hertz) investigated. Also shown is the basic image quality at the

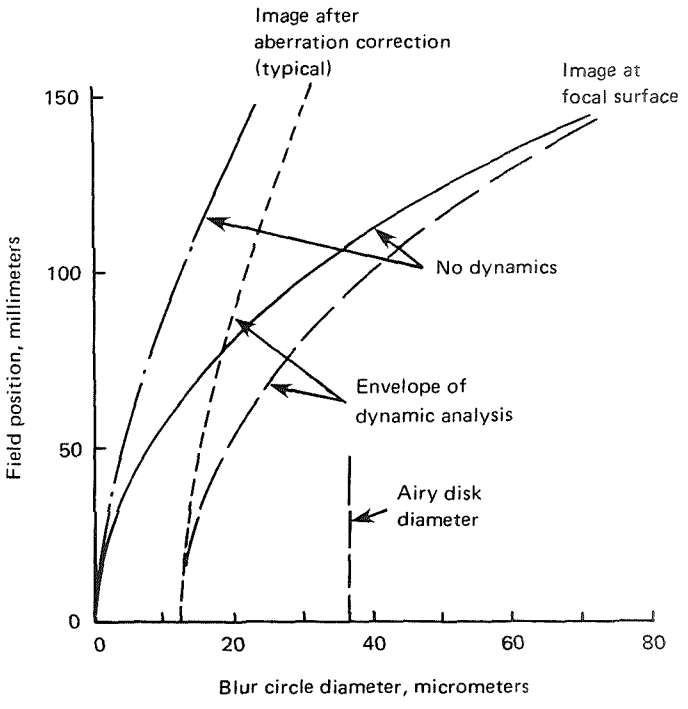

Figure 2.–Blur circle diameter–composite dynamics.

focal surface both with and without typical compensation for aberration. In all cases, the degradation caused by dynamics is a small but significant percent of the Airy disk diameter. The dynamic blur circle diameter delta, in all cases, represents the dispersion at the maximum structural deflection.

CONCLUSIONS

The analyses summarized do indicate that the impact of focal plane dynamics on image quality can be controlled to an acceptable level. However, this does require that this facet of the Space Telescope design be carefully monitored and controlled during the design phase.

STRAY LIGHT FROM OUT OF FIELD SOURCES

Robert J. Noll
Perkin-Elmer Corp.

Typically, there are three classes of stray light problems of concern:

(1) Scatter from primary optics
(2) Diffraction effects from various telescope edges
(3) Specular and diffuse reflections from telescope walls

In this paper an attempt to describe these effects in terms of a bidirectional reflectance function (BDRF) is presented.

MIRROR SCATTER

Stray light from mirror scatter is typically the result of high spatial frequency random irregularities in the surface profile of the mirror. With a plane wave incident upon the primary optic, the reflected amplitude in terms of the aberration function is well known and can be used to write the BDRF for normal incidence as

$$\mathrm{BDRF}(\theta\phi|00) = \left(\frac{k}{2\pi}\right)^2 \frac{1}{A_0}\left|\int_{A_0}\int d\mathbf{r}\, e^{i[k\Phi(-\mathbf{k})\cdot\mathbf{r}]}\right|^2 \tag{1}$$

where the quadratic Fresnal phase factor, as well as all dependence on the dielectric constant of the mirror, has been neglected.

When the aberration spatial frequencies are large (mirror scatter), it is convenient to consider a statistical representation for the scattered light. The average scattered intensity can be written as

$$\langle I\rangle = \langle U\rangle^2 + \langle |U - \langle U\rangle|^2\rangle \tag{2}$$

The first term in equation (2) describes specular reflection and the second, diffuse or scattered light. If the BDRF is taken as the average intensity scattered per unit of incident flux, it can be written as the sum of two terms, a specular and a diffuse term. The effects of nonnormal incidence as well as dielectric constant effects are far from negligible. The physical importance of the dielectric constant of the mirror appears to be most significant when the

incident light wavelength is in a range where mirror dispersion effects such as surface plasmons (particle excitations in metal) are important.

To obtain a qualitative understanding of mirror scatter, only the dependence on the autocorrelation will be considered. For this case the specular BDRF can be written for a circular mirror as

$$\text{Specular BDRF} = \pi\left(\frac{a}{\lambda}\right)^2 \left[1 - (2k\sigma)^2\right] \left[\frac{2J_0(ka\theta)}{ka\theta}\right]^2 \tag{3}$$

and the diffuse BDRF can be written as

$$\text{Diffuse BDRF} = \frac{1}{2\pi}(2k\sigma)^2(Tk)^2F(kT\theta) \tag{4}$$

where

$$F(y) = \int_0^\infty xC(x)J_0(yx)\,dx \tag{5}$$

The specular term is simply the aperture diffraction pattern modified by a factor that depends only on the root-mean-square height variations of the surface, sometimes called the Strehl factor. The diffuse or scatter term depends on both the root-mean-square height and correlation lengths and is functionally the Fourier transform of the surface autocorrelation function. Effects such as polarization, index of refraction, and arbitrary angles of incidence have been omitted because these effects generally perturb the results only slightly.

EDGE DIFFRACTION

Diffraction as a stray light problem in telescopes was studied many years ago by B. Lyot. He found that diffraction effects could be minimized by introducing a stop at the image plane of the diffracting edge. An analytic evaluation of the efficiency of such a stop has been given by the author. The Lyot stop is effective because diffraction comes only from edges. At an image plane of a circular entrance aperture, the out of field source produces a bright ring image. The energy in this ring is the diffracted energy that reaches the focal plane.

At Perkin-Elmer, extensive analysis of edge diffraction has been performed using a general unwanted energy rejection program that not only traces rays reflected from various telescope surfaces, but also the diffracted rays. The conclusion of this analysis is that typically there are only a few points on an edge that determine the magnitude of the diffracted light reaching a detector. This fact greatly reduces the amount of computer ray tracing required to compute diffraction effects. The edge points act as sources of astigmatic rays that are the diffracted rays. To calculate the diffraction BDRF, the points on

the edge that give rise to diffraction must first be determined and then the strength associated with each point must be found.

SPECULAR AND DIFFUSE REFLECTIONS

Baffle fins are placed inside telescopes for two reasons: to make specular rays undergo many more reflections before reaching the detector and to reduce the illuminated area inside the telescope seen by critical surfaces. Generally, baffle fins make specular reflections from walls a negligible contributor of total stray light. In a well-baffled system, the primary cause of stray light will result from either diffraction or diffuse reflection from the baffle fin edges. Diffraction tends to dominate for diffraction angles less than 20 degrees and reflection for scatter angles greater than 30 degrees.

Computer calculations at Perkin-Elmer show that sources less than 17 degrees off axis illuminate the primary mirror, making mirror scatter the dominant stray light mechanism. From 17 to 30 degrees, diffuse reflection from the support struts is important; and from 30 to 90 degrees diffuse reflection from baffle edges followed by diffuse reflection from the primary mirror dominates. Stray light diffusely scattered to the detector from the secondary mirror, inside the secondary baffle, and inside the primary baffle are all negligible. The secondary baffle calculation was done with no baffle fins anywhere in the telescope. The scattered flux reaching the detector for this system from any given source is easily obtained by substituting the BDRF shown in figure 1 into equation (1).

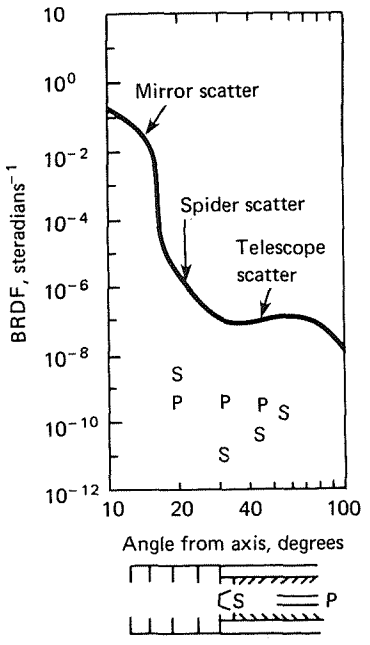

Figure 1.–Telescope BDRF. (S = secondary baffle, no fins (double diffuse); P = primary baffle.)

CONCLUSION

The specific concept of a BDRF as a surface reflectance characteristic has been extended to include general telescope stray light performance. It is shown that the BDRF is proportional to the telescope point spread function in the field and describes scatter outside the field. It has been determined that the three basic classes of stray light can be described by a BDRF. In particular, the Perkin-Elmer GUERAP program allows BDRF computation for rather complicated but realistic telescope stray light problems. The program has been applied to a prototype Space Telescope design, and the results are given in figure 1.

DESIGN OF HIGHLY STABLE OPTICAL SUPPORT STRUCTURE

Michael H. Krim
Perkin-Elmer Corp.

As spaceborne optical systems increase in diameter to achieve improved resolution, the stability requirements imposed on structures approach values that were unthinkable only several years ago. To achieve the potential of these apertures, optical path errors must not exceed a specific fraction of the wavelength λ of light. This fraction typically $\lambda/20$ root mean square in the focal plane, is independent of system size. The optical telescope assembly is installed in the Space Telescope spacecraft. The vertex-to-vertex spacing of the primary and secondary mirror is 490 centimeters (193 inches). To achieve satisfactory optical performance, this spacing must be maintained constant to a precision of ±1 micrometer for observation periods up to 10 hours. During this time it may be necessary to alter the spacecraft attitude with respect to the Sun, which would change the temperature levels and gradients within the structures. It is believed that by exploiting the use of novel, turnable graphite epoxy truss elements, the stringent alinement requirements can be satisfied with a nominally passive structure.

THERMAL LOADS

It will be shown that the thermal changes that occur between factory and orbit are not critical to system performance, but the thermal changes that can occur subsequent to arrival on station are of consequence. The thermal design envelope was developed from analyses of various vehicle pointing attitudes and heater system control accuracies. The envelope represents the maximum anticipated change that might occur during a single target observation.

ALINEMENT REQUIREMENTS

The working depth of focus at the $f/24$ image plane is ±432 micrometers at 0.63-micrometer wavelength. By applying the simple lens makers' formula to the two mirrors successively, the following relationship is obtained relating

defocus to changes in mirror radii and spacing:

$$\Delta f = \frac{[(2l_1 - R_1 + R_2)R_2/2 + R_1R_2/2 - R_2l_1]\ \partial R_1}{(2l_1 - R_1 + R_2)^2} + \frac{[(2l_1 - R_1 + R_2)(R_1/2 - l_1) - (R_1R_2/2 - R_2l_1)]\ \partial R_2}{(2l_1 - R_1 + R_2)^2} + \frac{[(2l_1 - R_1 + R_2)(-R_2) - 2(R_1R_2/2 - R_2l_1)]\ \partial l_1}{(2l_1 - R_1 + R_2)^2} \quad (1)$$

With this equation the tolerance on despace ∂l_1 is developed. Based on the system thermal analysis, temperature-induced defocus contribution of the optical elements alone is 175 micrometers. Allowing for a focus sensing and correction (initial alinement) error of 100 micrometers and another 50 micrometers for growth of l_2 (13.5 micrometers per degree Celsius (7.5 micrometers per degree Fahrenheit)) and location uncertainty of the four scientific instruments, 107 micrometers remain for the effect of a change in l_1, as ∂l_1 equals approximately 1 micrometer.

DESIGN APPROACH

To calculate the truss axial expansion, an equation was developed relating the axial expansion of a truss bay (which can be summed over the total number of bays) to the ring and strut geometry:

$$\Delta S = \frac{1}{S}\left[l^2\alpha_S T_S + R^2\alpha_R\ (\cos\theta - 1)\right](T_B + T_T) \quad (2)$$

From this equation, the truss member expansivities α_S (strut) and α_R (ring) can be determined. This equation shows that $\alpha_R/\alpha_S = 10.6$ for a nominally balanced design and also that $\alpha_S = 0.018 \pm 0.018 \times 10^{-6}$ K^{-1} $(0.01 \pm 0.01 \times 10^{-6}\ (°F)^{-1})$. The fundamental problem facing the structural designer is twofold. First, the variability of α from a design nominal is on the order of $\pm 0.09 \times 10^{-6}\ K^{-1}$ $(\pm 0.05 \times 10^{-6}\ (°F)^{-1})$ for graphite epoxy laminates, and, second, the expansivities at the various nominal temperatures along the truss length may be different.

To solve the variability problem, a means of adjusting the expansivity of the elements forming the structure is required. Ideally this adjustment should be performed in the postcured condition so that process variables can be compensated. Further, the adjustment on tuning should not introduce additional process variables but should be a discrete operation. Finally, the

tuning elements should not locally alter the thermal diffusivity of the member, otherwise transient behavior would be compromised.

The dual-α tunable graphite epoxy strut accomplishes these objectives. Here a single strut is constructed from a single graphite epoxy system but with different laminate (i.e., layup) geometry in the left- and right-hand sections. On the left, for example, the laminate would be designed so that its expansivity, considering the process variables, is $0 \pm 0.18 \times 10^{-6}$ K^{-1} ($0 \pm 0.1 \times 10^{-6}$ $(°F)^{-1}$). To the right of the transition zone it would be $(0^{+0.18 \times 10^{-6}}_{-1}$ K-1 $(0^{+0.1 \times 10^{-6}}_{-0}$ $(°F)^{-1}$. Obviously a net thermal expansion of zero could be achieved if the left- and right-hand sections could be proportional such that

$$\alpha_L l_L + \alpha_R l_R = 0$$

It is initially constructed oversize and trimmed after curing to satisfy the equation

$$\alpha_0 = \frac{\alpha_1 l_1 + \alpha_2 l_2}{l_0} = 0$$

Expansion measurements are made, using coupons cut from either end, to determine the as-cured values of α_1 and α_2 such that

$$\alpha_1 = -\frac{\alpha_2}{\alpha_1 - \alpha_2} l_0$$

These coupon measurements are made at the nominal temperature the strut will operate at, thus solving the $d\alpha/dT$ problem. The sensitivity of the overall truss assembly of off-nominal (nonzero) values of α may be assessed by use of the ΔS equation. This equation was also employed as a check on a finite element model of the truss that was then used to determine the deformations caused by more complex thermal conditions, such as axially varying side-to-side temperature gradients. From the closed-form solution, the change in length of each truss bay is given by

$$\Delta S = 74.75\alpha_S T_S - 3.53 L_R (T_B + T_T) \tag{3}$$

Note that if α_R is $10.6\alpha_S$, ΔS is identical to zero when

$$T_S = T_B = T_T$$

or the temperature change of the system is uniform, or when

$$T_S = \frac{T_B + T_T}{2} \tag{4}$$

This form of temperature desensitization of structures has previously been used in telescope structures before the use of composites. In those instances, the geometry of the structure was configured to satisfy α ratio constraints for titanium/aluminum combinations. However, because this form of athermalization depends on the small difference of relatively large numbers (α in the case of metallic pairs), it is impractical except in those situations of precisely uniform soak or static gradient situations.

For the Space Telescope truss design under discussion, equation (3) can be used to examine the effect of laminate α tolerance on performance. For a $\pm 0.09 \times 10^{-6}$ K^{-1} ($\pm 0.05 \times 10^{-6}$ $(°F)^{-1}$) uncertainty or spread in the nominal strut (α_S) and ring (α_R) tolerances, the despace error is 2.5 micrometers (99×10^{-6} inches). This is in excess of the 1-micrometer budget.

If tuned struts are employed where the nominal strut uncertainty is 0.009×10^{-6} K^{-1} ($\pm 0.005 \times 10^{-6}$ $(°C)^{-1}$) and the ring tolerance remains 0.09×10^{-6} K^{-1} ($\pm 0.05 \times 10^{-6}$ $(°F)^{-1}$) the uncertainty is reduced to 0.33λ. The wider ring tolerance is retained because the system is less sensitive to ring α uncertainties and the ring is more difficult to tune. To accomplish uniform soak athermalization, as opposed to a zero-α approach,

$$\frac{\alpha_R}{\alpha_S} = \frac{74.75}{2 \times 3.53}$$

$$= 10.588$$

If, in this instance $\alpha_S = 0.09 \times 10^{-6}$ K^{-1} (0.05×10^{-6} $(°F)^{-1}$), the change in length caused by the gradient change is nominally zero as expected. But, by applying a 0.09×10^{-6} K^{-1} ($\pm 0.05 \times 10^{-6}$ $(°F)^{-1}$) tolerance on α_R and α_S, a 2.1-micrometer error in the first bay alone is possible. If the temperature change over a bay is not linear, then the relationship of equation (4) is invalidated and the α_R/α_S balance defeated. In this instance, low absolute values of α are demanded to insure satisfactory performance.

Based on the results of temperature uncertainty and α tolerance and despace, it was concluded that the struts need to be constructed with a nominal α no greater than 0.022×10^{-6} K^{-1} (0.012×10^{-6} $(°F)^{-1}$) and a dispersion not in excess of 0.018×10^{-6} K^{-1} (0.01×10^{-6} $(°F)^{-1}$). This implies individual parts measurements and, as a logical extension, tuning. The dual-α strut will accomplish this.

III

Instrument and Detector Development

LARGE FORMAT SECONDARY ELECTRON CONDUCTION ORTHICON INTEGRATING TELEVISION SENSOR FOR THE SPACE TELESCOPE

John L. Lowrance
Princeton University

In the mid-60's, NASA recognized that television-type sensors would be very useful in space astronomy if they could be made to integrate for long periods of time with high photometric accuracy. A study completed in 1965 concluded that a magnetically focused Secondary Electron Conduction Orthicon (SECO) tube made by Westinghouse had the best chance of meeting these requirements. This choice was based on the almost indefinite storage capability of the SECO potassium chloride target, which also exhibited a gain of approximately 100 to overcome readout noise.

Through a series of supporting research and technology grants and contracts, a magnetically focused SEC tube with a 70-millimeter (51- by 56-millimeter) (2.8-inch (2.0- by 2.2-inch)) format has been developed for scientific photometric applications; in particular, for the Space Telescope *f*/24 field camera and the high-resolution spectrograph. The basic image sensor requirements for these two instruments are summarized in table 1.

The SECO-type television camera tube has been described in detail elsewhere and will only be summarized here (refs. 1 and 2). The Westinghouse WX-32193, 70-millimeter (2.8-inch) magnetically focused SECO tube is shown in figure 1. The image section is made of ceramic rings to make the tube more rugged. This also makes it possible to process various photocathodes in the tube using metal tabulations that can be pinched off after the photocathode is evaporated. Considerable design effort has gone into eliminating most of the

TABLE 1.–*Sensor Requirements*

Instrument	Format	Spectral response
f/24 field camera	2000 by 2000 pixels; 50- by 50-millimeter (2.0- by 2.0-inch) format	S-20 on MgF_2
High-resolution spectrograph	2000 by 2000 pixels; 50- by 50-millimeter (2.0- by 2.0-inch) format	CsI on MgF_2; bialkali on MgF_2

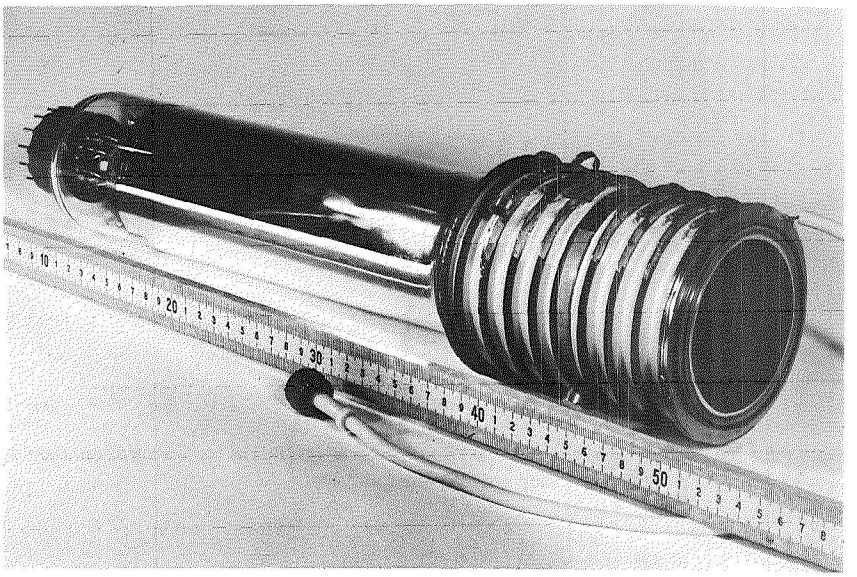

Figure 1.–Westinghouse WX-32193 70-millimeter (2.8-inch) SECO tube.

magnetic Kovar parts normally used in making these types of tubes. The ultraviolet transmitting magnesium fluoride window is sealed to the tube's metal flange using a heavy gold foil that allows for the differential expansion of the MgF_2 and the metal flange.

RESOLUTION

We are currently working on optimizing the image quality over the 70-millimeter format. The video signal corresponding to an image of 20 cycles per millimeter on the photocathode of the 70-millimeter SECO tube is shown in figure 2. Sixteen scan lines have been averaged together in a digital computer to reduce the noise and thereby allow more accurate measurements at high spatial frequencies where the statistical fluctuation in the number of photoelectrons per half cycle is a correspondingly greater percentage of the signal. The spatial frequency response is lower. The modulation transfer function curve obtained in this way is shown in figure 3.

PHOTOMETRIC PERFORMANCE

The photometric performance of the SECO tube is of considerable importance in the Space Telescope mission. Accurate photometric measurements are difficult to make and have been found to be very time consuming in dealing with a detector with such a large number of picture elements. Work has

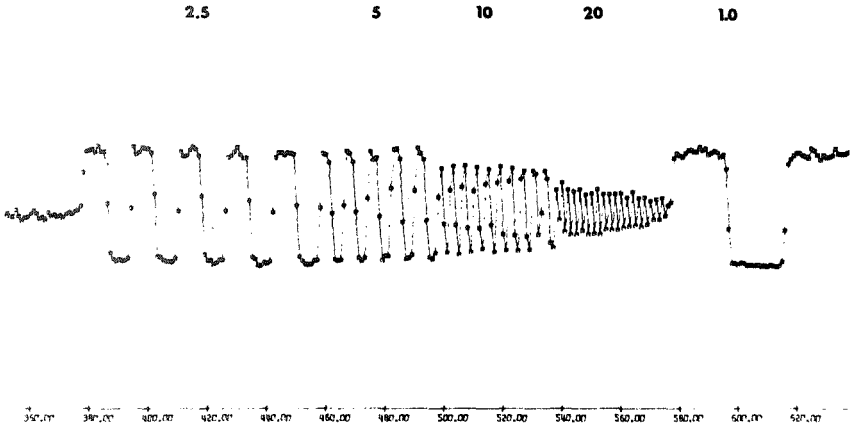

Figure 2.–Average of video signal from 16 scans across resolution test pattern; numbers at top are frequency in hertz.

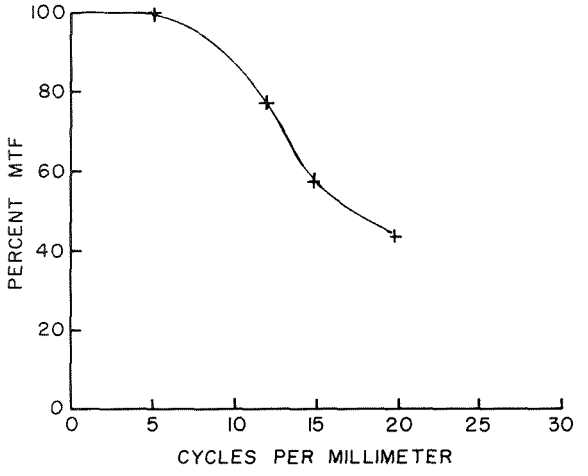

Figure 3.–70-millimeter (2.8-inch) SECO square wave modulation transfer function.

been going on for the past year to measure the stability of the photometric transfer function and to measure the signal-to-noise characteristics (ref. 3). The data in table 2 have been obtained with the 35-millimeter (1.4-inch) format SECO tube but are expected to be the same for the 70-millimeter (2.8-inch) tube because the target characteristics are the same. In an ideal tube, the signal S, defined as the total number of photoelectrons measured in a single pixel,

TABLE 2.–*Signal and Noise in 50 Pixels*

S, photoelectrons per pixel	79	156	312	625	1250	2500	5000
N, photoelectrons per pixel	20	26	35	50	70	122	265
S/N, photoelectrons per pixel	4	6	8.8	12.5	17	21	19
$\sqrt{S}/(S/N)$, photoelectrons per pixel)$^{1/2}$	2.2	2.1	2.0	2.0	2.1	2.4	3.7

would be related to the corresponding noise N by the equation

$$N = \sqrt{S} \tag{1}$$

The tests show that within a square pixel 50 micrometers on a side the noise level is increased above equation (1). Representative results are shown in table 2 from a tube cooled to -50° C, but are representative of operating the tube at about -10° C. The dominant thermal effect is the photocathode dark current.

As shown in table 2, the S/N ratio is evidently less than the ideal value predicted from equation (1). At low exposure the signal-to-noise is dominated by the readout noise, which is primarily the preamplifier noise. At intermediate exposures the signal-to-noise ratio S/N is about half the ideal value, presumably because of statistical fluctuations in the electron multiplication in the KCl target and some loss in photoelectrons due to reflection and absorption by the Al_2O_3 target substrate and aluminum signal plate. At high exposure the target begins to be saturated, the electrical signal per photoelectron decreases, and the tube becomes noisier, resulting in a decline in S/N. The net result is a dynamic range from about 50 to 2500 photoelectrons per 50-micrometer pixel, with a S/N ratio over this range that is about half the value for an ideal detector.

ASTRONOMICAL OBSERVATIONS

The 35-millimeter format SECO tube WX-31718 has been used by Morton and Crane at Princeton for a number of ground-based observations. There has been one Aerobee rocket flight carrying an ultraviolet echelle spectrograph with the 35-millimeter (1.4-inch) SECO as the data sensor. Unfortunately, the optics became contaminated during launch, but the SECO camera worked during the flight and after the parachute landing.

Figure 4 shows the spectrum of a Seyfert galaxy (*A New General Catalog of Nebulae and Clusters of Stars (NGC)* no. 1068 taken by Morton with the SECO camera on the Hale 5-meter (200-inch) telescope coudé spectrograph. The spectrum is from 387 to 412 nanometers and is 27 seconds-of-arc wide. This galaxy has strong emission lines as well as absorption. It is interesting to note

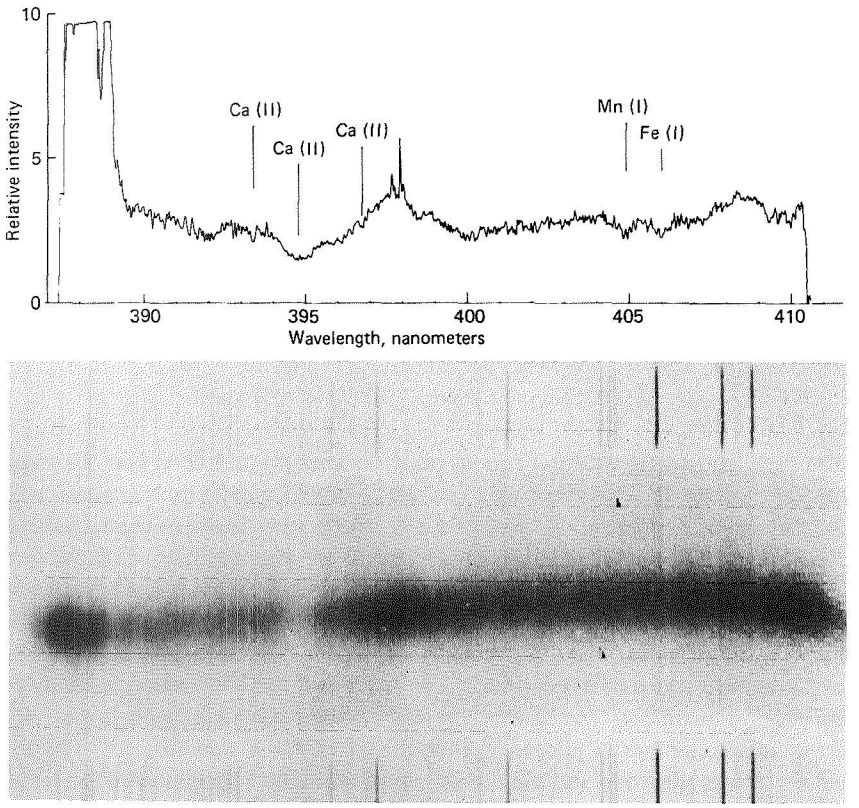

Figure 4.–Spectrum of NGC 1068 made with SECO television cameron on Hale 5-meter (200-inch) telescope coudé spectrograph.

the strong calcium (II) absorption in the Seyfert galaxy caused by the rotational velocity of the stars about the nucleus of the galaxy.

ENVIRONMENTAL TESTS

The Space Telescope-Space Shuttle launch environment has been interpreted in terms of quantification test levels for the subsystems as shown in table 3.

RADIATION BACKGROUND

Trapped energetic charged particles and cosmic rays are of particular concern in sensitive electrooptical detectors because of the background signal generated by these particles striking and/or passing through the windows and dynodes of the detector. Recent measurements by Viehmann et al. (ref. 4) of the fluorescence of MgF_2 indicate that in the Space Telescope orbit one can expect about 100 photoelectrons per centimeter per second from an S-20

TABLE 3.–*Subsystem Tests*

Test	Level	Range, hertz
Acceleration	33*g*	–
Acoustic	152 decibels	8 to 8000
Shock	57*g* to 225*g*	200 to 400
	225*g*	400 to 1250
	225*g* to 300*g*	1250 to 1600
	300*g*	1600 to 4000

photocathode. This is comparable to the night sky surface brightness of magnitude 23 per square second of arc when imaged at *f*/24 through an optical filter 3 nanometers wide. Therefore, the radiation background will not be significant for most of the *f*/24 camera observations. The radiation background from the bialkali photocathodes planned for the high-resolution spectrograph is expected to be less than 20 percent of the S-20 photocathode's radiation-induced background because of the long wavelength insensitivity of these photocathodes. However, the radiation background will probably set the lower limit on the system sensitivity because, in this case, the spectral filtering on the night sky background is much greater.

Radiation background measurements on the SECO tubes over a wide energy range are planned for later this year to confirm these estimates.

ACKNOWLEDGMENTS

Most of the results reported in this paper were obtained by Paul Zucchino and Don Long. Dr. D. Klinglesmith, Goddard Space Flight Center, has been helpful in the video image processing. The astronomical observations of NGC galaxy no. 1068 were made by Dr. D. C. Morton of Princeton. The tubes were made under the supervision of Dr. J. Pietrzyk at Westinghouse. This work is supported by NASA contract NAS-5-20833.

REFERENCES

1. Goetz, G. W.: *Advances in Electronics and Electron Physics,* vol. 22A, Academic Press, Inc., 1966, pp. 219-227.
2. Boerio, A. H.; Beyer, R. R.; and Goetz, G. W.: *Advances in Electronics and Electron Physics,* vol. 22A, Academic Press, Inc., 1966, pp. 229-239.
3. Lowrance, J. L.; and Zucchino, P.: *Methods of Experimental Physics,* vol. 12, pt. A, ch. 6.3, Academic Press, Inc., 1974, pp. 277-313.
4. Viehmann, W.; Eubanks, A. G.; Pieper, G. F.; and Bredekamp, J. H.: "Photomultiplier Window Materials Under Electron Irradiation: Fluorescence and Phosphorescence." *Applied Optics,* vol. 14, no. 9, Sept. 1975, pp. 2104-2115.

THE INTENSIFIED-CHARGE-COUPLED DEVICE AS A PHOTON-COUNTING IMAGER

Jack T. Williams
NASA Goddard Space Flight Center

The sensor is the limiting factor in any imaging system. This is especially true in astronomy where imaging low light level requirements are extreme. Sensors currently in use such as film, photomultiplier tubes, and TV cameras have severe limitations in astronomical applications that we feel can largely be overcome using a solid-state intensified-charge-coupled device (ICCD) as a photon-counting sensor.

MECHANICS

The ICCD is an extremely simple device consisting of three basic parts:

(1) The photocathode for wavelength discrimination and generation of electrons
(2) A focusing method, which can be proximity, electrostatic, or magnetic, as required
(3) A charge-coupled device (CCD) for signal storage and readout

The CCD itself is a near-perfect analog shift register in which photon- or photoelectron-generated signal charge is transported over large distances within a silicon chip to a low-noise charge sensitive amplifier. The arrays being used are Texas Instruments Inc. 100 by 160 arrays that have been thinned for back-side illumination to eliminate problems with the front-side gate structure. These devices are three-phase buried-channel arrays with a resolution element size of 23 by 23 micrometers (0.9 by 0.9 mil). The use of a thinned back-side-illuminated device allows us to overcome the degradation in performance that occurs in front-side-illuminated devices due to the necessity of acquiring signal either through or between the electrode gate structure with resultant absorption and interference effects. Buried channel devices were selected because of their higher charge transfer efficiency and low noise characteristics at room temperature. When operating, a CCD charge is stored within the pixel elements; then by proper sequencing of the gate electrodes, the signal is clocked in a parallel manner, one line at a time, into a serial shift register where it is clocked out through a charge sensitive amplifier one pixel at a time.

PERFORMANCE

In any photon-counting device, the goal is to be photon noise limited. This means that in CCD application, the inherent CCD noise must be less than the noise associated with the photoelectron generation process at the photocathode. To accomplish this, a number of factors must be considered:

(1) Gain, which is accomplished by secondary generation of electrons within the CCD at the rate of one for each 3.5 electron volts of accelerating potential
(2) Losses within the CCD because of surface dead layers and charge transfer efficiency
(3) The possibility that the signal from a photon event may be divided evenly among four adjacent pixels

Once all these factors are taken into account, one finds that the required performance characteristics are as shown in table 1. Table 1 also shows the measured values of currently available CCD arrays, indicating that current CCD technology can produce arrays of sufficient quality for photon counting.

TABLE 1.—*Performance Characteristics*

Parameter	Required	Measured
Gain	6000	<6000
Charge transfer efficiency	0.9992	0.9996
Root-mean-square noise electrons	100	80

RESULTS

To date, actual laboratory results show that CCD will operate in the intensified mode and can survive the processing required to place the array in a tube bottle with a photocathode. This was accomplished in a cooperative program with the Army Night Vision Laboratory that resulted in the successful fabrication of a proximity-focused ICCD that is currently undergoing testing at Goddard Space Flight Center.

FUTURE

The proximity tube cannot, nor was it intended to, do photon counting; however, a magnetically focused device has been designed and is being fabricated for delivery late in 1975 that should be able to do single photoelectron detection.

INFRARED CAPABILITIES

R. T. Hall
Aerospace Corp.

T. Kelsall
NASA Goddard Space Flight Center

D. E. Kleinmann
Center for Astrophysics

and

G. Neugebauer
California Institute of Technology

One of the seven instruments proposed for the four instrument bays aft of the primary mirror of the Space Telescope is the infrared photometer. Its design requirements have been specified by us, in our capacity as the Infrared Instrument Definition Team. This instrument will use at least two detector channels to cover the 2- to 1000-micrometer-wavelength range; present plans call for either a Si:As or a Si:P photoconductor for use from 2 to 24 micrometers or ∿30 micrometers, respectively, and a bolometer for the longer wavelengths. The photometer will feature cooled interchangeable field stops and filters for each channel. The passband of the filters will nominally be 10 percent of the effective wavelength, although some may be as wide as 50 percent. The field stops will range from the diffraction-limited beam size for the shortest wavelength in a channel up to 10 times the diffraction-limited beam size for the longest wavelength in that channel. The detectors, filters, and apertures will be placed in a dewar and maintained at a temperature less than 2 K for an in-orbit lifetime of at least 1 year. Chopping will be accomplished by wobbling a mirror on which the primary mirror is imaged. This chopping mirror is located in the warm relay optics forward of the dewar. The chopping frequency will be adjustable from 5 to 35 hertz, and the amplitude will be adjustable from 0.4 to 210 seconds of arc on the sky.

DETERMINANTS OF SYSTEM PERFORMANCE

Absence of Atmosphere

For the Space Telescope there will be no atmosphere to attenuate the signal; to produce a position-dependent, time-varying background; or to degrade the

angular resolution because of "seeing." In giving the angular resolution of several large telescopes, figure 1 shows that unless the seeing disk is smaller than 1 second of arc, the Space Telescope will provide higher angular resolution than any ground-based telescope out to approximately 5 micrometers. It also shows that the larger ground-based telescopes do not enjoy the full advantage of their size until 20 or 30 micrometers, where atmospheric attenuation begins to preclude all ground-based observation out to 1 millimeter, except for a rather occasional window at 350 micrometers.

Noise Power

Figure 2 shows the individual noise powers of each of the most significant contributors to the system noise power, which is the square root of the sum of the squares of the noise power from each element. The curve labeled Space Telescope is the fluctuation in the background power that is incident on the detector through a diffraction-limited beam. It is the noise equivalent power that could be obtained if a perfectly efficient detector were available (ref. 1). The background noise equivalent power is a fundamental limit that can be relaxed only by reducing the background on the detector; e.g., by lowering the

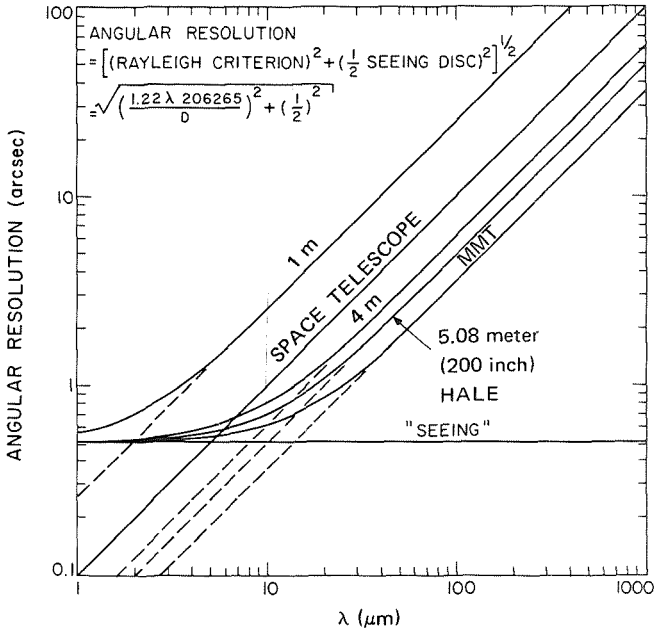

Figure 1.–The effect of atmospheric seeing on angular resolution. (Diffraction-limited optics and a seeing disk 1 second of arc in diameter are assumed; MMT = multimirror telescope.)

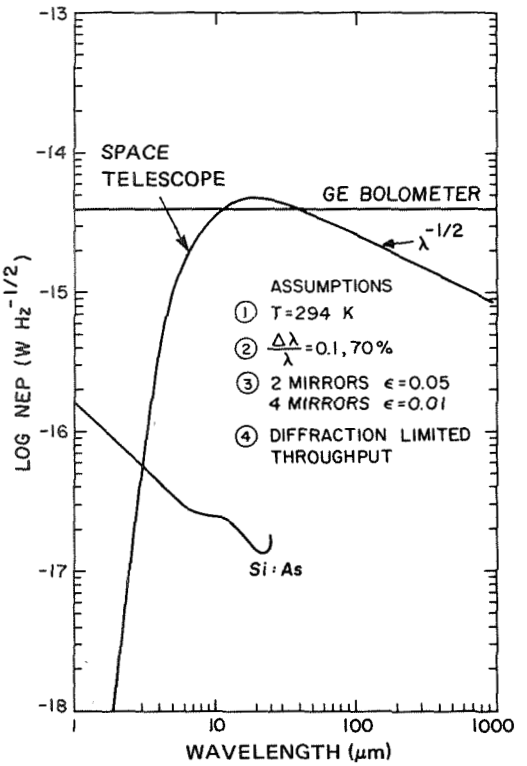

Figure 2.–Individual contributions to the system noise. Specific inputs to the calculation of the background radiation noise power conform to the properties of the Space Telescope and of the infrared photometer. (NEP = noise equivalent power; ϵ = emissivity.)

temperature or emissivity ϵ of the background, by reducing the optical throughput, or by reducing the bandpass of the cold filter.

Figure 2 also shows the intrinsic noise for two detectors of possible application on the Space Telescope. The performances indicated for these detectors have not yet been achieved; nevertheless, the projections are modest and do not require significant development in the state of the art.

SYSTEM PERFORMANCE

The noise equivalent power measures the system performance at the detector. From an astronomical point of view, it is more useful to know the system performance at the entrance aperture, indicated by the noise equivalent flux density given in figures 3 and 4. This value gives the flux into the telescope

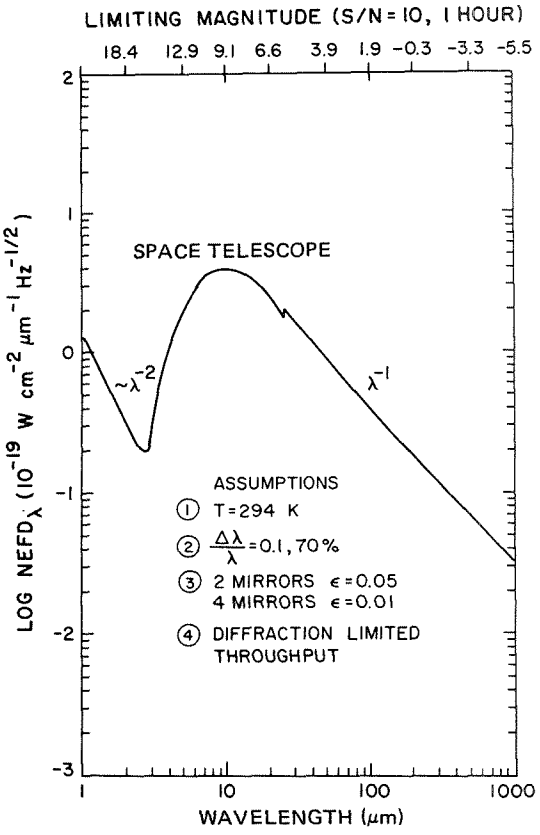

Figure 3.–Noise equivalent flux density (NEFD) and limiting magnitude as functions of wavelength.

that would produce a root-mean-square signal-to-noise ratio of 1 in a 1-hertz bandpass; or, equivalently, in 1/2 second of integration time.

Limiting magnitudes are also shown at the top of figures 3 and 4. For this paper these are defined to be the visual magnitude of the A-0 star (T = 9200 K) that could be measured with a root-mean-square signal-to-noise ratio of 10 in a 1-hour integration.

SOME POSSIBLE APPLICATIONS IN FAR INFRARED ASTRONOMY

Figure 5 puts the performance of the Space Telescope into astronomical perspective by addressing the question, "How far could some of the bright, well-known far infrared sources be removed before the Space Telescope would require 1 hour to make 10-σ measurement?" Galactic objects are shown on the

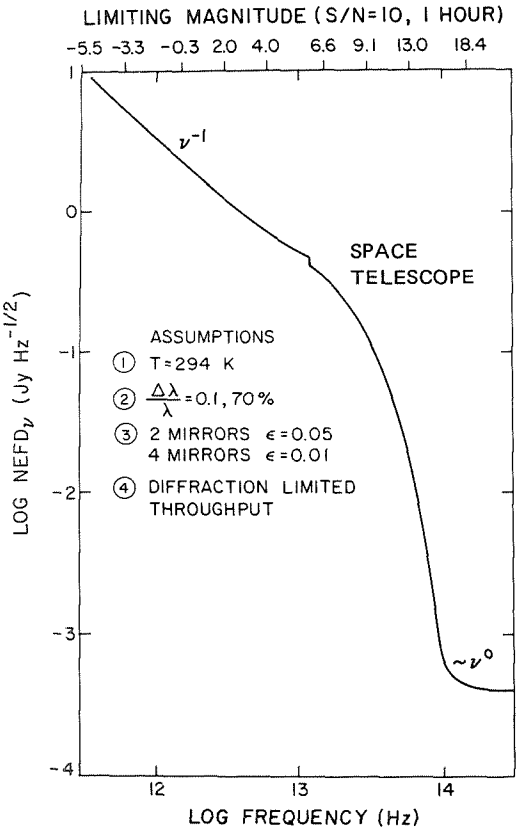

Figure 4.—Noise equivalent flux density and limiting magnitude as functions of frequency.

left in figure 5 and extragalactic objects are shown on the right. Several distance milestones are indicated by the dashed horizontal lines, each of which is labeled on the right. The actual distance of each source is indicated by the x on its line, except for NGC 2024 and Orion, which are too close to be accommodated within the boundaries of this figure. Figure 5 was prepared by comparing figures 3 and 4 with far infrared flux measurements (preferably those with effective wavelengths between 65 and 100 micrometers) compiled from the literature (refs. 2 to 7). Note however, that neither 3C 273 or Markarian 231 have been measured at approximately 100 micrometers. An estimate of the 100-micrometer flux from 3C 273 was obtained by interpolating between the approximately 20 jansky seen at 3 millimeters (ref. 8) and the 0.4 jansky seen at 10 micrometers (ref. 9). The far infrared flux from Markarian 231 was estimated by assuming that that resemblance between

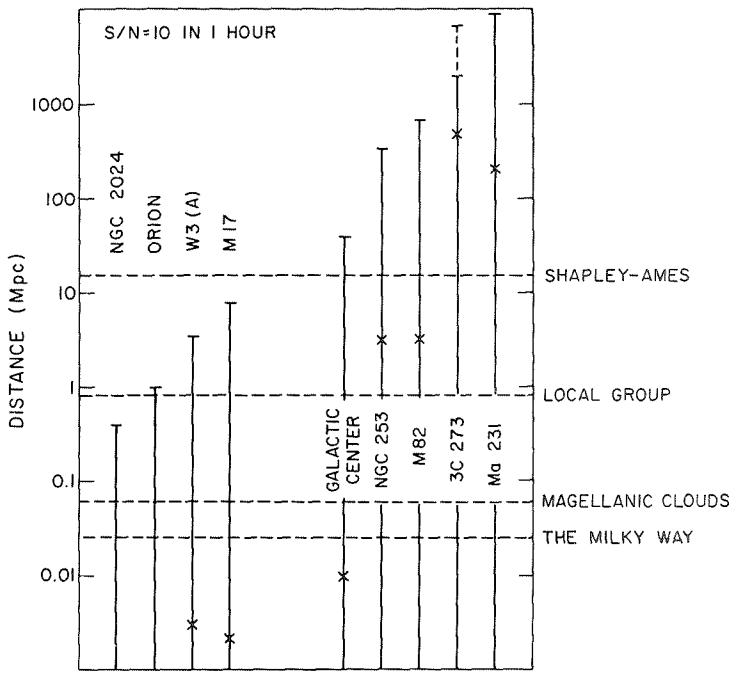

Figure 5.–The far infrared observability of galactic and extragalactic sources. (Mpc = million parsecs; x is the actual distance of each source; Ma = Markarian.)

M82 and Markarian 231 from 10 to 20 micrometers (Rieke, private communication) continues out to approximately 100 micrometers. From the observed ratio of their 10-micrometer fluxes (ref. 10), one therefore would expect that the 100-micrometer flux for Markarian 231 would be about 1/20 as bright as that observed for M82.

Figure 5 suggests several intriguing observational programs. It would be possible, for example, to determine the number and location of all the sources similar to the Orion nebula, W3(A), or M17 in each of the galaxies in the local group. It should be possible to monitor the quasi-stellar source, 3C 273, to determine whether there is variability at 100 micrometers, and, if so, to compare it with that reported at 3 millimeters (ref. 8). It would be possible to make a far infrared survey of all 1149 galaxies in the *Shapley-Ames Catalogue* to determine which have phenomena like those found in the galactic Center.

REFERENCES

1. Smith, R. A.; Jones, F. E.; and Chasmar, R. P.: *The Detection and Measurement of Infra-Red Radiation*. Second ed. Oxford University Press, Inc., 1968, pp. 214, 288.

2. Hoffmann, W. F.; Frederick, C. L.; and Emery, R. J.: *Astrophysics Journal Letters,* vol. 170, 1971, p. L89.
3. Harper, D. A.; and Low, F. J.: *Astrophysics Journal Letters,* vol. 165, 1971, pp. L9-L13.
4. Harper, D. A.; and Low, F. J.: *Astrophysics Journal Letters,* vol. 182, 1973, pp. L89-L93.
5. Emerson, J. P.; Jennings, R. E.; and Moorwood, A. F. M.: *Astrophysics Journal,* vol. 184, 1973, pp. 401-414.
6. Fazio, G. G.; Kleinmann, D. E.; Noyes, R. W.; Wright, E. L.; Zeilik, M., II; and Low, F. J.: *Proceedings European Space Laboratory Symposium* (Frascatti, Italy), 1975, pp. 79-85.
7. Olthoff, Henk: Ph.D. dissertation, 1975.
8. Fogarty, W. G.; Epstein, E. E.; Montgomery, J. W.; and Dworetsky, M. M.: *Astrophysics Journal,* vol. 76, 1971, pp. 537-543.
9. Kleinmann, D. E.; and Low, F. J.: *Astrophysics Journal Letters,* vol. 161, 1970, pp. L203-L206.
10. Rieke, G. H.; and Low, F. J.: *Astrophysics Journal Letters,* vol. 176, 1972, pp. L95-L100.

THE EUROPEAN SPACE AGENCY STUDY OF PHOTON COUNTING IMAGING FOR THE SPACE TELESCOPE

R. J. Laurance
European Space Agency

In early 1974 an agreement was reached between the European Space Research Organization (ESRO; now the European Space Agency (ESA)) and NASA on possible cooperation on the Space Telescope program. It was agreed that ESRO would consider the possibility of providing one of the focal plane instruments for the telescope. During 1974 preliminary studies were conducted and two focal plane instruments, the faint object spectrograph and the *f*/96 high resolution camera, were selected as possible candidates for European development. One of the important features of these instruments was that they were proposed to use imaging detectors working in the photon counting mode. This requirement was established by the NASA Instrument Definition Teams for these instruments to achieve the full potential of Space Telescope performance.

During 1975 the instrument choice has been narrowed down to the camera, and a change of name to the faint object camera has been made. Imaging faint objects is so important to the cosmological studies to be made by the Space Telescope. The European Space Agency is now actively engaged in studies of the faint object camera and its detector system.

OPERATIONAL CONCEPT OF THE DETECTOR

The operational concept of the Image Photon Counting System is shown in figure 1. Incoming photons are first converted to photoelectrons by photoemission from a photocathode. By means of a suitable image intensifier, each photoelectron is amplified to a sufficient degree so that unambiguous detection can take place. The detectors in the systems we are considering are image tubes, but other detectors like charge-coupled devices could also be considered. The coupling between intensifier and image tube may be fiber optic coupling or a lens relay, if sufficient gain is available. A number of solutions are possible for the intensifier/image tube combination ranging from solutions with high gain in the intensifier and low sensibility in the image tube to those with low gain intensifiers and high sensitivity image tubes.

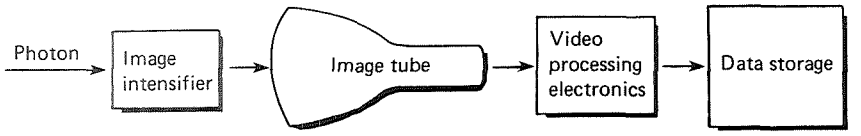

Figure 1.–Concept of Image Photon Counting System.

The image tube continuously scans the output of the intensifier. The photoelectron events appear as light scintillations and will be detected on several lines of the television scan. It is, therefore, necessary to identify the center of each photon event. Failure to do this would give different weight to each detected photon, resulting in a loss in image signal-to-noise ratio. This is carried out by a set of pattern recognition logic signals in the video processing electronics. The output of the processing electronics are the x and y coordinates of each detected photon. This information is passed to the data storage and the work location corresponding to these x, y coordinates is incremented by 1. Prior to an exposure, all locations in storage are set to 0. While the exposure is in progress, the image may be examined and the exposure terminated when the image signal-to-noise ratio is adequate.

One advantage gained by the inclusion of centering logic is the reacquisition of some of the resolution lost in amplifying the image. Most systems will require more than one stage of amplification, as shown in figure 2. A photoelectron leaving a point on the primary photocathode A deviates slightly from the axis according to the magnitude of its initial velocity components and lands on the first dynode B at a position governed by a two-dimensional probability function, the shape of which is identical to the large signal point spread function of the first stage (i.e., the integrated electron density profile at the first dynode B resulting from a large number of input electrons). Due to multiplication at the dynode, a large number of input electrons is emitted, and acceleration through subsequent stages of the system results in a recorded scintillation (with a finite spatial profile determined by the imaging characteristics of the system after the first stage) on the final target C. The video processing electronics locates the center of the scintillation and records its position in a memory location D, which is conjugate with the position in which the primary photoelectron struck the first dynode B.

For a large number of electrons originating from the same point on A, integration in the external memory ΣD of the image-processed events results in an "image-processed point spread function" very similar to the first stage ΣB, and considerably sharper than the point spread function normally obtained by analog integration of the final target ΣC (= convolution of first stage point spread function and scintillation profile).

It is also possible to eliminate the effect of ion scintillations in the video processing electronics. Ion scintillations occur in nearly all image intensifiers.

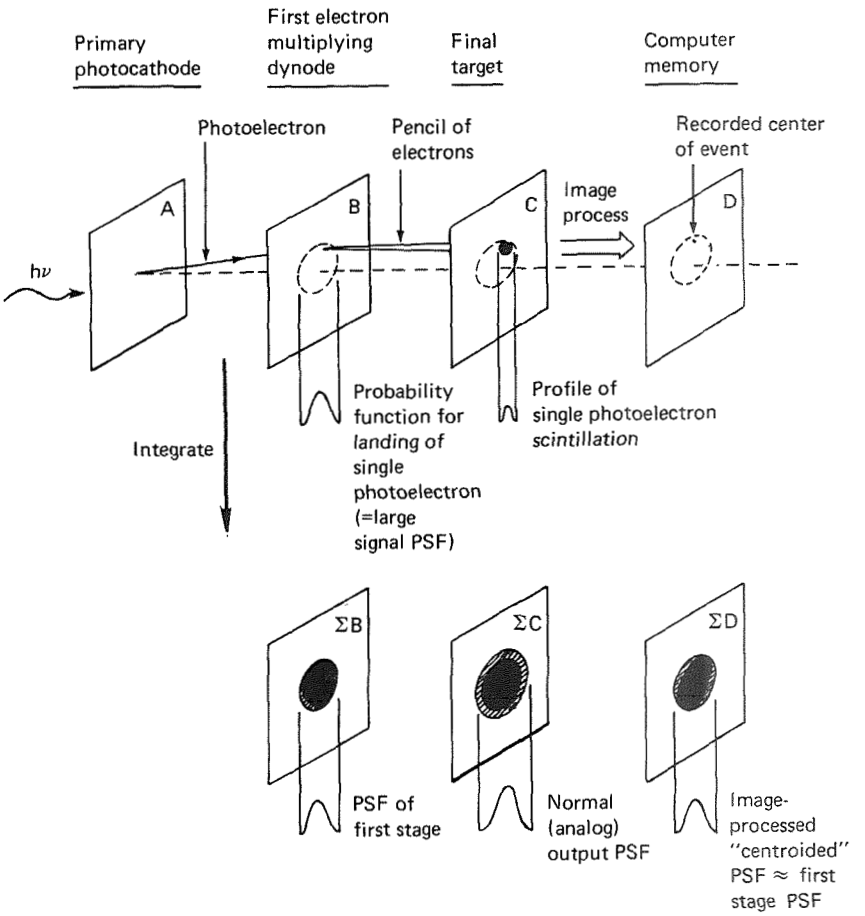

Figure 2.–Diagrammatic representation of the effect of centroiding on system point spread function (PSF).

As they consist of a group of some 15 electrons, they are given disproportionately higher recording weight in analog systems. However, because of their large amplitude compared with a single photoelectron scintillation, they are easily discriminated against in the logic of the Image Photon Counting System.

CONFIGURATIONS UNDER STUDY

At the beginning of 1975 two studies were initiated by ESA with the task of defining the preferred configuration of components for an Image Photon Counting System. These studies identified three configurations worthy of further consideration.

The first configuration identified is based on a system developed at University College in London that is now in extensive use for ground-based astronomical observations. It consists of a four-stage magnetically focused cascade intensifier having a blue light gain in excess of 10^7 which is optically coupled via a lens relay to a plumbicon image tube. This system has been well described (refs. 1 and 2).

For use in the Space Telescope, a number of changes must be made. The image intensifier must first be made sensitive to the vacuum ultraviolet, and for this it is necessary to change the input window to MgF_2. In the ground-based system, the focus solenoid of the four-stage intensifier dissipates ≈350 watts to obtain the double loop focus field of 280 gauss. This power is far in excess of the power available to the instrument in the Space Telescope.

It may be possible by careful optimization of the coil design and by operating the intensifier at single-loop rather than double-loop focus to reduce this figure to 70 watts. A scheme using this concept is shown in figure 3. Even this power level is likely to be excessive in the Space Telescope application; therefore, an alternative system using a permanent magnet focus assembly has also been studied. A scheme using this concept is shown in figure 4.

Because of the good resolution performance of the intensifier magnetically focused first stage, the system is capable of achieving a high number of independent pixels although the resolution when measured in an analog mode will be poorer. For a usable image diagonal of 35 millimeters on the input faceplate, it is possible to obtain 1230 square pixels, which is in excess of our requirements. The pixel size is 20 micrometers, and therefore only modest cooling will be required to keep the dark current to an acceptable level.

The disadvantage of this system for the Space Telescope is its large size and mass compared with the other detector systems being considered. The

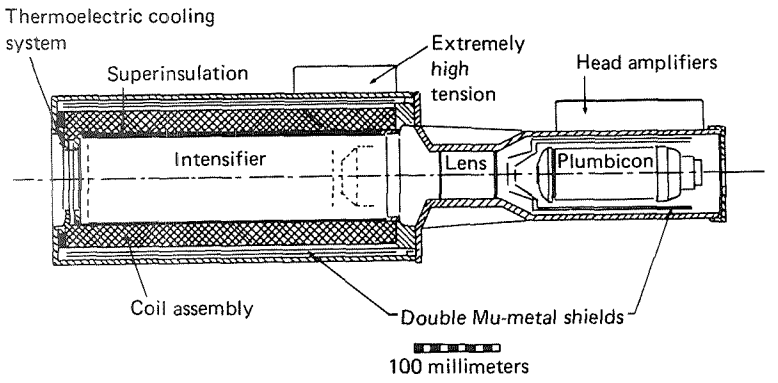

Figure 3.–Image Photon Counting System using four-stage intensifier with magnetic focus solenoid.

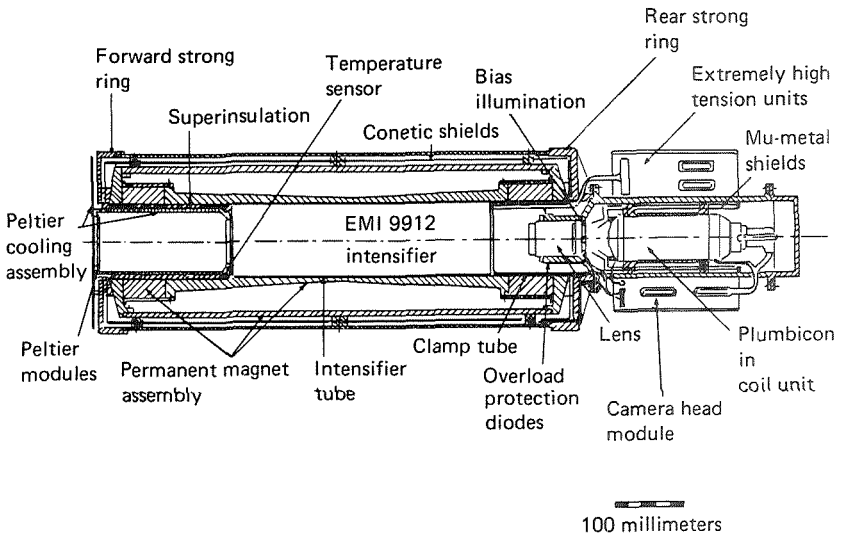

Figure 4.—Image Photon Counting System using four-stage intensifier with permanent magnet assembly.

attraction, however, is its good performance and its already proven operation in ground-based systems. The only problem foreseen is in the modification of the four-stage intensifier to meet the launch and landing environments. A program of work is currently under way to procure modified intensifiers; a breadboard system will be evaluated next year.

The second configuration being considered is an intensified electron bombardment silicon (EBS) system. The EBS image tube (because of its higher sensitivity) allows a lower gain in the image intensifier. If the EBS system is operated with an electrostatic intensifier, it is also possible to fiber optically couple them together. This is not possible in the first solution because the magnetic field of the intensifier would disturb the operation of the image tube. This leads to a further lowering of the required intensifier gain because of the absence of the loss in lens coupling (usual efficiency $\approx$ 1 degree). It is not possible however to operate the system with a single stage of electrostatic intensification because the input photocathode is curved. When working in the visible, it is customary to use a fiber optical input window to correct from the flat input to the curved photocathode. This is not practical in the ultraviolet because of absorption of fiber optics in this range. It is, therefore, necessary to include a proximity-focused image converter tube fitted with a flat MgF_2 input window at the input of the system.

Such a system is shown in figure 5. It uses a 40-millimeter (1.6-inch) proximity-focused converter (EEV-P-8103 or ITT-F-4122), a single stage intensifier (Varo 8605), and an EBS camera tube with DEMC target

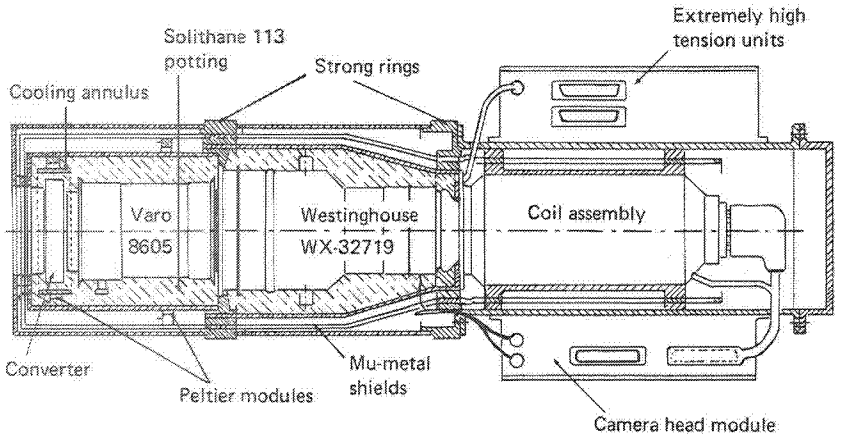

Figure 5.–Image Photon Counting System using EBS tube.

(Westinghouse WX-32719). This system will provide 465 square pixels when operating with a 32-millimeter (1.3-inch) target EBS (WX-32432) system or 575 square pixels with a 40-millimeter (1.6-inch) EBS (WX-32719) system.

It should be noted that the long-term integration is being performed in the data storage and the EBS tube is only integrating and storing photon events for a maximum of a frame time (<100 milliseconds). It is, therefore, not necessary to cool the EBS target as is usually the case when working in an analog mode. Cooling the converter photocathode to 0° C may be required to keep the dark current to an acceptable level.

Although an EBS Image Photon Counting System has never been practically demonstrated, it uses commercially available components that should not be too difficult to space qualify. Theoretical analysis indicates it has a good chance of successful operation, with a well-peaked pulse amplitude distribution. The only uncertainties are whether the effects of structure in the fiber optical coupling and EBS target could produce practical problems. A breadboard of the EBS detector system will be assembled and evaluated as part of the program of Space Telescope detector development by ESA.

The third detector system identified uses a microchannel plate image intensifier. Considerable interest in this system has been raised because of its high gain and compact size. Its negative exponential pulse amplitude distribution (characteristic of the microchannel plate image intensifier with straight channels) is, however, unsatisfactory for an Image Photon Counting System. The development of the microchannel plate image intensifier with curved channels allows operation in the saturated mode and gives a well-peaked pulse amplitude distribution ideal for this application. The configuration proposed for the Space Telescope detector system is shown in figure 6. The microchannel plate image intensifier with curved channels is incorporated into

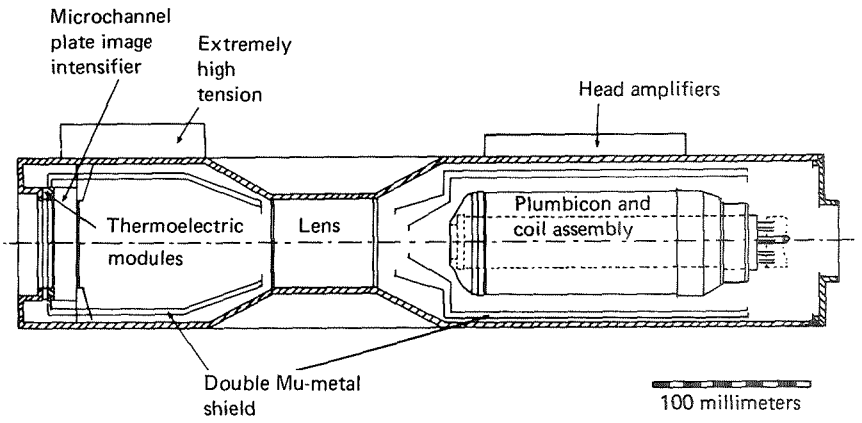

Figure 6.–Image Photon Counting System with microchannel plate image intensifier using curved channels.

a tube with proximity-focused input and output. This allows the use of a flat-faced MgF_2 input window and results in zero image distortion. With a microchannel plate image intensifier with a length-to-diameter ratio of 70 to 80, a gain of 10^6 should be possible. The tube can either be fiber optically coupled to a 5.1-centimeter (2-inch) Vidicon, or, as shown in figure 6, lens coupled to a Plumbicon. It is expected that a 40-millimeter (1.6-inch) microchannel image intensifier with 12- or 15-micrometer channels would provide a picture format of 500 by 500 pixels. The system is likely to have a higher detective quantum efficiency than either of the other two solutions because of the increased detection efficiency of the wafer structure. Because of the uncertain development problems of the microchannel plate image intensifier with curved channels, this system is not presently being proposed as a candidate detector for the Space Telescope. It is thought to be a worthwhile area of development for future Image Photon Counting Systems, and plans are being prepared for its further development on a longer time scale.

DATA STORAGE REQUIREMENTS

All the detector systems discussed are dependent on the provision of data storage for performing the image integration. This storage forms part of the Image Photon Counting System and its performance may well limit the capability of the total system. The baseline design being considered has 500 by 500 pixels. Data storage must therefore have a quarter of a million words, each word consisting of 16 bits; this will allow the accumulation of approximately 65×10^3 photons per pixel. One of the most important parameters of the data storage is its access time. The image tube will be capable of reading at a rate of 10 million pixels per second, which dictates an access time of 100

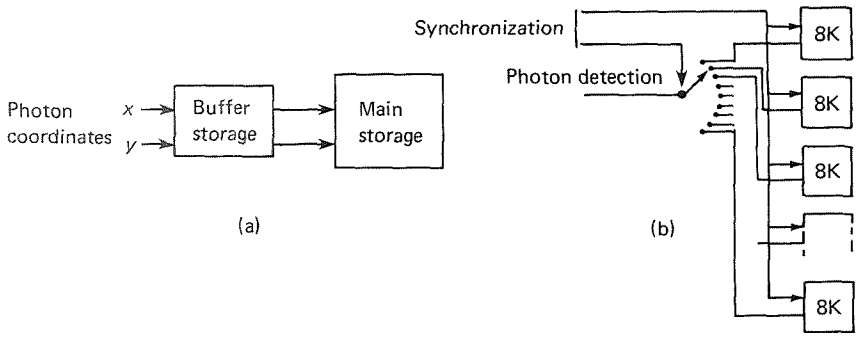

Figure 7.–Two possible configurations of the data storage.

nanoseconds. However, the counting rate of photons will not be greater than 1 million photons per second because dead time corrections and counting losses will be excessive for rates greater than this. Two approaches to data storage have been considered. The first consists (see fig. 7 (*a*)) of main storage buffered by a fast shift register that temporarily stores the x, y coordinates of each photon event recorded. The shift register has a speed capable of accepting the highest instantaneous rates expected from the video processing logic. The main storage can thus work at a slower speed corresponding to the average photon counting rate.

The second approach is to have a multiplexed storage as shown in figure 7(*b*). Each section of the storage need only have $n \times 100$-nanosecond access time, where n is the number of sections used. The sequencing of the storage is synchronized to the scanning of the image tube; when a photon is detected, the data work addressed at that instant is incremented by 1. Hybrids of these two schemes are also possible. The second approach is presently favored.

A number of technologies are possible for data storage. Among the most promising are C-mos, magnetic bubbles, and core. The baseline design presently being considered by ESA is a core storage based on technology developed for Helios. It consists of 32 sections of 8000 words, each with an access time of 2.5 microseconds. It will consume less than 50 watts when working at 10 percent duty cycle (corresponding to a maximum counting rate of 1 million photons per second). The required reliability will be obtained by including spare sections. The estimated mass of the data storage is approximately 40 kilograms (88 pounds) and the volume approximately 50 liters (1.4 cubic feet). ESA will be undertaking a detailed examination of this storage and the other technologies during the next 6 months.

DETECTOR ACCOMMODATION IN THE FAINT OBJECT CAMERA

Preliminary studies have been undertaken by ESA on the Space Telescope faint object camera, and these demonstrate the satisfactory accommodation of

the Image Photon Counting System. This analysis has been restricted to the version of the system using the four-stage intensifier fitted with a permanent magnet focus assembly and using a core data storage. This configuration is considered to be the most difficult to accommodate. The camera includes a set of relay optics to allow the focal ratio of the camera to be chosen so that the resolution of the camera will be determined only by the optical telescope assembly. The system with magnetic focused intensifier has a modulation transfer function of 50 percent at 25 line pairs per millimeter (625 line pairs per inch) after centroiding, thus a slight magnification of the optical telescope assembly image will be sufficient to make the influence of the detector on the resolution negligible. This leads to a focal ratio of $f/36$. A switchable element allows the focal ratio to be changed to approximately $f/200$, allowing a speckle mode of operation to be used. In this mode, each pixel corresponds to 0.01 seconds of arc. Other modes of operation are also possible including a coronographic mask mode for the selection of faint companions to bright stars and a dispersive mode.

Two detector heads are included in the faint object camera for redundancy, a plane mirror being used to switch from one to the other. The electronics of the faint object camera are isolated thermally from the optics because of the large and variable dissipation of the data stored. A general purpose computer may be included to control the various modes of operation of the camera.

The overall design of the faint object camera has been shown to be feasible using the worst case Image Photon Counting System presently under consideration. The design presented includes redundancy where required and provides a flexible instrument having a number of different modes of operation. This instrument and its detector system should make a significant contribution to the operational performance of the Space Telescope program.

REFERENCES

1. Boksenberg, A.: "Image Photon Counting." *Applications Spatiales des Tubes de prises de vues,* National Center for Space Studies, Nov. 1971.
2. Boksenberg, A.; and Burgess, D. E.: "Image Counting System." *Astronomical Observations With Television Type Sensors,* a conference held at the University of British Columbia (Vancouver), May 1973.

DEVELOPMENT OF AN INFRARED SPECTRORADIOMETER

W. H. Alff and J. G. Thunen
Lockheed Missiles & Space Co., Inc.

An infrared spectroradiometer for the Space Telescope is being planned that will allow astronomers to perform observations in the infrared with sensitivities and angular resolutions impossible to achieve using Earth-based, balloon-borne, or aircraft-mounted instruments. To perform the required measurements, the basic instrument has been designed to operate diffraction limited over the spectral range from 2 to 1000 micrometers with approximately 10 percent resolution. The dynamic range capability (target brightness) will be at least 10^5, and special emphasis will be given to automated operation and data processing. The detectors will provide essentially background-limited detection over the spectral range. To approach this sensitivity, it will be necessary to cool the detectors to approximately 2 K with supercritical liquid helium. The cooling system is thus integral to the performance of the radiometer and must have a lifetime of at least 1 year.

BACKGROUND-LIMITED PERFORMANCE

The background noise results from statistical fluctuations in the radiation incident on the detector from thermal background sources. For example, the primary and secondary mirror of the Space Telescope and the optical elements in the relay optics radiate according to Planck's law. The magnitude of the statistical variations in the power radiated from the various background sources is defined as the noise equivalent power, a function of electrical bandwidth detector area and wavelength. The noise equivalent power defines the system ability to detect low-level signals. To achieve background-limited performance, the detectors must be cooled to eliminate generation and recombination noise that is internally generated in the case of photodetectors and thermal noise (phonon noise) in bolometers. This requires the short wavelength detectors to be cooled to 4 K and the long wavelength detectors to be cooled to 1.8 K.

CRYOGENIC SYSTEM

The infrared detectors are maintained at 2 K or lower by a superfluid liquid cryostat. The ^{4}He (II) is maintained nominally at 1.8 K at its saturation pressure of 12.466 millimeters of mercury. These conditions are controlled by

a vent line orifice the diameter of which determines the flow rate for a given dewar heat leak. The heat load governs the evaporation rate. An increase in heat load, caused by use of the electronics, for example, causes an increase in dewar pressure. This increases the vent rate and pushes the system back toward the design point. A similar reaction occurs for a decrease in heat leak. The vent gas first passes through a porous plug that prevents the expulsion of liquid in zero gravity. The vapor then circulates through two vapor-cooled shields that are used to intercept the heat leak through the multilayer insulation, fiber glass struts, fill line, wiring, and detector cavity aperture. The warm vapor then passes through the vent orifice and is dumped overboard through a pair of opposed nozzles directed tangentially to the Space Telescope skin.

MODULATION NOISE

It is necessary to have the detector alternately view the source and then the background alone to remove the background radiation during measurement of a source signal. This can be accomplished using many different techniques. The method used in this design is to place a tilt in a pupil plane to generate the image translation. The telescope pupil (primary mirror) is imaged onto a flat mirror in the relay optics that is oscillated angularly with variable frequency (3 to 30 hertz) and variable amplitude (0.4- to 210-second field angle). No more than 10 percent of the cycle time is required to move the mirror frame from one position to the other.

In practice, the most difficult source of thermal radiation to predict and control is that which can cause a difference in the background between the signal and reference channels. The most common sources of this noise are emissivity and temperature gradients in the telescope baffles and optics and in the relay optics prior to the scan mirror. Scanning of these gradients develops a modulation noise. In the long wavelengths, diffraction effects further complicate the analysis.

Several steps have been taken in the design of this radiometer to reduce the level of modulation noise. Initial analysis indicates these steps will minimize thermal radiation differences seen by the detector to a level that can be successfully handled in the data processing.

DIFFRACTION EFFECTS

It can be assumed that all optical aberrations throughout the radiometer are negligible for wavelengths greater than a few micrometers. Diffraction, on the other hand, is not negligible. At wavelengths over 100 micrometers, the finite size of several critical instrument apertures diffracts energy that can significantly degrade the expected performance. Some of the results are as follows:

(1) Loss in signal intensity from a point source
(2) Incomplete modulation due to diffracted energy from the object into the adjacent field

(3) Increased background emission (higher noise equivalent power) reaching the detector from diffracted baffle sources just outside the pupil
(4) Increased modulation noise caused by variations in diffracted background radiation

Predicting the distribution of diffracted energy at the detector is accomplished by initially considering coherent imaging that treats diffraction from a point source in object space. The other half of the problem considers diffracted energy from a source originating in the plane of the primary mirror. Coherent imaging describes the effects of diffraction on predicted signal levels, while incoherent imaging is used to describe the background noise level.

For the specific design considered here, this analysis predicts a signal-to-noise degradation over that predicted geometrically by a factor of 4 at 1000 micrometers. A revised instrument design is not expected to improve on this loss. These effects are relatively minor, however, when compared to the major increases in signal level offered by the large aperture optics and space environment of the Space Telescope.

FAINT OBJECT SPECTROGRAPH

William P. Devereux
Ball Brothers Research Corp.

A faint object spectrograph is an instrument specifically designed to record the distribution, as a function of wavelength, of the energy emanating from a faint celestial object. Such an instrument is desired by the astronomical community to provide more data, hopefully leading to a better understanding of the nature of quasi-stellar objects and the validity of Hubble's law when applied to very distant galaxies.

THE NATURE OF A FAINT OBJECT SPECTROGRAPH

Several factors combine to make a faint object spectrograph. These factors include a telescope with a large collecting area, a detector that conserves the information content of every photoelectron generated, a design that is highly efficient in terms of the number and quality of surfaces used, and a spectrograph concept that makes efficient use of the available detector format and does not provide resolution higher than is necessary. The first two items are the Space Telescope and the intensified-charge-coupled device, both of which are discussed in separate papers. The design features are the subject of this paper.

DESIGN FEATURES

To assure high efficiency in design, three separate detectors are used in the spectrograph, each peaked for a different region, namely the visible, the near ultraviolet, and the vacuum ultraviolet. In addition, each of the detectors is used with two gratings so that operation is always near the blaze. The astronomy community agreed on a resolution of 1000 as meeting its needs, so that is the design value. The number of reflections was kept low by using a Wadsworth mount, and all mirror surfaces are coated to provide highest reflectance. A further increase in observing efficiency is achieved by the use of an image slicer that effectively triples the length of the detector format and allows the recording of more of the spectrum for each observing hour.

RESOLUTION-CHANGING OPTIONS

To permit the observation of even fainter objects, a collapsed dispersion is made available. In this mode, the mean resolution is decreased by a factor of

10, permitting more photons to fall on each picture element. In the visible and near ultraviolet ranges, prisms are used as the dispersing elements, and a grating is used in the vacuum ultraviolet where a suitable prism material does not exist.

For occasional observation of the fine detail of spectral features, there is also a high-dispersion mode with a resolution capability 10 times greater. This is achieved at the expense of sensitivity and simultaneous spectral coverage and can be used either with or without the image slicer.

A fourth mode of operation removes dispersion altogether by positioning an imaging mirror in the grating station and providing a near-diffraction-limited, photon-counting camera for viewing the area in the immediate vicinity of the target object.

ACCESSORY FEATURES

Other features of the instrument include a slit jaw camera, which is used as an aid in pointing the telescope at the object of interest, and a wavelength calibration lamp, which makes possible absolute wavelength determination of spectral features.

CONCLUSION

With the spectrograph it is possible to record spectra of magnitude 21 stars at a resolution of 1000 with 3 percent photometric accuracy in a 10-hour exposure. By reducing the accuracy to ±10 percent, and using the collapsed dispersion, this threshold can be dropped to magnitude 26 or 27. A faint object spectrograph worthy of the Space Telescope is within our grasp.

ACKNOWLEDGMENT

The encouragement provided by Space Telescope program personnel at NASA, by the scientific community represented by the Faint Object Spectrograph Instrument Definition Team, and by my colleagues at the Perkin-Elmer Co. and the Ball Brothers Research Corp. is gratefully appreciated.

HIGH-SPEED POINT/AREA PHOTOMETER CONCEPTUAL DESIGN AND INTEGRATION

William Bloomquist and Fred Steputis
Martin Marietta Corp.

The photometer will have the highest sensitivity and radiometric precision of all ultraviolet and visible instruments used on the Space Telescope and will provide a vast improvement over ground-based photometry. Advantages of orbital operation, exploited by the photometer, are accessibility of ultraviolet wavelengths absorbed by atmosphere, reduced veiling effects of air-glow and auroras, and freedom from spurious intensity and position modulation by inconstancies in the atmosphere.

Orbital operation makes the instrument inaccessible and places it in a harsh environment, requiring a highly reliable and tough instrument. The use of the Space Shuttle makes possible the recovery of a malfunctioning or obsolete instrument but does not relieve the photometer design from the necessity of meeting environmental challenges and performing well over a great period of time without maintenance.

The design presented here has both point and area photometry capability with provision for inserting filters to provide spectral discrimination. The electronics provide photon-counting mode for the point detectors and both photon-counting and analog modes for the area detector, which produces small field images with high resolution, precise photometric accuracy, and wide dynamic range. The analog mode allows the area detector to be used as a target locating device for the point detectors.

The original design allowed analysis of the state of polarization. The elements to provide this have been removed from the optical trains; however, the design is such that these elements could easily be restored.

The design and development approach will reflect the capability of the Space Shuttle to retrieve a Space Telescope that is not performing, either initially or as a result of failure during operation. The retrieval capability justifies the assumption of greater risk and the resultant savings through reduction of expensive design verification, development, qualification, and acceptance testing.

INSTRUMENT INTEGRATION

All the Space Telescope scientific instruments are packaged into common axial modules that are identical in exterior dimensions and in mechanical,

structural, and electrical connection interfaces. The photometer will be assembled as two submodules: optomechanical and electronics. These will be integrated into the larger common axial module.

INSTRUMENT GENERAL DESIGN

The instrument design concept introduces light from the optical telescope assembly past a contamination shutter and dark shutter to focus on the entrance aperture wheel where the desired portion of the image is selected. The light then diverges to two filter wheels in tandem. After spectral filtering, the light is reflected by one of four mirrors selected by a carrousel. Two of these mirrors are used to image the telescope's exit pupil on point detectors. Two mirrors are used as relay mirrors with secondary mirrors to reimage the light at either *f*/24 or *f*/96 and simultaneously to correct the optical telescope assembly astigmatism.

All the optical elements and detectors are attached to graphite epoxy optical bench rods. With an almost negligible coefficient of thermal expansion, the rods maintain the alinement. The rods are supported at midpoint and aft end on flexures to minimize stresses induced from deformations in the shell.

An aluminum radiator rejects heat from the thermoelectric device that cools the area detector to 230 K.

Mechanism Design and Mounting

Typical of the mechanisms that operate the optical elements is the aperture wheel assembly containing a variety of apertures used to limit the field of view. The smallest has a diameter of two Airy disks, or 72 micrometers. The need to center a point source within this opening is a controlling requirement on alinement tolerances. Initially calibrated using the area detector, it is required to have precise repeatability in the positioning of the apertures.

The wheel is driven by a stepper motor and positioned by a spring-loaded cam that seats into detents on the rim of the aperture wheel to assure repeatability of positioning. An optic encoder controls the positioning and indicates position. The entire assembly is mounted to the graphite epoxy bench rods and is adjustable to slide along the bench rod for initial adjustments with clamps to lock the assembly in place.

Instrument Electronics Support

Functionally, the electronics consists of several elements. Area detection consists of the detector, its intensifier and grid, high voltages, drive clock, signal conditioning, and a 16 000- by 16-bit memory. In photon-counting mode, the 160- by 100-element array is read out when information reaches 4-bit accuracy, and then, through use of an adder, is added into the memory.

Point detection is accomplished by either of two channel electron multiplier phototubes. There are two discriminators and photopulse counters for

redundancy. Output from the point detectors can be stored in the area detector's memory.

A microprocessor handles the timing and control functions and stores sequences of instrument operations. A small buffer memory stores commands from outside the photometer.

OPTICS DESIGN AND PERFORMANCE

The photometer consists optically of two conventional or point photometers and two imaging photometers that resemble cameras. Fabry mirrors are used for the point modes, and relay primary mirrors are used for area detection magnifications.

The first optical element encountered by the light in the photometer is a set of entrance apertures located at the telescope cassegrain focus that serve as field stops to select the portion of the sky the brightness of which is to be measured or which is to be imaged. There are circular, slit, and rectangular apertures.

Spectral discrimination is accomplished in either point or imaging modes through use of two filter wheels each having eight positions including an open position, thus allowing each filter to be used separately or in combinations.

Area photometry, performed by the camera-type optical system, accepts the astigmatic off-axis image from the telescope and reimages the light onto an intensified-charge-coupled device at either *f*/24 or *f*/96. The reimaging adjusts the plate scale of the image and removes virtually all the telescope's image aberration.

The *f*/24 system image resolution is limited almost equally by optical image quality and by inherent detector resolution, depending on the wavelength. At *f*/96 the system image resolution is limited by the optical image quality, which in turn is limited by diffraction. The *f*/96 pictures are expected to contain nearly all the image information possible from the 2.4-meter (94-inch) telescope. The high resolution of *f*/96 is obtained at a price, of course. The image irradiance is less than that at the *f*/24 input image by a factor of at least 16. For many astronomical objects, the obtainable resolution will be limited by photon statistical fluctuations.

SYSTEM PERFORMANCE

The photometer will have the highest light sensitivity of all Space Telescope instruments—to magnitude 26.5 or better. It will have the highest time resolution—100 microseconds or better. It is designed to have the highest photometric precision; the goal is 0.1 percent. The photometer will also have spatial resolution limited only by diffraction to about 0.1 second of arc over a relatively small field of view. With minor modification, the photometer can also do highly precise polarimetry.

The photometer provides a useful scientific instrument that fully uses and complements the unique astronomical capabilities of the Space Telescope.

HIGH-RESOLUTION SPECTROGRAPH

Keith Peacock
Bendix Corp.

The high-resolution spectrograph is one of four instruments sharing the focal plane of the Space Telescope. It occupies a 90-degree segment centered on the optical axis of the Space Telescope. The telescope is an $f/24$, 57.6-meter (189-foot) focal length Ritchey-Chretien. Its primary aberrations are astigmatism and focal plane curvature.

The design requirements have been established by a team of astronomers under the chairmanship of Dr. A. Boggess of Goddard Space Flight Center. It is required to cover the spectral range of 115 to 410 nanometers with resolutions of 10^3, 3×10^4, and 10^5. The detector is a Secondary Electron Conduction Orthicon (SECO) with a 51- by 56-millimeter (2.0- by 2.2-inch) target and is available with Bialkali/SiO_2 and CsI/MgF_2 photocathode/window combinations.

The design presented here meets the requirements, supplies all the desired modes of operation, has minimum aberrations, and yet contains a minimum of moving parts.

OPTICAL DESIGN

The optical layout of the high-resolution spectrograph is shown in figure 1. A slit mechanism permits the selection of any one of eight fields-of-view between 0.1 and 10 seconds-of-arc square. After collimation by an off-axis parabolic collimator with a focal length of 800 millimeters (31 inches), the beam falls on an echelle carrousel that supports four selectable echelle gratings and a plane mirror. The carrousel has a sinusoidal rotation with ±15 second-of-arc amplitude for correction of the orbital doppler shift. The diffracted beam passes to a second carrousel, which holds three selectable, spherical, cross-disperser gratings and two off-axis parabolic mirrors. One cross disperser is blazed to send the diffracted beam to folding mirror $M1$, which reflects the spectrum to short wavelength detector $D1$. The CsI/MgF_2 photocathode/window combination of this SECO limits its range from 115 to 170 nanometers. Any of four images can be displayed on this detector: (1) a cross-dispersed spectrum at a resolution of 3×10^4 using one of the echelle gratings, (2) a cross-dispersed spectrum at a resolution of 1×10^5 using another echelle, (3) a single low dispersion spectrum at 10^3 resolution using

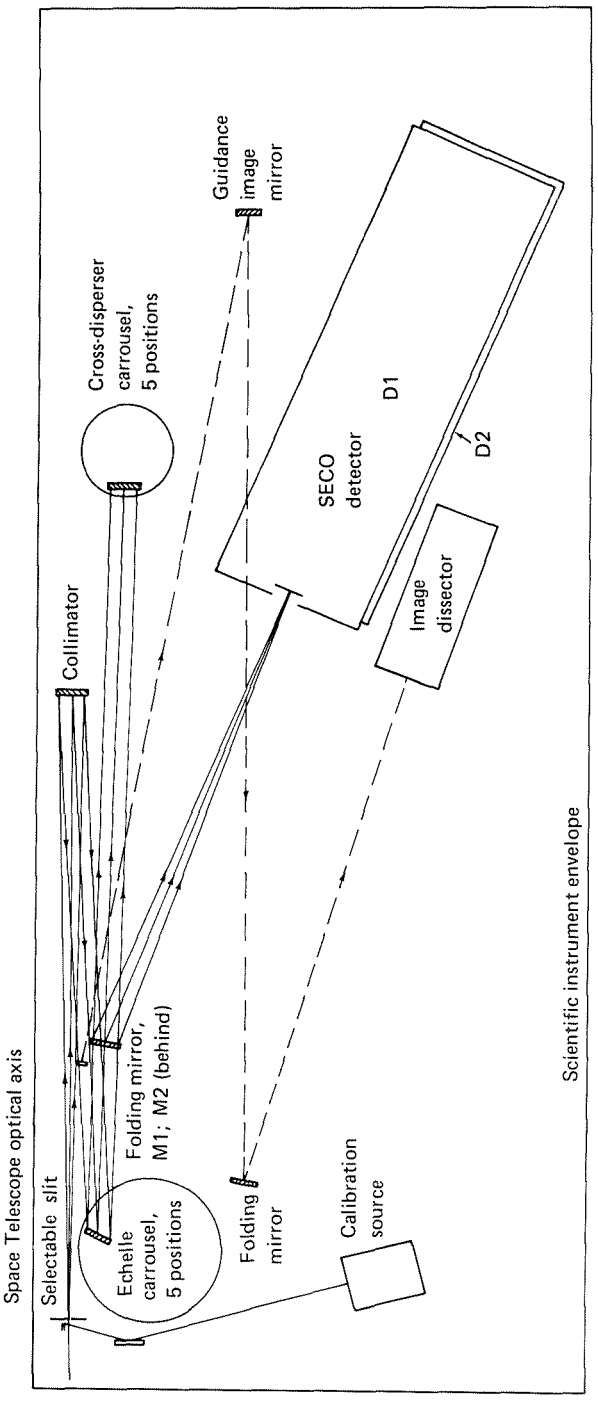

Figure 1.—Optical schematic of the high-resolution spectrograph.

cross dispersion only with the plane mirror in place of the echelles, and (4) a direct image using a figured mirror in place of the cross disperser.

Two other spherical gratings image either of the wavelength bands 170 to 265 or 265 to 410 nanometers across the bialkali photocathode of detector *D*2. With the additional two echelle gratings, the total operational modes are the 11 listed in table 1.

A small folding mirror picks off a small portion of the collimated beam to provide an image at the image dissector. The dissector is used for target identification, acquisition, and reacquisition after an exposure interruption. It operates in a closed-loop mode through the systems support module to the telescope guidance system.

The high-resolution spectrograph contains a hollow cathode lamp to act as a spectral calibration source. Its energy is reflected through a pinhole close to the target slit. The system optical efficiency, including detector quantum efficiency, varies between 0.2 and 1.5 percent in the required wavelength range. The aberrations of the instrument are very small and do not significantly degrade the image. Diffraction, wavefront error, detector resolution, and image motion are the main limitations and they produce a resolution of 3.5 line pairs per second of arc at 50 percent modulation transfer function and 9 line pairs per second of arc at 10 percent modulation transfer function for a wavelength of 171.4 nanometers.

MECHANICAL, THERMAL, AND SYSTEMS DESIGN

The optical components and mechanisms are mounted to an "optical bench" that consists of two longitudinal beams attached to a manufactured piece at each end. These end pieces attach to the three instrument package support points; one on either side near the focal plane and one three-quarters

TABLE 1.–*Modes of Operation*

Mode	Echelle carrousel	Cross-disperser carrousel	Spectral range, nanometers	Spectral resolution	Detector
1	*E*1	*G*1	115 to 170	3×10^4	1
2	*E*2	*G*2	170 to 265	3×10^4	2
3	*E*2	*G*3	265 to 410	3×10^4	2
4	*E*3	*G*1	115 to 170	1×10^5	1
5	*E*4	*G*2	170 to 265	1×10^5	2
6	*E*4	*G*3	265 to 410	1×10^5	2
7	*M*1	*G*1	115 to 170	1×10^3	1
8	*M*1	*G*2	170 to 265	1×10^3	2
9	*M*1	*G*3	265 to 410	1×10^3	2
10	*M*1	*P*1	115 to 170	–	1
11	*M*1	*P*2	170 to 600	–	2

of the way along the package. The optical bench must be kept at a constant temperature to maintain alinement, focus, and to allow precise reacquisition of the spectrum after an exposure interruption by Earth occultation. A thermal control subsystem adjusts the power to various heaters so that the temperature at strategic points is constant. The weight of the spectrograph including the package is estimated to be 203 kilograms (448 pounds).

The electronic system is autonomous and requires inputs of power, reference clock, and gross operational commands only from the support systems module. A continuously powered digital interface unit links the instrument with the rest of the spacecraft. After recognition of the high-resolution spectrograph command, a microprocessor assumes control, and using stored or transmitted functions, it controls power, heaters, detectors, and exposures. The main mode of exposure control is electronic shuttering of the detector high-voltage power supply using one of the system clocks for timing. The SECO target is read out as straight video at 10^6 bits per second with frame synchronization supplied by the microprocessor through the output selector gate and the digital interface unit line driver. The average operating power drawn by the spectrograph is 120 watts; the peak power is 160 watts.

CONCLUSION

This design study has revealed no major technical problems that could prevent manufacture of a high-resolution spectrograph capable of accomplishing the scientific objectives of the investigators.

ACKNOWLEDGMENT

The work described in this paper was supported by Itek subcontract 8237-A-0001 under prime NASA contract NAS8-29949.

IV

Mirror Development

MIRROR SUBSTRATE MATERIAL AND MANUFACTURING

William C. Lewis
Corning Glass Works

Corning code no. 7971 U.L.E.™ (ultra low expansion) glass has been selected as the material for the primary mirror substrate for the Space Telescope.

The basic process for producing this material is the same as that used widely for the manufacture of pure synthetic fused silica. Vapors of highly purified silicon tetrachloride are introduced into the flames of burners where they react with the water vapor produced by combustion of natural gas to form hot silica soot particles.

The process variation that produces U.L.E.™ material is primarily the introduction of titanium tetrachloride as well as silicon tetrachloride to the flame, thereby producing a binary glass composed of titania and silica.

The titania/silica system has many unique characteristics. For example, titania lowers the coefficient of thermal expansion of silica in direct proportion to its concentration. At 20° C, the instantaneous coefficient of 7.4 percent titania/92.6 percent silica is zero compared with a value of 0.50 part per million per degree Celsius for 100 percent silica. U.L.E.™ material is defined as that part of the titania/silica family in which the coefficient of thermal expansion taken over the 5° to 35° C temperature interval is in the range of 0.00±0.03 part per million per degree Celsius.

A second unique characteristic of this system is that a difference in coefficient of thermal expansion caused by differing titania levels is a constant that is independent of temperature. This means that it is not necessary to measure the inhomogeneities for coefficient of thermal expansion at the specific temperature of interest. Measurement may instead be made at a temperature most conducive to accurate data; the difference found would also be found at the temperature of interest.

A third unique characteristic is that not only is the coefficient of thermal expansion lowered in direct proportion to the concentration of titania, but so also is ultrasonic velocity. This means that by the use of a precision ultrasonic intervalometer and accurate thickness gaging, the coefficient of thermal expansion of various parts of an actual substrate can be determined

nondestructively to within a few parts per billion (refs. 1 and 2), a very important feature as regards forecast of change in image quality as a function of thermal excursions of the substrate.

The fourth unique characteristic of U.L.E.™ material is that it is truly weldable in the full sense of the word. Because of the low expansivity, two parts can be welded by heating the edges with gas-oxygen flames until the material is softened on each part. The pieces can then be merged, the flames removed, and the parts allowed to cool. The entire operation can be done without need for controlled heating or cooling. This feature enables a substrate to be fabricated of parts preselected for quality appropriate to the needs of each part of the substrate for each specific application.

The Corning Glass Works equipment used in the production of U.L.E.™ material consists of a multiplicity of burners, vertically disposed so as to point down toward a rotating table as the target for the accumulation of the soot. The material builds up slowly over a period of weeks until it produces a boule or disk that is about 150 centimeters (60 inches) in diameter and normally 8 to 13 centimeters (3 to 5 inches) thick. All articles to be made of U.L.E.™ material must be made from these disks.

In the manufacture of a mirror substrate we need to convert the material into two plates, an egg-crate-like core, and usually both an inner and an outer ring. The front plate is the one that is accurately figured and polished, and usually ends up either flat or concave. The piece of glass selected for this is one of selected quality for low inclusions to provide for favorable polishability.

If the mirror is over 150 centimeters (60 inches) in diameter, the material for plates is cut from the boule in extra thickness as necessary so that when the piece is taken to about 1600° C and allowed to flow to the large diameter, the thickness at the new diameter is appropriate. Plates up to 300 centimeters (120 inches) in diameter and 4 centimeters (1½ inches) thick have been obtained in this manner.

Manufacture of the core is more complex. First, if a 30-centimeter (12-inch) high core is wanted, the necessary number of boules are stacked vertically to produce a stack that is 150 centimeters (60 inches) in diameter and at least 30 centimeters (12 inches) high. This entire stack is placed in a furnace and heated to about 1600° C, at which temperature the boules fuse to form a single monolithic piece.

The stack is then used to saw out individual cell struts and ring sections, which are then ground to exact thickness; i.e., 5.08 millimeters (0.200 inch). The individual struts are then welded together to form a number of 90-degree ells, which are the building elements for the core. A number of these are initially welded to a flat plate in an adjacent position, and then the square cell accomplished by welding a second row. This procedure is continued row by row until the overall size is adequate, at which point the core is circled and ground to exact height.

The rings are made by sagging sections of straight plates to the proper radius

by heating them to about 1600° C on a male mold. The individual sections are then welded together to form complete rings.

The completed parts are then placed in their proper positions to make the complete structure, and the entire assembly is heated to about 1600° C, at which temperature it fuses to initially form a plano-plano monolithic structure. For the convex-concave configuration, the entire monolith is placed on a male mold, heated, and sagged to conform to the mold.

To provide optical performance, the two plates must be closely matched for coefficient of thermal expansion. This is commonly done to within 0.01 part per million per degree Celsius.

However, differences in expansivity are also purposely employed to enhance the strength of the final substrate. The ends of the struts are geometric stress concentrators, so it is desirable to produce residual compressive stress at these locations. This is done by purposely mismatching the expansivity of the ring and core materials. As the blank cools from the set point of 925° C, the differential expansion of the two is such that the rings pull the plate down against the strut ends, putting desirable residual compression at those points, and yet modest tension in the rings.

REFERENCES

1. Hagy, Henry E.: "High Precision Photoelastic and Ultrasonic Techniques for Determining Absolute and Differential Thermal Expansion of Titania-Silica Glasses." *Applied Optics,* vol. 12, no. 7, July 1973, pp. 1440-1446.
2. Hagy, Henry E.; and Shirkey, W. D.: "Determining Absolute Thermal Expansion of Titania-Silica Glasses: A Refined Ultrasonic Method." *Applied Optics,* to be published.

FABRICATION AND TEST OF 1.8-METER (71-inch) DIAMETER, HIGH-QUALITY U.L.E.™ MIRROR

Richard J. Wollensak and Clarence A. Rose
Itek Corp.

The demand for large-diameter, high-quality optical surfaces requires that many engineering disciplines participate in the design and development of a suitable support system for the mirror during fabrication and test and in the constant upgrading of the test equipment, test optics, and methods of data reduction. One of the key factors in the successful endeavor is providing the support equipment with appropriate sensitivity and a high degree of repeatability in testing the surface. It is critical that the total system used in developing the mirror surface demonstrate confirmed uniformity and repeatability from test to test.

The mirror blank used in this experiment was a lightweight, monolithic U.L.E.™ blank manufactured by Corning Glass Works. The mirror blank was initially an *f*/2.7 meniscus-shaped element that was subsequently reslumped to an *f*/2.2 curvature prior to the start of any optical fabrication. The purpose of the reslumping was to demonstrate fabricability of a faster mirror that would be compatible with the requirements currently planned for the Space Telescope program. The mirror blank was successfully reslumped by Corning Glass Works and the finished weight of the mirror was 546 kilograms (1203 pounds).

Properly designed support and test equipment is crucial in the development of any high-quality surface. We can categorize these requirements in essentially three areas:

(1) Mirror support system—this is used to repeatably maintain the surface figure during polishing and testing.
(2) The optical test equipment—the most important component of this equipment was a three-element null lens. It was decided in the definition phase of this activity that the most reasonable surface to demonstrate would be an *f*/2.2 parabola. Consequently, a null lens was required in order to produce a spherical wavefront that would be compatible with the interferometer requirements.
(3) Optical tooling—a number of different-sized laps with varying degrees of stiffness and flexibility were used during the fabrication of the surface.

The support system chosen for this program was a multipoint, passive liquid mount, consisting of 27 fluid pistons properly spaced and interconnected so as to allow flow from one piston to another. The type of support is shown schematically in figure 1 and an actual photograph of the finished mirror mount is shown in figure 2. A comprehensive structural analysis was undertaken to determine the number, diameter, and location of the fluid piston supports. To minimize any deformation contribution by the mount to the mirror surface, primary considerations in mount design are total amount of sag between any two support points and the area of the fluid pistons to minimize any highly stressed areas on the back of the mirror blank. Normally, loading on the fluid pistons is kept in the area of 21 to 34 kilonewtons per square meter (3 to 5 pounds per square inch). A theoretical goal for the total error contribution of the support system was set at $\lambda/150$ root mean square (λ = wavelength.) As shown in figure 2, there were 18 separately adjustable assemblies that were used to laterally restrain the mirror blank from any transfer motion. The restraint assemblies were designed so as to contact the mirror blank on the edges of both the top and bottom plates. These restraints were firmly adjusted to contact the mirror during the actual polishing cycle, and then backed off completely during the testing of the surface so as not to influence the mirror surface.

Figure 3 schematically shows the null lens configuration. This optical system consists of three elements, each having easy-to-fabricate spherical surfaces. The null lens design also accounts for a 2.5-centimeter (1-inch) thick BK7 window, which was the entrance port in the vacuum test chamber. The lens was designed with a certain amount of flexibility in terms of spacing the elements to permit compensation for the differences in the refractive index

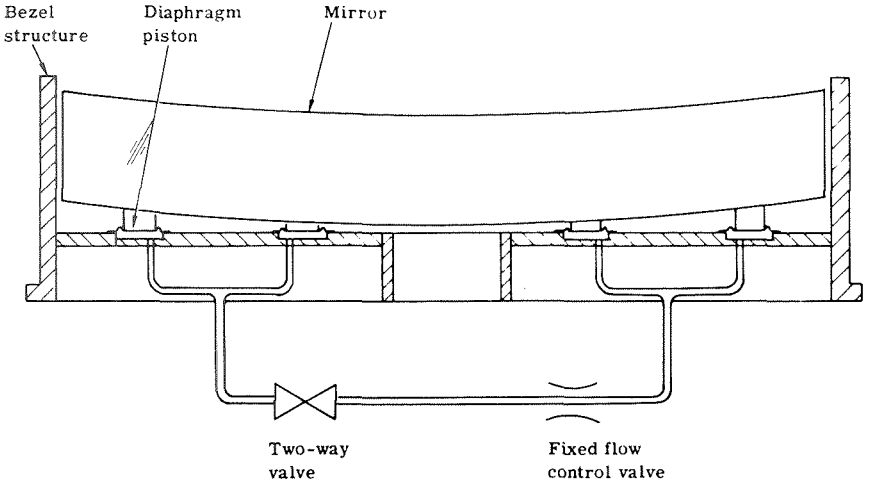

Figure 1.–Passive liquid mount.

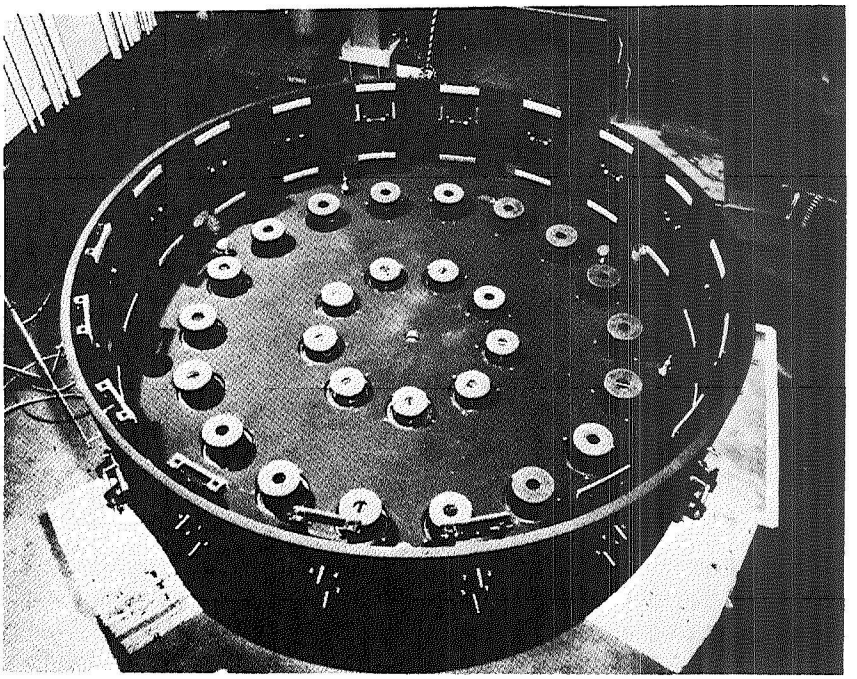

Figure 2.–Top view of bezel.

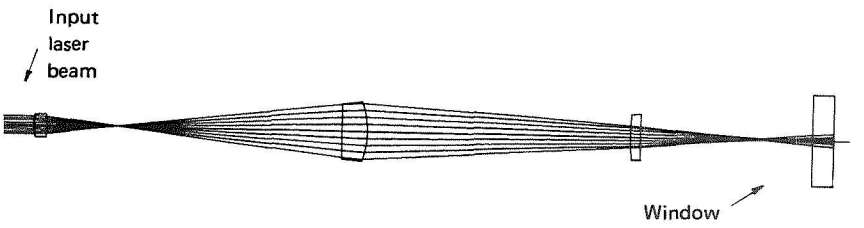

Figure 3.–Preliminary null lens design to be used in conjunction with laser unequal path interferometer. This design uses three small easy-to-fabricate refracting elements and all spherical surfaces.

between air and vacuum. In the initial phases of fabrication, the majority of the tests were conducted in a 1-atmosphere environment. As the quality of the surface improved, it was necessary to perform the optical testing in a partial vacuum, normally on the order of 20 kilonewtons per square meter (150 millimeters of mercury) to minimize the effects of air turbulence during measurements (refs. 1 and 2).

Critical to the performance of the null design is proper mounting and support of the optical elements. Figure 4 shows a photograph of the finished

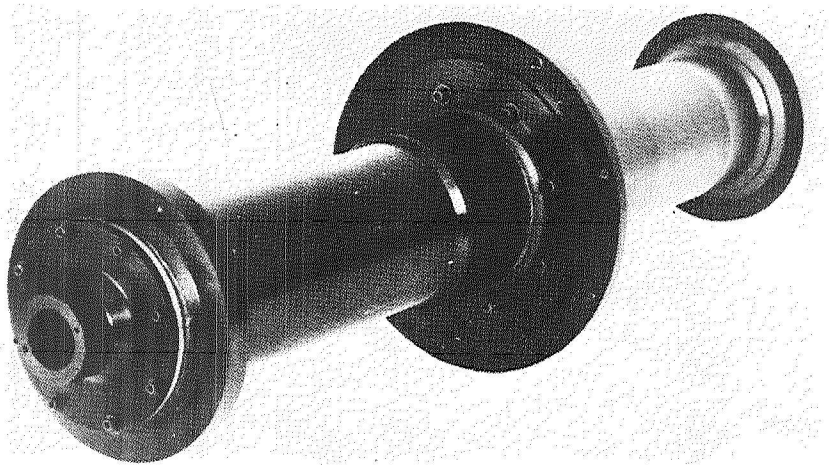

Figure 4.–Null lens.

null lens cell prior to its attachment to the laser unequal path interferometer. As shown in the photograph, the null lens cell was made of several components with highly precisioned internal mounting surfaces. In terms of concentricity and alinement of the optical elements, the design goal for the total mechanical error contribution of the three-element null lens was $\lambda/200$ root mean square.

As previously stated, a number of variously configured tools and laps were used in the fabrication process, ranging from full-size stiff laps for the initial generating work, through to laps with varying degrees of flexibility for the final polishing, down to laps on the order of 15 and 20 centimeters (6 and 8 inches), which would be used during the final hand correction. The basic fabrication technique employed in this demonstration was to first generate and partially polish a spherical surface of the proper radius. The spherical surface establishes a baseline and also insures a surface generally free of astigmatism prior to starting the aspherization process. Conventional techniques were then used to rough grind in the proper aspheric departure from the base sphere. The piece was then polished, tested, and figured using a variety of ring laps and special pitch lap configurations to obtain a smooth surface of $\lambda/50$ root mean square. From this point on, the major activity was one of hand correction to reduce the local zonal errors until a mirror surface of the required quality was achieved. Figure 5 shows an overview of the handling equipment used in transferring the mirror and its support system from the polishing machine into the test chamber. Figure 6 shows the workpiece during the initial phases of polishing.

Critical to the production of large-diameter, high-quality optical surfaces is a well-conceived test and data analysis program. Figure 7 shows a block diagram of the test and data handling sequence. When an optical fabrication cycle has been completed, the piece is removed from the machine to the test chamber

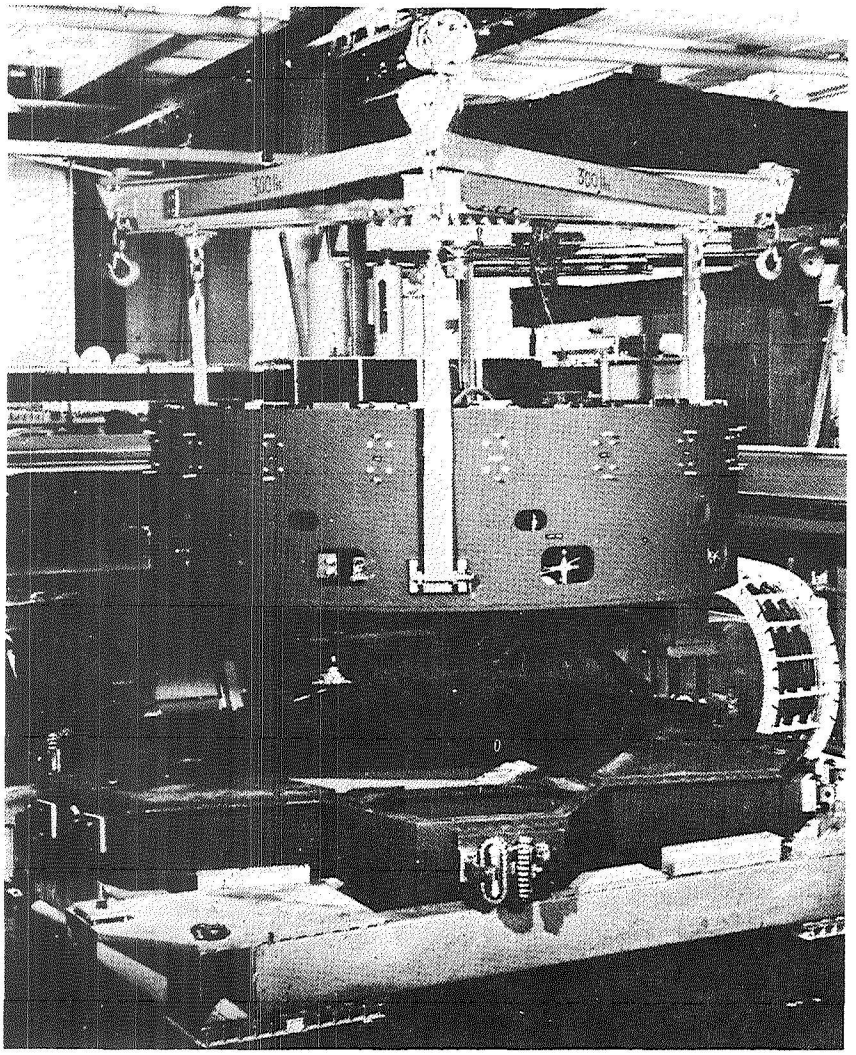

Figure 5.—Overview of handling equipment.

for an interferometric test. Figure 8 schematically describes the mirror positioned in the vacuum tank for a typical test cycle. The interferograms produced by the laser unequal path interferometer (ref. 3) are recorded on Polaroid film. The first stage of the fabrication, nominally to about the $\lambda/10$ root-mean-square level, is normally reduced and interpreted by the optician directly. This can be done quite readily using a straight edge or set of parallel rulers and counting the fringes.

Beyond the tenth wave level, the reduction becomes more challenging. At

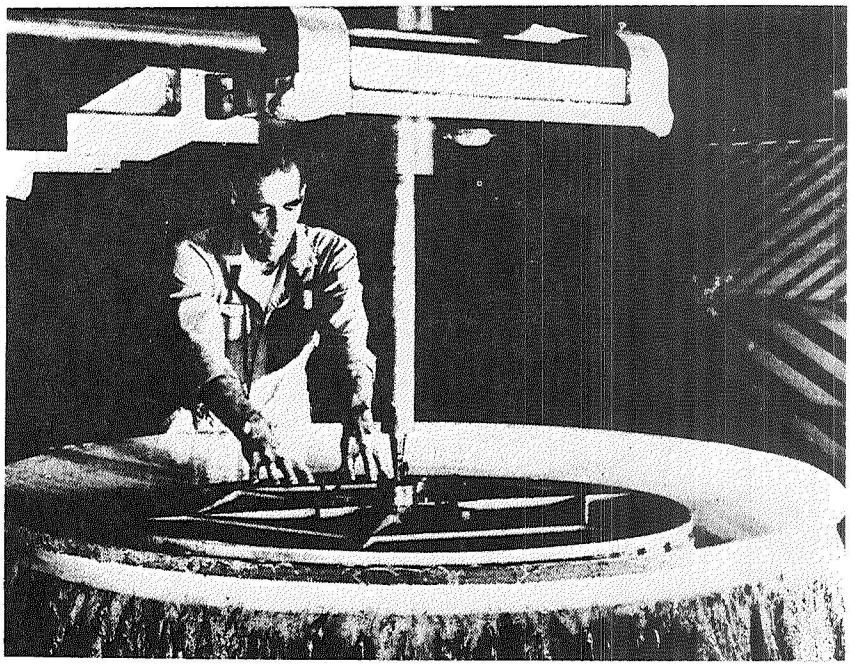

Figure 6.–Mirror during polishing.

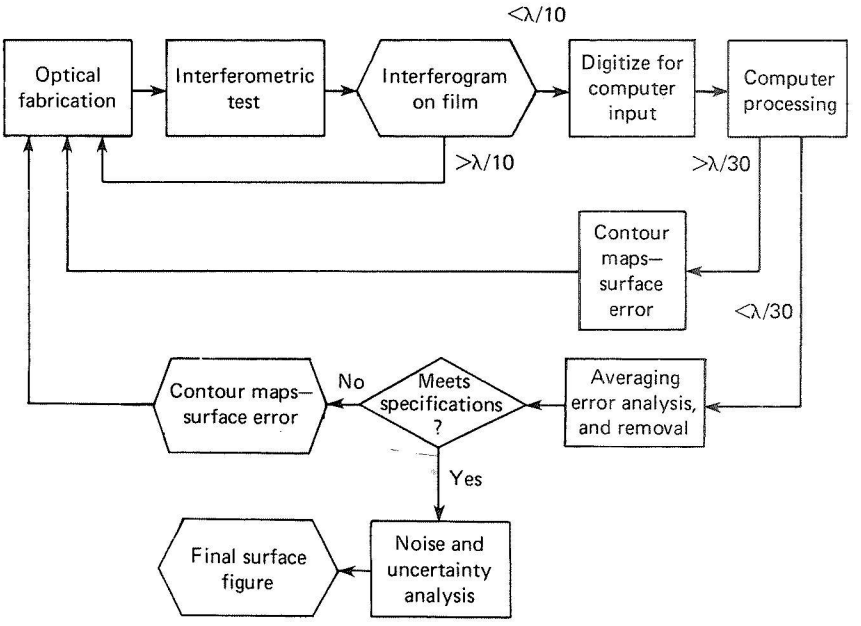

Figure 7.–Test and data analysis sequence.

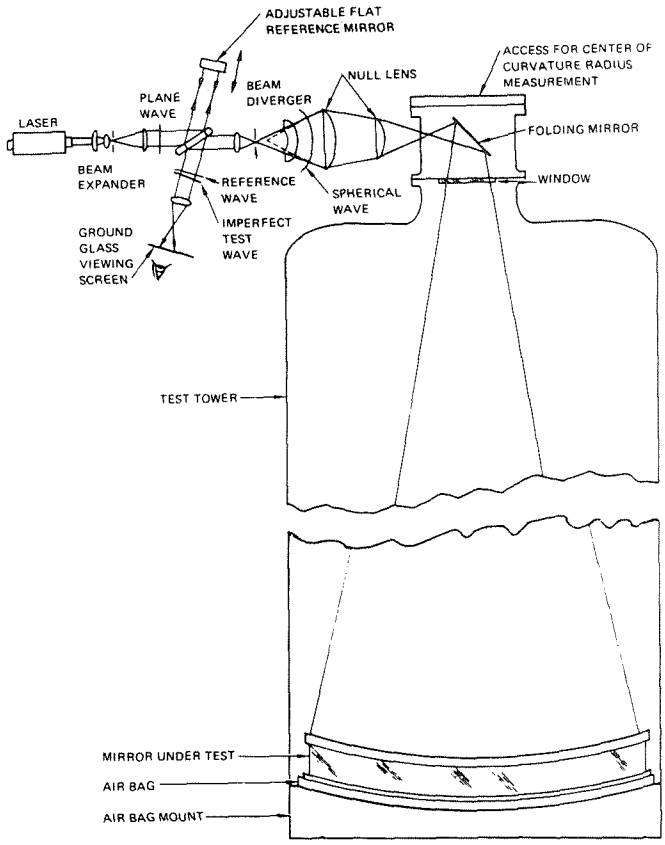

Figure 8.–Typical test configuration.

this point a test set of interferograms (e.g., usually 12 photographs, six showing horizontal fringe orientations and six showing vertical fringe orientations) is digitized, sent through the computer, and contour maps of the surface areas are produced. The contour maps are used by the optician in determining the length and location of his next fabrication cycle. This technique is used until the surface quality approaches the order of $\lambda/30$ root mean square.

From the $\lambda/30$ root-mean-square level to completion of the surface, errors in the total system are considered and subtracted from the contour plots that are produced by the computer. These errors are basically those contributed by the null lens, the primary mirror support system, and the test optics. Several tests are run during the course of the fabrication to determine the magnitude of these errors. The determination of these errors is accomplished by rotating various components in the test system with respect to each other. In this manner, errors that rotate with the test system components may be separated from the residual errors actually present on the optical surface. This is readily

accomplished using a computer program that evaluates the mirror or the optical test component in three rotational orientations. As an example, a set of test data would be taken in the -45-, 0-, and +45-degree rotational orientation. These interferograms would then be digitized and reduced, and by a subtraction routine, the -45-degree position would be subtracted from the 0-degree position and the +45-degree position would be subtracted from the 0-degree position. These errors would then be averaged and subtracted to determine the magnitude of the residual error in the workpiece. Figure 9 schematically demonstrates this procedure.

There are basically three error sources that must be considered in the interferometric error removal process. These are asymmetrical errors, symmetrical errors, and random errors. The asymmetrical errors can readily be defined by the rotation of the workpiece with respect to the test optics. This would hold true for the null optics system with respect to the test piece as well as the primary mirror support system with respect to the workpiece. These rotations can be done individually, and analyzed and accounted for. Symmetrical errors can generally be accounted for in the original error budgets. This is accomplished by precisely measuring the radius, element thickness, and spacing of the null lens assembly. Considerable previous experience has developed a high degree of confidence in accepting these measured values. Random errors in the interferometric testing are generally accounted for by averaging several

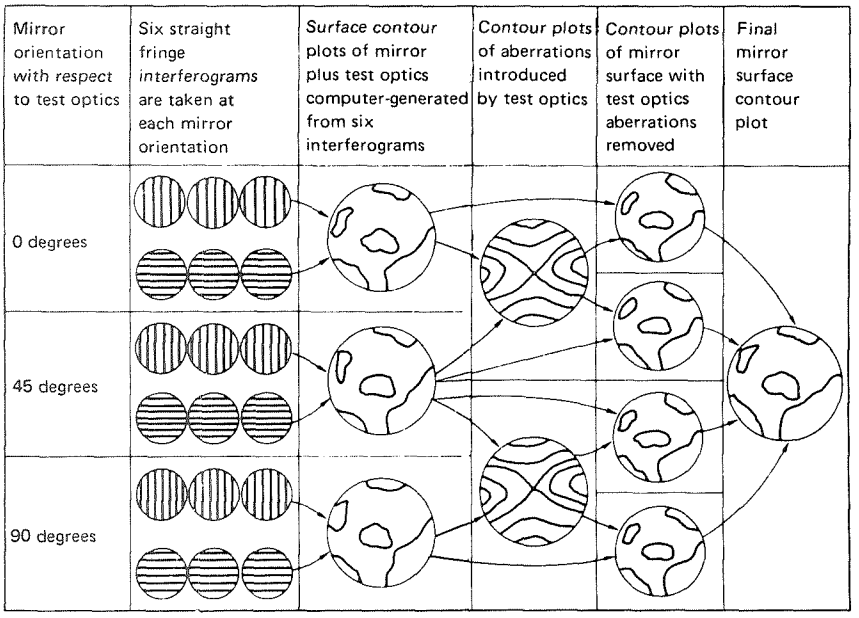

Figure 9.–Flow diagram of data reduction process.

interferograms. In the initial stages, fewer interferograms are digitized and reduced. As mentioned previously, 12 photographs are acceptable up to a level of λ/30 root mean square. Beyond this point, depending on the test conditions, primarily influenced by vibration and turbulence effects, it may be necessary to take as many as 20 pictures in any one data set. The main objective is to reduce a sufficient number of interferograms to obtain confidence in the repeatability of the test data and minimize the noise contribution.

Figure 10 shows a plot of actual optician hours plotted against root-mean-square surface improvement. The numbers directly above the curve indicate the hours expended in such functions as grinding and polishing since the last data point. The numbers directly below the curve show the number of test cycles that were used throughout the total fabrication cycle. As shown by the curve, there were approximately 25 test cycles performed to achieve a figure λ/2 root mean square. In total, the mirror was cycled from the polishing machine or through a hand figuring operation into the test chamber, interferograms were taken, the data were reduced, and an evaluation was made, totaling 108 cycles.

Figure 11 shows a typical contour plot of the finished mirror. The contour increments in this plot are 0.01 wave peak to peak. Figure 12 is the contour of the mirror surface at 0.02-wave increments. These contour plots are the result of an average of approximately 24 interferograms, 12 with horizontal fringe orientations, and 12 with vertical fringe orientations. Typical interferograms

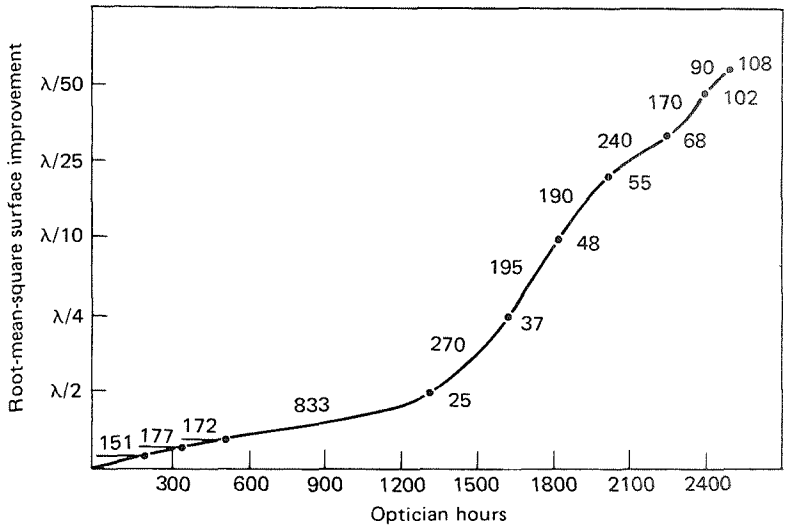

Figure 10.–Curve showing root-mean-square improvement versus optician hours–phase 1 (λ/62 root mean square = 0.16; null lens subtracted). Numbers above curve indicate optician hours since last data point; numbers below curve indicate cumulative number of test cycles.

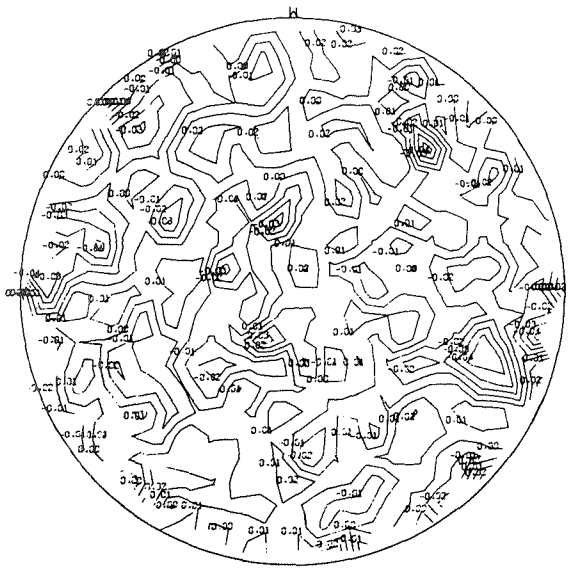

Figure 11.–Contour plot (contour increment = 0.01λ; mirror: 0.015λ root mean square, λ/65.1 at surface).

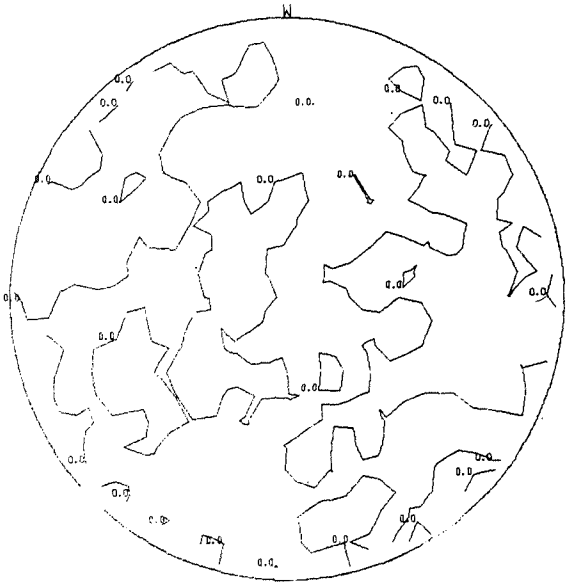

Figure 12.–Contour plot (contour increment = 0.02λ; mirror: 0.015λ root mean square, λ/65.1 at surface).

for data reduction contain approximately 20 to 22 fringes across the surface of the mirror (fig. 13).

This gives us a data density on the mirror surface of approximately 1 fringe for every 7½ centimeters (3 inches) of mirror surface. These interferograms are digitized, scanning the interferogram with 21 scans that produce nominally on the order of 367 data points on the mirror surface for each interferogram. These interferograms are then averaged, the known error sources in the system are subtracted, and the result is the contour plot of the actual mirror surface.

The described experiment resulted in a mirror with a surface quality of $\lambda/65.3$ root mean square over a 178-centimeter (70-inch) diameter clear aperture (fig. 14). The average error contribution of the primary mirror support and the test optics resulted in a combined error of $\lambda/114$ root mean square.

While this program has resulted in a substantial step forward in developing the technology associated with the production and testing of large-diameter, high-quality surfaces, it is not at all clear that we have reached an upper limit of fabrication and test capabilities. Clearly, a substantial step forward has been achieved. The production of these surfaces is a painstaking and demanding task requiring much attention to detail and a constant upgrading of the various components of the total system. Much progress has been made in the last 5 to 10 years in the production of high-quality surfaces. Better test equipment and

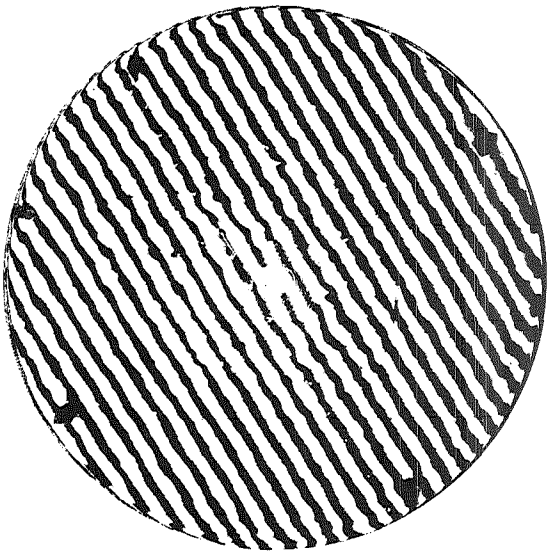

Figure 13.–Final interferogram of NASA 183-centimeter (72-inch) mirror ($\lambda/65.3$ root mean square).

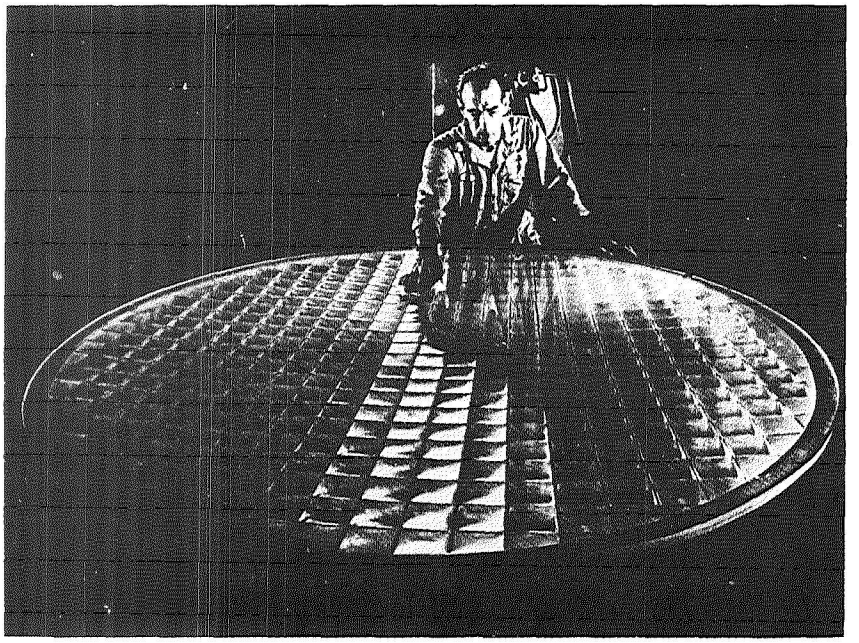

Figure 14.–Mirror overview.

better analytical tools have helped us to predict and anticipate many of the complex problems that have arisen. It would, therefore, seem reasonable to anticipate that higher quality surfaces can be fabricated and that surfaces of comparable quality could certainly be fabricated on large-diameter mirrors.

REFERENCES

1. Fischer, R. E.: "Null Optics for Testing a 1.8-Meter-Diameter Paraboloid." *Journal of the Optical Society of America,* vol. 64, 1974, p. 1369.
2. Fischer, R. E.: "Null Lens Mapping Errors." *Journal of the Optical Society of America,* vol. 61, 1971, p. 655.
3. Houston, J. B., Jr.; Buccini, C. J.; and O'Neill, P. K.: "A Laser Unequal Path Interferometer for the Optical Shop." *Applied Optics,* vol. 6, no. 7, 1967, p. 1237.

DESIGN AND TESTING WITH A REFLECTIVE NULL SYSTEM

L. Montagnino and A. Offner
Perkin-Elmer Corp.

To obtain aperture-limited performance from a large optical system such as the proposed 2.4-meter (94-inch) aperture Space Telescope, the component elements, their spacings, and their relative orientations must be very close to nominal. In particular, to keep the contribution to image degradation of figure errors of the large concave primary mirror consistent with this goal, it is necessary to manufacture this mirror with a root-mean-square figure error of about $\lambda/100$ at $\lambda = 632.8$ nanometers (λ = wavelength). Auxiliary optical systems that can be manufactured and used to measure the contours of a large concave aspheric mirror to this order of accuracy are the subject of this paper. These auxiliary optical systems are retroreflective null correctors. In these systems, the spherical wavefront from a point source is modified by the auxiliary optical system so that its shape is that of the desired aspheric. This wave is then reflected back through the auxiliary optical system, which restores its spherical shape. The retroreflected spherical wave can then be compared with an accurately known spherical surface in a high finesse spherical wave interferometer (ref. 1).

Three forms of null-correcting optical systems have been developed (ref. 2). Each of these consists of a small field lens and one or two spherical mirrors so that each of the components can be tested by itself. A form that consists of two spherical mirrors and a field lens arranged in line was designed as a null corrector for a 2.4-meter (94-inch) *f*/2.3 Space Telescope Ritchey-Chretien primary mirror. For null mirror diameters of 15 and 25 centimeters (6 and 10 inches), the nominal residual wave aberration of the retroreflected wave was less than $\lambda/1000$ root mean square. When practical tolerances are applied to the manufacture of this null corrector optical system, it is shown that when used in conjunction with a high finesse interferometer, the contours of the hyperboloid can be measured with an uncertainty that results in a root-mean-square contribution of less than 0.02λ to the imagery obtained with the Ritchey-Chretien system of which the hyperboloid is the primary mirror.

TOLERANCE ANALYSES

To build and use a null corrector of the form shown in figure 1, it is necessary to know the effects of departures from nominal values of the null

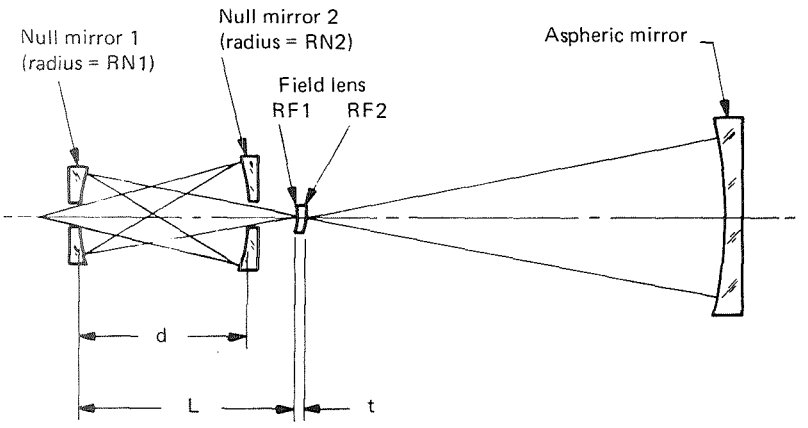

Figure 1.–Null-corrector optical system.

corrector elements and of their positions and orientations with respect to each other and with respect to the aspheric mirror being tested. For this purpose, a two-mirror null corrector was designed for use with both a 2.4-meter (94-inch) *f*/2.3 hyperboloidal mirror to be used for the Space Telescope Ritchey-Chretien primary and a 152-centimeter (60-inch) model mirror. This form was chosen because it is the easiest to aline and use and because its dual application requires only a slight respacing of the mirrors and a new field lens. It can be used in conjunction with a spherical wave interferometer (ref. 1) with no additional elements except for the interferometer field lens the aberrations of which can be compensated by a slight modification of the spacings of the null corrector.

To obtain accurate values of the tolerance sensitivities, the residual root-mean-square wave aberration of the null-corrector design was reduced to less than $\lambda/1000$ at $\lambda = 632.8$ nanometers.

The effects of departure from nominal of the various parameters on the root-mean-square wavefront departure from the closest reference sphere were determined. At the same time, changes in spacing or orientation that compensate for departures of parameters from nominal were determined. The results indicate that manufacturing tolerances on the radii of the null mirrors and the radii and thickness of the field lens are not prohibitively tight provided that these quantities are measured accurately after manufacture so that their departures from nominal may be compensated by changes in the spacing. Manufacturing tolerances of ±0.1 millimeter (0.004 inch) on the radii of the null mirrors and the thickness of the field lens are not difficult to achieve. The resulting maximum departure of the figure of the aspheric mirror from its nominal value will then be determined by the accuracy of the measurement of the radii and separations of the null corrector. A set of uncertainties resulting

from measurement we can meet with a high degree of confidence with our present measuring techniques was chosen. These measurement uncertainties and their influences are shown in table 1. As can be seen, the total null-corrector/interferometer measurement uncertainty in terms of mirror figure contour is approximately 0.01λ root mean square.

CELL DESIGN

To reduce the reflective null lens design to practice, a cell design was formulated that could achieve the objectives of mirror figure quality, optical alinement, and figure stability. Stability is of utmost importance because the null-corrector performance must be certified by the evaluation of individual elements and alinements. Once certified, it is essential that the optical performance remain within tolerance throughout the period of performance under all required environmental conditions.

A schematic of the cell design is shown in figure 2. The null corrector will be mounted to a vibration-isolated vacuum tank with its optical axis alined vertically.

Axial spacing of key elements is controlled by design configuration and selection of materials. Lateral alinement is controlled by symmetry about the optical axis. The mirrors are Cervit. The outer shell is aluminum. Lateral

TABLE 1.–*Measurement Uncertainties and Influences*

Parameter[a]	Measurement uncertainty	Figure uncertainty, wavelength, root mean square
t	±0.010 millimeter	0.0018
L	±0.010 millimeter	.0018
d	±0.010 millimeter	.0017
RN1	±0.010 millimeter	.0026
RN2	±0.010 millimeter	.0016
RF1	±0.100 millimeter	.0008
RF2	±0.020 millimeter	.0016
Field lens decenter	±0.025 millimeter	.0004
Field lens wedge	10 seconds of arc	.0004
Field lens tilt	10 seconds of arc	.0004
Field lens index	±0.00002	.0004
Null and reference mirror figures	0.004λ wavelength, root mean square	.0086
Longitudinal position	±0.30 millimeter	.0020
Lateral position	±0.67 millimeter	.0020
Tilt orientation	±0.33 second of arc	.0020
Total		∿.010

[a]See figure 1 for definition of some of these parameters.

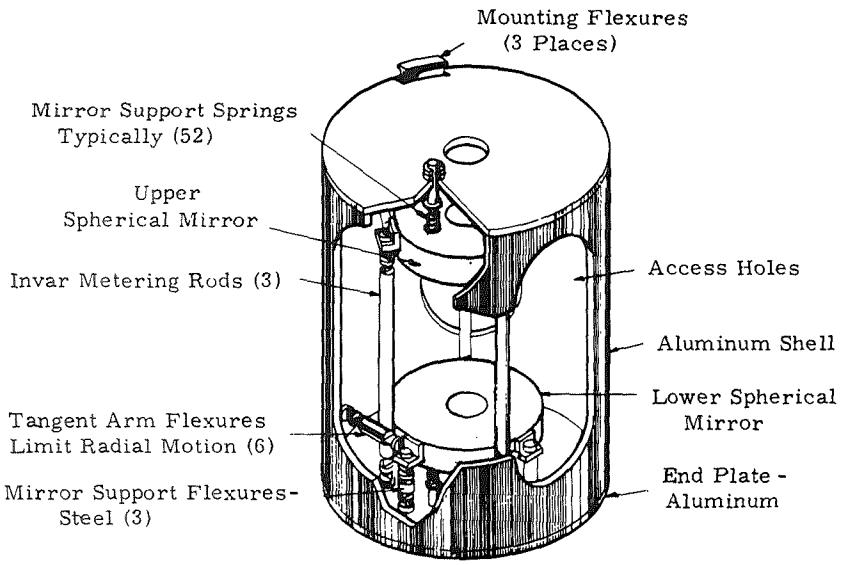

Figure 2.–Null-corrector cell design schematic.

spacing of each is controlled by three steel tangent bars equally spaced at 120 degrees that connect the outer shell to the mirror.

The effect of gravity on mirror figure is controlled by supporting the weight of each mirror by 52 low rate springs arranged in a grid pattern. The force of each spring is adjusted to a level that is calculated to minimize mirror deflection. The spring forces are trimmed at assembly to provide minimum net reaction at the three position control points to avoid local figure effects. The number of springs supporting each mirror is more than required for adequate figure control. To enable in situ measurements of the mirror figures, ports in the aluminum shell were provided that give access to the mirror centers of curvature.

REFERENCES

1. Heintze, L. R.; Polster, H. D.; and Vrabel, J.: *Applied Optics*, vol. 6, 1967, p. 1924.
2. Offner, A.: "Reflecting Null Correctors for Conicoid Mirrors." Paper presented at Spring Meeting, Optical Society of America (Washington, D.C.), Apr. 25, 1975.

TEST RESULTS ON HOMOGENEITY OF EXPANSION FOR A 1.8-METER (71-INCH) U.L.E.™ LIGHTWEIGHT MIRROR

G. Friedman and G. Gasser
Itek Corp.

OBJECTIVES

Interferometric measurements of figure changes caused by inhomogeneity in expansion coefficient for various low expansion mirror substrate materials were performed most recently by Paquin and Goggin (ref. 1) and in the past several years by Goggin et al. (ref. 2) and Bloxsom et al. (ref. 3). These measurements were obtained on samples less than 25 centimeters (10 inches) in diameter and, therefore, could not account for material variations in a large optical element and the technique used to fabricate lightweight elements. It was the intent of this experiment to measure the overall optical effects resulting from inhomogeneity in expansion coefficient in a large lightweight optical element. The element tested was fabricated of Corning code no. 7971 U.L.E.™ fused silica.

The specific objectives of the program were to (1) measure the effect of material inhomogeneities on mirror surface figure under uniform temperature changes, (2) determine the hysteresis level remaining after temperature cycling, and (3) verify the analytical model used to predict surface figure changes.

Testing was conducted in two parts. To accomplish the first objective during part 1, the mirror temperature was uniformly changed from 24° to -18° C, and interferograms were compared under both conditions. During part 2, data were obtained at an intermediate temperature level, -1° C, and apparent figure-time changes observed during part 1 were further investigated. To accomplish the second objective during part 1, interferograms were taken on return to ambient and compared with initial interferograms. Data after cycling between 24° and -18° C were obtained during part 2, in addition to obtaining data after temperature cycling between -12° and 55° C. To develop an understanding of the mechanism of figure change, a structural model of the test mirror incorporating local values of coefficient of expansion was developed.

The conclusions of the experiment were as follows:

(1) The root-mean-square value of surface figure changes caused by material inhomogeneities was found to be equal to 0.036λ over 42° C at 632.8 nanometers (λ = wavelength).

(2) Time variations of surface figure change were found to be insignificant.
(3) No hysteresis remained after returning to figuring temperature. (The measurement uncertainty was less than 0.023λ root mean square at 632.8 nanometers.)
(4) Predictions of surface figure change were in close agreement with measurements (within ±20 percent).

ANALYTICAL MODEL

An integrated thermal/structural/optical analytical tool developed at Itek was used to predict surface figure changes resulting from material inhomogeneities. The major element in this tool is an 880 node EASE structural model of the test mirror. EASE is a structural analyzer computer program developed by the Engineering Analysis Corp. In addition to standard material properties, local values of the coefficient of expansion for material constituting the faceplate, backplate, core, and ring stack were determined on the basis of edge-measured values and estimates of manufacturing variation of expansion coefficient by Corning Glass Works.

Edge-measured values of the coefficient of expansion for the faceplate, backplate, core, and ring stack are shown in table 1. A radial variation of coefficient of expansion α in any boule was estimated to be $0.035 \times 10^{-6}/°C$ (lower at the center than at the edge). This was attributed to oven temperature variations during the early production of U.L.E.™ Recent improvements in oven design have reduced this variation to $0.015 \times 10^{-6}/°C$. No circumferential variation in the coefficient was found to exist in a boule. Random distribution of this material property was assumed for the core. Surface deflections from the EASE model were analyzed and restated in terms of residual root mean square surface errors after removal of phase and tilt coefficients and change of focus.

TABLE 1.—*Measured Expansion Coefficient of U.L.E.™ Lightweight Mirror*

Part	Edge measured α, $(°C)^{-1} \times 10^{-6}$
Front faceplate	0.000
Back faceplate	−.017
Core and ring stack	−.009
	−.003
	−.017
	−.010
	.018

TEST CONFIGURATION

The test configuration is shown schematically in figure 1. The mirror was positioned on a three-point kinematic mount. The mirror (fig. 2), a monolithic U.L.E.™ lightweight structure, was 1.83 meters (6.00 feet) in diameter with an overall height equal to 30.0 centimeters (11.8 inches). The core consisted of cells 7.62 centimeters (3.00 inches) square. The faceplate and backplate thicknesses were 2.09 and 1.20 centimeters (0.822 and 0.472 inch), respectively. The surface figure prior to testing was approximately 0.1λ root mean square over 90 percent of the clear aperture.

TYPICAL RESULTS

The values of the surface contours were obtained, as was pointed out, by averaging the surfaces obtained from several interferograms. For each point in the mean difference contour, the standard deviation of the mean was computed. By examining the magnitude of the apparent surface changes in comparison with the uncertainty of measurement, on a point-by-point basis, the significance of the results may be appreciated.

Figure 3 compares the mean profile of the mirror difference surface, across one diameter, for two conditions. The profile for each condition is plotted

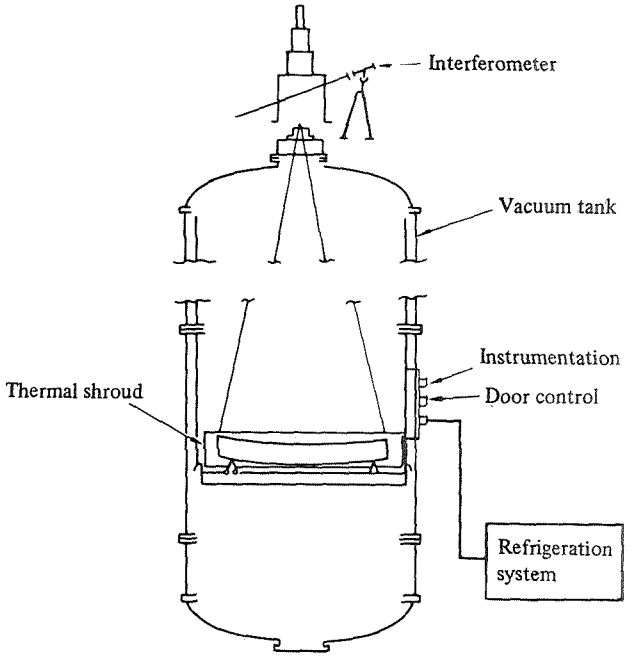

Figure 1.–Test configuration.

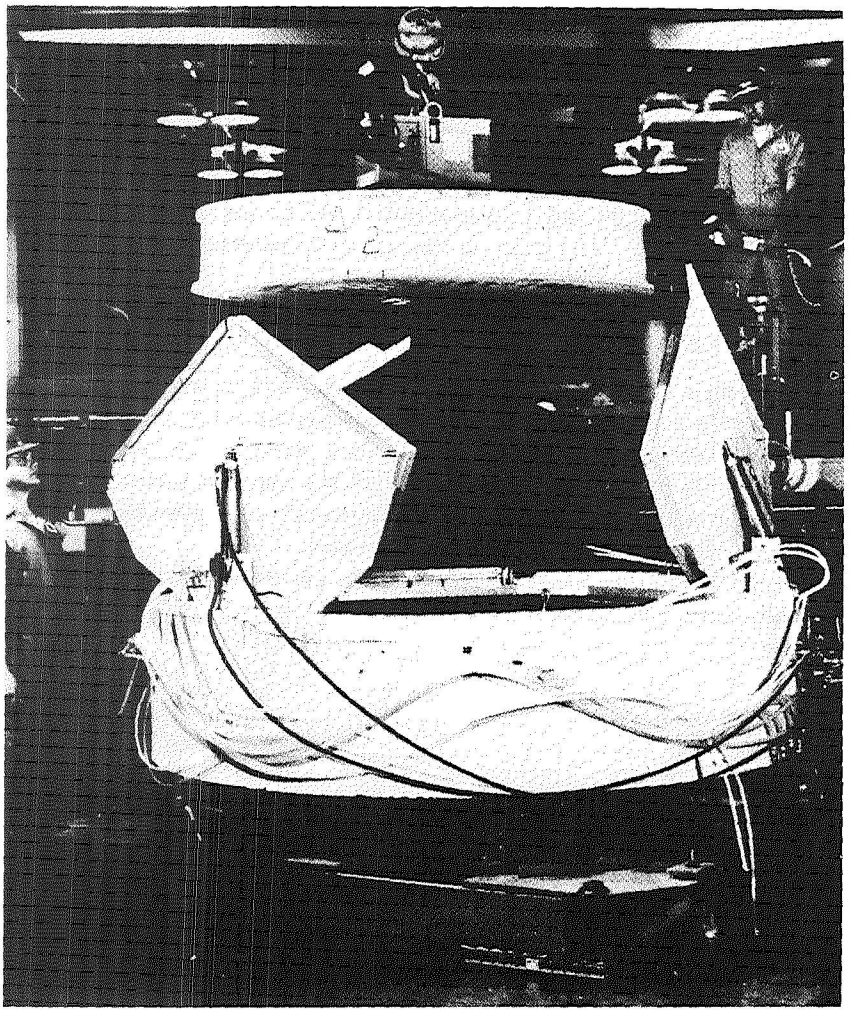

Figure 2.–Test mirror installation into thermal shroud.

along with a curve bounding twice the standard deviation determined for each point. The probability that the real surface difference lies between the two boundary curves is 0.95 and only 0.05 that the real surface lies outside the band.

COMPARISON OF MEASUREMENTS WITH PREDICTIONS

Measurements and predictions of the change in surface figure under uniform temperature changes are shown in figure 4. Calculations were made both for a

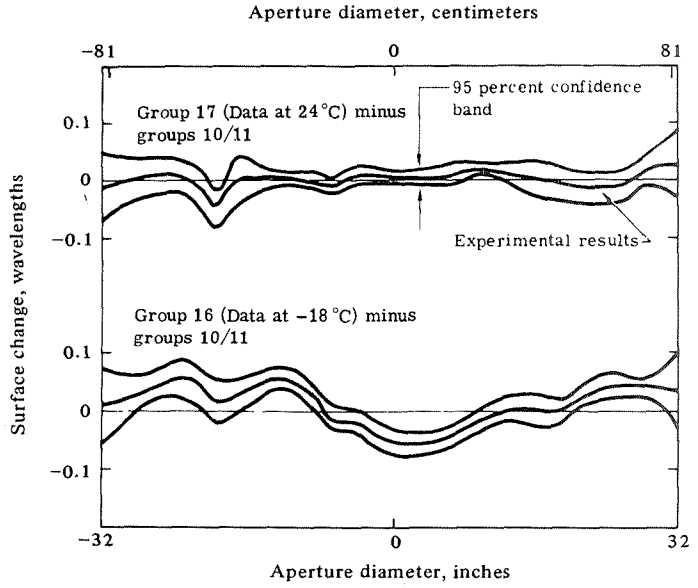

Figure 3.–Comparison of mirror difference surface mean profiles across one diameter for two test conditions.

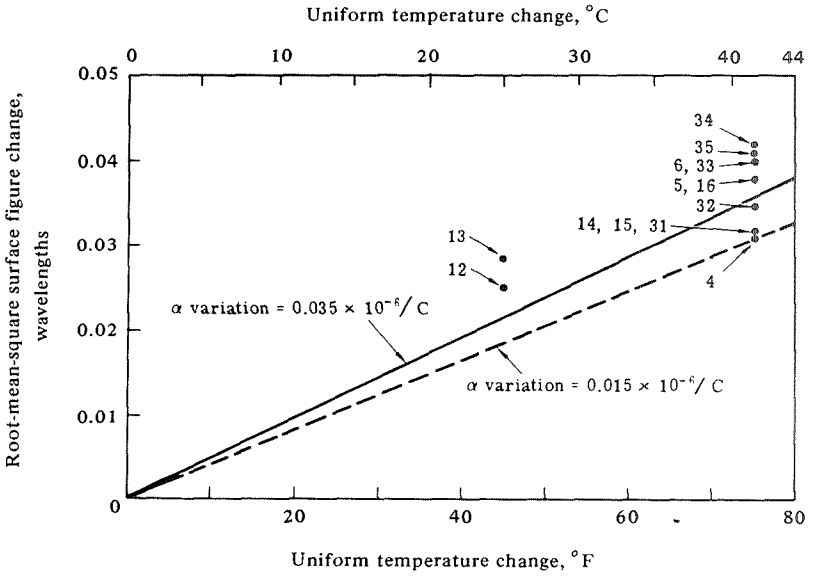

Figure 4.–Uniform temperature change comparison of predictions and measurements. (λ = 632.8 nanometers.)

radial variation in expansion coefficient within the boules from which the mirror was fabricated equal to $0.035 \times 10^{-6}/°C$ (early material) and $0.015 \times 10^{-6}/°C$ (current material). A random distribution of material within the core was assumed. Due to the uncertainty involved in knowing the actual distribution of expansion coefficient within the mirror, agreement between predictions and measurements within ±50 percent would have been considered reasonable. The data are in good agreement with predictions and further are grouped about the upper line (within ±20 percent), which is representative of the material variations typical at the time material for this mirror was produced. Data taken at an intermediate temperature of $-1°C$ were also in reasonable agreement with predictions.

REFERENCES

1. Paquin, R. A.; and Goggin, W. R.: Perkin-Elmer report 10657 (contract NAS5-11327), May 1971.
2. Goggin, W. R.; et al.: Perkin-Elmer report OOD-41 (contract DAAH-01-68-C-0018), Feb. 1970.
3. Bloxsom, J. T.; et al.: Perkin-Elmer report 9383 (DDC AD 842-227; contract DAAH-01-68-C-0018), Sept. 1968.

V

Precision Pointing and Control Systems

AN ANALYTICAL AND EXPERIMENTAL EVALUATION OF ACTUATOR VIBRATION ON SPACE TELESCOPE IMAGE DISTORTION

A. D. Houston, L. W. Hodge, Jr., and T. J. Kertesz
Lockheed Missiles & Space Co., Inc.

Described in this paper is a program conducted at Lockheed Missiles & Space Co., Inc., that addressed the overall question of pointing control in the presence of actuator vibrations. The intent of the project was to reduce the technical uncertainties associated with programs in which pointing control is critical.

The program was conducted in three phases. Phase 1 consisted of exploratory shaker testing to evaluate measurement techniques and to develop experimental transfer functions. Phase 2 testing, in which operating Bendix MA500 control movement, gyroscopes (CMG) were used, employed the same analog data acquisition and processing system used in the phase 1 tests. Phase 3 of the experimental work was conducted with an advanced analog-to-digital data acquisition and processing system (MODALAB) and included additional transfer function studies and preliminary evaluation of Sperry reaction wheel.

DISCUSSION

Test Specimen

The Space Telescope structural developmental test vehicle used in the experimental program consists of three basic sections: the optical telescope assembly; the support system module; and 46-centimeter (18-inch) deep conical monocoque adapter connecting them. The optical telescope assembly section consists of a cylindrical semimonocoque ring-stiffened aluminum shell and contains the basic elements of the optical system, including primary and secondary optical surface and focal-plane simulators. The specimen accelerometer and shaker locations are shown in figure 1.

Instrumentation

Ultrasensitive vibration transducers (1000 millivolts per gram sensitivity) were installed on the structural developmental test vehicle to monitor motions of the primary and secondary optical surface simulators and at the focal plane. Both Kistler QA116 and Unholz-Dickie 100 PA transducers have been used

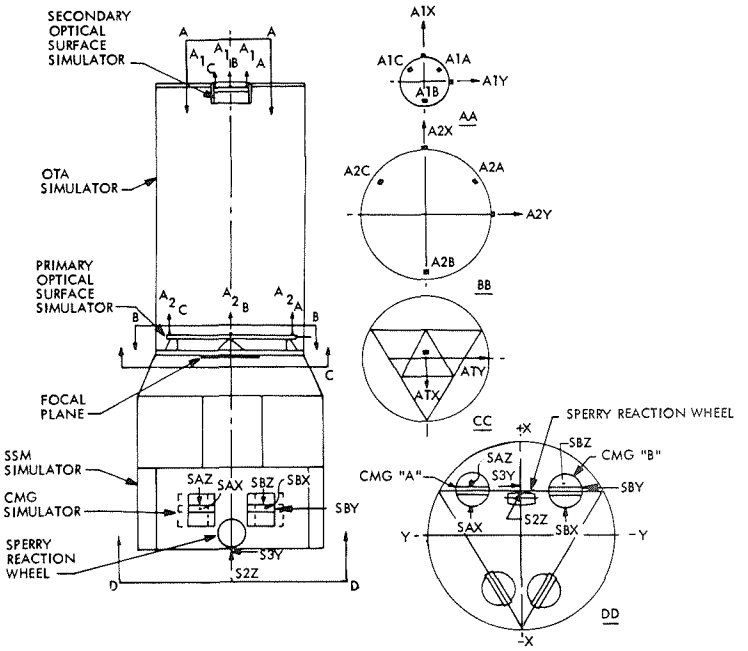

Figure 1.–Structural developmental test vehicle instrumentation and actuator locations. (OTA = optical telescope assembly; SSM = support systems module.)

successfully in the program. The location and orientation of this instrumentation (fig. 1) was such that translational and rotational motions of the primary and secondary optical surfaces relative to the x- and y-axes could be determined. Instruments were installed to monitor translation of the focal plane along the x- and y-axes.

Data Acquisition

Phase 2 testing on the specimen employed an analog data acquisition and processing system. Signals proportional to shaker force, which were held constant, provided absolute value ($|A|$) inputs to each of two coquad analyzers. Image distortion signals ($\ddot{e}_x$ and $\ddot{e}_y$) were passed through 2-hertz tracking filters and provided absolute value ($|B|$) inputs to the coquad analyzers.

Phase 3 testing used the bulk analog-to-digital capability of MODALAB as the primary data acquisition, storage, and processing system.

Analytic Simulation

The conical adaptor structural developmental test vehicle mathematical model was constructed using a half-model approach and the Lockheed finite

element code SNAP. The final model consisted of 2600 equivalent full model degrees of freedom. The model used 417 plate and 366 beam elements.

Major line of sight error contributions will result from modes (see fig. 2) involving significant relative optical element and focal plane motions with respect to local support structure.

Transfer Functions

Using computed optical eigenvectors, transfer functions are computed directly for force and moment inputs by using Lockheed steady-state response code STEDY9. All transfer functions are computed assuming uniform damping of 0.5 percent, based on previous structural development test vehicle experience.

EXPERIMENTAL AND ANALYTIC RESULTS

A typical comparison of analytic and empirical results is shown in figure 3. Note that the significant analytic modes 13 and 25 have excellent correlation with empirical results.

CONCLUSIONS

Transfer function tests conducted with a force amplitude of 27 grams (0.05 pound), which is typical for allowable disturbance on spacecraft such as the

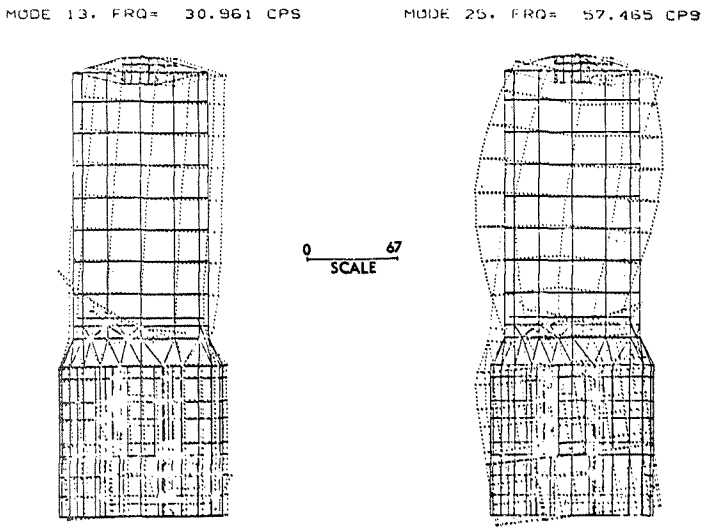

Figure 2.–Significant line of sight error analytic model modes.

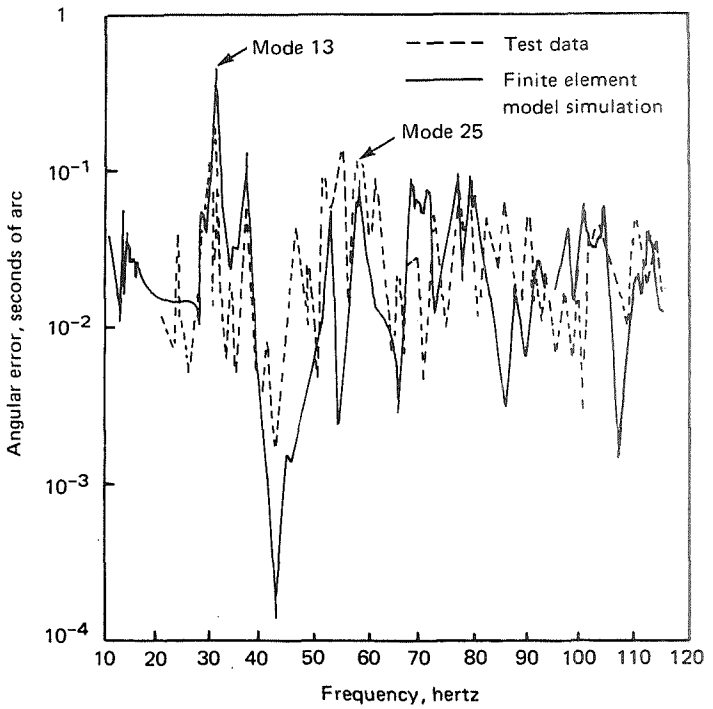

Figure 3.–Test and analyses simulation results. (0.5 percent uniform damping.)

Space Telescope showed that–

(1) State-of-the-art instrumentation and data processing can reliably measure dynamic response to such a small force in a 6120-kilogram (13 500-pound) structure.

(2) Pointing errors in different directions are about the same regardless of the direction of excitation in the range from 30 to 40 hertz.

(3) Analytical simulations based on detailed finite element models can predict in a conservative manner the frequency and amplitude characteristics of the response in the plane of excitation; however, they tend to underestimate the response in directions normal to the plane of excitation.

(4) Assuming the vector sum of an analytically obtained response to be applicable in any direction proves to be a good estimator.

(5) Large amplitude regions of the response, particularly at high frequencies, are clustered in frequency bands associated with resonances of secondary mirror supports.

(6) The key to insuring high pointing accuracy is to have CMG whose speed can be changed by 10 to 15 percent, thus moving them from the regions of frequency cluster, or to design secondary mirror supports that have no resonances within 10 to 15 hertz of the operating speed of the CMG.

(7) Three-axis isolators can attenuate disturbance caused by very low level forces; however, the effectiveness of attenuation varies by as much as 10 decibels, depending on the orientation of the CMG spin vector.

(8) Variation of isolation effectiveness with direction can be minimized by insuring that the center of gravity of the CMG is in the plane of the four isolators and that the CMG support structure has resonance three to four times greater than the isolation frequency.

(9) Nonlinear "beating" could not be induced in the experimental structure with a 45-decibel amplitude range with reference to the response at the CMG spin frequency.

(10) Pointing stability requirements budgeted for high-frequency vibration, such as 0.0035 second of arc for the Space Telescope, are attainable with state-of-the-art CMG designs and isolation systems; furthermore, the performance of structures at typical spin speeds can be predicted with a high degree of confidence, thus lowering development risks.

DEVELOPMENT OF A LARGE-INERTIA FINE-POINTING AND DIMENSIONAL STABILITY SIMULATOR

R. L. Gates, D. H. Wine, R. W. Seiferth, and N. A. Osborne
Martin Marietta Corp.

The Space Telescope attitude control requirements have placed an increased emphasis on simulation techniques to prove the validity of the requirements. The 0.007-second-of-arc stability requirement and the long-term pointing requirements require that the hardware component models be more complete for scientific computer simulations. Proper experiment design requires that the errors in physical simulation equipment, particularly the instrumentation, be about an order of magnitude less than the spacecraft operational performance requirement.

In 1972 Martin Marietta built a fine-pointing simulator that obtained a pointing stability below 1 millisecond of arc. This physical simulator, which demonstrated excellent pointing stability, is considerably below the desired Space Telescope spacecraft inertia. It has a maximum inertia of 2000 kilograms-square meters (4.5×10^4 pounds-square feet) instead of the 6×10^4 kilogram-square meter (2×10^6 pound-square foot) inertia of the 2.4-meter (94-inch) Space Telescope. This meant that the data had to be scaled by a factor ranging from 30 to 90. When nonlinearities are involved, scaling becomes questionable. With a full inertial simulator, scaling becomes unnecessary.

Other limitations of the first generation simulator are that the rotation axis is vertical and the main beam is made of aluminum. Long-term testing of gas bearing rate integration gyros is difficult because vertical Earth rate required compensation and the aluminum truss is susceptible to dimensional changes due to temperature variations.

A new physical simulator referred to as the fine-pointing and dimensional stability simulator was completed early in 1975. The unique features of this simulator are a mercury mass augmentation system to provide 10^5 kilogram-square meter (2×10^6 pound-square foot) inertia and a graphite epoxy instrument truss to insure long-term stability to gyro testing (fig. 1).

This simulator has a single degree of freedom and its pivot axis is oriented east-west to minimize Earth rate effects on gyro testing. The pivot freedom is provided by specially designed flex pivots that provide a rotation angle of 2 degrees. The pivot support and the inner truss, which is center connected with the flex pivot, are made of graphite epoxy. A larger outer aluminum truss is

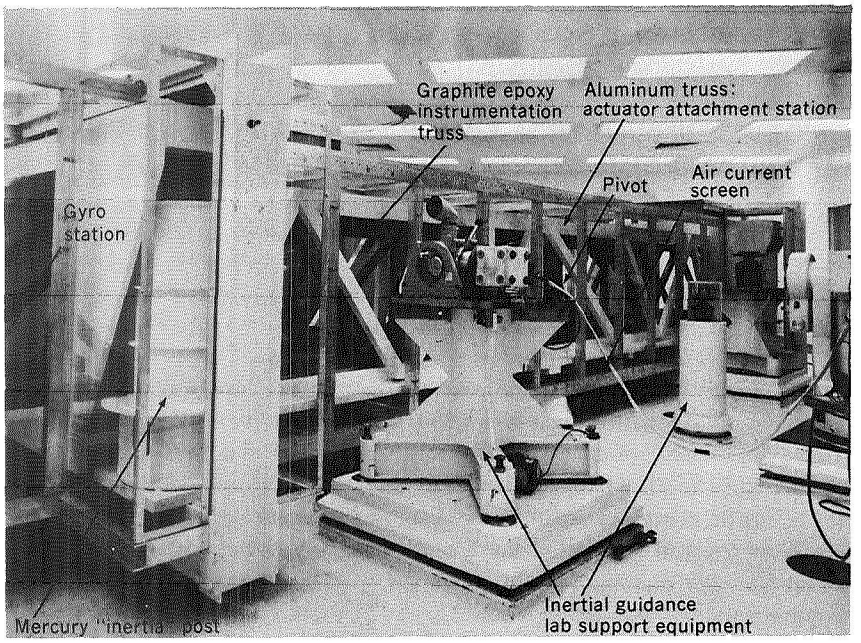

Figure 1.–Fine-pointing and dimensional stability simulator.

then connected to the graphite truss by flex hinges, which are stiff in rotation but allow the aluminum truss to change dimension with temperature while keeping the graphite stress to a minimum. Four mercury mass augmentation systems are connected to the aluminum truss. These systems not only provide proper equivalent mass but also give approximately 1800 newtons (4000 pounds) of buoyant force to float the larger aluminum truss so that its pivots are nearly unloaded.

The total simulator is enclosed in Plexiglass to isolate it from the room air currents. The system is quite sensitive to acoustical coupling.

The pivot support, mass augmentation system, and reference piers all are mounted to a very large inertia block that rests on bedrock. This particular location has very low seismic background noise and provides a very precise testing environment. The floor area is spring isolated from the testing piers.

EVALUATION OF COMMUNICATION ANTENNA DRIVE SYSTEM DESIGN REQUIREMENTS TO ALLOW TRACKING AND DATA RELAY SATELLITE TRACKING DURING SPACE TELESCOPE FINE POINTING

A J. Besonis and C. J. Chang
Lockheed Missiles & Space Co., Inc.

Orbiting telescope systems such as the Space Telescope have to provide a pointing stability accuracy of ±0.007 second of arc (root mean square). This accuracy has to be maintained over a frequency spectrum from essentially zero to frequencies ranging beyond several hundred hertz.

The effects of all potential disturbance sources have to be evaluated to insure that such extreme pointing accuracies can be maintained in the operational environment of the telescope. Major attitude disturbances to the system include external torques such as gravity gradient, aerodynamic, solar, and reaction torques produced by operating equipment internal to the Space Telescope. The latter category of disturbances includes those that would be produced by communications antenna motion if required to track the Tracking and Data Relay Satellite.

A major tradeoff in terms of cost savings through the use of existing antenna and drive system design has been identified. This would require antenna tracking during certain periods of Space Telescope observations. An additional important payoff would result with this design because the required transmitter power would be limited to levels compatible with the state of the art. This again can have a significant impact on cost and will certainly minimize potential design risks.

The use of fixed as opposed to tracking antennas would involve the following considerations:

(1) Line of sight from the Space Telescope to the Tracking and Data Relay Satellite changes a maximum of 11° during an orbit.
(2) Baseline configuration has open-loop high-gain antenna tracking to maintain a boresight gain of 25.7 ± 0.2 decibels.
(3) Use of optimized fixed pointing (one slew per orbit pass) causes antenna boresight to be a maximum of ±5.5° off angle to the Tracking and Data Relay Satellite, giving a gain loss of 4.9 decibels.
(4) Transmitter power is increased 3.1 times over baseline (from 10 to 31 watts).

Therefore, the advantages of fixed pointing are that antenna inertial compensation is not needed and computer use is needed for only one slew as opposed to continuous pointing. The disadvantages of fixed pointing are that it requires three times more power, the amplifier is a new development, and there may be interference with other multiaccess users because of the 4.9-decibel signal strength variation over a single pass.

An existing communication antenna design developed by TRW, Inc., has been identified for Space Telescope application. The system is depicted in figure 1. The counterbalance system statically balances the antenna; the inertia seen by the azimuth drive is independent of elevation angle. Azimuth and elevation inertias are equalized, allowing identical azimuth and elevation drives. A flexible coaxial cable wrap, a power cable wrap, and a compensating inertia ring are added to an existing stepper motor harmonic-type drive. The ring virtually eliminates disturbances and allows antenna motion during fine pointing.

The major objective of this study was to determine by computer simulation if such a design with a half-power bandwidth of 8 degrees would be adaptable to the Space Telescope. The selected approach was to simulate the complete dynamic system consisting of the Space Telescope, the antenna with its drive system, and the antenna structural support system. Required antenna motion was then introduced while the Space Telescope was inertially stabilized with a control system bandwidth compatible with the fine-pointing requirements dictated by considerations other than antenna tracking motions.

SIMULATION RESULTS

Evaluated were the existing configuration (1.1-meter (39-inch) antenna with the dish offset from the elevation drive axis), the effect of mass balancing of the antenna, and the effect of adding momentum compensation to each axis of the antenna drive. Two types of antenna mounting support (booms) were also considered. The first type of support consisted of aluminum alloy booms configured in an A-frame in the Space Telescope y-z plane stabilized in the x-z plane by guy wires of stainless steel. The aft guy wires imparted a preload to the forward guy to achieve a suitable stiffness. The A-frame had a natural frequency in the y-z plane of 16.4 hertz, and the guy wire support had a frequency of 2.25 hertz.

The alternative type of support considered was a rigid single boom of graphite epoxy. The reason for an antenna support that would shift about either axis is that control actuators such as reaction wheels would more readily excite a soft boom, producing large dynamic errors. Boom excitations of 8.0 and 11.0 hertz were considered.

The level of compensation considered was 95 percent for static balance and 90 and 80 percent of momentum compensation.

Table 1 summarizes simulation results for the different antenna drive systems considered for the soft antenna support. Results show that with mass

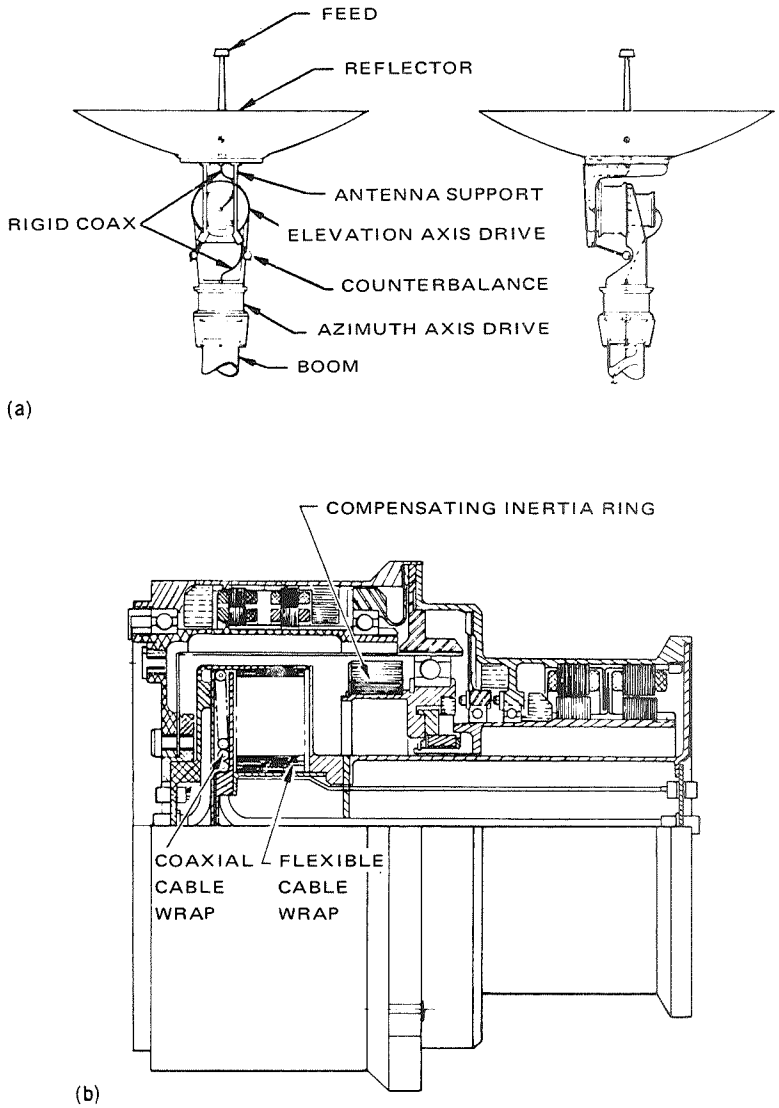

Figure 1.–High-gain antenna design used in the study. (*a*) Counterbalance system. (*b*) Antenna drive–cutaway view.

balance alone, Space Telescope pointing errors of the order of 10^{-3} seconds of arc can be produced. This level is considered excessive based on the error budget allocated for the total system. Results for two levels of momentum compensation are also shown in table 1. As shown, momentum compensation reduces the attitude error to below an order of magnitude of the allowed total

TABLE 1.—*Comparison of Maximum Space Telescope Pointing Errors Produced by Antenna Tracking (Stepping[a]) in Azimuth and Elevation*

Antenna position	Condition	Attitude error, seconds of arc		
		Roll	Pitch	Yaw
Antenna vertical (elevation: 90 degrees)	No mass balance; no momentum compensation	0.011 2	0.001 28	0.005 63
	Mass balance: 95 percent; no momentum compensation	.003 09	.001 16	.001 37
	Mass balance: 95 percent; momentum compensation: 80 percent	.000 62	.000 23	.000 275
	Mass balance: 95 percent; momentum compensation: 90 percent	.000 29	.000 115	.000 138
Antenna horizontal (elevation: 0 degree)	No mass balance; no momentum compensation	.009 4	.001 27	.006 53
	Mass balance: 95 percent; no momentum compensation	.002 87	.001 13	.001 5
	Mass balance: 95 percent; momentum compensation: 80 percent	.000 55	.000 23	.000 30
	Mass balance: 95 percent; momentum compensation: 90 percent	.000 285	.000 113	.000 148

[a]Step size: 0.0375 degree per step.

pointing stability error for the Space Telescope. Momentum compensation to within 80 percent is quite easily attainable in the drive system considered without incurring a significant design cost.

Simulation for the rigid single boom supports showed little difference for the same level of momentum compensation.

CONCLUSION

Antenna tracking of the Tracking and Data Relay Satellite can produce significant attitude disturbances on the Space Telescope if proper design procedures are not adopted to compensate the antenna system. With moderate mass balance and momentum compensation, the pointing errors can be held to below one order of magnitude of the pointing stability error specified for the Space Telescope. Considerable latitude exists in the design of the antenna structural support system from the standpoint of stiffness, provided, of course, it is sufficiently stiff to avoid interaction with the dynamics of the Pointing

Control System and to prevent large errors caused by excitation from momentum actuator unbalance.

ACKNOWLEDGMENTS

Support by TRW, Inc., and by Roy Acker in particular for providing design data on the antenna system is gratefully acknowledged.

SPACE TELESCOPE INTERFEROMETRIC FINE GUIDANCE SENSOR

A. B. Wissinger and R. H. Carricato
Perkin-Elmer Corp.

This paper describes the Space Telescope fine guidance sensor preliminary design by answering three questions: What does the fine guidance sensor have to do? How does the sensor function? What is the sensor's predicted performance?

FUNCTIONS

The fine guidance sensor has several functions. Its primary function is to detect mispointing of the telescope by measuring the positions of auxiliary or guide star images in the telescope focal plane. The measurement is converted to an electrical error signal for the use of the support system module in correcting the pointing direction to 0.007 second of arc (root mean square).

Because the guide stars will occur at arbitrary (but known) positions relative to the star or object of scientific interest, the fine guidance sensor must be capable of performing its primary function for any accessible star location. The accuracy of some of the spectrographic instruments depends on the location of the star image in the entrance slits, and it is the null point of the fine guidance sensor that locates the star image; therefore, the fine guidance sensor must have the capability of accurately positioning the guide star relative to the science instrument. This means that the null point of the fine guidance sensor must be adjustable and repeatable with an accuracy of 0.01 second of arc to meet the needs of the spectrographs.

The fine guidance sensor must also have sufficient sensitivity to measure faint guide stars. It is required to have sufficient field area and sensitivity to insure an 85 percent probability of acquisition in the area of the sky where stars are the least dense (at the galactic poles).

Given a field area for the fine guidance sensor sized to achieve 85 percent probability of acquisition, the system must then have the capability of searching for the guide star. Once a star is detected, the sensor must check it with the brightness of the selected guide star. When the detected star is the correct star, pointing error signals are sent to the spacecraft so that it can reduce the pointing error to less than 0.007 second of arc. The simulation described later in this paper includes the spacecraft dynamics.

One final function that is included in the fine guidance sensor is the ability to continuously offset the tracking point (sensor null) to make a time exposure of a moving planet and to compensate for the effects of the differential velocity aberration. Differential aberration is the apparent change in the radial position of stars in the telescope field caused by the spacecraft velocity vector. The sensor will correct for this gross direction change, but stars in different parts of the telescope will have slightly different shifts. The effect is as large as three times the Space Telescope stability requirement (0.007 second of arc) and must be compensated.

COMPONENTS AND OPERATION

A single sensor is capable of detecting errors simultaneously and continuously in pitch and yaw. A second sensor is used to measure the motions of a second guide star caused by roll motions around the axis defined by the line of sight to the star used to control pitch and yaw pointing.

The Perkin-Elmer concept uses an interferometer to detect the tilt of the wavefront that results from a change in the telescope pointing direction relative to the guide stars. The wavefront tilt is best measured at a pupil (which is an image of the primary mirror) because all the rays pass through the pupil for any guide star positions.

A small gimbaled mirror is also placed at a pupil formed by the relay mirror in the fine guidance sensor. Its purpose is to direct the star light to a fixed reference location regardless of the guide star position. At this location, there is a mirror with a small aperture at its center and a beamsplitter in the aperture area.

The gimbaled mirror is preset precisely to an angular position corresponding to the guide star location. The signal for setting the mirror is a single ground command. However, the mirror can also be used for planet tracking by sorting a series of commands representing the trajectory of the planet.

The action of the mirror and beamsplitter is to reflect the star image to the image dissector when the image is outside the field stop and to evenly split the light between the image dissector and interferometer when the image is within the field stop.

The interferometer output is split into four quadrants and directed to four photomultiplier tubes. The outputs of the photomultipliers are amplified by photon-counting-type amplifier/discriminators. The pulse trains from each amplifier output are used to drive up/down counters, which produce the error signal between opposing pairs of photomultiplier tube/amplifiers.

THE SPACE TELESCOPE POINTING SYSTEM SIMULATION

To test the performance of the fine guidance sensor, a digital computer simulation program was written.

The emphasis of the simulation is placed on the fine guidance sensor. A

simple single-axis model of the Space Telescope vehicle and its pointing control system is included. The only nonlinearity included in the vehicle control system is a torque limiter.

A fine guidance sensor consists of two error detectors: the image dissector, which is used to sense errors from 2.5 to 0.1 second of arc, and the fine error sensor, which is used to sense errors less than 0.1 second of arc. The outputs from these two error detectors are called the coarse error signal and the fine error signal, respectively.

The input to the simulation is a star direction with respect to the vehicle pointing angle; the difference angle is the pointing error. Initially, the fine guidance sensor is in the coarse mode, and it remains in the coarse mode until the coarse error ϵ_c indicates less than 0.1 second of arc.

As the star image traverses the beamsplitter field stop, an apparent centroid shift takes place. This shift is computed and added to any system offsets that might occur within the coarse sensor to form the error signal generated by the image dissector star tracker. A 0.1-second time delay is inserted to account for aperture scanning and dwell time required by the image dissector. It is this processed and delayed signal that is used to determine when the error is within the fine error detector capture range.

Once the coarse error signal shows an error less than 0.1 second of arc, control is passed to the fine error sensor. The interferometer transfer function computation simulates the polychromatic transfer function of the fine error detector. Gaussian noise is generated using conventional techniques and is added to the error signal.

The error signal is then fed to the pointing control system. After the fine guidance system has been in the fine mode for 10 seconds, a root-mean-square pointing error varies between 0.0011 and 0.0014 second of arc. It must be remembered that this is only the error caused by fine guidance internal noise and quantization.

CONCLUSIONS

The fine guidance sensor described has ample performance margins. The effects of nonlinearities, noise, quantization, and mode switching have been included in the simulation of both the fine guidance sensor and the support system module. In spite of these effects, performance requirements are met for a variety of simulated operational conditions.

The wide-field image dissector, with its 5-minute-of-arc acquisition field, relieves the initial pointing accuracy requirements for the support system module. When compared with earlier requirements, the requirement is reduced by a factor of 5.

The combination of photon-counting electronics and the interferometer for fine guidance sensing permits operation on fainter guide stars. The margin of probability for acquiring guide stars is thereby appreciably increased over the 85 percent requirement.

PRISMATIC GRATING STARTRACKER

Allen H. Greenleaf
Itek Corp.

LINE OF SIGHT STABILIZATION FOR THE SPACE TELESCOPE

The Space Telescope will observe celestial objects much too dim to provide line of sight stabilization error signals by some kind of target lock-on sensor. The stabilization error signals must be provided therefore by a device that locks onto a brighter star image somewhere else within the telescope field of view. In the Itek version of the Space Telescope, there are three fine guidance sensors situated radially around the focal plane area so that star images appearing within three areas at the edge of the field of view can be used for stabilization. The fine guidance sensors must be capable of searching for and acquiring the guide star image within a 1-minute-of-arc-diameter initial pointing error and then providing pointing commands to bring the telescope to the correct orientation.

OPERATION OF PRISMATIC GRATING SENSOR

The basic concept of the fine guidance sensor is to use a fixed, coarse grating at the focal plane upon which the guide star is imaged. This grating breaks the beam from the guide star into different optical channels, and the precise location of the guide star image on the grating determines the relative balance of power in the different channels. The only element in the sensor, the stability of which is critical for stabilization of the telescope line of sight, is the grating itself.

Figure 1 is a schematic of the fine guidance sensor as it is to be used in the Space Telescope. The converging beam from the guide star is first passed through an optical micrometer, which consists of two gimbaled plane parallel glass plates. The optical micrometer provides accurately controlled displacements of the guide star image over a range equal to the 4-second-of-arc groove spacing of the grating plate. This provides the means to guide on any guide star image within the field of the grating plate while keeping the guide star image centered upon a groove intersection. Next, the guide star beam converges to focus at the grating plate. The grating plate is a curved element whose front and rear surfaces conform, respectively, to the tangential and sagittal focal surfaces of the telescope. The grooves on the front surface form concentric rings because the star image at that surface is blurred tangentially.

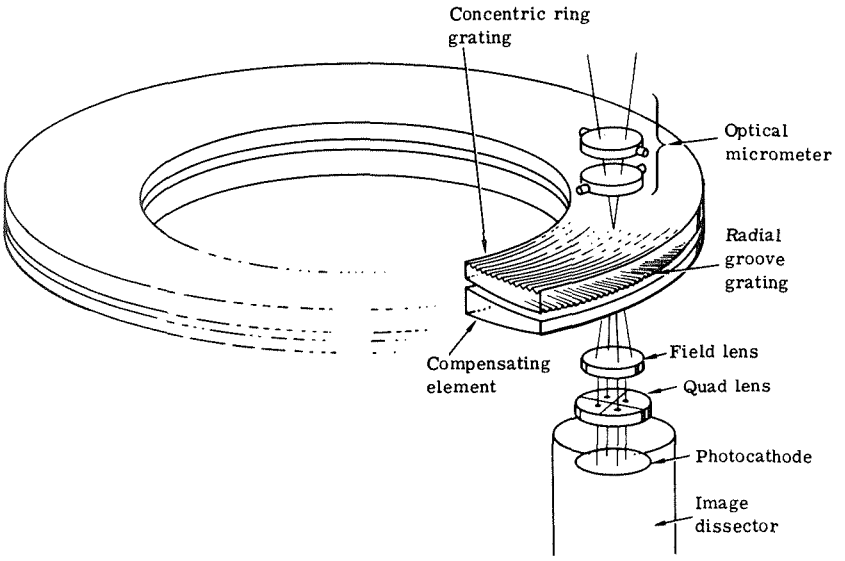

Figure 1.–Schematic diagram of a fine guidance sensor.

The grooves at the rear surface run radially because the star image at that surface is blurred in the radial direction. The grating on the front surface divides the light into two beams–the relative power of each depends upon the radial location of the star image. The grating on the rear surface divides each of the two light beams at that point into two more beams; the relative power of each of these beams is dependent upon the tangential position of the star image. This configuration automatically compensates for the astigmatism in the telescope image without the need for additional correctors. The error signal from the sensor is essentially that of a diffraction-limited optical system.

Behind the grating plate is the sensor head, which contains the optical relay elements and the image dissector. The four beams from the guide star image formed by the grating plate are projected onto different points of the image dissector. During fine tracking the image dissector samples these four beams in sequence and develops tracking error signals proportional to their differences in power. During initial acquisition the image dissector also measures the positions of the four beams on the image dissector and uses this information to provide coarse tracking information. This controls telescope pointing until the guide star image has been brought to the appropriate groove intersection on the grating plate, when fine tracking commences.

Figure 2 shows an isometric view of one of the fine guidance sensors. The optical micrometer, relay, and image dissector are assembled to constitute the sensor head and can be positioned at the point in the grating at which the guide star is to appear. The grating is mounted to an Invar structural bulkhead to which the mounting feet for the instrument are attached.

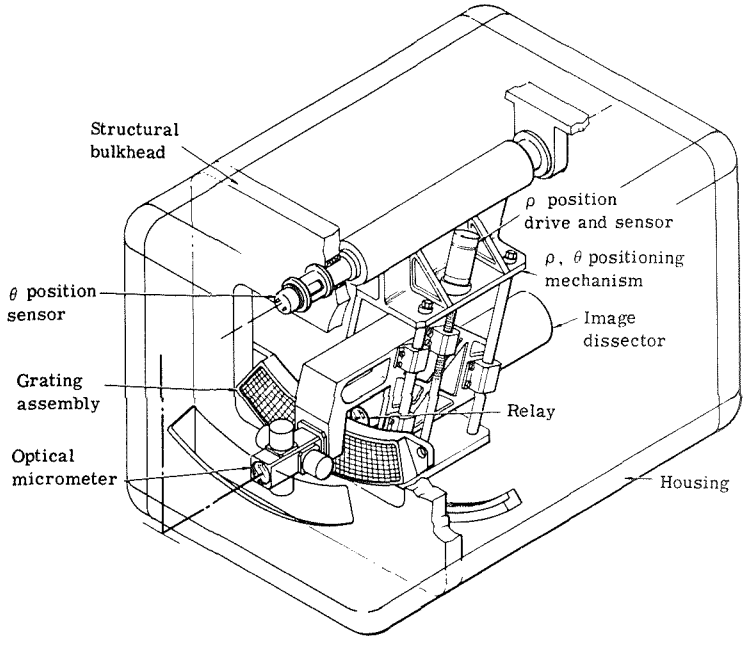

Figure 2.–Isometric view of a fine guidance sensor.

By selecting the photon-counting mode of operation for the nulling loops within the sensor, sources of noise other than shot noise in the signal current may be made negligible. At the same time, the background counts in the signal are insignificant compared to the counts received from the guide star; therefore, virtually the only system limitation is the photon noise of the guide star. The noise equivalent angle as a function of the visual stellar magnitude of the guide star and the effective integration time of the control system is shown in figure 3. A control system with a 5-hertz noise equivalent bandwidth has an effective integration time of about 0.1 second; so for a magnitude 13 star, a stabilization error contributed by the sensor noise of about 0.002 second-of-arc root mean square can be expected.

The sensor, by virtue of its basic concept, is remarkably free of stabilization errors other than the photon noise error. The bandwidth-independent errors add up to about 0.001 second-of-arc root mean square. This also represents the sensor capability in reacquiring a guide star following occultation by Earth.

ASTROMETRIC MEASUREMENTS

The fine guidance sensor is suitable for making astrometric measurements for star parallax and proper motion determinations because the basic astrometric measurement consists of measuring changes in the angular separation between stars over an extended period of time.

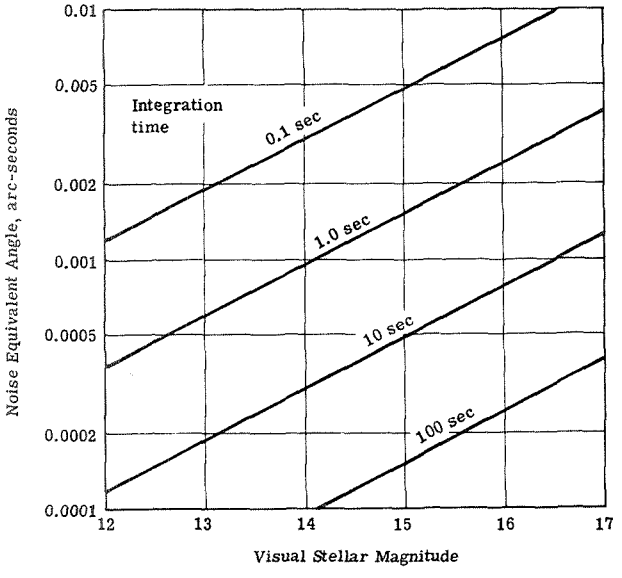

Figure 3.–*Photon noise of a fine guidance sensor.*

BREADBOARD VERIFICATION OF THE CONCEPT

A breadboard built at Itek, with astigmatism-accommodating gratings, relay optics, and image dissector, fully demonstrates the performance capability of the tracker in searching for, acquiring, and locking onto a guide star. Performance limited by diffraction and photon noise is achieved. The gratings were produced by Bausch and Lomb in the circumferential and radial groove form on curved surfaces as would be required for the Space Telescope. Figure 4 shows the breadboard and electronics.

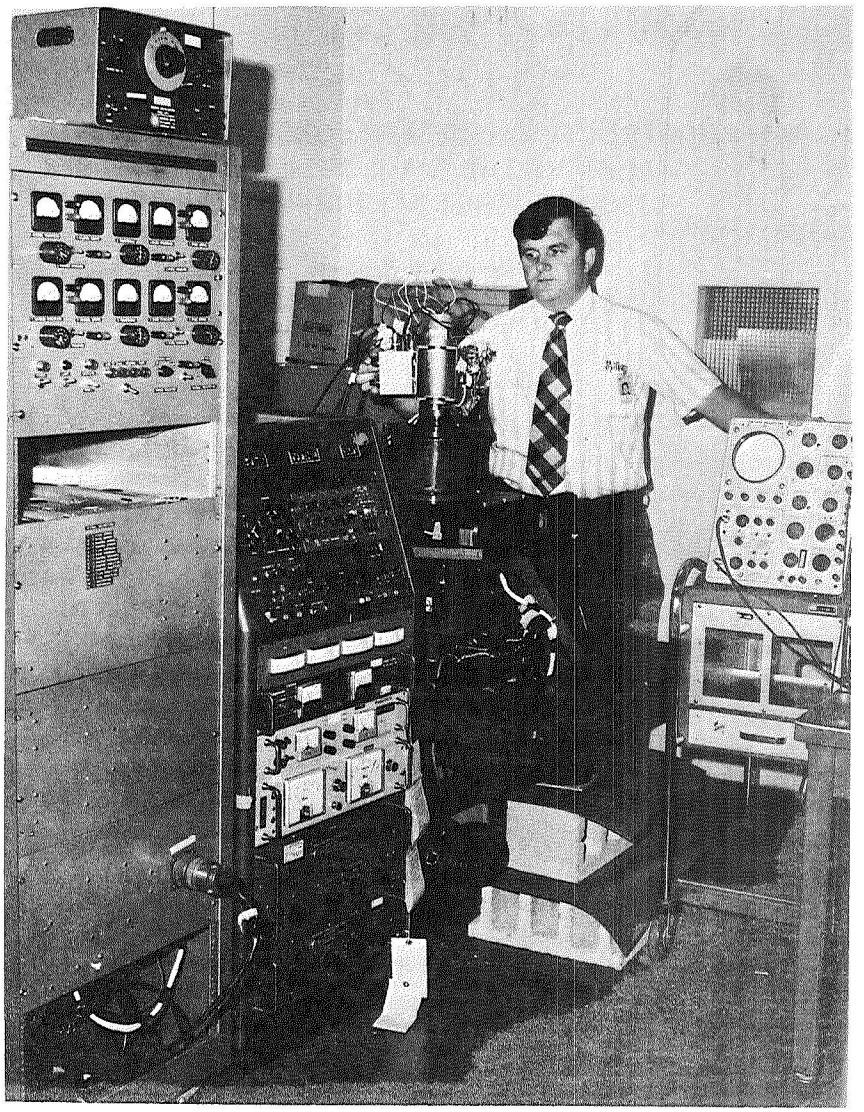

Figure 4.–Startracker breadboard.

THERMOSTRUCTURAL DESIGN CONSIDERATIONS TO ACHIEVE THE SPACE TELESCOPE LINE OF SIGHT REQUIREMENTS

Domenick J. Tenerelli
Lockheed Missiles & Space Co., Inc.

The Space Telescope, which is scheduled for launch in 1982, is a long-life precision-pointing, Earth-orbiting satellite requiring structures that provide high dimensional stability, minimum thermal distortion, and minimum response to onboard dynamic environments (e.g., reaction wheels). The Space Telescope must be developed, tested, and manufactured at the lowest system cost. This vehicle will be placed in orbit by the Space Shuttle, which will also be used for orbital servicing and return of the Space Telescope.

Some of the design, analysis, and test studies that have been conducted to meet the requirement goals stipulated for the structure are described in this paper.

The Space Telescope is to be an astronomical facility developed by the National Aeronautics and Space Administration under the direction of the George C. Marshall Space Flight Center in Huntsville, Alabama. It will be designed as a national observatory, capable of using a wide range of scientific instruments.

As currently configured, it will be an assemblage of three major modules: an optical telescope assembly (OTA), scientific instruments (SI), and a support systems module (SSM). The OTA will be a Ritchey-Chretien optical system consisting of a 2.4-meter (94-inch) diameter, clear aperture reflecting telescope with an $f/2.3$ (approximately) primary and a secondary mirror combination. The SI package will include field cameras, low- and high-dispersion spectrometers, and ultraviolet and infrared sensors to give the Space Telescope a broad capability for spectral analysis.

Located within the SSM will be the Space Telescope's very precise stabilization system for attitude sensing and control. NASA's development goal of 0.007-second-of-arc guidance stability for periods of up to 10 hours is akin to keeping the view within the area of a dime nearly 400 miles away, or from Washington, D.C., to Boston. Such fine-pointing accuracy is necessary to obtain full use of the OTA's optical capabilities. The SSM will also contain power and communications systems and provide environmental control and data management for the scientific instruments. Electrical power for the system will be supplied with the aid of solar panels.

The orbiting telescope will measure approximately 13 meters (43 feet) in length and from 3 to 4¼ meters (10 to 14 feet) in diameter. This vehicle will circle Earth at an altitude of approximately 500 kilometers (270 nautical miles) and at an inclination to the Equator of 28.8 degrees.

The Space Telescope will contribute significantly to studies relevant to the origin and structure of the universe, the study of energy processes that occur in galactic nuclei, the study of early stages of stellar and solar systems, and observation of such objects as supernova remnants and white dwarfs. It will be capable of viewing galaxies 100 times fainter than those seen by the most powerful ground-based optical telescopes.

The Space Telescope configuration was modeled for analysis by the Structural Network Analysis Program finite element computer code. The purpose of the analysis was to determine the effect of SSM thermal deformations on the alinement of the optical system. The early designs had the OTA/SI and SSM meeting at the main ring. It was assumed that if the in-orbit thermal deflections of the OTA/SI structure could be maintained to the listed requirements, the performance of the Space Telescope would be guaranteed. A representative finite element computer model was developed depicting a design configuration that had the OTA/SI and the SSM joined at the main ring. To insure the ability to differentiate thermal deformation effects of the SSM structure on the optical system from those of the OTA/SI structure, the OTA/SI structure was maintained at ambient conditions. The results of this detailed thermostructural computer analysis of the total Space Telescope structural system showed that an accumulated tilt and decenter misalinement of over 100 seconds of arc will exist between the optical elements and the focal plane during certain orbit conditions. This amount of misalinement results in unacceptable performance output of the telescope. A solution to this situation is to design the OTA/SI structural system such that it is essentially isolated from the external structure; i.e., the SSM. Isolation of the optical system can be achieved by a three-point support with either flexure joints or spherical bearings. This type of design was also modeled for finite element computer analysis. Results of a thermostructural deformation analysis showed that the optical system is unaffected by SSM thermal deformations when the Space Telescope structural system is designed with a thermal isolation joint between the OTA/SI and the SSM.

A strong candidate for the type of configuration that should be used as the main element of the metering structure that maintains the alinement between the primary and secondary mirrors is a ring-stiffened, thin-walled circular cylinder made from graphite epoxy. An analysis was performed to determine the effect on the despace between the primary and secondary mirrors because of the incompatibility of displacements occurring at the ring-shell junctures of a ring-stiffened, thin-walled cylinder as the result of a uniform increase in temperature (3° C (5° F)) in the rings and shell. The results indicate that the shell axial deformation is minimized as the coefficient of thermal expansion of the ring in the hoop direction is increased in the positive direction. This result

is logical; i.e., when the hoop expanison of the ring approaches the hoop expansion of the shell, the normal forces between two components are mininuized. This trend in turn reduces the Poisson ratio effect. The results also showed that the coefficient of thermal expansion of the ring base should be close to that of the shell in the axial direction, although a complete match at $-0.07425\ K^{-1}$ ($-0.04125\ (°F)^{-1}$) still causes an increase in shell length. This is due to the Poisson ratio effect caused by the mismatch of the hoop deformations between the ring and the shell. The variation of the shell length with the adhesive thickness indicates that the axial deformation of the shell is significantly affected by the thickness of the adhesive layer. Large adhesive thicknesses result in large increases in the length of the shell as a direct result of the adhesive extensional stiffness increase.

ACKNOWLEDGMENT

The work described in this paper was supported by NASA contract NAS8-31313.

DESIGN OF LOW THERMAL DISTORTION SPACE TELESCOPE METERING STRUCTURE

John R. Lager
Martin Marietta Corp.

High-precision performance of the Space Telescope proposed for future astronomical observations from Earth orbit requires that the lens support structure remain dimensionally stable under variable environmental conditions. A fibrous structural material—continuous graphite filament—offers potential for design of structures with near-zero thermal distortion characteristics. This is possible because, unlike other structural materials, individual graphite fibers have a negative coefficient of thermal expansion (i.e., contract when heated) in their axial direction. Composite laminates using these fibers and epoxy matrix material can be used to design truss structures that remain dimensionally stable when subjected to temperature variations.

The Space Telescope metering structure shown in figure 1 was designed and a representative section was fabricated and tested to demonstrate the potential of a near-zero thermal distortion structure. The selected overall structural concept shown in figure 2 is a truss with individual members fabricated of continuous graphite fiber, epoxy resin, and fiber glass cloth. A zero thermal distortion truss structure is defined as one for which the node points at truss member joints do not move when the overall truss is subjected to gross thermal gradients. However, other points on the individual truss members can and, in general, will move. For example, the requirement for angle-plied materials in the end regions of truss members (e.g., for attachment purposes) causes these regions to have a slightly positive axial thermal coefficient that is offset in the center portion of the member by a laminate configuration that provides a slightly negative coefficient. Therefore, the overall gross axial movement of the truss member is a net zero even though there is relative movement of individual points along the truss member. The truss members also exhibit relatively large radial movement, which is not detrimental because relative movement of truss node points remains near zero.

Finite element analysis of overall truss performance and application of basic strength-of-materials-type theory to truss components have been shown to be entirely appropriate and satisfactory for predicting structural response. Fortunately, the type of structure and basic composite laminates required to provide a zero thermal expansion coefficient lend themselves to the use of

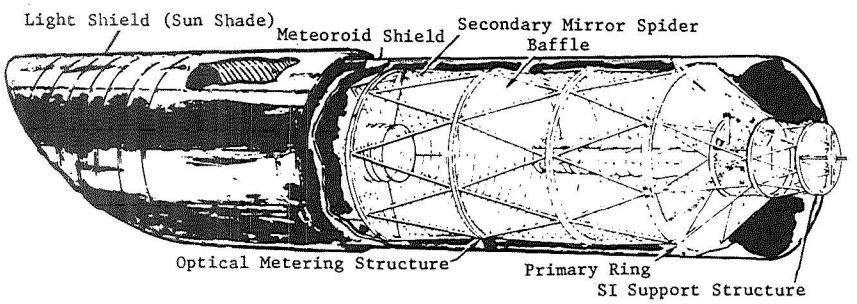

Figure 1.–Space Telescope structural support assembly.

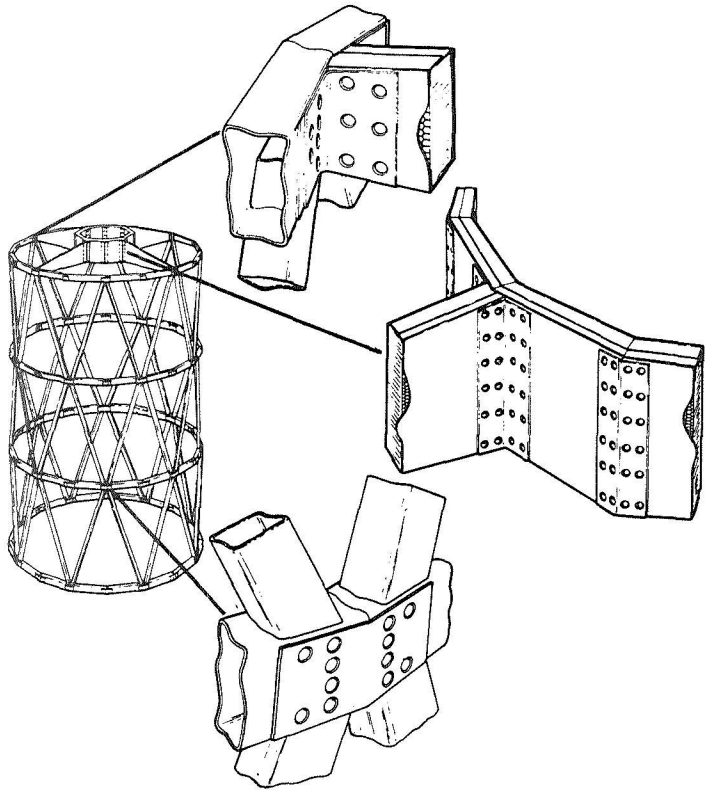

Figure 2.–Low thermal distortion graphite epoxy metering truss concept.

uncomplicated theoretical analysis methods. A unique feature of Space Telescope truss design is that a specific value of overall thermal expansion (i.e., zero) is required, with very little tolerance for error on either side of the desired value. This is in contrast to typical aerospace structural characteristics,

such as stiffness and strength, in which minimum values are established, with a relatively large margin for error on the overdesign side. Therefore, the analytical expression used to predict the axial thermal expansion coefficient of individual truss members was subjected to a Monte Carlo probability analysis. Each of the 14 influencing variables was assigned a mean value and assumed to have a normal distribution of variation with an assigned standard deviation. The mean value and standard deviation of the strut axial thermal expansion coefficient determined from the Monte Carlo analysis indicated that design allowables of the Space Telescope metering truss could be satisfied without imposing undue restrictions on the normal variation of the influencing parameters.

A triangular section (fig. 3) of the full-scale metering truss was fabricated to demonstrate feasibility and refine proposed techniques. Fabrication of a single truss strut member used a dissolvable plaster mandrel that was grooved along two opposite sides to provide potential for fabrication of high-quality wrinkle-free components. The truss strut was debulked several times before final cure. Each debulk cycle involved applying a resin bleeder system and vacuum bag and then heating the bagged system to 71° C (160° F) for 2 hours. After debulking, a considerable amount of epoxy resin had bled off; however, the component remained uncured. The debulking cycles provided high fiber content of the final component, which is required for a low axial thermal expansion coefficient. Intermediate debulking also minimized resin removal during final cure, resulting in good surface appearance.

Final cure used a vacuum bag system and autoclave with applied pressure of 690 kilonewtons per square meter (100 pounds per square inch) and maximum cure temperature of 191° C (375° F). After final cure, the plaster mandrel was washed out by passing hot water through the center aluminum tube. The ends of the struts were cut to finished dimensions using a diamond cutoff wheel on a standard table saw.

Struts, frames, and splice plates were assembled using the attachment concept shown in figure 3. In general, fibrous composite laminates have low interlaminar shear and bearing strength. The effect of these characteristics on the design of mechanical attachments is that fasteners in single shear should be avoided and fasteners with a large bearing area are desirable. The attachment concept shown has these desirable features, with the added advantage that it is lightweight, inexpensive, and very rigid. The fastener consists of a hollow aluminum tube that is shrunk fit, bonded, and swaged in place.

Successful fabrication of the metering-truss A-frame fully demonstrates the potential for fabricating high-quality low thermal distortion truss structures. Fabrickability and fabrication cost were given full consideration throughout design concept development. The result is that the final truss concept uses component parts that are very easy to fabricate; the attachment concept is lightweight, rigid, and inexpensive; and the process techniques developed result in a very appealing appearance of the finished structure.

	Millimeters (mm)	Inches (in.)
104 glass		
+45° graphite epoxy	0.05	0.002
−45° graphite epoxy	0.05	0.002
0° graphite epoxy	0.2	0.008
104 glass		
0° graphite epoxy	0.2	0.008
0° graphite epoxy	0.2	0.008
104 glass		
0° graphite epoxy	0.2	0.008
0° graphite epoxy	0.2	0.008
104 glass		
0° graphite epoxy	0.2	0.008
0° graphite epoxy	0.2	0.008
104 glass		
0° graphite epoxy	0.2	0.008
0° graphite epoxy	0.2	0.008
104 glass		
−45° graphite epoxy	0.05	0.002
+45° graphite epoxy	0.05	0.002
104 glass		

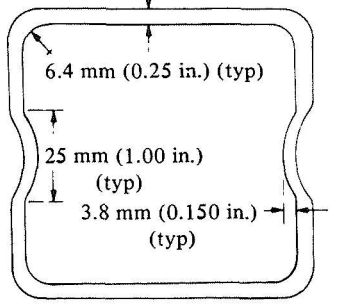

Section A-A

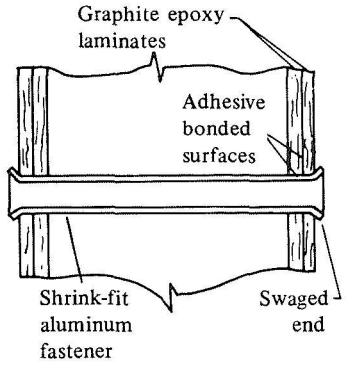

Section B-B

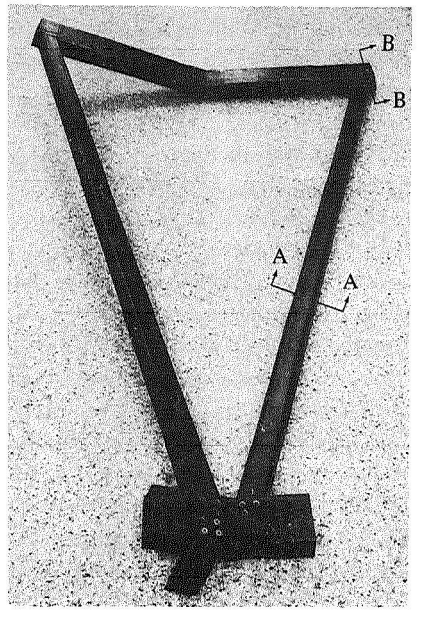

Figure 3.—A-frame section.

Predicted strength and stiffness of the end attachment method were verified through successful structural tests of a series of test specimens. The ultimate failure load of approximately 11 120 newtons (2500 pounds) of a single-pin unbonded specimen provides for design of joint attachments in which the pins resist all the design ultimate load, and the epoxy adhesive, although significantly strengthening and stiffening the joint, need not be relied on for structural integrity.

One of the full-scale 185-centimeter 5- by 5-centimeter (73-inch 2- by 2-inch) truss struts was tested to verify the predicted low value of the thermal expansion coefficient. The optical extensometer used has the ability to detect relative motion of approximately 0.0005 centimeter (0.0002 inch); therefore, a relatively large change in temperature is required so that small movements associated with the expected low thermal expansion coefficient can be properly monitored. This method of measurement was used because it was relatively inexpensive and satisfied the test objectives to determine feasibility rather than fully and precisely characterize the thermal distortion characteristics of the strut. The measured coefficient of thermal expansion was $-0.09 \times 10^{-6}\ K^{-1}$ ($-0.05 \times 10^{-6}\ (°F)^{-1}$ over the temperature range of 22° to 93° C (72° to 200° F).

THREE-AXIS SIMULATION OF THE POINTING CONTROL SUBSYSTEM—A MULTIDISCIPLINE ACTIVITY

W. W. Emsley, T. D. Fehr, D. C. Fosth, and D. L. Knobbs
The Boeing Co.

The Boeing Co. started research related to orbiting telescopes in 1965. The initial effort was a laboratory investigation of precision pointing capability where a "rigid" vehicle was three-axis stabilized with performance indicated at better than 0.05-second-of-arc peak to peak. This early demonstration of the feasibility of precision pointing led to detailed studies of actual spacecraft implementation of pointing control systems.

The analog control systems were judged inflexible and costly relative to long life and diverse operating modes. The follow-on research emphasized digital control technology to overcome the limitations. The initial efforts were analytically oriented to develop the background and tools for advanced digital control concepts. An interdisciplinary approach resulted in the development of a succession of analytic tools followed by hardware prototypes and software development to validate the analyses. This tool evolution resulted in two key computer simulations for Space Telescope application: the Vibration Analysis Program and the Digital Three-Axis Attitude-Control Simulation. These programs allow analysis of the Space Telescope Pointing Control Subsystem, and interfaces including structures and optical paths, in the frequency and time domains, respectively.

With the establishment of the analytic base, the emphasis shifted to investigations of the multidisciplinary aspects of synthesizing a Pointing Control Subsystem. The proof-of-performance testing was being actively pursued by Marshall Space Flight Center. The Boeing decision was to complement this effort with a three-axis air-bearing simulation emphasizing the total range of Pointing Control Subsystem functions and interfaces. (This choice was prompted in large part by the difficulties experienced in this area by NASA and DOD contractors in applications related to the Space Telescope.) The three-axis air-bearing simulation is shown in figure 1. The sensory inputs for the simulated Pointing Control Subsystem are provided by an array of state-of-the-art, strapdown, rate-integrating gyros; two cadmium sulfide star-trackers with a 1-milliwatt helium laser and collimating mirrors for a source; and a modified Canopus tracker with a collimated star source. The actuators of the simulated Pointing Control Subsystem are six prototype control moment

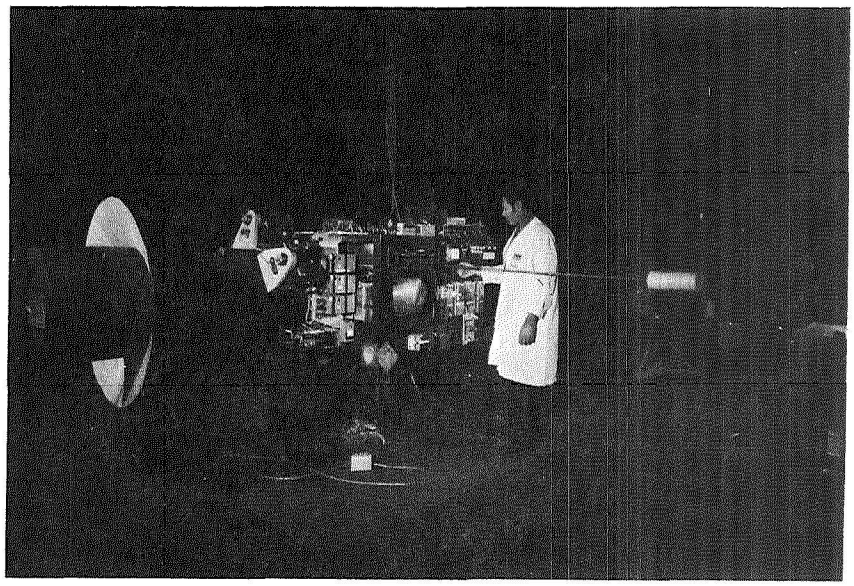

Figure 1.–Three-axis air-bearing simulator.

gyroscopes mounted in a skewed array. The signal processing is provided by a prototype aerospace computer (24-bit, 8000-word memory, 0.8-microsecond add, 3.4-microsecond multiply) interfacing with 16 channels each of 15-bit analog-to-digital and digital-to-analog conversion and three channels of voltage-to-frequency converter-updown counters. Other interfaces for the Pointing Control Subsystem included the onboard power system, simulated structural modes, and articulated appendages including an antenna gimbal system. (See fig. 2.) The antenna gimbal system base motion simulator duplicates the motion of the air-bearing simulated vehicle. Software for the system was developed at the assembly level and tailored to the simulated Space Telescope application.

The test program is progressing successfully. The integration of the various interfaces (and disciplines) has been demonstrated. The actuator control law (pseudoinverse) has been verified and a low-gain caging loop added to retain a nominal null configuration permitting maximum momentum utility. The pointing demonstrations were followed by an assessment of the slew mode performance. The slew law was developed and validated, which applied jerk (derivative of acceleration), acceleration, and rate limits to a single axis (Euler) rotation for any maneuver. Appendage motion was monitored in these tests to assess slew excitation and has been judged minimal. Reacquisition was assessed and implemented effectively using the slew law for even the smallest rotations. The antenna gimbal system performance was assessed and pointing perform-

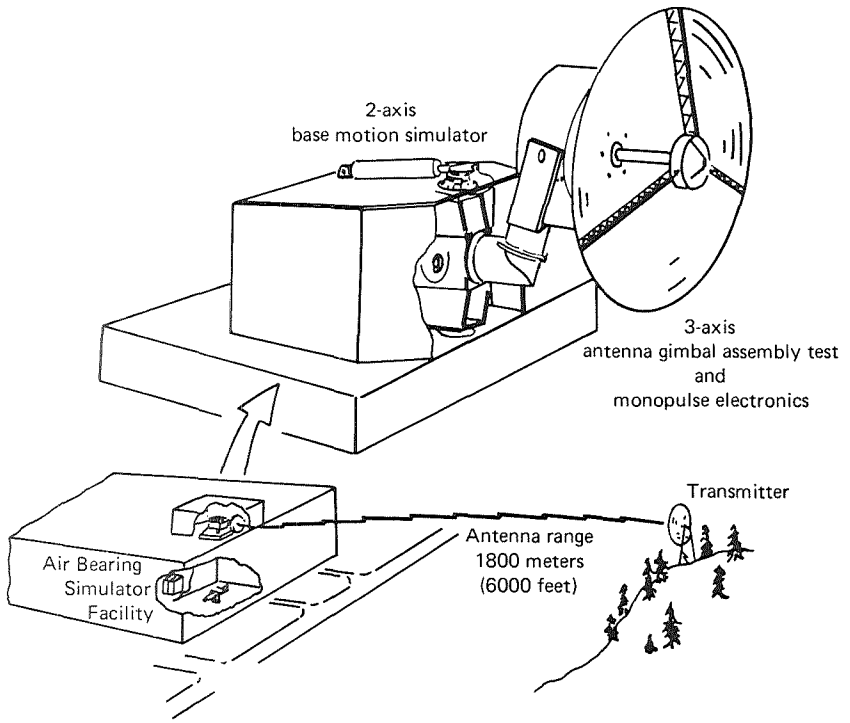

Figure 2.–Communication system test facility. Functions: acquisition, autotrack, and disturbance sequence through the air-bearing simulator tie in.

ance approaching 5 percent of the beamwidth was demonstrated using monopulse tracking data. Signal lock was maintained during simulator vehicle slewing (with base motion following).

A significant result of this test program is a detailed preliminary design and validation of the Pointing Control Subsystem software. The pointing performance of the simulated vehicle, on the order of 0.05-second-of-arc peak to peak, is not representative of the Space Telescope application. However, the correlation of the measured performance with that predicted using the analytic simulations serves to validate the digital computer program models. This validation lends credibility to the analytic predictions for Space Telescope pointing performance. Furthermore, the air-bearing simulation has resulted in further detailed definition of the interface and subtier requirements.

VI

Data Management

DATA MANAGEMENT AND MISSION OPERATIONS CONCEPT

R. Walker, F. Hudson, and L. Murphy
International Business Machines Corp.

Space Telescope studies in progress have accentuated the need for a clear understanding of the interaction between spacecraft and ground facilities. This paper describes a candidate design concept for a Space Telescope ground facility. The design objective was strongly influenced by a desire to use NASA institutional (existing or planned) hardware, software, and facilities whenever practical to reduce development cost. A second objective was to maximize efficiency of telescope usage.

The Space Telescope is a space-based observatory with a complement of scientific instruments that may be changed upon retrieval of the vehicle. The telescope is oriented so as to place the target to be viewed on the focal plane of the viewing instrument and within the field of view of the selected electronic detector. Fundamental to the operation are the pointing accuracies and the stability of the telescope, once acquisition of the object has been achieved. Table 1 shows the performance requirements of the Pointing Control Subsystem, which is being designed to maintain a stability of 0.007 second of arc for all viewing states where guide star pairs are available.

The nominal sequence for experiment pointing is as follows. A slew maneuver to the commanded celestial coordinates is accomplished by use of navigation instrumentation. Fine guidance sensors are used to acquire two guide stars within 30-second-of-arc field of view. Closed-loop commands through the Pointing Control Subsystem position the telescope to the accuracies stated for modes II and III, shown in table 1. However, knowledge of the position of the target with respect to the guide star without direct target viewing is expected to be ±0.3 to 1.5 seconds of arc. This level of accuracy is a natural goal because this is the type of accuracy one can expect to routinely derive from all-sky ground-based photographic surveys. Further refinement of pointing in mode II is accomplished by onboard direct object viewing with loop closure through the Pointing Control Subsystem. In mode I, correction commands are derived from direct target display on the ground referenced to the Space Telescope body coordinator.

On an average day it is expected that 30×10^8 bits of science data including calibration, engineering, and housekeeping data will be generated by the Space Telescope. Approximately 10 percent of the science data will be processed in real time for quick look or for target acquisition verification.

Figure 1 shows the major data interfaces of the candidate ground system.

TABLE 1.–*Pointing Control Performance Requirements*

Instrument	Line of sight accuracy (diameter), seconds of arc	Stability (root mean square), seconds of arc	Maximum exposure period, minutes	Target acquisition mode[a]
Infrared photometer	0.1	0.03	60	III
Faint object spectrograph	.03	.03	600	I^1
High-resolution spectrograph	.01	.01	600	II
Astrometer:				
Wide	1.0	.007	10	III
Narrow	.03	.007	10	III
High-speed point/area photometer	.03	.05	300	I^2
f/24 field camera	1	.03	60	III
f/48 and *f*/96 planetary camera	1	.007	5	III

[a]Mode I^1: ground control, real-time operation slit jaw camera, 160- by 100-pixel frame; mode I^2: ground control, real-time operation, 160- by 100-pixel frame; mode II: onboard, image dissector detection, closed-loop Pointing Control Subsystem; mode III: onboard, program coordinates used for pointing.

All data from the Space Telescope are communicated to the Mission Operations Center (MOC) in real-time and to the Telemetry Operations Processing System (TELOPS) as well. MOC and Science Operations (SO) real-time operations are performed with the Science Institute (SCI) acting in an advisory and monitoring role. In the non-real-time mode, engineering data are processed through TELOPS and MOC, but the science data go only to TELOPS and subsequently to SCI. This does not preclude SO from requesting a real-time operation on demand. From the time the science data are received by TELOPS, the data processing may be viewed as a "batch operation." The SCI uses the Master Data Processor (MDP) and Image Data Processor (IDP) Facilities to perform specific image processing with Space Telescope unique algorithms.

Of considerable interest for display and computer manipulation of data by the SCI and SO in the Space Telescope program is the Earth Resources Interactive Processing System, which is designed to analyze data from Landsat (formerly the Earth Resources Technology Satellite). Primary analysis software presents lists of interactive questions for callup of data manipulation programs, imaging of digital data, pattern recognition, and statistical handling of multispectral images.

CONCLUSION

The Space Telescope, as a vehicle, has highly autonomous guidance, navigation, and control functions. This uncouples ground mission operations

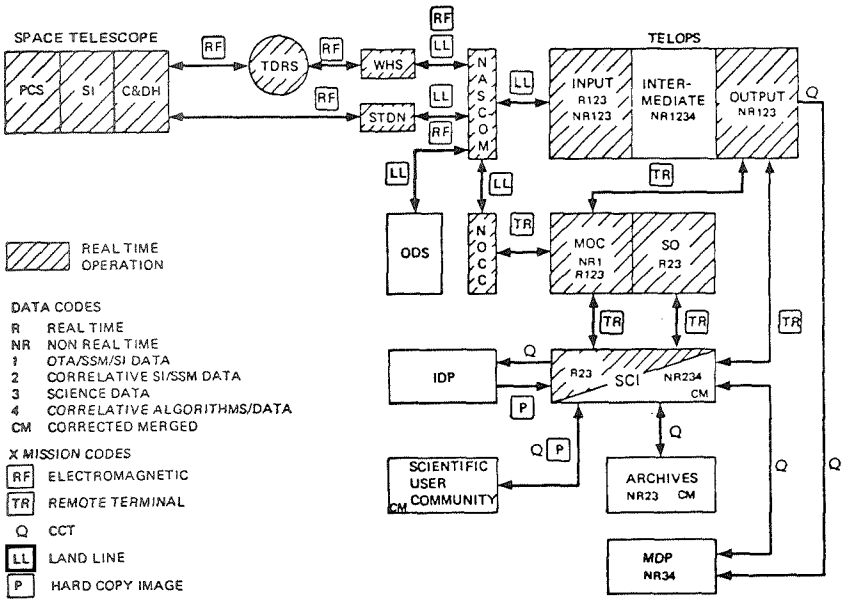

Figure 1.—Major data interfaces. (CCT = computer-compatible tape; C&DH = command and data handling; NOCC = Network Operations Control Center; ODS = Orbit Determination System; PCS = Pointing Control Subsystem; SI = scientific instruments; STDN = Spaceflight Tracking and Data Network; TDRS = Tracking and Data Relay Satellite; WHS = White Sands, New Mexico.

from serious time constraints, facilities workaround, and interactive science procedural investigations. The criterion of high efficiency in data taking is best achieved by exact modeling, mission planning, and execution of the mission plan in such a way as to minimize lost time resulting from vehicle slewing to new targets and occultations. Once the science data cross the NASCOM interface, the problem switches to one of management of high data rate information and data processing. The thesis of this paper is to encourage in these formative years the formulation of Space Telescope requirements for NASA multiuser institutional facilities. Development cost is a prime concern, and it must be realized that image data processing is extremely demanding of data processing capacity and that the facilities now being procured for work in the allied field of Earth resource digital image processing must be shared by the Space Telescope.

ACKNOWLEDGMENT

The work described in this paper was supported in part by NASA Marshall Space Flight Center contract NAS8-31312.

DATA MANAGEMENT FOR THE SPACE TELESCOPE

G. R. Hope, Jr.
Lockheed Missiles & Space Co., Inc.

and

T. J. Rasser
Bendix Corp.

The Space Telescope is an orbiting national astronomical observatory that will provide useful data for the scientific community from a variety of scientific instruments. The present complement of instruments includes an *f*/24 field camera, *f*/48 and *f*/96 planetary camera, faint object and high-resolution spectrographs, astrometer, infrared photometer, and a high-speed point/area photometer. Major detectors envisioned for use in the scientific instruments are a 70-millimeter (2.8-inch) Secondary Electron Conduction Orthicon (SECO) with a format of 2000 by 2000 picture elements (pixels) and two types of semiconductor devices: A 400 by 400 element charge-coupled device and a 100 by 160 element intensified-charge-coupled device. In addition, auxiliary sensors, intensified charge-coupled devices, and image dissectors are used for target centering in instrument and guidance sensor apertures.

Because the Space Telescope will be a useful observatory for many years, provisions are being made in the design to allow instrument replacement as technology or observational needs warrant. Instrument replacement may occur in orbit using the Space Shuttle and crew extravehicular activity or by means of ground return, refurbishment, and subsequent relaunch. Flexibility is therefore the keystone upon which data management for the Space Telescope must be founded. There must be sufficient flexibility to accommodate different instruments, different detectors, and different observational requirements in response to changing needs of science. The challenge to the system designer is to provide this flexibility while also providing a system at minimum cost.

There are two significant differences between the Space Telescope and previous NASA programs. The first difference is, of course, the advent of the Space Shuttle (also referred as the Space Transportation System or Orbiter). The capabilities and flexibility of the Space Shuttle have a profound impact on system design. For instance, we are no longer facing the severe weight constraints of the past; in fact, we can trade addition of weight in structure to provide larger factors of safety against costs of both static and dynamic

structural tests. Probably the largest impact, though, is the capability the Space Shuttle provides to perform in-orbit maintenance of components or modules, which are called orbit replaceable units. Thus, a failed transmitter can be replaced or a scientific instrument updated in orbit, or, if need be, the Space Telescope can be brought back to Earth for more extensive refurbishment.

The other difference between the Space Telescope and current systems is the support provided by the Tracking and Data Relay Satellite System (TDRSS), a new addition to the Spaceflight Tracking and Data Network (STDN). There is no longer the constraint of relatively short and infrequent ground station contact opportunities for command, telemetry, and payload data dumps. TDRSS provides both forward (command) and return (telemetry) narrowband services over about 85 percent of the orbital period at the present altitude (500 kilometers (311 miles)). The operational ground rules are that science data transmission (at 1.1 million bits per second exclusive of the 1/2 rate convolutional coding required by TDRSS) can be scheduled for up to 30 minutes per orbit when in view of either or both relay satellites. The capabilities of TDRSS exceed present needs, so no constraint due to high-rate data communication services exists. This nearly full-time command and engineering data coverage contributes to the ability to provide flexibility. In addition, as a contingency mode of operation in the event that the Tracking and Data Relay Satellite (TDRS) link is unavailable, the ground stations of the post-1980 STDN can be used to receive science and engineering data and transmit command loads, although at greatly reduced coverage.

Both onboard and ground-based elements (fig. 1) must be considered because Space Telescope data management addresses the end-to-end flow of data from the scientific instrument to the ultimate user, the astronomer/scientist, and also the command/control and health monitoring of the vehicle. The key requirements for data management are as follows:

(1) Acquire, format, transmit, and process science data quantities of from one frame (1.6×10^8 bits) per revolution to 3×10^9 bits per day, at rates through the system of up to 1 million bits per second
(2) Use TDRSS, both S-band single access and multiaccess channels, as primary space link; use post-80 STDN as backup for forward and return links; use NASCOM for point-to-point data transmission
(3) Generate onboard software and hardware requirements for vehicle command/control, health and status data acquisition, formatting, science data acquisition and routing, telemetry transmission, and command receiving
(4) Generate ground software requirements for vehicle control, mission planning, science scheduling, science processing and display, test and checkout, software maintenance/update, health/status processing, and display

The onboard portion of data management consists of the instrumentation,

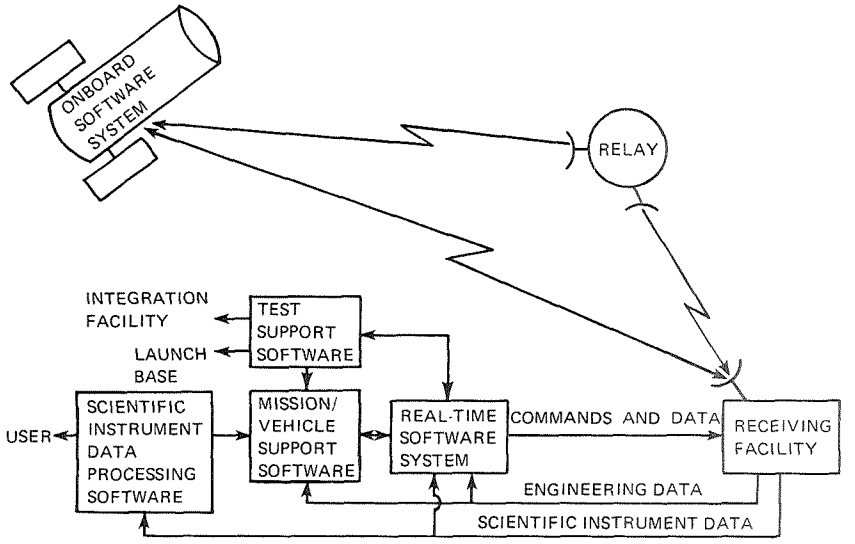

Figure 1.–Function allocation overview.

communications, and data management subsystems. The instrumentation subsystem provides the transducers and sensor that monitor the vehicle and payload health and status. The instrumentation system isolates, by telemetry processing, failures on the vehicle and payload to the orbit replaceable units. The communications subsystem provides the facilities to transmit scientific instruments and engineering data to the TDRSS or STDN ground station and receive commands from the relays or ground stations.

The data management subsystem functions are as follows: (1) acquisition, formatting, storage (if required), and routing of engineering and science data to the communications subsystem; (2) decoding, verification, storage, and distribution of commands to the vehicle subsystem and instruments; and (3) data processing to support the pointing control subsystem in maneuvering, stabilizing, and fine pointing the vehicle to allow scientific observations. Stabilization and target reacquisition requirements necessitate extreme accuracy: 0.007 second of arc. Observations can last from several milliseconds to several hours.

The ground-based portion of the data system has two major facilities: the Mission Operations Center (MOC) and the Science Institute (SCI), supported by the TDRSS ground terminal (TDRST) located in the continental United States, and NASCOM, which provides point-to-point communications services between NASA facilities.

Determination of the functions to be performed and allocation of functions to and among the system elements are the primary tasks of the system designer who must then configure hardware and software to implement the functions.

The functions that must be performed by the data management system are divided by area as follows:

(1) Vehicle support
  (*a*) Vehicle commanding
  (*b*) Vehicle health and status
  (*c*) Telemetry processing
  (*d*) Subsystem control
  (*e*) Calibration update
  (*f*) Telemetry formatting
(2) Mission support
  (*a*) Pointing control
  (*b*) Mission planning
  (*c*) Command generation
  (*d*) Ephemeris table construction
  (*e*) Scientific instrument control
  (*f*) Scientific instrument data processing
(3) Software support
  (*a*) Data base management
  (*b*) Executive control
  (*c*) Assembler/loader
  (*d*) Display handler
  (*e*) Maintenance and update
(4) Test system support
  (*a*) Command generation
  (*b*) Telemetry processing
  (*c*) Vehicle modeling
  (*d*) Calibration processing
  (*e*) Real-time test support/control
  (*f*) Vehicle status

The allocation of these functions to spacecraft and ground elements is as follows:

(1) Online vehicle support
  (*a*) Real-time execution
  (*b*) Command processor
  (*c*) Telemetry processor
  (*d*) Display handler
  (*e*) Pointing control (selective)
  (*f*) Scientific instrument data processing (selective)
(2) Airborne software
  (*a*) Executive processor
  (*b*) Command processor
  (*c*) Telemetry formatting and system status
  (*d*) Pointing control and update

(3) Off-line (batch) processor
   (*a*) Calibration processor
   (*b*) Mission planning
   (*c*) Command generation
   (*d*) Orbit determination and space positioning
   (*e*) Data base management
   (*f*) Telemetry processor
   (*g*) Onboard computer assembler/loader
(4) Test software
   (*a*) Calibration processor
   (*b*) Vehicle logic model
   (*c*) Command generation
   (*d*) Executive processor
   (*e*) Command transmission
   (*f*) Telemetry processor
   (*g*) Post-test analysis
   (*h*) Onboard computer assembler/loader
(5) Scientific data processing
   (*a*) Executive processor
   (*b*) Data content interrogator
   (*c*) Ancillary data processor
   (*d*) Telemetry processor
   (*e*) Calibration processor
   (*f*) Scientific instrument data processor

Because a careful balance must be maintained between minimum cost and flexibility, each function must be examined to determine where it can best be performed. The philosophy is that functions that can only be performed onboard will be performed onboard, and all others will be performed on the ground. Experience has shown that space hardware and software is many times more expensive than ground hardware and software.

It has also been shown that software to perform real-time processing is several times more expensive than batch processing software. Therefore, only those functions that must be controlled by real-time data feedback or that require near-real-time analysis in the MOC or SCI will use real-time software.

Consider, for example, spacecraft health and status processing. This function could certainly be performed onboard, and, in other systems, is. However, with TDRSS, there is near full-time orbital coverage of telemetry and command. Review of each spacecraft and payload subsystem for time-criticality of response to an anomaly revealed few areas that could not stand the time delay of transmission of telemetry to the ground and formulation and transmission of a command to the Space Telescope in response to the anomaly. Review of the relative costs of software onboard and on-the-ground to process the health and status data led to choosing to perform the function on the ground.

A similar decision was reached concerning pointing the high-gain antennas at TDRS. Ephemerides of both spacecraft are known and the necessary software and computing capacity could be made available onboard; however, cost of software led to a decision to do the computation on the ground and uplink stepping commands to control the high-gain antenna. Availability of only near full-time TDRS coverage and the delay caused by the space/ground/space communication forced us to incorporate processing capability for fine pointing of the spacecraft onboard. But slewing between target objects, and the computation required to formulate the steering commands is done on the ground and uplinked to the Space Telescope. These examples serve to show the interplay between the elements of the total data system and the tradeoffs that must be made to achieve a minimum cost but flexible data management system.

Mission planning and spacecraft control must be addressed early in the conceptual design of the overall system because they can have a profound impact on data management.

Spacecraft control is the responsibility of MOC (fig. 2) while mission planning is a cooperative effort between MOC and SCI (fig. 3). A typical sequence of events would be as follows. Months before an experiment or observation is performed by the Space Telescope (typically 6 months to as much as a year) the astronomer/scientist submits his proposal for observation/experiment; it is screened and put in a roughly outlined observation sequence. About 3 months prior to observation, the detailed planning begins, with an ordering of observations/experiments, and this is transmitted to the SCI for more detailed work. Software processed in the MOC computer sorts the

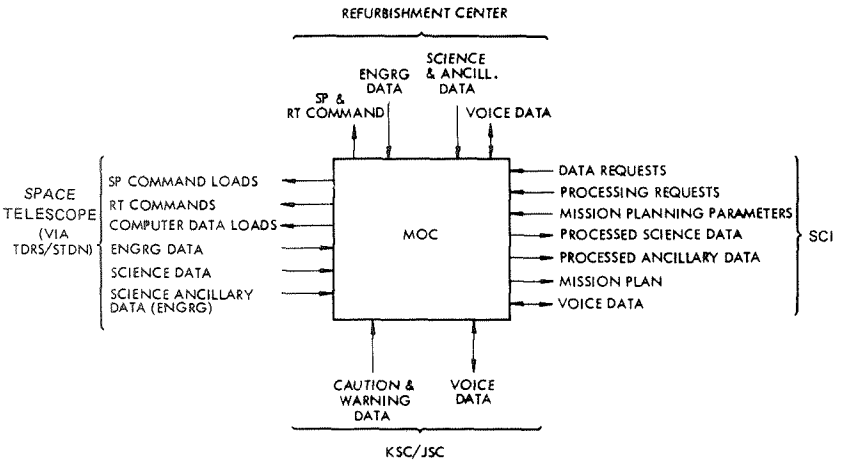

Figure 2.–MOC interfaces. (JSC = Johnson Space Center; KSC = Kennedy Space Center; RT = real time; SP = stored program.)

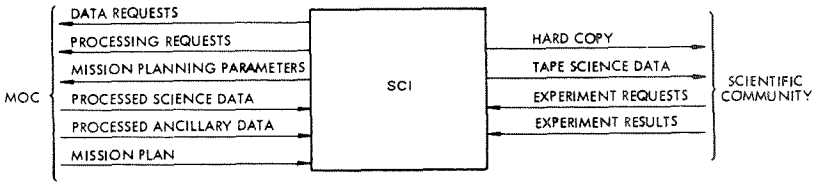

Figure 3.–SCI interfaces.

observations using criteria such as viewing constraints and state of health of the request instrument.

About 1 month prior to observation, details of the observation are produced; for example, slewing constraints are added, a preliminary time line of events constructed, and a final integrated sequence of observations is produced. About 1 week prior to observation, MOC produces and SCI reviews the detailed observational sequences required. Based on these sequences, a spacecraft command load required to command/control the spacecraft and instrument is produced. This command load is verified in a software logic model of the spacecraft. Twelve to 25 hours prior to the observation, the command load is uplinked via the TDRS to the Space Telescope. This command load provides the command/control of the instrument, the support systems, slewing commands to the pointing control subsystem, tracking commands for the high-gain antennas, schedules for the onboard storage devices if required, and the other functions that support the observation. In the meantime, scheduling of TDRSS, NASCOM, and other support functions and services has taken place.

The observation begins with the onboard Data Management Subsystem issuing the slewing commands to the pointing control subsystem. The spacecraft settles, and the required guide stars are acquired. If quick-look data are required to verify the validity of an observation or insure target acquisition, the first frame of data from a given observation will be processed under control of SCI in near real time and displayed immediately in SCI and at the astronomer position in MOC. Based on the quick-look analysis, any necessary commands to implement pointing corrections or modifications to the scientific instrument functions will be generated and transmitted as real-time commands. After quick-look processing and analysis and after necessary adjustment of pointing and scientific instrument parameters, observation continues. Instrument data are acquired and routed by the onboard data system to the relay and then to MOC/SCI. There the data are formatted, corrected and enhanced if necessary, calibration applied, and presented to the observer in the form requested.

The foregoing sequence shows the heavy involvement of the data management system (fig. 4). MOC with extensive computer support prepares the rough observation list; sorts the observation for optimum spacecraft use, subject, of

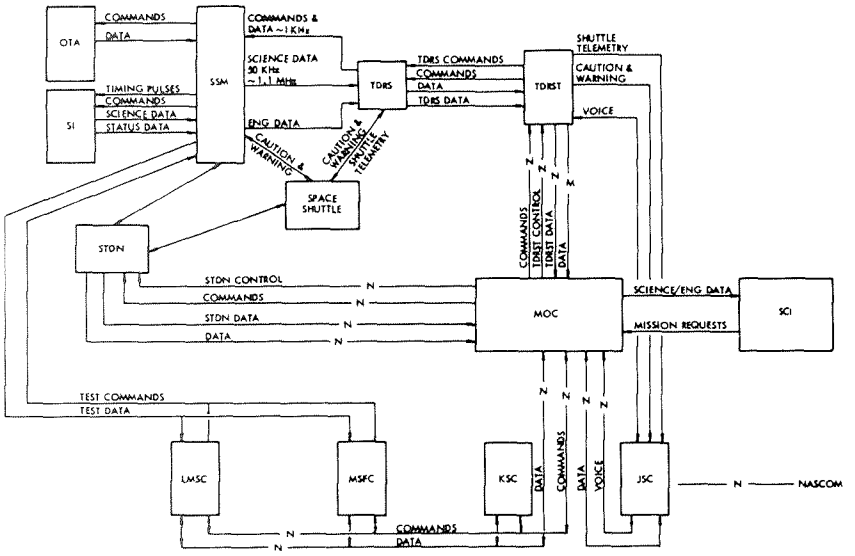

Figure 4.–Space Telescope system data interfaces. (LMSC = Lockheed Missiles & Space Co., Inc.; MSFC = Marshall Space Flight Center; N = network; OTA = optical telescope assembly; SI = scientific instruments; SSM = support systems module.)

course, to manual override; prepares and checks the command load; and, under control of the SCI, processes the resultant science data. Concurrently controlled by the real-time software, MOC determines the state of health of the spacecraft and maintains the interactive operation data base and the terminal system that distribute data throughout MOC and SCI.

Data management does not stop with design of the onboard system but runs the gamut of vehicle, control/command, ground-data handling and processing, and user interface. For a system such as the Space Telescope, the planning functions are as important as the actual handling and processing of the data. Efficient use of all the capabilities of the vehicle, its dedicated command/control and processing facilities, and the supporting systems, such as the Space Shuttle, STDN/TDRS, and NASCOM, provides the system designer with the means to configure a flexible and minimum cost system.

ACKNOWLEDGMENT

The work described in this paper was supported by NASA Marshall Space Flight Center contract NAS8-31313.

A COST-EFFECTIVE DATA MANAGEMENT SUBSYSTEM

John A. Dougherty, Thomas D. Patterson, and Albert E. Cole
Martin Marietta Corp.

The Space Telescope Data Management Subsystem concept development and selection challenge lies in the need to provide a low-cost, simple and reliable approach to meeting the data management requirements of all Space Telescope modules. That approach must be fitted to the initial science payload and subsystem requirements and provide the operations flexibility that is responsive to near-real-time changes by the astronomer in the observing requirements. In addition, reasonable hardware flexibility and growth margins must be provided that minimize the impact of the science payload and subsystem changes that can be anticipated over the long mission life. Finally, the Data Management Subsystem approach must be responsive to the overall project requirements (ref. 1) and to the use of presently and potentially available NASA standard components and subsystems (ref. 2). (Note that the Space Telescope was formerly called the Large Space Telescope or LST.)

The Space Telescope is currently projected for launch in the last quarter of 1982. As an unmanned Space Shuttle Orbiter (SSO) payload, it will be inserted into a near-Earth orbit to perform a science mission of many years in accumulated in-orbit life. The Space Telescope will consist of an optical telescope assembly (OTA), scientific instruments (SI), and a support systems module (SSM). The overall objective will be to acquire spectral, imaging, and astrometric data from celestial objects and planetary bodies, with a significant improvement over data obtainable from Earth observation.

DISCUSSION

The approach to solving the problem required accomplishing the activities identified in figure 1. These included rigorous definition of immediate and potential Data Management Subsystem requirements and the identification and performance of key analyses. Results of the analyses supported the development of candidate Data Management Subsystem concepts for trade study and subsequently resulted in selection of the most cost-effective approach for the Space Telescope.

Seven SI are being considered for accomplishing the initial scientific objectives. NASA provided the primary definition of SI Data Management

Figure 1.—Data Management Subsystem concept development activities. (I/O = input/output; TLM & CMD TDRSS = telemetry and command Tracking and Data Relay Satellite System.)

Subsystem requirements (ref. 3). Using these and other selected NASA, Space Telescope SI documentation, firm requirements were derived for each of the SI. Potential SI requirements were also examined, and this assessment was factored into the Data Management Subsystem concept evaluation.

OTA and SSM Data Management Subsystem requirements were derived. These were telemetry, command, timing, and control. OTA optical performance control and thermal control subsystems do not require onboard computer support. The Pointing Control Subsystem drives the onboard computer sizing. Computer growth margins for throughput speed and memory were added based on an assessment of the maturity of individual requirement definition and the potential growth, after initial definition, as experienced for similar requirements on the Gemini, Viking, and Skylab programs.

Key analyses performed were (1) ground versus onboard functional allocation, (2) SI internal/external functional analysis, (3) distributed versus centralized telemetry, command and computer systems, and (4) definition of a standard SI Data Management System interface. In addition, software analysis was performed to determine a low-cost approach.

To examine flexible cost-effective approaches to the Data Management Subsystem, two basic concepts were developed using results obtained from the analyses previously discussed. One provides integration of the Data Management Subsystem functions while the other implements maximum separation of the functions. In the integrated concept, the computer I/O is a data bus. For the separated concept, a digital hybrid computer I/O is employed. The functionally integrated concept is shown in figure 2. This approach uses a powerful central SSM computer and would require a throughput speed and main memory of 40 000 operations per second and 8000 words, respectively, larger than that of the SSM computer of the functionally separated concept (fig. 3). Separate command and telemetry hardware elements are used. The central SSM computer is limited primarily to implementation of onboard, closed-loop pointing of the Space Telescope.

Computer decentralization is an intended option for each concept, should future SI requirements dictate its feasibility.

RECOMMENDATION

A functionally separated concept having a central SSM computer with hardwired digital I/O, separate telemetry and command systems, and individual SI random access memory/read only memory (RAM/ROM) subsequencers is the recommended Space Telescope Data Management Subsystem (fig. 4). This concept has the following advantages:

(1) Most cost effective
(2) Greatest potential for use of NASA standard components
(3) Least interface complexity
(4) Good approach for selective use of redundancy

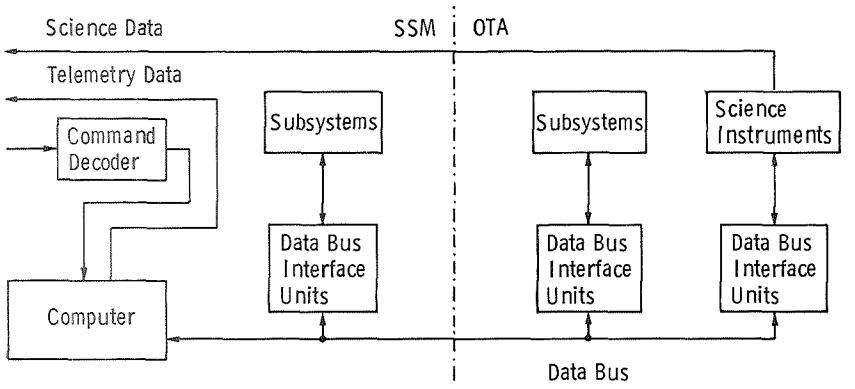

Figure 2.–Functionally integrated Data Management Subsystem.

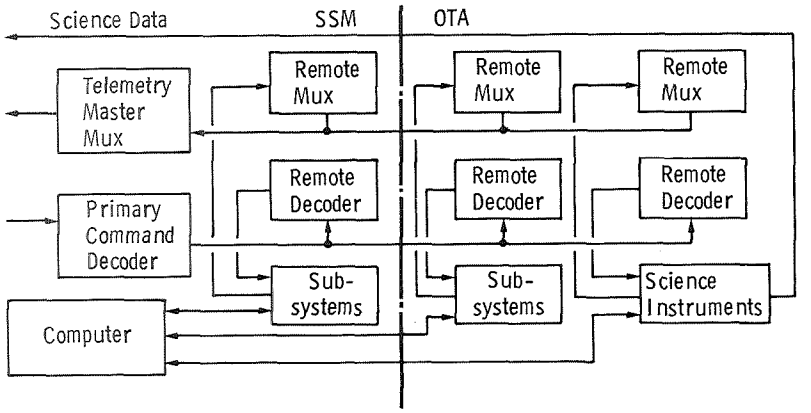

Figure 3.–Functionally separated data management concept. (Mux = multiplex.)

(5) Increased operations flexibility because of separation of functions
(6) Hardware flexibility/growth permits addition of telemetry and command remotes and potential for SI computer at a later date
(7) Low schedule/development risk
(8) Software is minimized by limiting computer function primarily to onboard pointing of the Space Telescope

The selected Data Management Subsystem is cost effective in satisfying the Space Telescope project design goals. Its development and selection is based on a thorough understanding of the firm and potential Data Management Subsystem requirements and on the results of analyses of the critical considerations that drive the design.

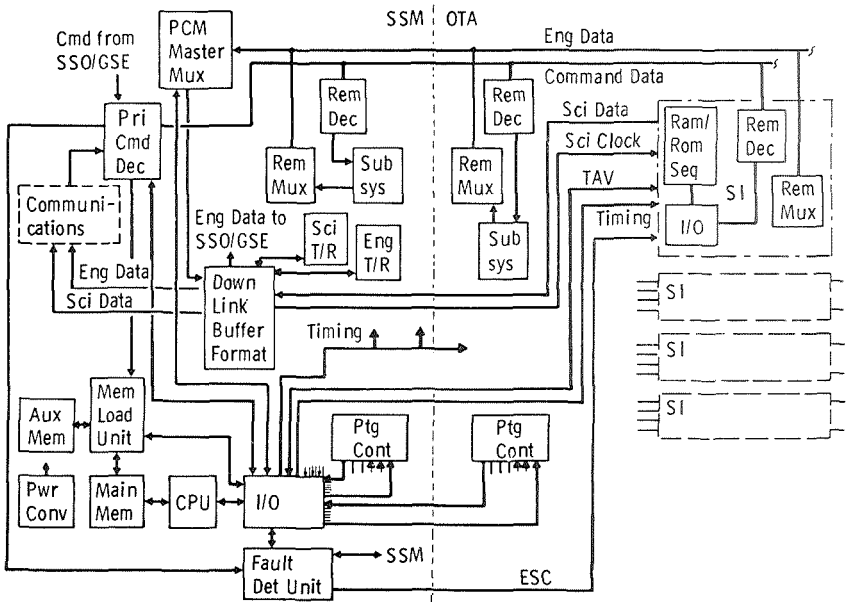

Figure 4.–Recommended Data Management Subsystem concept. (CPU = central processing unit; ESC = emergency shutter control; GSE = ground support equipment; PCM = pulse code modulation; Ptg Cont = pointing control; and TAV = target acquisition/verification.)

ACKNOWLEDGMENT

The work described in this paper was supported by NASA Marshall Space Flight Center contract NAS8-31312.

REFERENCES

1. *LST Project Requirements and Guidelines Document,* revision 2, NASA Marshall Space Flight Center, June 25, 1975.
2. *NASA Standard Modular Spacecraft Specification,* sec. 5.0, NASA Goddard Space Flight Center, May 1975.
3. Data Systems Laboratory, Branch Technical Notes, EF23-75-1A through EF23-75-7A, NASA Marshall Space Flight Center, Apr. 4, 1975.

SYSTEM CONSIDERATION, DESIGN APPROACH, AND TEST OF A LOW-GAIN SPHERICAL COVERAGE ANTENNA FOR LARGE SPACE VEHICLES

Richard E. Ferguson, Thomas D. Patterson, and Manuel R. Moreno
Martin Marietta Corp.

The objectives of this paper are to assess the system requirements on an antenna with spherical coverage using the Space Telescope as an application example, to develop a design approach, and to describe the antenna and modeling measurement techniques that were used to obtain the early empirical antenna pattern data essential to the overall command and data system definition.

SPACE TELESCOPE APPLICATION

The prime communications links will be through the Tracking and Data Relay Satellite System (TDRSS) (ref. 1). The Spaceflight Tracking and Data Network (STDN) (ref. 2) ground stations will be used normally for backup and during the deployment and retrieval of spacecraft by the Space Shuttle. In summary, the needed communications operational capabilities with the omnidirectional antenna system are as follows:

(1) *During orbital deployment and retrieval operations by the Space Shuttle*—receive commands from and transmit engineering data to the STDN remote sites under conditions of both retraction and deployment of the solar arrays
(2) *After deployment from the Space Shuttle*—receive commands and transmit engineering data to both TDRSS subnet and STDN remote site subnet; transmit science data to STDN remote site.

ANTENNA PLACEMENT CONSIDERATIONS

The antenna elements should be placed so as to provide an overall spherical gain pattern and to avoid occlusions and distorting multipath reflections by the vehicle structure. If the elements are to be arrayed to provide a fixed omnidirectional pattern, the placements must also minimize the gain reductions caused by the interferometry effect. To fulfill these criteria, two turnstile-over-cone right-hand circular polarized antenna elements, each having hemispherical response patterns, were tentatively selected to be on the ends of the solar panel booms, as shown in figure 1.

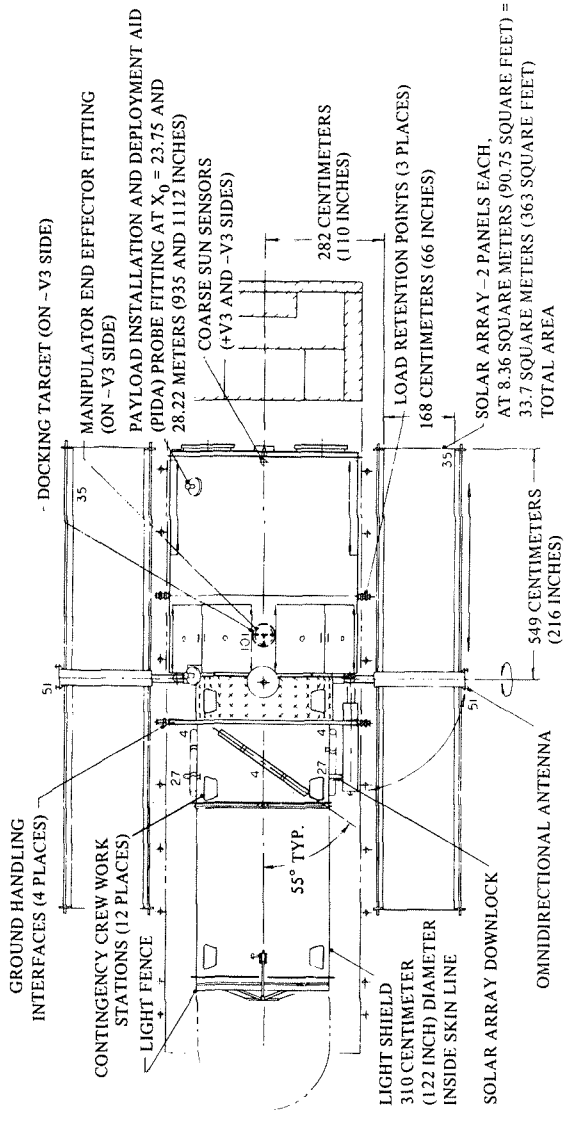

Figure 1.–Space Telescope with solar panels and omnidirectional antennas deployed.

TRIAL RADIOFREQUENCY LINK PERFORMANCE ANALYSIS

A trial radiofrequency link performance analysis was accomplished to determine the required antenna gain versus bit rate for command reception, and for engineering and science transmission links appropriate to TDRSS and to STDN, considering the services available. Tables were constructed, with the known factors included and summarized, of the quantities available for dividing between antenna gain and bit rate for the command link, and, additionally, of the Space Telescope radiofrequency transmitter power for the data return link. For STDN and TDRSS services, the command bit rate is plotted versus the Space Telescope antenna gain in figure 2, and return data bit

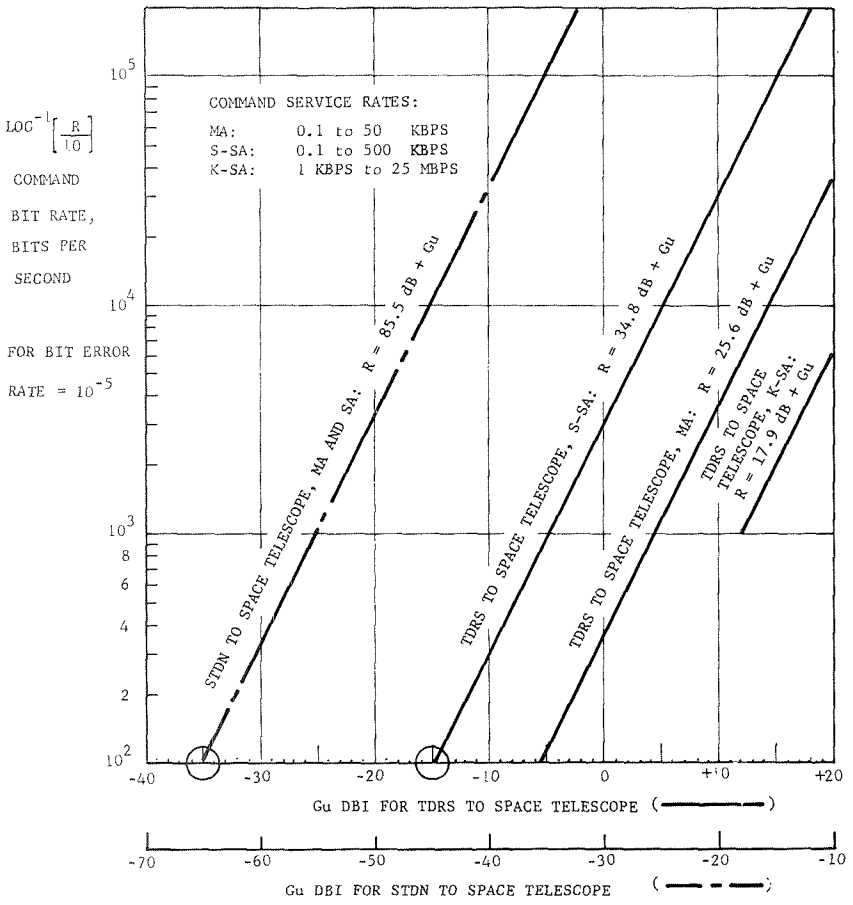

Figure 2.–Command bit rate versus Space Telescope antenna gain. (dBI = decibels isotropic; Gu = gain; K-SA = K-band single access; MA = multiaccess; R = rate; SA = single access; and S-SA = S-band single access.)

rate is plotted versus antenna gain and Space Telescope transmitter radiofrequency power in figure 3. Note that in figure 2 a 3.5-decibel loss is included in the known factors for passively splitting the received signal power to the redundant receiver to make it unnecessary to command a switchover to the redundant receiver in the event of prime receiver failure.

OMNIDIRECTIONAL ARRAY SCALE MODEL PATTERN MEASUREMENTS

Gain pattern measurements were conducted on a one-fifth scale model of the Space Telescope with the antenna elements mounted at the ends of the

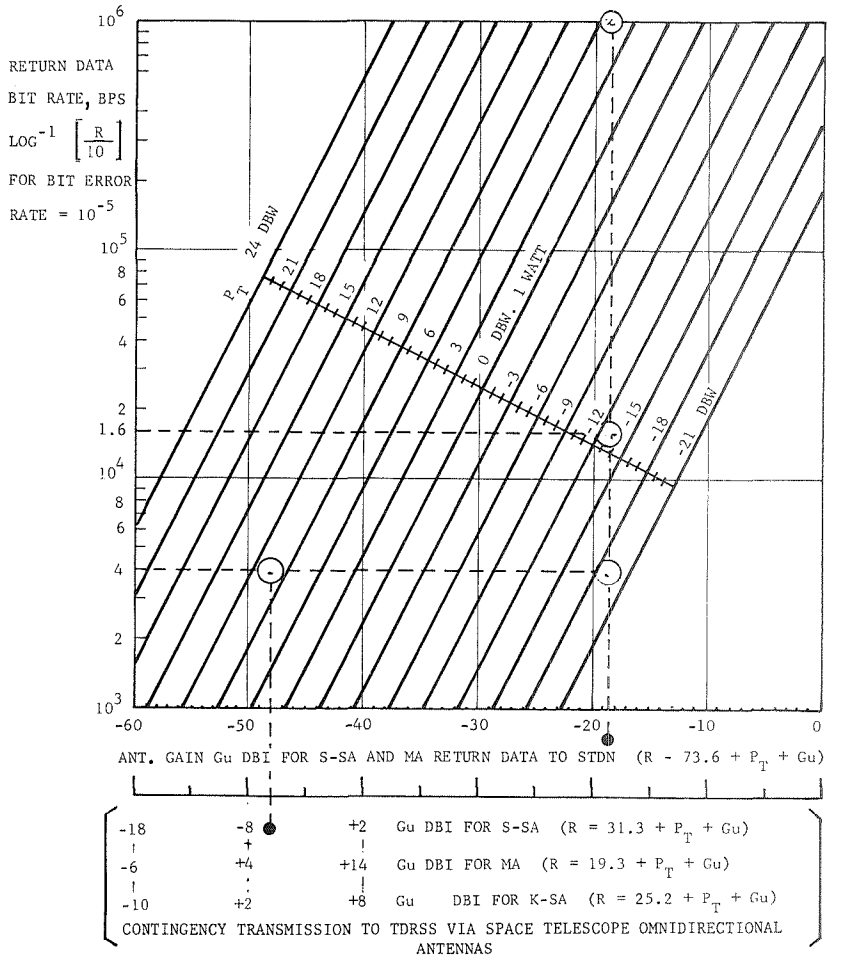

Figure 3.–Return data bit rate versus Space Telescope antenna gain and radiofrequency power. (P_t = power of transmitter.)

booms of simulated solar panels. The model was constructed to set up the conditions of solar panel deployment, retraction, and angular positioning of the deployed panels about the axis of the boom. Outputs of the antenna elements were connected in phase by a coaxial T-junction to the test receiver. The minimum pattern response in a 360-degree rotation of the Space Telescope about its longitudinal axes (Φ) at each azimuth look angle Θ increment is plotted versus Θ in figure 4. Because the antenna gain minima reduce by nearly the same amount versus Θ as Θ approaches the longitudinal axis at either end of the Space Telescope, a model for spherical coverage is suggested. The angle Θ to a selected response minimum approximates the half angle of cones at both

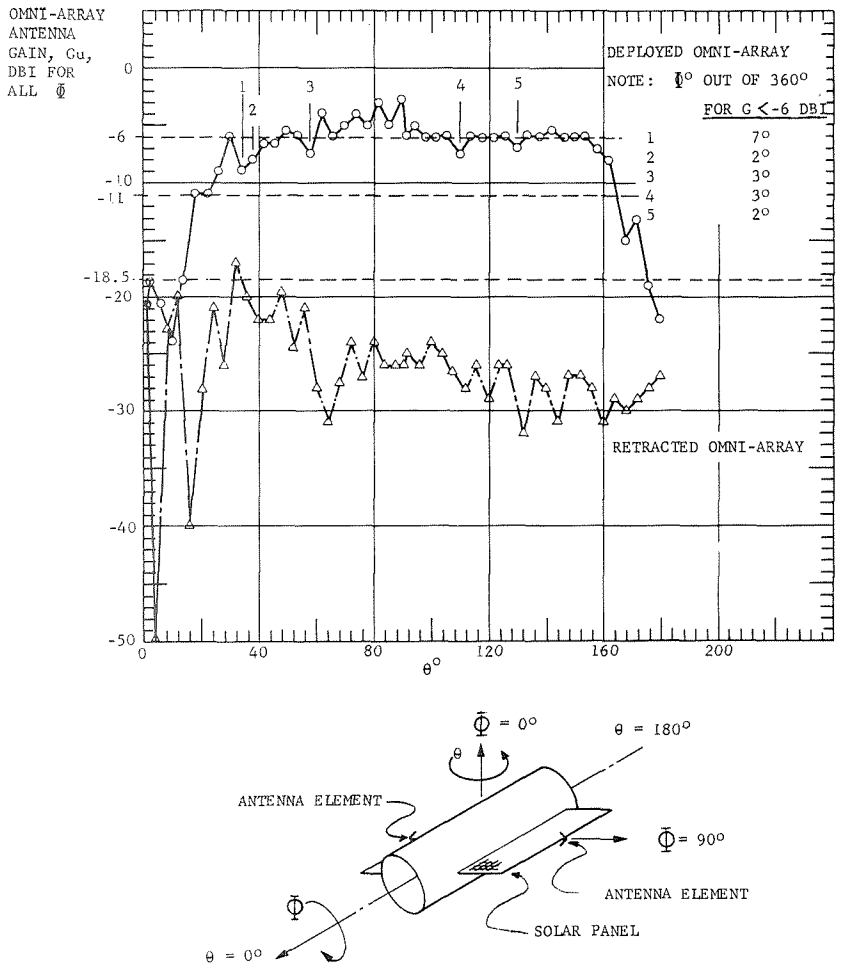

Figure 4.–Space Telescope omnidirectional array antenna gain Gu versus azimuth look angle Θ for all Φ.

TABLE 1.—*Space Telescope Communications Interface With the TDRSS and STDN*

Communication element	REIRP, dBW	Transmit channel	Modulation	Space Telescope antenna type	Antenna response, dBi	Percent coverage	Command and data rates, kilobits per second				Tracking and range rate	Radio-frequency link margin from design case, decibels	Average access time[a] per orbit, minutes
							Forward commands	Return data		Deployment, contingency return engineering			
								Engineering	Science				
TDRS:													
S-SA receive	–	–	SQPN	Omni	-11	96	0.1	–	–	–		3.8	30
Transmit:													
Data group 1	8.9	I	SQPN	High-gain	–	–	–	4	–	–	√	3.9	30
Data group 1	14.9	Q	SQPN	High-gain	–	–	–	16	–	–	√	3.9	30
Data group 2	28.7	I and Q	PSK	High-gain	–	–	–	–	1000	–		4.7	30
Data group 2	2.1	I and Q	PSK	Omni	-6	80	–	–	–	4		2.1	30
STDN:													
S-SA receive	–	–	SQPN	Omni deployed/ retracted	-50	100	.1	–	–	–		15	11.5
Transmit:													
Data group 1	30.2	I	SQPN	Omni	-18.5	97	–	4	–	–	√	7.2	11.5
Data group 1	-24.1	Q	SQPN	Omni	-18.5	97	–	16	–	–	√	7.2	11.5
Data group 2	-10.4	I and Q	PSK	Omni	-18.5	97	–	–	1000	–		7.9	11.5
Data group 2	-33.6	I and Q	PSK	Omni retracted	-40	99.9	–	–	–	4		8.7	11.5
Data group 2	-17.6	I and Q	PSK	Omni	-24	100	–	–	–	4		24.7	11.5

dBW = decibel above 1 watt; PSK = phase shift key; REIRP = radiated effectively instantaneously radiated power; SQPN = staggered quadraphase pseudorandom noise.
[a]Per satellite for TDRS; per station for STDN.

ends of the Space Telescope within which the antenna response is less than the minimum. From this geometry, the percent continuous spherical coverage is equal to at least 100 percent cosine Θ.

SELECTION OF THE COMMAND AND RETURN DATA SERVICE, RATES, AND ANTENNA

Analysis of observational sequences and command history shows that a 100-bit-per-second command bit rate is satisfactory. The S-band single access service is selected. Figure 2 shows that it requires a minimum antenna response of (-)14.8 decibels isotropic at 100 bits per second for communications with TDRSS. Figure 4 shows that the deployed arrayed antenna response is at least (-)11 decibels isotropic minimum to within 18-degree half-cone angles from the longitudinal axis at either end of the Space Telescope. Thus, 95 percent (100 percent cosine 18 degrees) continuous coverage is achieved with 3.8 decibels of margin. For commands from STDN ground station subnet, figure 2 indicates that a minimum antenna gain of -65 decibels isotropic is needed; figure 4 shows that all gain minima are no less than -50 decibels isotropic, which results in 100 percent continuous spherical coverage with 15 decibels of margin.

Based on the number of items to be monitored, the return data rates of 4 and 16 kilobits per second were chosen for engineering. A high rate channel of 1 million bits per second for science data is a requirement. Radiofrequency power allocated to the above rates is -7, -0.97, and 12.8 decibels above 1 milliwatt, respectively. The minimum antenna response needed is obtained from figure 3. Add to the minimum antenna response for the engineering rates the factors 3.9-decibel noise loss caused by multiplexing with the science data channel and 1-decibel channel loss caused by a multiplex with a pseudorandom noise range and tracking code. The percent continuous spherical coverage may be obtained from figure 4 as found for the command channel.

Table 1 contains the summary of the Space Telescope communications interface with TDRSS and STDN using the proposed fixed beam omnidirectional array for the Space Telescope. Included also for completeness is the interface for the high-gain antenna.

ACKNOWLEDGMENT

The work described in this paper was supported in part by NASA Marshall Space Flight Center contract NAS8-31312.

REFERENCES

1. *Tracking and Data Relay Satellite System (TDRSS) User's Guide,* revision 2, STDN no. 101.2, Goddard Space Flight Center, Greenbelt, Md., May 1975.
2. *STDN User's Guide Baseline Document,* revision 2, STDN no. 101.1, Goddard Space Flight Center, Greenbelt, Md., May 1974.

SYSTEM APPLICATIONS OF THE FAULT TOLERANT MEMORY

L. J. Murphy
International Business Machines Corp.

In recent years there has been a marked increase in the long life and high reliability required of computers. Attaining these goals is complicated by an attendant increase in required equipment capability. Computer memories with large, fast arrays and memory sizes in the range of 24 000 to 64 000 words are not uncommon. These larger memories present some system design challenges in meeting overall program reliability goals.

IBM has been involved in recent studies that required long-term, highly reliable performance of an onboard computer system. Two of the more stringent sets of reliability requirements are imposed by the Solar Electric Propulsion Stage and the Space Telescope.

The reliability goal for the Solar Electric Propulsion Stage Command Computer System is 0.95 for a 3-year, unmaintained mission. The system includes a central processing unit, memory, input/output, power supply, and tape recorder.

The initial reliability goal for the Space Telescope Computer Subsystem is 0.975 for a 1-year, unmaintained mission. The most current Space Telescope Computer System concept includes a central processing unit, memory, input/output, and digital interface units. Three redundant power supplies (an optimization of the basic design) are used to increase system reliability slightly. Both the reliability goal and the configuration may be modified in the current phase B studies, but the trade study described in this paper will remain valid.

Reliability analyses were conducted as part of the computer system selection trade studies performed. The results led to the selection of a fault tolerant memory over standard memory modules for both the Solar Electric Propulsion Stage and Space Telescope applications because of savings in cost, weight, and volume.

RELIABILITY AND TRADE STUDY ANALYSIS

To determine the computer system configuration, a reliability analysis of candidate configurations was performed to determine the number of redundant elements required in each candidate configuration to meet the

established reliability goal. The candidate configurations chosen for analysis encompass both single-string and cross-strapped concepts and systems with conventional as well as fault tolerant memories. After the candidates were sized, a trade study was performed to determine the most cost-effective solution. Trade study parameters were cost, weight, power, and volume.

The candidate configurations evaluated for the Solar Electric Propulsion Stage included redundant simplex systems with conventional memories, cross-strapped systems with conventional memories, simplex systems with a shared fault tolerant memory, and cross-strapped systems with a shared fault tolerant memory. Cross-strapped systems have higher reliability but suffer the disadvantage of having more complex interfaces. When the best candidate was selected, the design was optimized to minimize the hardware required to meet the reliability goal. Based on the reliability analysis, the design selected was the three cross-strapped system with a five fault tolerant memory. This design was further optimized to a cross-strapped system with three central processing unit/translators, three power supplies, two input/outputs, two tape recorders, and a 16 000 16-bit-word five fault tolerant memory. The reliability of the optimized system was 0.950 39 for a 3-year unmaintained mission.

The configurations evaluated for the Space Telescope were similar to those considered for the Solar Electric Propulsion Stage. The major differences were memory size (32 000 16-bit words) and the absence of a tape recorder in the critical reliability path. The reliability goal used for the Space Telescope Computer System was 0.975 for 1 year without maintenance.

The system selected for the Space Telescope was two single strings with a five fault tolerant memory. This was optimized to include three cross-strapped power supplies leading to a system reliability of 0.977.

To demonstrate the advantages of the fault tolerant memory system over those using conventional memories for these particular applications, an analysis of relative costs, weight, power consumed, and volume of the competing configurations was performed. All costs were recurring and all parameters were normalized to the selected configuration in each case. The best value for each selection criteria was given the value one (example: lowest cost earns a one) and designated the winner. In both cases a fault tolerant memory configuration was lower in cost, weight, and volume, with a penalty of 20 to 30 percent in power.

FAULT TOLERANT MEMORY ADVANTAGES

A detailed technical description of memory operations is given in a recent technical paper by McCarthy, Carter, and White (ref. 1).

The fault tolerant concept is not totally new. Error correcting codes have been used in some models of the IBM System/360 and System/370 for some years. Field experience showed that significant increases (10:1) in reliability could be achieved by using an error-detecting, error-correcting scheme. This is based on the fact that many memory errors are transient in nature, and if

detected and corrected, the system could continue to operate. The concept that is new in the fault tolerant memory discussed here is the memory plane replacement, which represents the limiting case modular memory replacement.

Strategies for replacement of memory planes will depend upon program needs. If desired, a plane could be replaced when a single bit error occurs. However, because bit errors are frequently random and are corrected by error correcting logic, a better scheme may be to replace a plane after either a hard failure or multiple single errors in the same plane. The selected strategies can be implemented in software.

SUMMARY

The fault tolerant memory has much to offer when the system requirements include high reliability, long life, and large memory size. The reliability of the memory approaches unity for missions as long as 2 years and memory arrays as large as 32 000 16-bit words. This improved memory reliability allows a reduction in the redundancy required (as compared with designs using conventional memory techniques), which results in reduced cost, weight, and volume. Power penalties for the system using the fault tolerant memory approach 30 percent.

The fault tolerant memory concept has been proven in nonaerospace applications. Field experience has shown a 10:1 improvement in reliability. It appears that, based on performance experience to date and anticipated requirements in the future, the fault tolerant memory deserves the attention of system designers.

REFERENCE

1. McCarthy, C. E.; Carter, W. C.; and White, J. B.: "A Memory System Design Which Can Tolerate Multiple Storage Array Faults." *Southeastern Symposium on System Theory,* sponsored by the Institute of Electrical and Electronics Engineers (Auburn, Ala.), Mar. 20-21, 1975.

VII

Maintainability and Operations

SPACE TELESCOPE EXTERNAL INTERFACES

Richard E. Collart
Lockheed Missiles & Space Co., Inc.

The Space Telescope is the first of the permanent space observatories made possible by the development of the Space Shuttle. It is designed for in-orbit maintenance from the Space Shuttle as well as retrieval for ground-based refurbishment if required. This capability will permit high-confidence cost estimating and lower total costs. The Space Telescope will be an international facility similar in operation to ground-based observatories such as Kitt Peak.

The success of the Space Telescope as an outstanding science achievement in the latter part of this century will be directly affected by the definition of its interfaces. The requirements of its external interfaces will determine its design and operation. Also, its requirements will impact those areas with which it interfaces. The earlier the interfaces can be defined, the lower the total program costs.

Interfaces have been established for expendable payloads of the past, but the Space Telescope presents unique new interfaces because it is one of the first large satellites that will use the Space Shuttle as both a launch and a service vehicle. Because the Space Telescope will be an international facility operating for years to come, long-term operational and scientific interfaces are of paramount importance. An important new interface will be with the Tracking and Data Relay Satellite System (TDRSS), which will be developed in the same time frame as the Space Telescope and will augment the Spaceflight Tracking and Data Network (STDN). Figure 1 shows the key external interfaces for the Space Telescope project.

KEY INTERFACES

Key interfaces can be directly related to the mission phases, which include ground test and integration, prelaunch and launch operations, ascent, deployment, operations, in-orbit maintenance, retrieval, deorbit and landing, and refurbishment.

Test and Integration Interfaces

The Space-Telescope-to-test-and-integration interfaces are primarily in two areas: facilities and ground support equipment. A typical Space Telescope

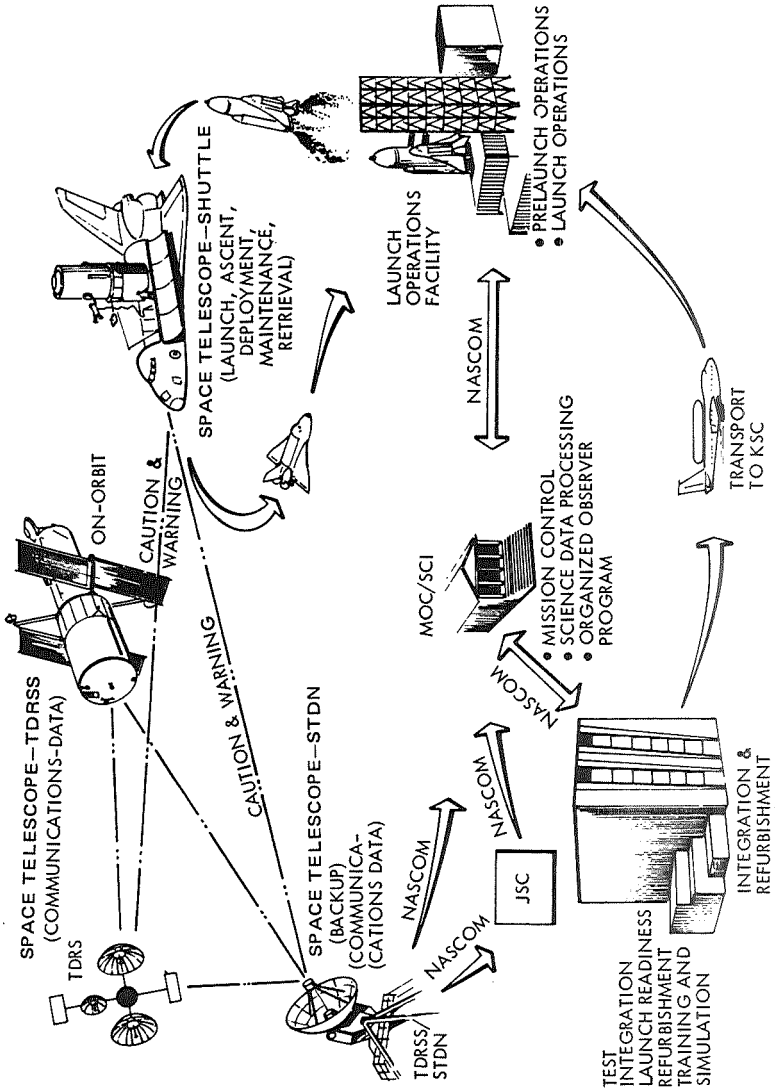

Figure 1.–External interfaces. (JSC = Johnson Space Center; KSC = Kennedy Space Center; MOC = Mission Operations Center; SCI = Science Institute.)

integration facility such as that located at Lockheed provides the interfaces required to integrate and test the spacecraft prior to launch operations. Floor area, crane capacities, hook heights, door sizes, and test chamber capabilities are adapted to Space Telescope requirements and configurations. The close grouping of the pertinent areas will keep handling/mobility operations and risk of contamination to a minimum and will require little relocation of ground support equipment throughout operations prior to shipment to the launch base.

Lockheed has a common boundary with the Moffett Field Naval Air Station, thus precluding the need to transfer the Space Telescope over public roads and permitting virtually door-to-door air shipment from the integration facility to the launch site by means of the 747 payload pod.

Launch Operations Interfaces

The Space-Telescope-to-launch-operations interfaces are similar to those required for test and integration, primarily facilities and ground support equipment.

Shuttle Interfaces

The interfaces between the Space Telescope and the Space Shuttle are unique new interfaces that must be developed because the Space Shuttle will be used both as a launch and as a service vehicle. These interfaces are caution and warning, electrical, mechanical, and in-orbit maintenance.

The Space Shuttle places requirements on users to insure safety and provides facilities for monitoring potentially hazardous elements and initiating safing commands upon detection of a warning. All caution and warning signals from both the Space Shuttle and the Space Telescope are routed to the Integrated On-Orbit Crew Station on the aft flight deck. The Aft Crew Station has the capability to provide checkout and diagnostic services to payloads and Space Shuttle subsystems; it also has the caution and warning status panel for displaying parameters. A caution and warning annunciator panel in the Forward Crew Station relays alarm conditions from the Aft Crew Station.

To minimize interface and program costs, the electrical interfaces between the two spacecraft are simple and consistent with the factory-to-pad test concept. Several Space-Shuttle-to-ground umbilicals are available to the payload users, but at this time only the $t - 0$ umbilical with the digital forward (command) and return (health and status telemetry) data are planned for use. The caution and warning capability through the Space Shuttle will provide sufficient command and monitoring of the Space Telescope for the last few hours the Space Shuttle is on the ground. Other electrical interfaces include battery charging, deployment, instrumentation and monitoring devices, and status monitoring.

The Space Shuttle payload bay available for the Space Telescope mission is

4.6 meters (180 inches) in diameter and 18 meters (720 inches) in length, minus the orbital maneuvering system tank kit length. These net available payload bay dimensions (4.5-meter (15-foot) diameter by approximately 15 meters (50 feet) in length) must accommodate the Space Telescope and associated support equipment. The Space Telescope envelope must allow 122 centimeters (48 inches) clearance of the forward payload bay bulkhead for hatch opening. Mechanical connection of the Space Telescope to the Space Shuttle payload bay occurs at four points: three on a plane at Space Shuttle Station 1010.0 and a fourth at Space Shuttle Station 951.0.

The key interfaces for in-orbit maintenance of the Space Telescope are the Space Shuttle and its crew. The tilted payload system is an example of a system used to allow servicing of the Space Telescope while it is attached to the Space Shuttle. The Space Telescope is swung out of the payload bay on pivot points located on both its sides; firm sill bridge attachment of the payload is maintained throughout the vertical erection and locking process. The tilted payload position permits full 360-degree access to the Space Telescope. The astronauts are fully constrained with built-in crew aids (mostly equipment from Skylab and other NASA programs).

Data (TDRSS/STDN/NASCOM) Interfaces

The Space Telescope will be supported by an extensive network of existing and planned facilities; these will be an extension of the current STDN and NASA communications (NASCOM) network operated by the Goddard Space Flight Center. Other major facilities completing the total support network include MOC and SCI.

Mission Operations Interfaces

The principal operational interfaces are between the Space Telescope and MOC, SCI, and the science community. MOC personnel will control all real-time and near-real-time activity of the Space Telescope by the transmission and execution of real-time and stored-program commands. MOC mission controllers will use displays to monitor the onboard activities, health, and status in near real time. MOC will also provide near-real-time processing of a limited quantity of quick-look science data to SCI.

SCI will develop experiment requirements that are based on requests from astronomers and will transmit the data to MOC. SCI will use a remote terminal to control the processing of science data, preparation of output topics, listing of items for analysis by SCI, and transmittal of experiment requests. SCI will manage all current and archival science data libraries.

CONCLUSIONS

The Space Telescope external interfaces are presently being defined in detail as part of the phase B definition studies. These early definitions and tentative

agreements will lay the initial groundwork for the hardware phase of the program. NASA and its contractors understand the importance of this task because Space Telescope program costs will be directly proportional to the time used to reach the formal external interface agreements: the earlier in the program this task is accomplished, the lower the total program cost.

ACKNOWLEDGMENT

The work described in this paper was supported by NASA contract NAS8-31313.

REFURBISHMENT AND SUPPORT

John Henschke
Martin Marietta Corp.

In conjunction with LST Phase B Definition Study Contract NAS8-31312, the Denver Division of the Martin Marietta Corp. investigated the maintenance/refurbishment and support requirements of Space Telescope equipment. (Note that the Space Telescope was formerly called the Large Space Telescope or LST.) The results of the investigation, discussed in this paper, have been presented to Marshall Space Flight Center, but to date have not been approved by NASA.

MAINTENANCE REQUIREMENTS

Because maintenance requirements are based on predicted failures, a detailed reliability study of the Space Telescope design, as proposed by Martin Marietta, had to be completed. This was accomplished using available design data, plus that generated from previous space programs, in a Monte Carlo maintenance simulation computer model. The Space Telescope items that are most likely to fail in a relatively short time are bearings, image tubes, and batteries. A preliminary contamination analysis performed by Martin Marietta indicated that the Space Telescope optics may be degraded as much as 20 percent in the 100-nanometer wavelength range after 4 years of operation (ref. 1). The proposed silver-coated Teflon thermal coating/cover has a predicted lifetime of 10 years, but mechanical and/or thermal degradation will not occur uniformly on all sections. It can be assumed that after 4 or 5 years certain portions of the thermal coat will be degraded below the level that is acceptable. Other functional components may fail, but the predicted failures will occur at much greater intervals.

IN-FLIGHT MAINTENANCE

During the study it was confirmed that contingency in-flight maintenance must be included in all Space Telescope maintenance programs. Contingency in-flight maintenance in this case covers those in-orbit crew actions necessary to prepare the Space Telescope for deployment or return to Earth when the external equipment such as arrays or antennas do not operate as planned.

Limited In-Flight Maintenance

A limited type of in-flight maintenance was considered for the Space Telescope as a compromise between no such capability and complete in-flight maintenance capability. Only the batteries, reference gyros, two scientific instrument modules, and the fine guidance sensors would be replaced on every mission. During orbital operations, if another critical component fails prior to a scheduled in-flight maintenance mission, its replacement would be considered as part of the next in-flight maintenance mission. For these added tasks, the required tools and spares would be acquired, the additional procedures prepared, and the necessary training planned and conducted as special tasks.

In-Flight Maintenance Versus Ground Refurbishment

After a detailed analysis (ref. 2), it was determined that having all ground return or refurbishment would be the least expensive and having complete in-flight maintenance with minimum ground return would be the most expensive. A combination of minimum ground return plus limited in-flight maintenance would cost approximately 10 percent more than all ground return. Because the probability of requiring maintenance between 1 and 2 years is vastly increased without limited in-flight maintenance, it was decided to include limited in-flight maintenance in the Space Telescope maintenance program.

GROUND REFURBISHMENT

After analyzing the maintenance requirements and determining the extent of the planned in-flight maintenance, a complementary ground refurbishment program was established.

General Concept

After the Space Telescope has been removed from the Space Shuttle at Kennedy Space Center, it will be shipped in the assembled configuration to the refurbishment site. It will then be disassembled into the major modules, and each functional component will be removed and benchchecked. The optics assembly will be shipped to the optics contractor for recoating and realinement. Each failed or degraded and limited life item will be replaced, required in-place repairs accomplished, and all items including the optics assembly installed. The thermal coating will also be renewed. The controlling factor concerning the total ground time is the refurbishment of the optics assembly. Providing spare scientific instrument modules, a spare support systems module structure, as well as a spare optical telescope assembly including the metering truss would reduce ground time to the practical minimum, but the cost would be excessive. A spare set of mirrors would cost about 20 percent of one refurbishment and would reduce the ground time from 45 to 35 weeks; therefore, this was proposed.

Refurbishment Site

It was determined that the average cost of one refurbishment at a payload depot located at Marshall Space Flight Center would be about 75 percent of the estimated cost for a refurbishment at a contractor's facility. Furthermore, if a depot was not established and the refurbishment was accomplished at Marshall using personnel on temporary duty, the average cost would be increased by about 35 percent. Because cost was the primary evaluation factor, it was proposed that a Payload Depot be established at Marshall Space Flight Center and that it should be the Space Telescope refurbishment site.

Payload Depot Operation

For efficiency and cost effectiveness, it appears that other payloads for which Marshall Space Flight Center is responsible should be refurbished in the depot. This would require a great deal of detailed planning, especially with regard to the scheduling of work, to prevent unacceptable peaks and valleys in manning requirements. The depot could be organized similar to one of the laboratories at Marshall. The proposed method for manning the depot would be to have a permanently assigned group of aerospace-experienced personnel that would be augmented by personnel on a temporary basis from the payload contractors.

REFURBISHMENT SUPPORT

Transportation

The 747 (pod) is baselined, but it was determined that the Super Guppy should be considered as the primary backup mode for shipment of the assembled Space Telescope. The availability of the Super Guppy in the required time period is uncertain; therefore, the river barge could be the secondary backup. The C-5A could be a primary backup for the optics assembly.

Spares/Supplies

The proposed provisioning method is to procure or build the necessary new spares and supplies after the first launch and prior to the first refurbishment and to refurbish all repairable failed items. It is estimated that refurbishment of repairables would reduce the cost of spares approximately 40 percent.

Ground Support Equipment

The ground equipment necessary to support transportation, checkout, disassembly, repair, assembly, servicing, integration, and test will be required at the depot. If the same equipment is required at other locations, it will normally be shipped rather than duplicated. Ground support equipment not required elsewhere will be stored at the depot.

Technical Documentation

Necessary technical documentation to support the refurbishment must be provided, but available data should be used to the maximum. It is proposed that operation and maintenance procedures for Space Telescope ground support equipment be prepared. Detailed, step-by-step procedures are not believed to be necessary because the depot personnel will be experienced with aerospace hardware. For the same reason, it is believed that detailed formal procedures for shop repair of failed items removed from the Space Telescope are not necessary.

Personnel and Training

It is assumed that the present training at Marshall Space Flight Center can be expanded to cover Space Telescope requirements. In addition, courses will be conducted at the depot on the subsystems of the Space Telescope. Before any person will be allowed to operate, test, or maintain any Space Telescope equipment, he must be certified. Proper recertification of personnel will be especially important in the case of the Space Telescope because of the relatively long intervals between ground refurbishments.

Facilities

Building 4755 at Marshall Space Flight Center is scheduled to be the Central Integration Site and meets the requirements for refurbishment. Repair shops equipped with normal bench equipment are required to perform the benchcheck and repair of items removed during the flight article refurbishment; these already exist at Marshall.

CONCLUSIONS

Based on available reliability data, four in-flight maintenance missions and three ground refurbishments, scheduled alternately after every 2 years of orbital operations, is the optimum maintenance program for the Space Telescope.

From the overall program cost standpoint, the ground refurbishment of the Space Telescope, with the exception of the optics, should be accomplished at a central payload depot located at Marshall Space Flight Center.

Maximum use of existing equipment, data, facilities, and logistics systems should be emphasized to keep refurbishment support costs to the lowest practical level.

ACKNOWLEDGMENT

The data and helpful suggestions received during the preparation of this paper from A. Howard Kent, Jr., of Martin Marietta Corp. are gratefully

acknowledged and appreciated. The work described in this paper was supported by NASA contract NAS8-31312.

REFERENCES

1. Bareiss, L.: *Preliminary LST Contamination Analysis (2.4 m Option)*. Martin Marietta Corp. LST 75 203671-508, Mar. 1975.
2. Kent, H.: *On-Orbit and Ground Return Maintenance Vs All Ground Return.* Martin Marietta Corp. LST TSR 11.1V, July 1975.

SIMULATION OF THE IN-ORBIT MAINTENANCE CYCLE

J. A. Donnelly
Lockheed Missiles & Space Co., Inc.

Projected long system life for the Space Telescope is achieved through inherent reliability of the selected hardware, service revisit capability of the Space Shuttle, and ground support activity. Reliability of equipment determines the frequency of corrective maintenance, amount of spares required, and need for preventive maintenance. Therefore, an important input to the system maintenance model is reliability information, which is prepared to define the complete Space Telescope system process mode. The initial step in the description of the complete Space Telescope system is to establish basic and redundant elements and the functional relationship of each. The final configuration selection is made to achieve the best reliability within the constraints of system weight, volume, margin of safety, and life-cycle cost. The addition of a unit in redundancy to achieve stated reliability goals and a fail-safe capability is an iterative decision process. Level-of-repair optimization concepts must be designed into the system to take advantage of in-orbit as well as ground refurbishment. Optimum maintenance is achieved over the total life cycle of the system if the repair level alternatives selected minimize total support cost for a specified level of system effectiveness, as compared with other possible maintenance concepts, procedures, or design alternatives.

The maintenance analyses study flow encompasses the interaction of reliability, criticality assessment, maintenance threshold, program cost, and Space Shuttle revisit schedule.

DESIGN AND OPERATIONAL MODEL REQUIREMENTS

System Definition

The Space Telescope consists of three major groups: (1) the optical telescope assembly, which includes the primary and secondary mirrors plus associated electronics and thermal protection; (2) scientific instruments, which includes a high-resolution camera ($f/24$), a faint object spectrograph, an infrared photometer, and a photopolarimeter; and (3) the support systems module.

An essential part of the assessment of the Space Telescope configuration option is the development of the subsystem configuration with its required redundant units. The minimum equipment required to perform the mission constitutes the so-called single-thread reliability model. Redundant optical

telescope assembly and support systems module equipment is added to the single thread in a logical sequence as a function of the minimum weight, cost, and volume to provide the best incremental improvement in reliability. The so-called state of the system at a given interval is defined by the redundant equipment complement that exists at that time. Simply stated, equipment is added in the most logical order by the computer program until the desired reliability is achieved or the cost, volume, or weight constraints are exceeded. Reliability, therefore, becomes a key driver in the search for the best operational system. Variations in reliability and associated redundancy are directly related to the frequency of Space Shuttle visits, which is directly related to changes in total maintenance program cost.

Critical Equipment

Equipment criticality is determined through the identification of those functions that must occur to assure safe retrieval of the Space Telescope. One analytical method to quantify the system probability of loss is to use fault-tree computer graphics. The results of such an analysis determine redundant fail-safe requirements over and above those defined for cost or reliability.

Maintenance Threshold and Call-Up Criteria

The need for Space Shuttle visits to either retrieve or service the Space Telescope depends on the following factors:

(1) System redundancy depletion
(2) Performance of scientific instruments below an acceptable level
(3) Degradation of the optical solar arrays or other limited operational life equipment

Removal and replacement of failed equipment may be accomplished either on demand or it may be scheduled. The on-demand approach suggests a threshold of acceptability below which maintenance action is necessary. The number and type of spares carried by the Space Shuttle to maintain the Space Telescope above this threshold level is determined through fault isolation/detection or by analysis. The system is inoperative when no more redundant units are available. The degradation of scientific instrument performance (loss of channels) is identified as an output of the simulation. Once the threshold is reached, a call for the Space Shuttle and maintenance exits. In effect, the utility of the Space Telescope has reached some level at which it is not cost effective to continue without maintenance. Suppression of this threshold line in the model tends to reduce program cost at the expense of data acquisition. The simulation run identifies both in-orbit maintenance action and ground maintenance action such as refurbishment of the optics.

Programing the Simulation

The General Purpose System Simulator Univac version was selected to be used in the evaluation of the maintenance model. It is ideal because the

language is adaptable to event flow and requires a minimum of program statements.

As a computer programing language, the General Purpose System Simulator has the characteristic of being versatile but not very flexible. This is to say that a relatively short program written in this language can represent a complex problem, but that operations (such as data matrix manipulation) not specifically designed into the language are exceedingly cumbersome to program—if not impossible. As a result, the General Purpose System Simulator has the capability of interfacing with a more general programing language, FORTRAN, to accomplish these otherwise cumbersome operations.

The General Purpose System Simulator/FORTRAN interface is a subroutine entitled "HELP." The purpose of this subroutine in the Space Telescope maintenance simulation program is to produce plots and system parameters over time. In effect, the HELP subroutine is divided into three parts: an initializer, a recorder, and a plotter. The initializer is called at the start of the program to set up the data matrix. The recorder is called from the main program during the simulation each time there is a change in system data. The change and the time of the change are then noted in the data matrix. After the simulation is completed, the plotter portion of the HELP subroutine is called to draw a graph of the data matrix created during the simulation.

CONCLUSIONS

The maintenance model became a useful tool in the system evaluation process. A distinct advantage to this program is the quick-look capability with plots available for analysis of the results. Frequency distributions of the time to first maintenance action and the interval between maintenance Space Shuttle visits give an insight into system behavior.

A comparison of the case studies shows clearly that an on-demand maintenance policy is the most cost effective from a total program cost standpoint.

Spares provisioning becomes an integral part of cost sensitivity studies because it is directly linked to equipment selection, redundancy, and life-cycle failures.

ACKNOWLEDGMENTS

Reliability and cost models developed by E. A. Polgar were the key elements in his systems approach method in the search for the most cost-effective design alternative. C. J. Sheehan provided the General Purpose System Simulator model and developed the unique subroutine plot capability to display the simulation results.

The work described in this paper was supported by NASA contract NAS8-31313.

SPACE TELESCOPE POWER SYSTEM LONG-LIFE DESIGN TECHNIQUES

Owen B. Smith, Richard L. Donovan, and James L. Oberg
Martin Marietta Corp.

The challenge of the Space Telescope power system is to design a solar array/battery system with an operating life in excess of 2 years in orbit. The Space Shuttle provides the capability to replace the batteries and solar array in orbit, but the Space Telescope program must pay the cost of the Space Shuttle flight. Even if the cost of the maintenance mission is shared with another space program, the cost to the Space Telescope program will be several million dollars; therefore, it is imperative that the life of the components be the maximum possible within the constraints of the program.

SYSTEMS DESCRIPTION

The solar array selected is the flexible, rollup solar array designed and flown by Hughes on the STP71-2 mission. The selection of this design as the solar array for the Space Telescope permits additional area of active solar cells at an acceptable weight and cost penalty. To increase the flexible, rollup solar array 2-year design configuration to a configuration that would support a 5-year life results in a weight penalty of only 9 kilograms (20 pounds) and a cost increase of $240 000. Although this value represents a significant percentage increase in the cost of the Electrical Power System initial design, it decreases the spares requirement and is cost effective for the Space Telescope program as a whole.

The initial design requirement for the Electrical Power System specified a 2-year mission, which requires a battery design with a cycle life of 12 000 cycles. The remainder of this paper will address the design techniques of the nickel/cadmium battery system required to meet or exceed the 12 000-cycle requirement.

CHARGE CONTROL SYSTEM

The long-life design techniques addressed in the Space Telescope research project include the capabilities to provide individual cell level control, operate at a reduced state of charge, provide spare cells, and recondition in orbit. To accomplish the cell control function with reasonable size and weight, a relay interconnection network under microprocessor control is used.

FLEXIBLE CHARGE/DISCHARGE CONTROLLER

The 36-cell flexible charge/discharge controller system shown in figure 1 consists of the microcomputer, command decoder, relay drivers, relay interconnection network, multiplexer, current switch network, clock, and ancillary signal conditioning circuits (ref. 1). One relay is required for each cell. Magnetic latching relays, which are energized by a 50-millisecond pulse, are used to reduce power consumption. Relay contact position is under control of the microcomputer. If the microcomputer detects a cell out of limits (voltage high or low), a command is issued to a relay that removes the cell from the battery. The battery will normally have six cells not connected (spare cells). These cells will be used later in the mission for extending the battery life and in reconditioning other cells.

The flexible charge/discharge controller system also contains a clock that generates a real-time word. The provision for time indication permits numerical integration by the microcomputer of the battery charge and discharge ampere-hour integrals. The ampere-hour integrals can be used to implement charge control techniques that use recharge fraction in addition to cell voltage for terminating battery charging. Recharge fraction control will be the primary battery control with cell voltage as a backup.

A unique feature of the flexible charge/discharge controller is reconditioning the cells to regain useful ampere-hour capacity. The microprocessor controls the cell discharge until it detects a cell voltage equal to or less than the low voltage limit.

The discharged cell is then switched back into the battery and is recharged until it reaches 100 percent state of charge as determined by the recharge fraction. This process is repeated until all cells have been reconditioned. In addition to the cell control function, the flexible charge/discharge controller also performs a monitoring function. The system parameters monitored are individual cell voltages, battery current, battery voltage, and battery temperature.

Breadboard

The feasibility of the flexible charge/discharge controller design as presented herein has been successfully demonstrated by a breadboard system at Martin Marietta in Denver, Colorado. A 30-cell breadboard was developed to demonstrate the operation of a 24-cell battery with six spare cells using individual cell monitoring and charge/discharge control. The basic software for this system has been developed and the system is currently operational.

Packaging

Figure 2 shows the flexible charge/discharge controller mounted to a battery housing. A significant reduction in weight of the battery housing is

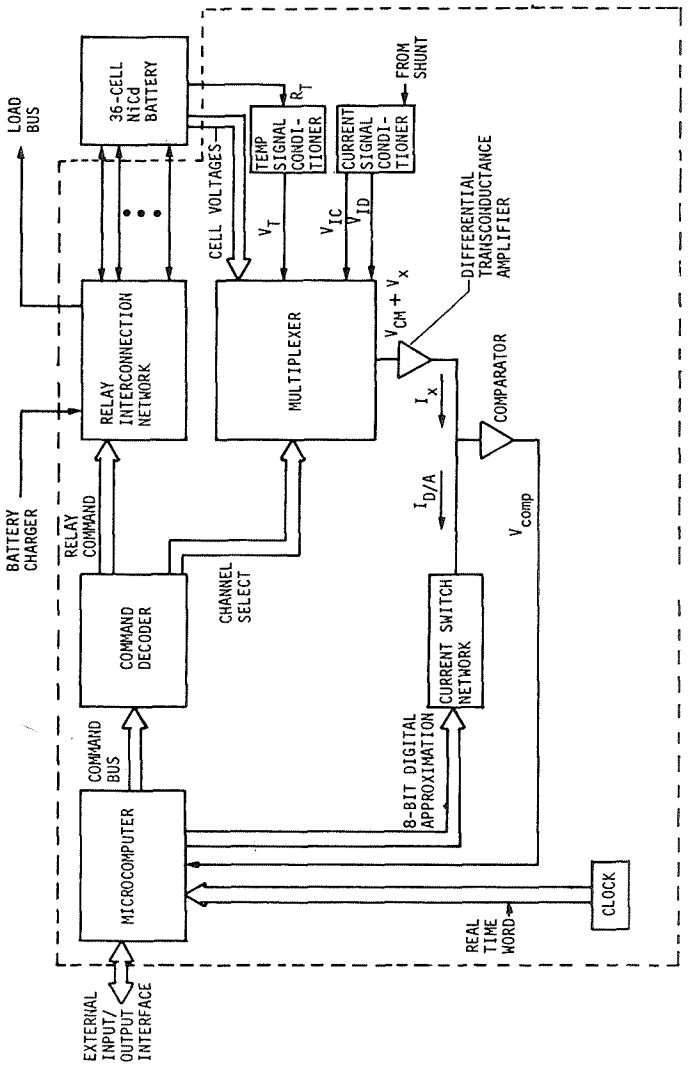

Figure 1.–Flexible charge/discharge controller block diagram. ($I_{D/A}$ = analog current estimate of the signal current I_x; I_x = signal current; R_T = temperature resistor; V_{CM} = common mode voltage; V_{comp} = comparator signal; V_{IC} = charge current signal; V_{ID} = discharge current signal; V_T = temperature signal; V_x = signal voltage.

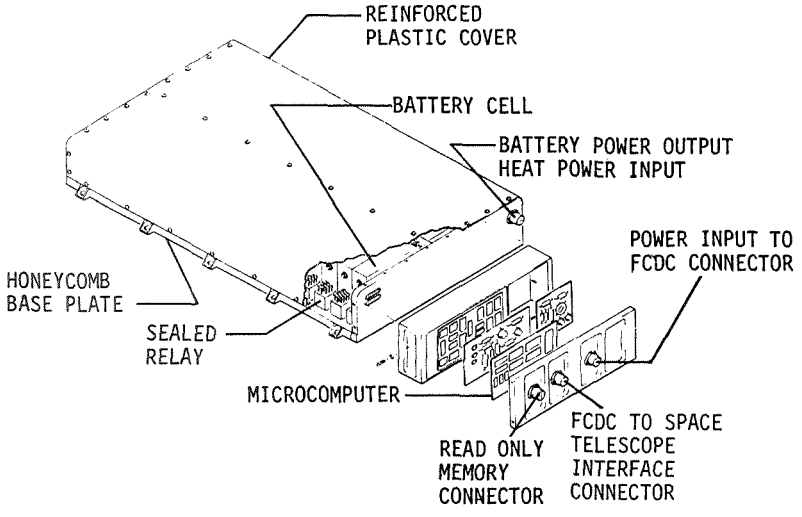

Figure 2.–Flexible charge/discharge controller (FCDC) mounted to a 36-cell battery.

obtained by using a honeycomb in a dual role of a heat conductor and load-carrying structure. Martin Marietta has studied the use of the honeycomb structure and has established the feasibility of its use in space applications (ref. 2). By using the honeycomb structure, the total weight of the 36-cell battery with the flexible charge/discharge controller would be about 56 kilograms (124 pounds). By comparison, the 36-cell Skylab housing weight would be about 62 kilograms (137 pounds) without the flexible charge/discharge controller.

SUMMARY

The individual cell charge and discharge control of the Space Telescope nickel/cadmium cells offers a potential design improvement that could result in batteries with cycle life well in excess of the 12 000 cycles. The exact value of the flexible charge/discharge controller concept must be proved by battery testing or in-flight operation. If indeed the battery tests prove that the flexible charge/discharge controller significantly increased the battery cycle life, the battery life increase can be weighed against the costs in designing the most cost-effective system for the Space Telescope.

ACKNOWLEDGMENT

The work described in this paper was supported by NASA Marshall Space Flight Center under contract NAS8-31312.

REFERENCES

1. Imamura, M. S.; Donovan, R. L.; Oberg, J. L.; Skelly, L. A.; and Julseth, D. H.: "Microprocessor-Controlled Battery Protection System." Paper to be presented at the 1975 Intersociety Energy Conversion and Engineering Conference.
2. Perreault, W. T.: "Lightweight Housing Study for Batteries and Electronic Packaging." Final Report, Martin Marietta Corp., MCR-74-71, 1975.

ORBITAL CREW EXTRAVEHICULAR MAINTENANCE OPERATIONS

H. T. Fisher
Lockheed Missiles & Space Co., Inc.

Initial human factors engineering analyses directly applicable to the Space Telescope were undertaken in support of the NASA-Industry 1965/1967 Optical Technology Experiment System studies. In mid-1972, Lockheed again undertook a major and since continuous Crew Systems activity including development of full-scale hard mockups and conduct of extensive man-in-the-loop simulations. During this time and in concert with NASA, program objectives were developed, interfaces identified, and ground and in-orbit crew system requirements established.

The primary objectives are to develop an in-orbit extravehicular maintenance capability to minimize program cost, reduce design/operations complexity, improve operational reliability, and reduce development uncertainties. Additional program objectives are to develop flexibility in candidate maintenance approaches, accommodate (where practical) off-shelf equipment items, provide for maximum safety of maintenance and flightcrew, and evolve a transitionally flexible and smoothly integrated crew subsystem.

HUMAN FACTORS PROGRAM

In analyzing the Space Telescope system and attendant maintenance modes, certain key issues predominate and therefore become the catalyst of crew systems operations and design development:

(1) Safety to crew, Space Shuttle, and Space Telescope (in that order)
(2) Compatibility with Perkin-Elmer, Itek, and NASA scientific instrument layout
(3) Space Telescope/Space Shuttle docking and/or berthing
(4) Philosophy for manual detract/expand deployable devices
(5) Axial versus radial scientific instrument removal/replacement
(6) Major scientific instrument module size and configuration
(7) Spares quantities, stowage, and volume (if in payload bay)
(8) Crew extravehicular time: integrated suit versus strap-on environmental control and life support system

(9) Manipulator versus crew versus combination of capabilities
(10) In-orbit checkout modes and verification

As the program evolved, several fundamental crew requirements have been generated. Each has been based on extensive analyses, mockup design verification, simulation results (both neutral buoyancy and 1*g*, and data extracted from the highly successful Apollo and Skylab extravehicular activities (both planned and emergency). These basic crew system requirements are as follows:

(1) Operations by one extravehicular crewman
(2) Translation aids designed into the Space Telescope
(3) Component/module changeout designed for one gloved hand or hand-held tool
(4) Orbit replaceable component modules
(5) All hardware and spaceframes designed for crew safety
(6) All access doors sized to permit module, scientific instrument, and component withdrawal/insertion on ground or in orbit
(7) All components/modules sized to be manageable by one or two on ground
(8) Adequate internal volume for ground or extravehicular crew internal access to and maneuverability with components, modules, and scientific instruments
(9) Least contaminable crew ground/extravehicular translation routes
(10) Shortest route to spares pallet and work platform
(11) Minimum need for special crew space support equipment
(12) Direct uncluttered escape route and rescue access
(13) Option for Remote Manipulator System use
(14) Maximum use of Space Shuttle crew/system capabilities

Extravehicular Maintenance Concept

The preferred maintenance approach, incorporating results of 4 years of human factors studies, is for unaided manned extravehicular suited operations. The maintenance crewman translates up rails to the equipment section for external maintenance of support system hardware. Figure 1 illustrates the maintenance mode configuration and the associated spares rack and work platform.

The primary maintenance mode is internal for the scientific instruments, and therefore is conducted radially. Instrument access is quite feasible and can be accomplished from the work platform by translating through either compartment "door," as seen in figure 1. Maintenance of the equipment section is conducted externally in a mobile work platform, also shown in figure 1. A series of external "doors" has been provided to permit radial access to the equipment section, and also to provide for ease of ground maintenance access.

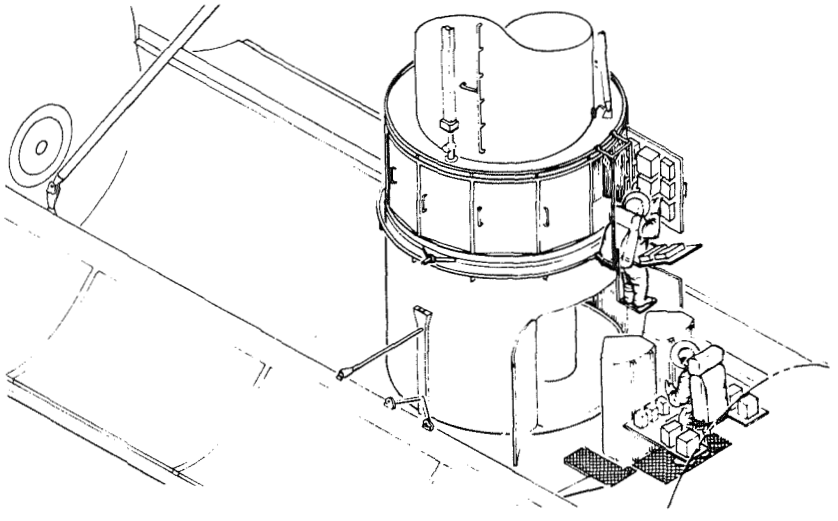

Figure 1.–Space Telescope berthed to Space Shuttle; spares pallet and work platform are illustrated.

Figure 2 illustrates the techniques for scientific instrument and equipment removal.

Berthing or Docking

A key element in the overall Space Telescope maintenance mode is the successful capture and berthing or docking of the Space Telescope to the Space Shuttle. On the basis of extensive trade studies conducted to date, it appears that the most simple and cost-effective docking technique is to soft berth the Space Telescope to the payload bay sill (fig. 1). Close proximity of the crew to the work platform (with spares) and the work platform to the Space Telescope is one of the driving factors in the selection of this approach.

Mockup Development and Simulation

In mid-1972 a program plan was prepared in concert with NASA Marshall Space Flight Center for the Lockheed independent development of a full-scale high-fidelity mockup to permit water immersion for potential neutral buoyancy man-in-the-loop simulation. The mockup was developed as a design and operations verification tool to be used by each of the major engineering and system disciplines. Results of mockup studies have indicated that installation and removal of equipment section hardware is rather straightforward.

CONCLUSIONS

All studies to date indicate that in-orbit extravehicular manned maintenance of the Space Telescope is not only feasible but can be designed to be

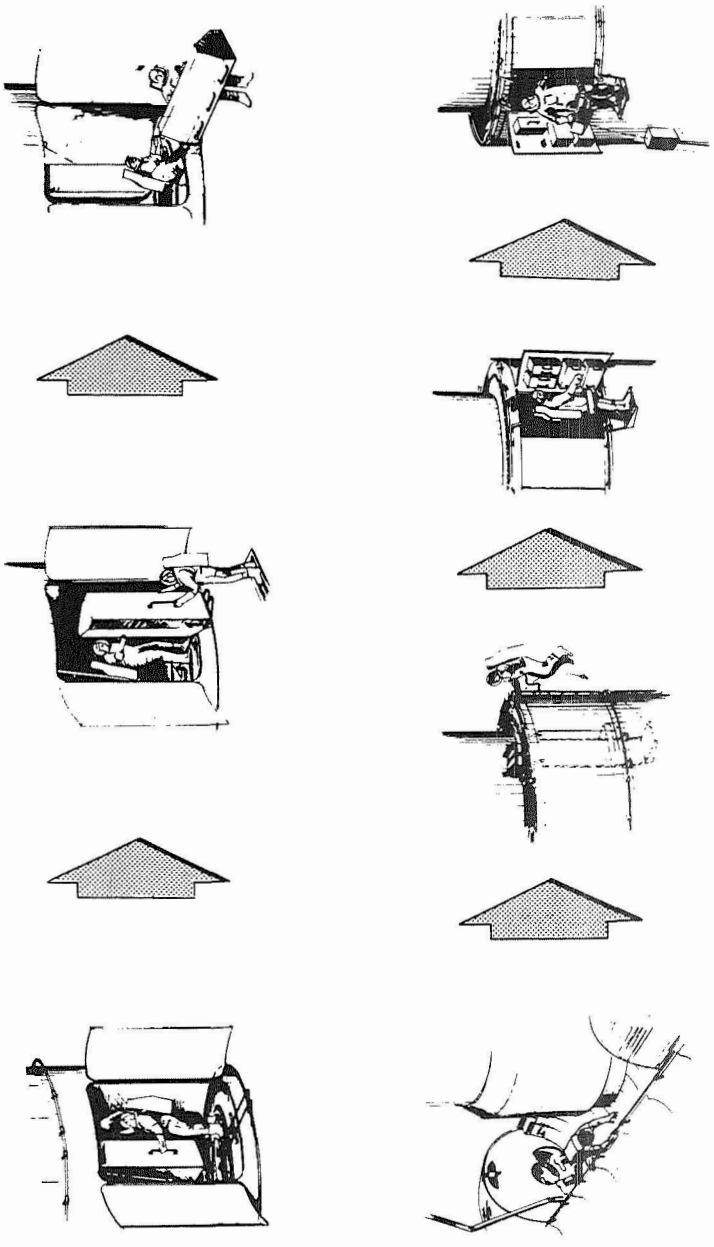

Figure 2.–Scientific instrument and equipment removal sequences.

easily within the capability of the extravehicular functioning astronaut. Both 1*g* and neutral buoyancy man-in-the-loop simulations further verify this point. It is important to recall the success of the Skylab crews in accomplishing the "impossible" mission saving tasks with few, if any, built-in extravehicular mobility and work aids. Therefore, this opportunistic success strongly suggests consideration of the following: What can future crews accomplish if payloads are designed for orbital maintenance? What potential time and cost savings can be realized by program developers and, ultimately, the principal users?

ACKNOWLEDGMENT

The work described in this paper was supported by NASA contract NAS8-31313.

ACRONYMS

CCT	computer-compatible tape
C&DH	command and data handling
CMG	control movement gyroscope
CPU	central processing unit
EPS	Electrical Power System
ESA	European Space Agency
ESC	emergency shutter control
ESRO	European Space Research Organization
FCDC	flexible charge/discharge controller
GSE	ground support equipment
GSFC	Goddard Space Flight Center
ICCD	intensified-charge-coupled device
IDC	image dissecting camera
I/O	input/output
IPCS	Image Photon Counting System
JSC	Johnson Space Center
KSC	Kennedy Space Center
LMSC	Lockheed Missiles & Space Co., Inc.
MA	multiaccess
MMT	multimirror telescope
MOC	Mission Operations Center
MSFC	Marshall Space Flight Center
NDL	near diffraction limited
NEFD	noise equivalent flux density
NEP	noise equivalent power
NGC	*A New General Catalog of Nebulae and Clusters of Stars*
NOCC	Network Operations Control Center
ODS	Orbit Determination System
OTA	optical telescope assembly
PCM	pulse control modulation
PCS	Pointing Control Subsystem
PSF	point spread function
PSK	phase shift key
Q.L.	quick look
REIRP	radiated effectively instantaneously radiated power
RT	real time
SA	single access
SCI	Science Institute
SECO	Secondary Electron Conduction Orthicon
SI	scientific instrument

SP	stored program
SQPN	staggered quadraphase pseudorandom noise
SSM	support systems module
SSO	Space Shuttle Orbiter
STDN	Spaceflight Tracking and Data Network
TAV	target acquisition/verification
TDRSS	Tracking and Data Relay Satellite System
TLM & CMD	telemetry and command
WHS	White Sands, New Mexico

AUTHOR INDEX

☆ U.S. GOVERNMENT PRINTING OFFICE : 1976 O—204-654

"The aeronautical and space activities of the United States shall be conducted so as to contribute . . . to the expansion of human knowledge of phenomena in the atmosphere and space. The Administration shall provide for the widest practicable and appropriate dissemination of information concerning its activities and the results thereof."

—NATIONAL AERONAUTICS AND SPACE ACT OF 1958

NASA SCIENTIFIC AND TECHNICAL PUBLICATIONS

TECHNICAL REPORTS: Scientific and technical information considered important, complete, and a lasting contribution to existing knowledge.

TECHNICAL NOTES: Information less broad in scope but nevertheless of importance as a contribution to existing knowledge.

TECHNICAL MEMORANDUMS: Information receiving limited distribution because of preliminary data, security classification, or other reasons. Also includes conference proceedings with either limited or unlimited distribution.

CONTRACTOR REPORTS: Scientific and technical information generated under a NASA contract or grant and considered an important contribution to existing knowledge.

TECHNICAL TRANSLATIONS: Information published in a foreign language considered to merit NASA distribution in English.

SPECIAL PUBLICATIONS: Information derived from or of value to NASA activities. Publications include final reports of major projects, monographs, data compilations, handbooks, sourcebooks, and special bibliographies.

TECHNOLOGY UTILIZATION PUBLICATIONS: Information on technology used by NASA that may be of particular interest in commercial and other non-aerospace applications. Publications include Tech Briefs, Technology Utilization Reports and Technology Surveys.

Details on the availability of these publications may be obtained from:

SCIENTIFIC AND TECHNICAL INFORMATION OFFICE

NATIONAL AERONAUTICS AND SPACE ADMINISTRATION

Washington, D.C. 20546